Natural Resources Canada | Ressources naturelles Canada

THE GEOLOGICAL FRAMEWORK OF SEDIMENT INSTABILITY ON THE SCOTIAN SLOPE: STUDIES TO 1999

Geological Survey of Canada Open File
3920

David J.W. Piper
Geological Survey of Canada (Atlantic)
piper@agc.bio.ns.ca phone: (902) 426 6580

with contributions from D. Bonifay, D.C. Campbell, J. Marsters, K. Moran, D. Pass, C.G.P. Pereira, K. Skene and R. Sparkes.

August 2001

Canada

Available from
Geological Survey of Canada
Bedford Institute of Oceanography
1 Challenger Drive
Dartmouth, Nova Scotia B2Y 4A2
Price subject to change without notice

Table of Contents

LIST OF FIGURES

Chapter 5

Chapter 6

Chapter 7

Chapter 8

Chapter 9

Abstract

Slope stability is a constraint for hydrocarbon development on the Scotian margin. Surficial debris flows and slides are widespread and cover more than 40% of the continental slope. Pockmarks (fluid escape craters) are widely seen on sidescan sonar records. Cores commonly contain gas and there is circumstantial evidence for the presence of gas hydrates.

The surficial geological framework of the continental slope is highly variable. Morphologically, the east Scotian Slope is much steeper and more dissected than the west. Everywhere, the surficial sediments on the slope are dominated by Pleistocene glacial deposits but the style of glacial sedimentation varied geographically. As a result, surficial sediment type and the potential for instability varies from one area to another.

Slope stability analysis shows that surficial sediment is generally stable (except on steep canyon walls) so long as there is not high excess pore pressure. Sources of excess pore pressure may include: (a) Migration of shallow petrogenic gas. (b) Residual excess pore pressure in rapidly deposited proglacial mud and debris flows. (c) Fluid expulsion from diapiric Pliocene deltaic shales. (d) Fluid expulsion associated with salt diapirs.

In water depths > 500 m, conditions are suitable for the formation of gas hydrates. Sediment cores and high-resolution acoustic profiles suggest that shallow gas is widespread. However, gas hydrates have not been proven. There is circumstantial evidence that they are implicated in many of the large failures on the slope. If present, they would influence the migration of shallow gas and their sublimation would pose a hazard if production changed the thermal regime of bottom sediment.

Many observed shallow surficial failures head in about 500 m water depth, perhaps because: (a) sediment in water depths of less than 500 m is overconsolidated as a result of either ice or iceberg loading in the past; (b) silty sediment prone to liquefaction is most common at this depth; or (c) failure takes place at the upslope limit of a gas hydrate "cap". There is scientific uncertainty about the role of ice loading on the outer shelf and upper slope in promoting both sediment failure and local seismicity, particularly in the few thousand years following ice retreat.

On the New England continental margin, large sediment slides many tens of metres thick originating in 700 to >2000 m water depth are associated with interstratal failure of late Pliocene to early Pleistocene sediment. Sediment of this age on the Scotian margin show similar instability features suggesting that there could be a potential hazard from failure at several hundred metres depth subbottom.

Seismicity is one trigger for sediment instability. In 1929, a catastrophic seafloor failure extending over at least 100 km was triggered by a magnitude 7.2 earthquake on the geologically similar margin of the western Grand Banks. Such earthquakes probably have a recurrence interval of at least many thousands of years. No large failures are known on the Scotian margin dating from the last 10 000 years, although several major failures (one near the Albatross well involving the upper 50 m of the seabed) date from 10 000 to 14 000 years ago, long after glacial ice had retreated from the shelf edge.

If comparison is made with sediment stability in other slope areas, then certain unusual features of the Scotian margin must be considered. The facies distribution of sediment on the slope is different from that in fluvial dominated slopes such as in the Gulf of Mexico, Brazil or Indonesia. The proglacial deposition resulted in very silty sediment being deposited in water depths down to several hundred metres and upper slope sediment are winnowed by storm-driven currents. Such silty sediment may be very prone to failure by cyclic loading. The cold bottom waters on the Scotian margin may promote the shallow occurrence of gas hydrates leading to excess pore pressures.

Mean sedimentation rates in the Holocene are of the order of 10-20 cm/ky. Sedimentation rates during the last glacial maximum are probably regionally variable but typically 100 cm/ky. Mean sedimentation rates over the last half million years are about 40 cm/ky and over the last 1.5 million years about 30 cm/ky.

Existing geological data suggest that while slope instability is a risk, it is likely to be a manageable risk and only severe in certain restricted areas. Additional studies are needed to establish the surficial geological framework affecting slope stability and to understand the various factors that may promote slope instability. Of particular importance is understanding what evidence of instability is a consequence of past conditions.

1. Introduction

1.1 The geological setting of sediment instability

The continental slope off southeastern Canada has a highly variable morphology (Fig. 1). The slope lies seaward of the continental shelf, extending from the shelf break in water depths of 100-400 m to the lesser gradients of the continental rise at 2000-2500 m. In some areas, the slope has prograded in the Quaternary: these areas generally have relatively smooth bathymetry and several hundred metres of Quaternary sediment. Other areas are highly dissected by submarine canyons that have exposed Tertiary strata: these areas tend to have a shallow shelf break. In general, the eastern Scotian Slope is steeper and more dissected; the central Scotian Slope has wide areas of relatively undisturbed sediment; and the western Scotian Slope has abundant debris flows.

The first systematic study of the continental slope off southeastern Canada was by King and Young (1977), who noted regional variability based on industry multichannel seismic profiles. Regional seismic interpretation has also been carried out by Woods Hole Oceanographic Institute (Emery et al., 1970; Austin and Uchupi, 1979; Swift, 1985a, 1985b, 1987). Detailed studies of a slopes with canyons south of Sable Island were made by Stanley and Silverberg (1969), and a synthesis of late Quaternary margin development was presented by Stanley et al. (1972). Hill studied in detail an area of smooth slope south of Emerald Basin (Hill, 1981, 1983, 1984; Hill and Bowen, 1983).

The original impetus for this research was to provide a knowledge base to assess constraints to hydrocarbon exploration and possible development on the continental slope. From 1979 to 1988, a total of 8 wells were drilled in water depths of more than 900 m on the southeastern Canadian margin, mostly on the central Scotian Slope and in Flemish Pass. Sediment failure, shallow poor hole conditions, and shallow gas were all perceived as possible constraints to exploratory drilling. Seismic risk from the area near the epicentre of the 1929 "Grand Banks" earthquake could not be quantified. The previous work on the continental slope did not provide a geological framework of sufficient detail or regional coverage to address such issues.

Systematic study of the continental slope has proved to be of value beyond the issues of constraints to hydrocarbons. The new fibre-optic cables of the late 1980's have required detailed knowledge of seabed conditions along their routes. For contemporary global change issues, the continental slope provides a long stratigraphic record of proxy-climate data near to the continent. This area is also a major site of methane gas release. The continental slope also provides a proxy-record of past seismic activity.

PERD[1] funding to the Geological Survey of Canada and the five deep-water wells drilled on the Scotian margin by industry in the 1980's accelerated our understanding of the Scotian Slope in the 1980's, but the pace

[1] Program of Energy Research and Development

of research diminished after 1990. The strategy of the GSC has been to focus research on areas of industry activity and to take advantage of well results and site-survey geophysical data. Mosher (1985), Marsters (1986), Hughes Clarke (1988), Berry (1992), Baltzer (1994) and Morrison (2000) all carried out graduate thesis work on instability features on the Scotian margin and the nearby Laurentian Fan and St Pierre Slope. The Lamont-Doherty SeaMARC I deep-water sidescan system was used on the Scotian Slope in 1982, 1983 and 1984; the IFREMER SAR deep water sidescan and "module géotechnique" were used in 1990; and submersibles were used in 1981, 1985 and 1986. Most of these field studies concentrated on geological issues and have been reported in the open literature and in various GSC Open File reports. As a result, we have a general knowledge of the geology of the Scotian Slope, although parts of the western and eastern Slope remain poorly known. This knowledge includes:

- Major bathymetric features
- some idea of whether canyons, debris flows, or smooth slopes predominate
- Pliocene - Quaternary overall sediment thicknesses, stratigraphy and predominant facies

In addition, we have a more detailed knowledge of the areas around the five wells drilled on the Scotian margin: Shelburne G-29, Albatross B-13, Acadia K-62, Shubenacadie H-100 and Tantallon M-41, which have been used as type examples for extending interpretations to less well-known areas.

Hazard assessment on the continental slope depends on an understanding of the Late Cenozoic evolution of the slope and the geological processes active there. We have therefore used both 1980s industry seismic and our own single channel seismic lines to intepret the Pliocene to Quaternary history of the slope, using biostratigraphic ties to wells (Table 1.1). Pliocene sediment in places forms small mud diapirs (Piper and Sparkes, 1987; Piper 2000) that are quite distinct from the Triassic salt diapir province further seaward (Wade and MacLean, 1990). Interstratal faulting is also present in some Pliocene sediment. The Late Cenozoic evolution of the slope was strongly influenced by sea level variations that resulted in similar sedimentation history over large areas of the margin (Piper and Normark, 1990).

We follow Piper and Sparkes (1987) in defining the upper slope as the region from the shelf break in 100-200 mbsl to the heads of widespread gullies in water depths of 400-600 mbsl (Table 1.2). The middle slope then extends to a diminution in gradient that typically occurs between 1000 and 1400 mbsl. The lower slope then extends to the top of the continental rise, typically at about 2000 mbsl, where a further reduction in gradient takes place (Heezen, 1959).

Piper (1991) mapped the principal surficial sediment types of the continental margin. In water depths to about 3000 m, 8% of the seabed was mapped as erosional into Late Cenozoic bedrock, 16% as dissected stratified late Quaternary sediment, 22% as covered by slumps and debris flows and 40% (largely in deeper water) as depositional. These bottom conditions result largely from sedimentation over the past few hundred

thousand years, particularly during glacial periods when continental ice extended to the edge of the continental shelf (Stea et al. 1998). There was considerable variation in the style of glacial sedimentation along the margin (Piper, 1988). The transverse troughs on the continental shelf were major outlets for glacial ice, leading to thick deposits of both coarse and fine-grained sediment. Glacial ice less frequently crossed the shallow outer-shelf banks, but commonly discharged proglacial meltwater across the banks, resulting in deltaic sedimentation at the shelf break. Fine-grained proglacial sedimentation predominated in some areas of deeper shelf break that were not emergent at lowstands of sea level. High-resolution seismic data and cores suggest that upper slope sediments are deposited in cycles corresponding to major glacial - deglacial phases. At the base of each cycle are acoustically amorphous sediment, corresponding to sands or debris flow deposits, that are overlain by acoustically stratified sediment with a draped architecture (principally muds) and then a thin veneer of post-glacial muds with a ponded architecture (Piper and Sparkes, 1987; Piper et al., 1990). There is thus a reasonably systematic pattern of proglacial sedimentation on the slope (Piper, 1987; Mosher et al., 1989), allowing predictions on the occurrence of drilling problems such as boulder beds and sticky clays.

Rates of sedimentation on the slope were as high as 1 m/ka during ice retreat on the continental shelf, but after about 10 ka, sedimentation rates decreased (Bonifay and Piper, 1988). Sedimentation rates are discussed in greater detail below. Holocene sediment appears to be derived in part from winnowing of topographic highs (Syvitski et al., 1983; Hill and Bowen, 1984). There is circumstantial evidence for Holocene turbidity currents initiated on the upper slope on the central Scotian Slope, where dendritic channel patterns have been mapped by sidescan, and on the Tail of the Banks, where sandy turbidity currents reach the continental rise every 4 ka (Savoye et al., 1989).

Several morphological types of submarine canyons and gullies cut the slope. Classical submarine canyons with pinnate morphology that head at the shelf break are common on the southern part of Grand Bank. On parts of the Scotian Slope, canyons head at about 400-500 m onto a smooth upper slope (Shor and Piper, 1989). Smaller canyons off Banquereau and Sable Island Bank show this morphology, but larger canyons breach the shelf break. Some canyons appear to be the continuation of buried subglacial tunnel valleys on the shelf (Boyd et al., 1988; McLaren, 1988). All these scales of canyons dissect early Pleistocene or Tertiary strata on the slope. Smaller gullies and channels, in areas lacking canyons, tend to cut only late Quaternary strata.

On many parts of the margin, sediment failure has occurred in water depths of 500-1000 m. Some of this failure appears to result from oversteepening by canyon incision. Other failure occurs on gentle slopes lacking canyons, notably around the epicentre of the 1929 earthquake on St Pierre Slope, and near the Shubenacadie well on the central Scotian Slope. Failure initially results in rotational slides, but on steep slopes there is evidence that slides pass into debris flows, eventually producing ignitive turbidity currents (Piper et al., 1985a; Piper et al., 1992a, 1999). Turbidity currents are probably the principal agents of canyon incision (Hughes Clarke et al.,

1990). Although some result from slope failure, others may result from hyperpycnal flow of glacial meltwater or subglacial outbursts (cf. Piper and Savoye, 1993).

On several parts of the margin, shallow gas is common in cores and industry seismic shows patchy occurrence of shallow gas. Pockmarks have been mapped with deep-water sidescan on St Pierre Slope and in the area between the Shubenacadie and Shelburne wells on the central Scotian Slope. Gas hydrates have been interpreted from well logs in some East coast wells (Thurber Consultants, 1985) and seafloor temperatures are sufficiently low for gas hydrates to form in water depths of more than 500 m. Neave (1990) has proposed that the widespread failures that begin in 500 m water depth represent sliding at the feather edge of a gas hydrate cap. Alternatively, this critical depth for failure may be related to the distribution of proglacial facies and/or overconsolidation by iceberg scour. Bottom-simulating reflectors (BSRs) have not been reported from seismic profiles on the Scotian margin.

Earthquakes are the most likely trigger for failure. Sparse earthquakes occur along the passive continental margin of eastern North America and the 1929 "Grand Banks" earthquake resulted in widespread sediment failure. Moran and Hurlbut (1986) demonstrated that in water depths of more than a few hundred metres, wave loading was not likely to be a trigger. The possibility of breaking internal waves triggering failure cannot be excluded.

1.2 **Technology and data acquisition**

Geological work in deep water presents special problems not generally experienced on the continental shelf. The greater distance to the seabed from surface or near-surface towed acoustic systems results in poor horizontal spatial resolution, compounded by the effects of steep and irregular topography in many areas. Instruments that operate at or near the seabed require long cables, thus large winches, and in many cases adequate pressure protection. Long wire times are required to lower instruments to the seabed; towing equipment near the seabed requires very low ship speeds (typically 2 knots) in order to reduce cable drag.

Most of the GSC research on the continental slope has been limited by the capability and availability of deep-water instrumentation (Table 1.3). Early work has been superseded by later work with more advanced technology. The lack of established instrumentation and geologic concepts on the continental slope result in long lead times being necessary to provide interpretations of particular problems.

During the 1980s, ship navigation has been by Loran-C (generally 100 m accuracy), with conventional GPS (10-20 m accuracy) and later differential GPS becoming available in the 1990s. Most cruises did not have any method of positioning equipment relative to the ship; short base-line navigation systems proved imprecise, but suggest that at times piston cores were located up to 500 m from the ship in water depths of 3000 m.

Bathymetric information is generally based on widely spaced 12 kHz surface echosounder profiles,

resulting in poor spatial resolution, particularly on steep slopes. Seabeam bathymetry is available only for part of the Laurentian Fan (Hughes Clarke et al., 1990). Bathymetric compilation in places is further hampered by extreme variability in sound velocity in surface waters associated with Gulf Stream rings.

A variety of deep-water sidescan systems have been used to image parts of the southeast Canadian margin (Fig. 1.2). The UK surface-towed GLORIA, with a 20-30 km swath and 10 m^2 resolution, has been run on parts of the Scotian Slope and Rise (Hill, 1984; Hughes Clarke et al., 1992). The US deep-towed SeaMARC I, with a 5 km swath and 5 m^2 pixel, was used on the central Scotian Slope near the Shelburne, Albatross, Acadia and Shubenacadie wells (Piper et al., 1985a; Piper and Sparkes, 1987; Shor and Piper, 1989). The similar Canadian SEAMOR system was used on the central Scotian Slope near the Shubenacadie well (Hutchins et al., 1985). The French SAR system, with a 1 km swath and 1 m^2 pixel, was used on the central Scotian Slope (Baltzer et al. 1994). The shorter swath systems use higher frequencies and thus image near surface sediment; GLORIA appears to image sediment at depths of several metres below the seabed.

Deep-towed sidescan vehicles have been used as platforms for near-bottom acoustic profiling systems. For a variety of technical reasons, such systems are typically restricted to pinger-type 2-4 kHz sounders with limited penetration and resolution. The SEAMOR system used a Huntec boomer source; some SeaMARC I tracks used an experimental Chirp sonar source. Such deep-towed profilers provide improved spatial resolution compared with surface-towed systems, but have limited penetration. The GSC has recently experimented with acquiring seismic data using a surface source and a deep-towed hydrophone array (Piper 1999).

Most surface seismic profiling has been carried out with a single channel analogue seismic system with a 40 cu. in. airgun source and a 100 ft SE 24 hydrophone streamer (Fig. 1.3). Some data were collected with similar sleeve gun and water gun sources. In 1981, the airgun source was used to acquire 1350 line km of multichannel seismic data from St Pierre Slope and the central Scotian Slope; in addition, some comparable well-site survey multichannel seismic is available. Ship-mounted 3.5 kHz profiles have been routinely collected since 1988; prior to that some towed 3.5 kHz data were acquired. A few Huntec boomer profiles have been collected.

Coring has been carried out principally by piston corer (Fig. 1.4); prior to 1987 using a 13 m barrel and 1000 kg head; since that time with the Long Coring Facility (LCF) using 17 or 20 m barrel and 1400 kg head (Moran et al., 1989). Measurements of shear strength (with a vane device), bulk density, water content and acoustic velocity have been made routinely on most cores collected since 1986. Samples for consolidation testing have been taken from some piston cores (Marsters, 1986). In situ measurements of the upper 2 m of sediment have been made with a cone penetrometer on the IFREMER module géotechnique. In situ pore-pressure measurements have been made with Lancelot on St Pierre Slope (Christian and Heffler, 1993). Direct sea-floor observations have been made with the submersible Pisces IV (Fig. 1.4). These proved invaluable in providing

ground-truth for interpretations made from sidescan sonar imagery. The submersible also provided a means of precise sampling in areas of complex geology.

A chronological framework is provided by AMS radiocarbon dating on molluscs from the mid slope (Table 1.4). Some pelecypod samples with paired valves appear to be in life position, but in most cores the only datable material is single pelecypod valves or gastropods, which may not necessarily be in life position. Nevertheless, in sediments with accumulation rates of >1 mm/a, dating of a series of molluscs by Bonifay and Piper (1988) and unpublished data shows that radiocarbon dates give an internally consistent down-core chronology and that lithologic correlations between adjacent cores are also consistent with the radiocarbon chronology. This suggests that there is little reworking of old shell material in high sedimentation rate sequences. Bioturbation, however, may give depth uncertainties of tens of centimetres.

Few measurements of the mechanical properties of sediments have been made on the Scotian margin. Conventional shear vane, water content and bulk density measurements are available for some piston cores (<10 m penetration) from the Scotian margin: some results are presented by Mosher (1986), Berry (1992), Mulder et al. (1997) and in cruise reports for HU88-010, 90-015 and 91-020. Similar data on the Grand Banks margin are reported by Marsters (1988). Interpretations of the data are made by Mosher et al. (1994), who used average undrained shear strength and bulk density profiles to perform an infinite slope analysis. Mulder et al. (1997) used similar measurements on debris flow deposits near the Albatross well site to calculate the degree of overconsolidation and hence the depth of failure in the source area. Baltzer et al. (1994) made in situ measurements with a 2-m piezocone penetrometer and obtained more precise shear strength data that confirms measurements made on cores and showed that the upper 1.5 m of sediment had an apparent overconsolidation as a result of biogenic processes.

1.3 **Strategy of project and purpose of this report**

The strategy of this project was to investigate three slope areas in substantial detail: these were the area around the epicentre of the 1929 earthquake, as an example of a major failure, and the two main areas of hydrocarbon drilling on the central Scotian Slope (between the Shubenacadie and Shelburne wells) and in central Flemish Pass. The results of these studies have been largely published elsewhere.

In addition, several less detailed transects were studied in order to cover the range of variation in shelf break and slope morphology and sedimentation. This report concentrates on the geology of these second level detail transects, although summaries are also provided of the three key areas. No work has been carried out on the Canadian margin off Georges Bank and Northeast Channel: there is a moratorium on hydrocarbon exploration in the area and baseline work was carried out by the US Geological Survey (e.g. O'Leary 1986). The deeper parts of the continental margin in this area were synthesised by Hughes Clarke et al. (1992).

In each transect, similar assessment is provided for: seabed morphology and bathymetry; the late Cenozoic geological framework; the surficial geology framework revealed by high-resolution seismic or 3.5 kHz profiles (typically the top 50 m of sediment); late Quaternary sedimentation as revealed by cores (Table 1.5); and a synthesis of geologic history and potential hazards.

Nomenclature of different parts of the continental slope has been standardised as far as is possible. The shelf break is the abrupt steepening at the edge of the continental shelf, occurring at 80-200 m in most areas (Table 1.2), but as deep as 380 m in Laurentian Channel. In most areas the upper slope has a convex-up profile and its lower limit is marked by an abrupt steepening marking the heads of gullies or sediment slides. The mid-slope zone commonly has much small-scale morphologic irregularity and seismic reflection profiles indicate that much of the seabed is erosional. On the lower slope, the morphology is less irregular and a greater proportion of the seabed shows continuous deposition in seismic profiles. The transition to the continental rise is marked by an abrupt decrease in gradient.

1.4 **Acknowledgments**

This report has been written by D.J.W. Piper, relying in part on data and internal reports prepared by other contributors. Not all contributors have had the opportunity to review the relevant parts of the manuscript, and may not necessarily agree with all aspects of this report. In addition, many colleagues with whom I have published joint papers have contributed to the development of ideas concerning the southeast Canadian slope: I particularly thank Harold Christian, Mike Gipp, Phil Hill, John Hughes Clarke, Kate Moran, Peta Mudie, Bill Normark, Chris Pereira and Sandy Shor. The figures have been largely prepared by Doris Fox, Adam Macdonald, and principally Ernest Douglas. I thank Calvin Campbell for editorial assistance.

This project has received help from a variety of petroleum companies and consulting companies, mostly in the provision of additional data: I thank Shell, Husky, and Geomarine Associates for their support in the 1980's and Mobil, Imperial, Exxon, Shell, Marathon, Pan-Canadian and Chevron for recent assistance. COGLA and its successor in the Canada-Nova Scotia Offshore Petroleum Board have provided access to data filed with them. In addition to dedicated cruises, the project has benefited from several cruises of opportunity: I thank senior scientists Ian Reid, Russ Parrott, Chris Pereira, Keith Manchester, and Larry Mayer. I also thank the Masters, officers and crew of CSS Hudson and CSS Dawson; Keith Manchester, Mike Gorveatt and the GSCA Technical Support Group; and all other shipboard colleagues who contributed to the collection of data at sea.

Table 1.1. Late Cenozoic stratigraphic markers used in this report

Reflector name	*Regional reflector*[2]	*Probable age*[1]
Light Red	A	
Light Yellow		
Brown		
Carmine	B	middle Pleistocene
Gold		
Rose		
Grey	C	basal Pleistocene
Magenta		
Blue		
Red	D	
Lavender	E	middle Pliocene
Orange		
Pink		basal Pliocene
Canary	F	early Miocene (deep water)
		Miocene/Eocene unconformity (shallow water)

[1] Ages based on Shubenacadie H-100, except for Grey, which is based on Acadia K-62

[2] Regional reflectors correspond approximately to the scheme of Piper and Normark (1989)

Table 1.2. Regional variation in slope gradient and depth of shelf break

Transect	**Shelf break** (mbsl)	**Upper slope Gradient**	**Heads of gullies** (mbsl)	**Mid slope Gradient**	**Lower slope Gradient**	**Upper rise Gradient**
Browns Bank	130-150	3.3°	300	3.8°	1.4°	1.0°
West La Have Basin	120-130	2.7°	500	2.5°	1.4°	1.1°
East La Have/ Emerald basins	150-180	3.1°	500	2.3°	1.4°	1.0°
Emerald Bank	110-120	7.4°	500	11°	1.5°	1.0°
Western Bank	110-120	1.3°	300	3.0°	2.2°	1.3°
Sable Island Bank	110-120	1.1°	300	5.0°	4.5°	1.1°
Banquereau	100-110	1.3°	500	5.2°	2.9°	1.4°

Table 1.3. Summary of cruises on which geological data has been acquired on the continental slope, with information on equipment used.

Cruise	Transects off	Principal operations
81050	Emerald Basin	Submersible dives
81044	Sable Bank Western Bank Emerald Basin	High resolution multichannel seismic
82014	Emerald Basin Western Bank	SeaMARC
83012	Emerald Basin	Piston cores, NSRF v-fin sparker
84044	Emerald Bank	SeaMARC, 40 cu in airgun, Chirp
85001	Emerald Bank	40 cu in airgun
86034	Banquereau Emerald Bank	Piston cores, Huntec DTS, 40 cu in airgun
87003	Sable Bank	Piston cores, Huntec DTS, 40 cu in airgun
88010	Sable Bank Western Bank Emerald Bank	Piston cores, Huntec DTS, 40 cu in airgun
90002	La Have Basin	Piston cores, 3.5 kHz, 40 cu in airgun
90015	Western Bank Emerald Bank	SAR, geotechnical module, piston cores, 3.5 kHz 40 cu in airgun
91020	Emerald Bank	Piston cores, 3.5 kHz, 40 cu in airgun
92003	Western Bank	Piston cores, 3.5 kHz, 40 cu in airgun
92052	Banquereau Sable Island Bank	Piston cores, 3.5 kHz, 40 cu in airgun
93026	Western Bank Emerald Basin	Piston cores, 3.5 kHz, 40 cu in airgun
95033B	Banquereau	Piston cores, 3.5 kHz, 40 cu in airgun
96029	Banquereau	3.5 kHz, 40 cu in airgun
98039	Sable Island Bank to Emerald Basin	3.5 kHz, 40 cu in airgun
99036	Sable Island Bank to Emerald Basin	Piston cores, 3.5 kHz, 40 cu in airgun, Excalibur Huntec DTS sparker

Table 1.4. New radiocarbon dates from the continental slope.

Core	Depth	Material	Age[1]	Lab No	Notes
Slope off Browns Bank					
90002-001	157	*Nuculana pernula* (pv)	13120 ± 90	TO-2389	
90002-001	316	*Colus togatus*	13380 ± 110	TO-2388	
Slope off La Have Bank					
90002-004	19	*Lischkeia ottoi*	2760 ± 60	TO-2450	
90002-004TW	48	*Bathyarca raridentata* (v)	10790 ± 90	TO-2033	
90002-004	109	*Yoldia thraceiaeformis* (v)	13190 ± 110	TO-2034	
90002-004	118	*Yoldia thraceiaeformis* (v)	13350 ± 160	TO-2035	
90002-004	263	*Tachyrhynchus erosus*	14240 ± 120	TO-2036	
90002-004	580	echinoid fragments	14350 ± 120	TO-2037	
80004-020	280	bivalve fragments	28100 ± 240	TO-6462	
80004-020	88	gastropod fragments	12490 ± 90	TO-3851	
81006-010	113	mollusc fragments	32950 ± 350	TO-6463	
90015-022	91	*Nuculana pernula* (v)	14100 ± 90	TO 2383	
Slope off Emerald Bank					
86034-36	256	*Macoma* sp. fragments	14270 ± 90	TO-5071	
86034-041	218	*Dentalium entale stimpsoni*	13280 ± 100	Beta 34305 ETH 6057	
86034-041	623	*Neptunea* sp.	16050 ± 220	TO-2387	
86034-040	690	*Portlandia arctica* (pv)	18700 ± 300	Beta 20733 ETH 2995	
90015-019	290	pelecypod fragments	12470 ± 100	TO-2084	
90015-019	600	*Dentalium entale stimpsoni*	13350 ± 110	TO-2085	
78005-42	55-65	bulk foraminifers	9750 ± 70	TO-5842	
78005-42	202-206	bulk foraminifers	12600 ± 80	TO-5843	
90015-018	90	*Lunatia heros*	9610 ± 80	TO-2390	
90015-018	49	carbonate fragments	7620 ± 80	TO-4484	
90015-018	110	*Nuculana* sp. valve	10860 ± 110	TO-4482	
90015-018	137	*Nuculana* sp. valves	10670 ± 90	TO-4483	
91020-013	680	bulk foraminifers	20910 ± 160	TO-3323	continental rise
Slope off Western Bank					
78005-077	58	shell material (small sample)	5050 ± 300	GX-7737	conventional age
78005-077	31	*Apporhais occidentalis*	8870 ± 80	TO-2451	
78005-077	42	*Pecten* sp.	10300 ± 160	TO-2452	
78005-077	68	*Nuculana tenuisulcata* (v)	10500 ± 80	TO-2453	
78005-077	75	*Dentalium entale stimpsoni*	11350 ± 90	TO-2454	
78005-077	102	*Astarte undata* (v)	13030 ± 100	TO-2455	
82004-01	490	*Aporrhais occidentalis*	12020 ± 1320	Beta-6283 (conventional age)	
82004-01	145	Aspodont pelecypod indet.	14900 ± 310	Beta-10988	
82004-01	308	*Astarte undata*	16100 ± 310	Beta-10989	
82004-02	84	*Propebela turricula*	13140 ± 195	Beta 15242	
82004-02	221	*Macoma* cf. *brevifrons*	14150 ± 250	Beta-15243	
82004-02	320	*Astarte undata*	14410 ± 205	Beta-15244	
82004-02	659	*?Colus spitsbergensis*	18320 ± 440	Beta-15245	
82004-02	75	*Nautica clausa*	15100 ± 310	Beta-10987	

[1] all ages expressed in radiocarbon years with no marine reservoir correction

90015-017	131	mollusc fragments	20780 ± 170	TO-2088	
82004-007	222	gastropod fragments	10840 ± 80	TO-5077	in DF0
82004-004	91	mollusc fragments	15830 ± 10	TO-5078	in DF3
82004-011	163	*Oenopota turriculata* (gastropod)	12330 ± 90	TO-5568	just above DF1
83012-6	445-448	*N. pachyderma* forams	36420 ± 420	TO-7747	
Slope off Sable Island Bank					
87003-007TW	78	*Colus obesus*	8200 ± 90	TO-4956	
87003-007	290-300	bulk foraminifers	9830 ± 70	TO-5844	
87003-007	343	unidentified mollusc frags.	10350 ± 300	TO-2386	
87003-007	442	bulk foraminifers	10770 ± 250	TO-2385	
87003-007	517-525	bulk foraminifers	11550 ± 100	TO-5845	
87003-007	715	*Mya truncata* fragment	14630 ± 100	TO-2384	
Slope off Banquereau					
86034-016TW	49	mollusc fragments	39290 ± 550	TO-4485	
86034-016TW	95	*Nuculana pernula* (pv)	15150 ± 120	Beta 28269 ETH 4720	
86034-016	442	*Aclis velleri*	15910 ± 130	Beta 28268 ETH 4265	
86034-016	630	*Nuculana pernula* (pv)	16480 ± 130	Beta 28270 ETH 4721	

pv = paired valve; v = single valve
All determinations by AMS except as noted

Table 1.5. Summary of sediment facies described from cores

Facies A: olive to olive-grey bioturbated sediment
1) silty mud to mud with rare or no IRD.
2) silty mud to mud with abundant IRD.
3) sandy muds to muddy sands.

Facies B: silty to sandy brownish muds with varying amounts IRD
1) brown with silty laminae (?destroyed by bioturbation) and/or dark (black) mottles.
2) reddish-brown sediment.

Facies C: thinly bedded marker mud beds
1) brick-red sandy mud beds
2) light grey silty mud to mud; generally having little sand; carbonate rich.
3) dark grey to greyish black mud

Facies D: coarse grained facies, with varying amounts of interbedded mud, various colours.
1) sand and sand-mud turbidites
2) coarse-grained debris flows
3) winnowed sands and gravels.

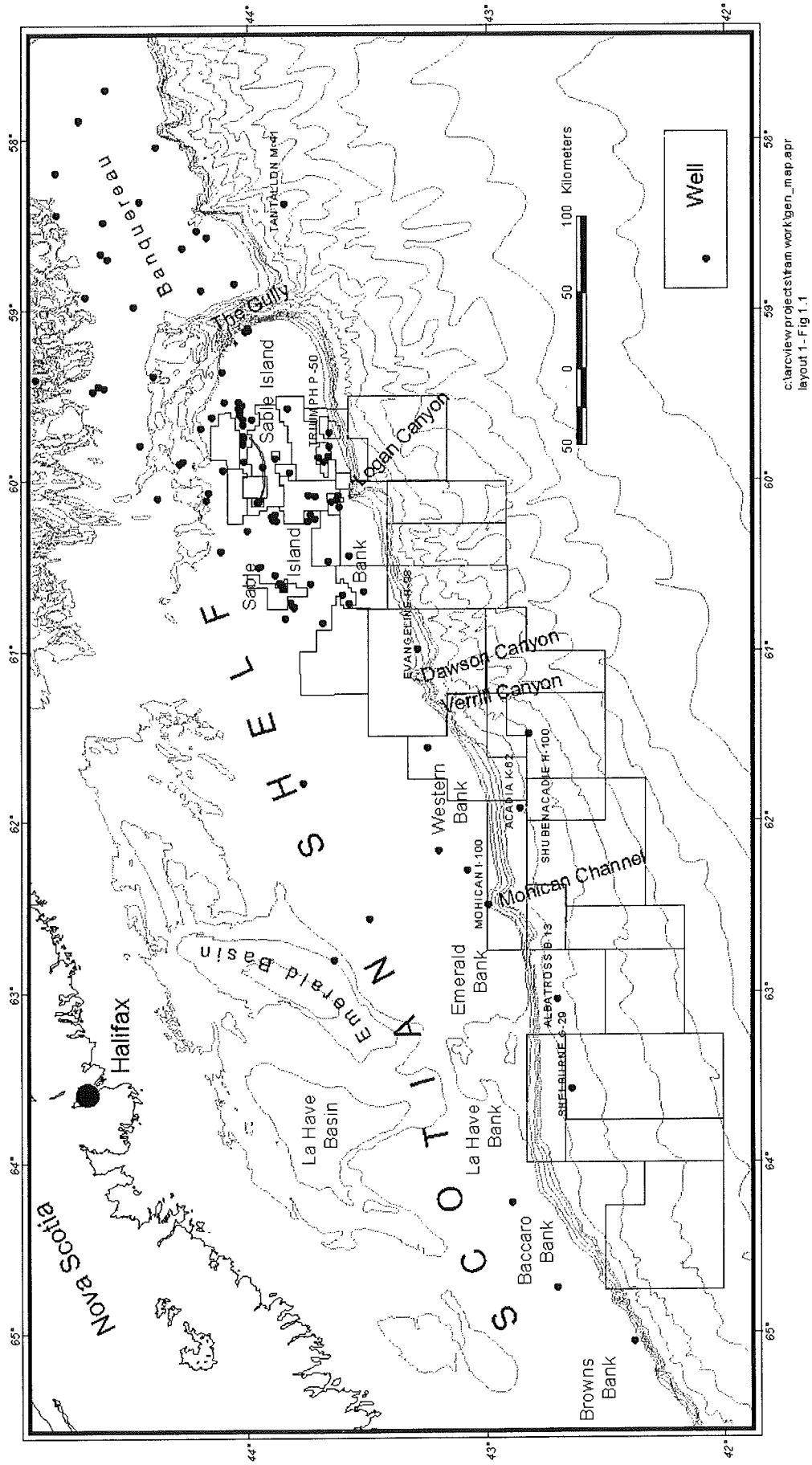

Fig. 1.1: General map of the Scotian margin showing current lease blocks and deep-water wells.

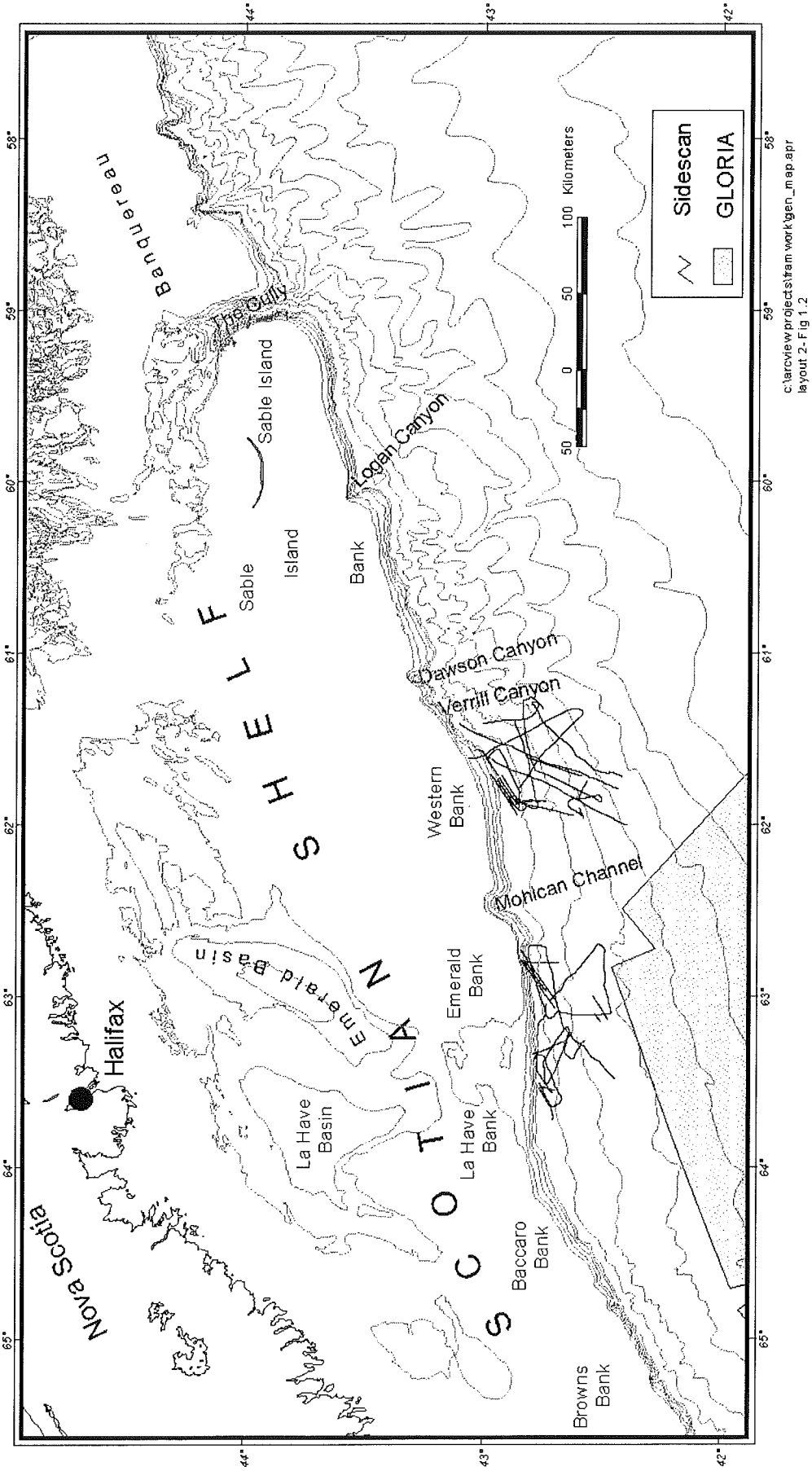

Fig. 1.2: Map showing distribution of sidescan and Seabeam surveys on the Scotian margin.

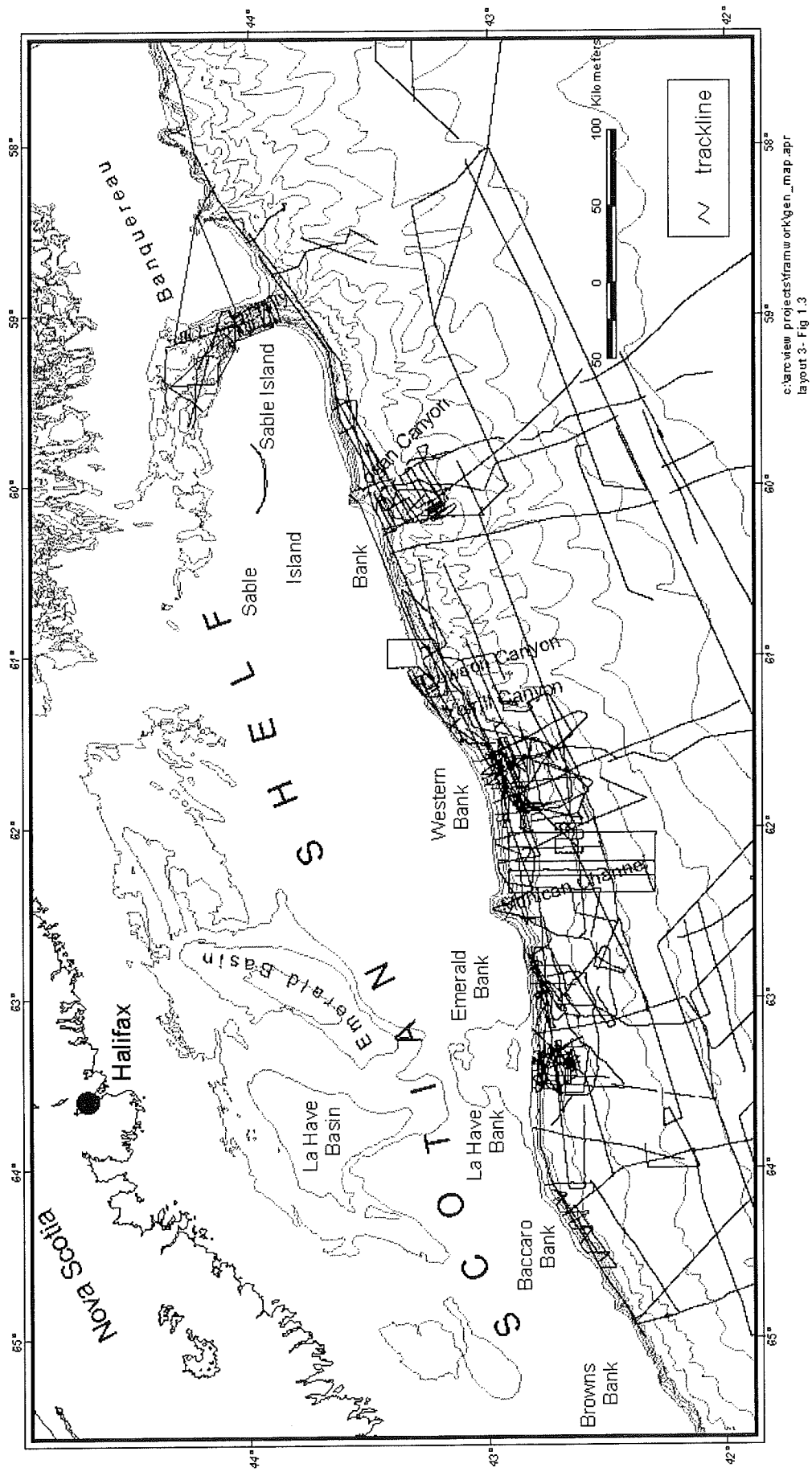

Fig. 1.3: Map showing seismic profile tracklines on the Scotian margin (small airgun and higher resolution profiles only).

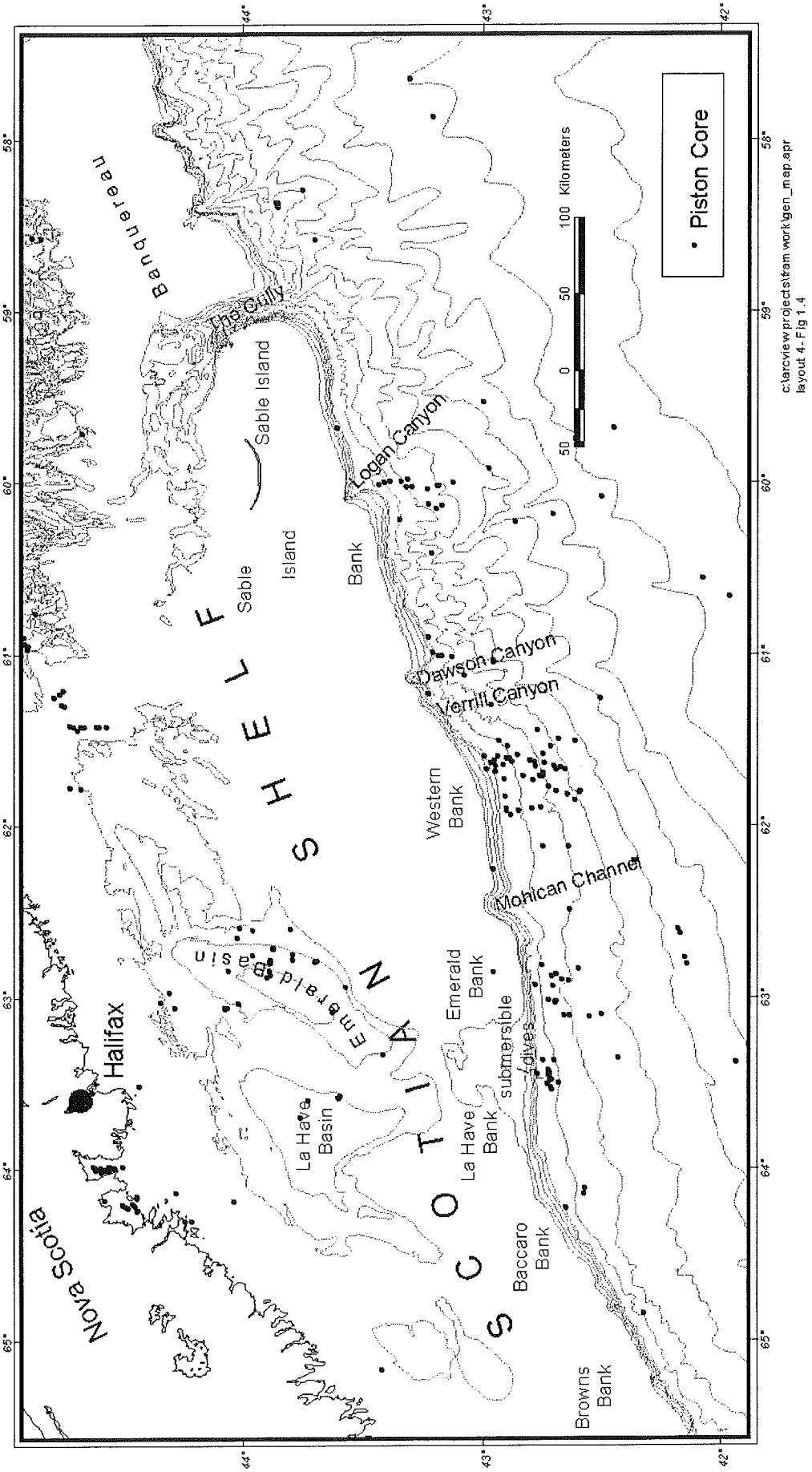

Fig. 1.4: Map showing piston cores and submersible dives on the Scotian margin.

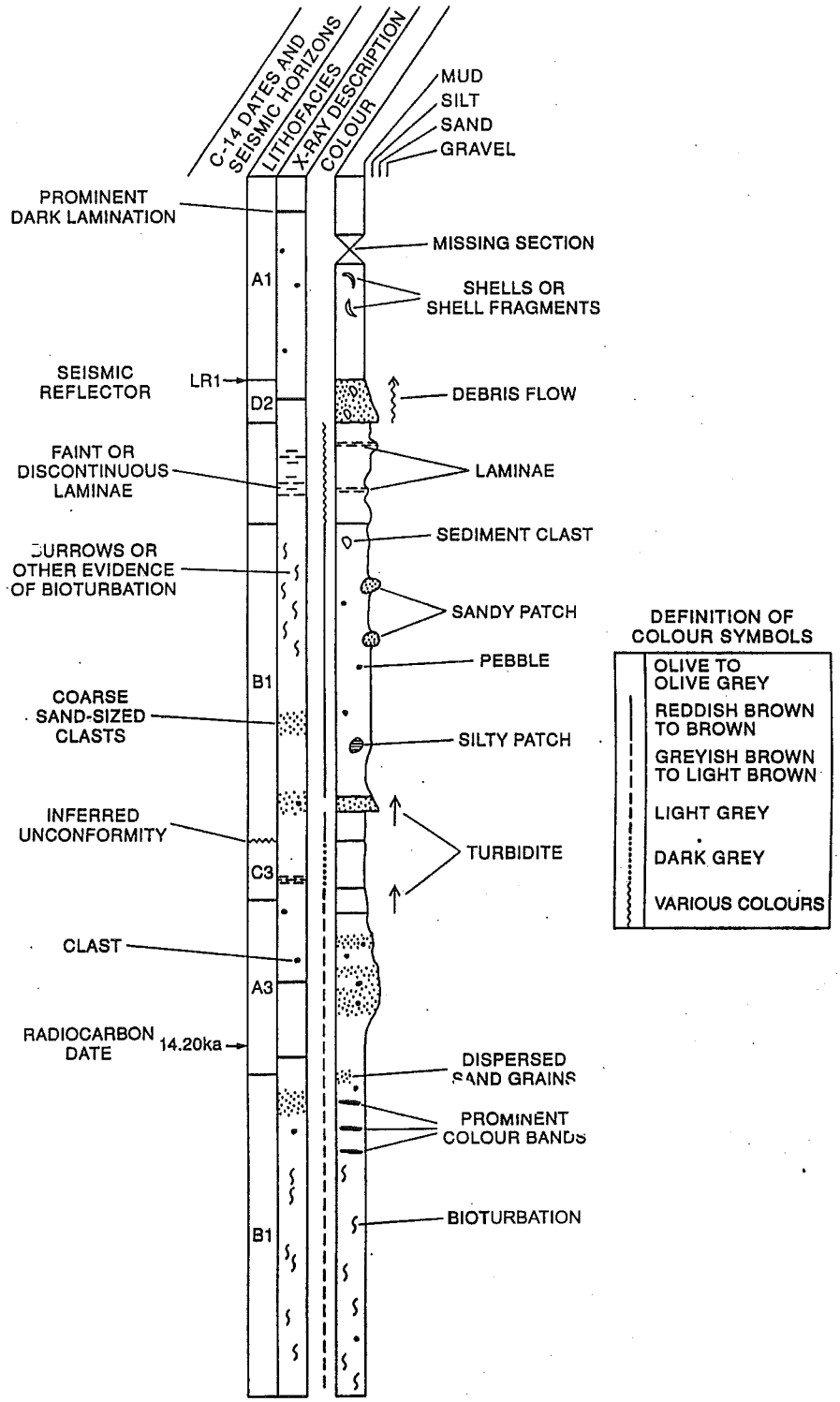

Fig. 1.5. Legend to core descriptions. Note that the distribution of clasts is most accurately shown by X-radiographs: clasts in the lithology column are shown conventionally.

2. Late Cenozoic geological framework

2.1 Introduction

The general late Cenozoic architecture of the southeastern Canadian margin was synthesised by Piper and Normark (1990). They suggested that several marker horizons could be recognised in places as disparate as Flemish Pass, St Pierre Slope and the central Scotian Slope. Reflector E marks a sea-level lowstand in the middle Pliocene, with valley cutting on the slope, followed by a return to draped even sedimentation on the continental slope during the succeeding highstand. The early Pleistocene lowstand of sealevel (reflector C) was marked by widespread gullying and in many parts of the continental margin, these gullies persisted through the Quaternary. Reflector B marked a pronounced change in the style of slope sedimentation associated with the onset of shelf-crossing glaciation in the middle Pleistocene (Piper et al. 1994).

2.2 Geological framework of the western Scotian Slope

The late Cenozoic geological framework of the Shubenacadie H-100 and Acadia K-62 area was interpreted by Piper et al. (1987), with modifications by Piper and Normark (1989) and Piper and Sparkes (1990) and is summarized here (see also Table 1.1). A prominent Oligocene or earliest Miocene reflector, identified as "canary" or F[1] by Piper and Sparkes (1990) occurs about 0.8 secs subbottom beneath the lower slope, and is deformed by large deep-rooted salt diapirs near the 3000 m isobath (Jansa and Wade, 1975). It rises toward the seabed on the upper slope, marking a major slope unconformity against which Neogene and Quaternary reflectors onlap. This unconformity marks the base of the section examined in this report.

The type seismic section for reflectors above F is defined in the vicinity of the Acadia K-62 well on lines HU85001 and DW81044-44 (Fig. 3), and is based on the stratigraphic scheme described by Piper et al. (1987) and Piper and Sparkes (1990). A series of key reflectors are defined in Fig. 4. These key reflectors have been chosen where there is an abrupt change in seismic character that can be traced over a large area, and at unconformities. Piper and Sparkes (1990) defined reflectors near the Acadia K-62 well (Table 1.1; Fig. 2.2) named red, blue, magenta, grey, rose, flesh, carmine, brown, and light red. Deeper reflectors canary, pink, orange and lavender were defined near the Shubenacadie H-100 well (Fig. 2.3). A general correlation with the stratigraphic scheme of Piper and Normark (1989) is that lavender = E, red = D, grey = C and carmine = B. These letter designations are used in this report, except where detail requires the use of the colour designations. In general, Quaternary and Neogene strata successively onlap older Tertiary strata on the continental slope. With

[1] Note that Piper and Normark tentatively suggested that F was of late Miocene age. In the scheme used in this report, the pink reflector is of late Miocene-early Pliocene age and F is older.

low frequency seismic profiles, it is difficult to correlate strata along strike near onlap pinchouts, and few deeper water strike lines are available. The deepest reflectors pink and lavender can be traced across the whole area in deep water, but onlap the F unconformity on the upper slope. Shallower reflectors grey, carmine and A are cut out in places by erosion.

The best biostratigraphic control is provided by the Acadia K-62 and Shubenacadie H-100 wells, as summarised by Piper et al. (1987) and Swift (1987). The Albatross B-13 and Shelburne G-29 wells provide additional control for the deeper part of the section. The grey reflector corresponds to the probable base of the Pleistocene in the Acadia well (Piper et al., 1987).

In the Shubenacadie H-100 well, the shallowest samples at 2140 m RT (corresponding approximately to red) are of mid to Late Pliocene age (foraminifera zones N19-N21: Gradstein in Piper et al., 1987). Definite mid Pliocene faunas (N19-N20) occur at 2300 m, corresponding approximately to the lavender reflector. The pink reflector corresponds to the Pliocene - Miocene unconformity in the Shubenacadie H-100 well and the canary reflector corresponds to a horizon at or just above the Miocene - Eocene unconformity in the well (Swift, 1987).

The grid of 1980's industry multichannel seismic data around the Shubenacadie H-100 well has been integrated with published work by Piper et al. (1987). The basic stratigraphy is illustrated in Figure 2.3. Between the seabed and the carmine reflector, reflectors are subparallel and continuous, but the unit thins to 40% between 650 and 1700 m water depth. The interval from carmine to grey is also characterised by parallel continuous reflectors, but this unit shows a reduction to only 75% of upslope thickness over the same depth range. Immediately below grey is a series of shallow erosive gullies, better defined on single channel 40 cu. in. airgun data (e.g. Fig. 6.8) as channels 40 ms deep and up to 4 km wide.

The interval from grey to red is characterised by high amplitude continuous parallel reflectors. Immediately below red are weak continuous reflections, but most of the sequence below this to lavender consists of short, discontinuous, shingled or scour-and-fill type reflectors. Indeed, lavender cannot be traced as a single reflector, but rather consists of a series of short reflectors. This irregular reflector character may in places extend down to the orange reflector. Over much of the area, the interval between orange and canary consists of fairly continuous subparallel reflectors. More detailed examination, however, shows that there is substantial variation in reflector amplitude, both along strike and down dip. In many areas of higher amplitude, the pink reflector is clearly a planar unconformity surface, with local toplap. The canary reflector (F) is a high-amplitude reflection from where it onlaps the Miocene/Eocene unconformity downdip for about 10 km, where it abruptly decreases in amplitude.

Swift (1987) interpreted the canary disconformity in the vicinity of the Shubenacadie well as resulting from bottom current erosion. The Late Miocene to Early Pliocene age of the canary, pink and orange

disconformities corresponds to a time of strong bottom current erosion and redeposition on the continental margin of Eastern North America (Mountain and Tucholke, 1985; Myers and Piper, 1988). It is therefore possible that some of the "channel" features visible in this interval might be related to bottom current erosion. The location of erosion in dip lines at the "orange" reflector close to the break in paleoslope where orange onlaps the mid-Tertiary unconformity is a feature that would be expected from bottom current erosion. However, the steep channel margins seen in some profiles[1] suggests that the channel erosion was due to downslope processes, although subsequent filling might be the result of bottom current sediment deposition. Downslope channels cut winnowed bottom current deposits in several places on the Canadian margin: for example, on the Labrador Slope (Carter and Schafer, 1983; Myers and Piper, 1988) and at Titanic Canyon (Cochonat et al., 1991). However, no constructional features related to bottom current deposition have been recognised in the seismic reflection profiles.

Piper and Sparkes (1990) reported isopachs on the principal Pliocene and Quaternary sediment intervals in a series of 1:250 000 maps of the central Scotian Slope. These isopachs are shown in Figures 2.4 to 2.7.

2.3 **Geological framework of the Eastern Scotian Slope**

The geological framework on the eastern Scotian slope is difficult to interpret because the late Cenozoic part of the seismic section is obscured by casing in wells and is severely dissected. Piper and Normark (1989) correlated an early Pliocene marker from the Triumph P-50 well downslope to an erosional event on the middle slope (E) off Sable Island Bank (e.g., Figs. 7.4, 7.5). Higher in the mid-slope section, the reflector at the top of a draping unit (D) and an irregular reflector marking the beginning of pronounced levee growth (C) were correlated on the basis of reflector character with similar reflectors in the Shubenacadie H-100 area and on St Pierre Slope. Reflector carmine represents the base of the well-stratified section on the upper slope west of Logan Canyon and is overlain by a thick, generally acoustically incoherent section. Skene (1994) extended this regional correlation along the upper continental slope between Logan Canyon and Banquereau, largely on the basis of the distinctive character of the grey reflector.

2.4 **Correlation with the Scotian Rise**

Correlation of slope failures with deposits on the continental rise is important because deposits on the rise provide information about the scale and timing of failures that leave little record on the slope. Such correlation is at present limited by available data. I summarize briefly the present state of knowledge.

---

[1] e.g., in line 521 (not illustrated)

There are no wells to provide an independent basis for chronostratigraphy on the rise and the salt diapirs prevent ready correlation with the continental slope (Swift, 1985). Berry and Piper (1993) established a late Cenozoic stratigraphic scheme for the area south of the Albatross debris flow, recognising nine key reflectors (A1 to A9). Reflector A9 can be tentatively correlated along industry line A160 (Fig. 2.1) to the slope, where it corresponds to a horizon just above blue, in other words of middle Pliocene age. West of this area, Mulder and Piper (in prep.) correlated a single prominent debris flow deposit that is interbedded with stratified sediment on the rise and overlies reflector A4[1] with a debris flow directly upslope on the middle continental slope west of Acadia just above grey that is also interbedded with stratified sediment. A third possible method of bringing in a stratigraphy to the rise is by seismic correlation from Laurentian Fan[2], where a middle Pliocene pick is available from outcropping mudstone (Piper and Normark, 1989).

Such correlations, if correct, are important because they show a history of debris flow deposition on the continental rise that goes back to the middle Pliocene. This means that the triggering mechanism for debris flows does not directly involve the presence of icesheets on the outer shelf, since Atlantic Canada was likely not glaciated in the Pliocene and shelf-crossing glaciations probably first occurred around isotopic stage 16 or 12 (450-650 ka) (Piper et al. 1994). We have not evaluated why some areas of the rise have abundant debris flow deposits since the Pliocene, whereas others accumulated principally stratified sediment (Fig. 2.8). We speculate that it might be related to sedimentation rates or rates of leakage of petroliferous gas; it does not appear to correlate with regional gradient.

2.5 **Late Pleistocene-Holocene stratigraphic framework revealed by piston cores**

A rather uniform Holocene - late Pleistocene lithostratigraphy is found in cores on the Scotian margin, summarized by Piper and Skene (1998).

On the Scotian margin, a distinctive lithostratigraphic sequence can be recognized (Hill, 1984; Mosher et al., 1994). This stratigraphy is described briefly here to provide a context for core descriptions in subsequent chapters. Middle to late Holocene sediment comprises foraminiferal ooze in water depths >3000 m, bioturbated olive-gray mud from 3000 to 600 m water depth, and silty sands on the upper slope. In many cores on the continental slope and rise, early Holocene and latest Pleistocene olive gray sediment is sandier and in deeper water includes sandy turbidites. It also contains scattered ice-rafted granules. The Holocene olive-grey sediment passes down into brownish and grayish sandy mud and uniform brownish muds with granules, which in turn overlie widespread red-brown clayey turbidites, in places with intercalated sands. On the Laurentian Fan, this

---

[1] 93026 JD222/2330 correlated with 88010 JD151/0700; this feature also illustrated in Fig. 4.9

[2] using seismic profiles from Skene (1998) on Laurentian Fan, then along lines HU98-039 and onto PZ93-026.

clay turbidite unit is about 10 m thick and overlies olive gray muds and sands interbedded with tan beds rich in detrital carbonate and less common brown muds.

Distinctive brick-red sandy mud beds occur within the sandy olive-gray sediment and the underlying brownish and grayish mud. These are interpreted as resulting from rapid ice-rafted transport from the Gulf of St Lawrence between 14 ka and 10 ka (Piper and Skene, 1998). In some cores, as many as four such beds are recognised, but in most cores only two beds, **b** and **d** are found. The lower bed, **d**, is commonly overlain by a light tan sandy mud bed correlated with Heinrich event 1 in the Labrador Sea, interpreted as derived from ice-rafting from Hudson Strait. Heinrich event 2 (21 ka) is recognised as a tan bed on Laurentian Fan.

Facies interpretations of the Holocene - Late Pleistocene sediment sequence have been made by Stow (1981), Hill (1984) and Mosher et al. (1994). The olive gray mud facies is hemipelagic and derived from reworking of glacial and Tertiary strata on the outer shelf. Interbedded sands and silts are principally turbidites (although some on the upper slope may result from storm reworking: Hill and Bowen (1983)) with a similar outer shelf source. Brown and gray muds and sands are interpreted as ice margin plume fall-out (uniform brown muds with granules) and turbidites (graded sands and interbedded muds) derived from ice that crossed the Scotian Shelf (Mosher et al. 1989). The distinctive red-brown clay turbidites are thickest on the Laurentian Fan and are probably associated with glacial discharge from the Gulf of St Lawrence. The facies boundaries may thus be diachronous, but are controlled overall by the retreat of glacial ice from the Scotian margin.

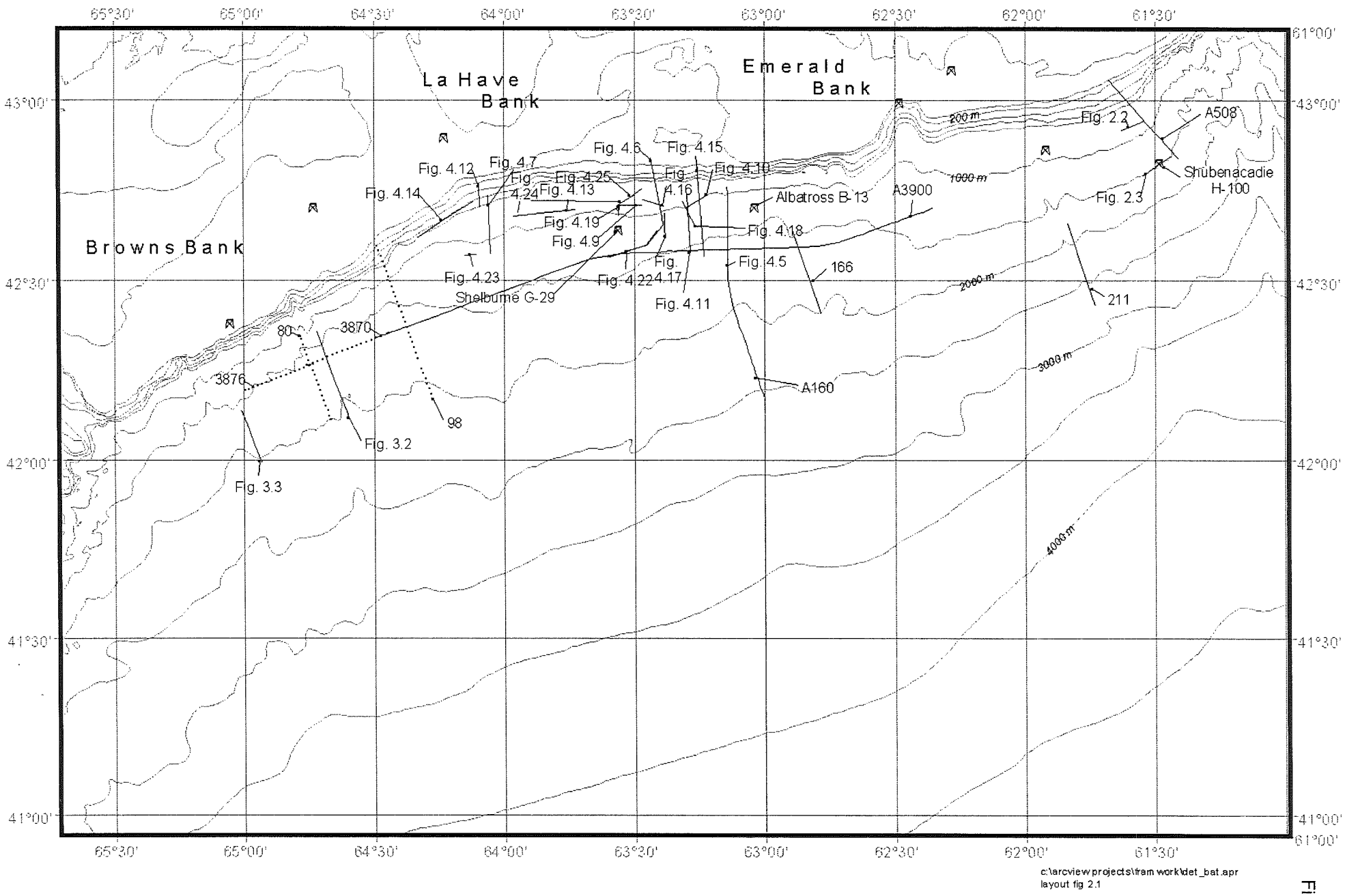

Fig. 2.1: Index map of illustrated seismic lines descibing the late Cenozoic framework of the Shubenacadie to Browns Bank area (chapters 2, 3 and 4).

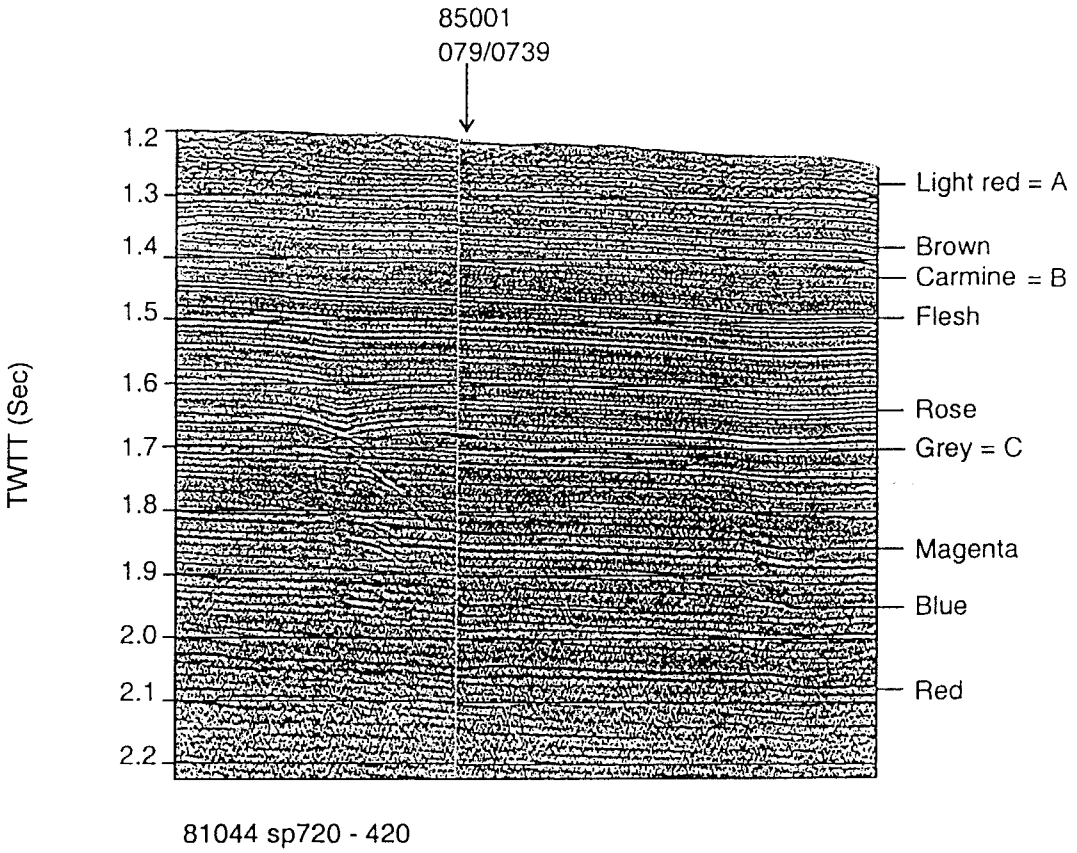

Fig. 2.2. Type section for Quaternary framework studies near the Acadia well site.

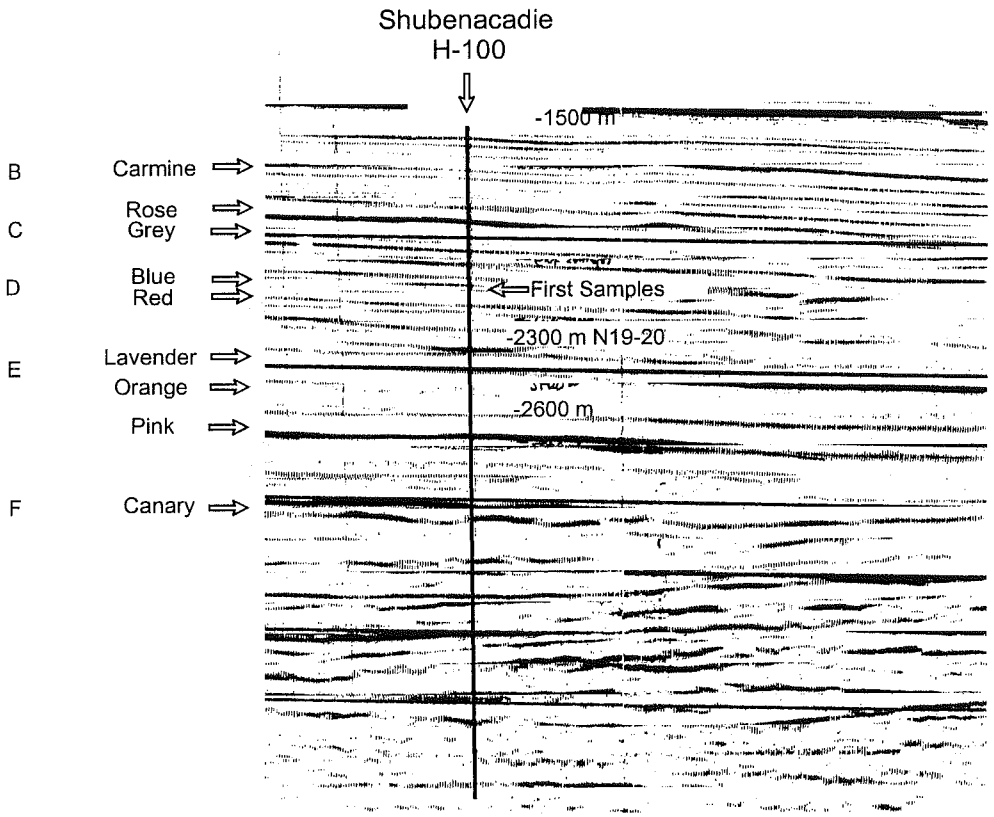

Fig. 2.3. Correlation of Shubenacadie well with adjacent seismic profile.

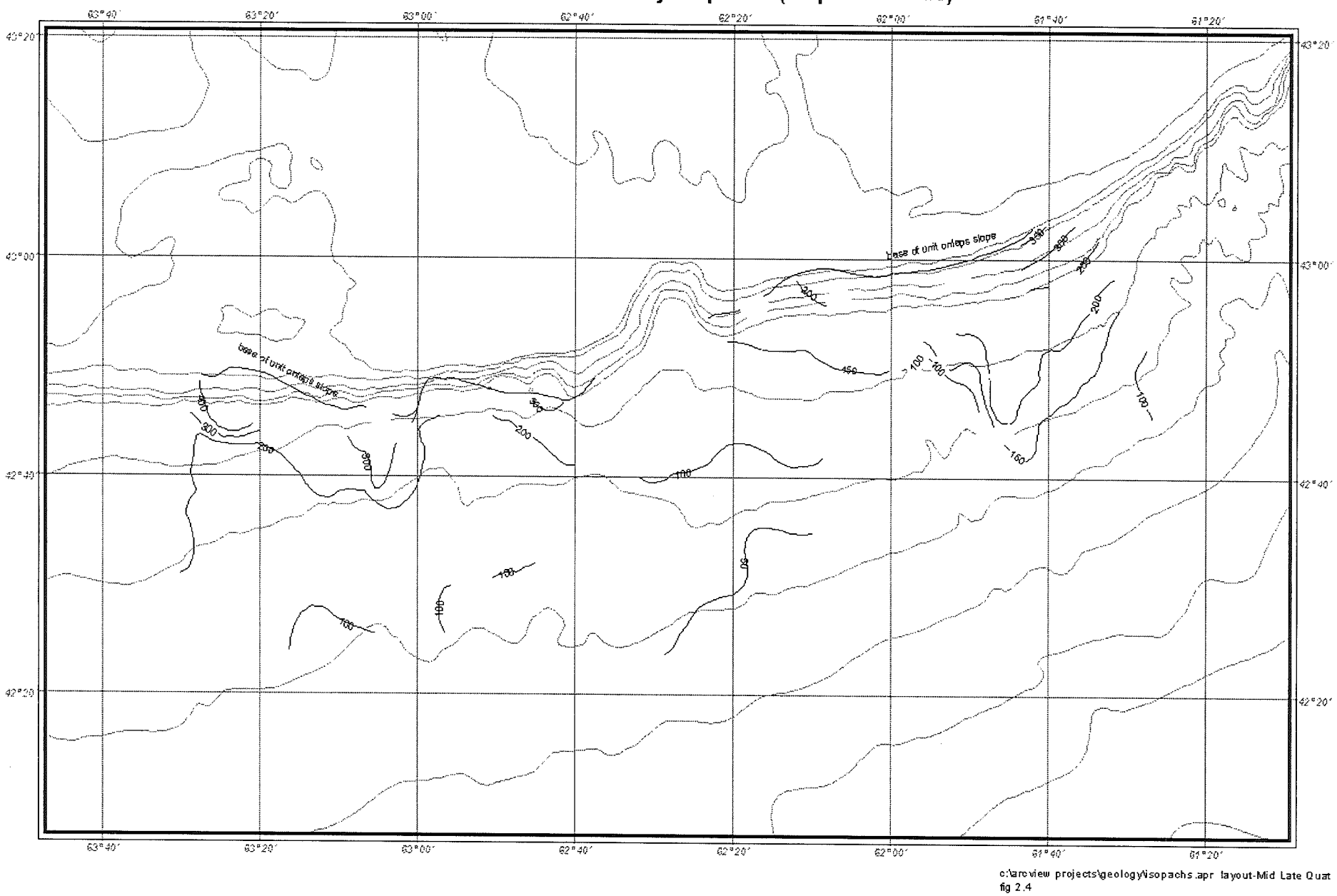

Fig. 2.4: Isopachs (in ms TWTT) of the Mid to Late Quaternary sequence, Shubenacadie to Shelburne wells (from Piper and Sparkes, 1990)

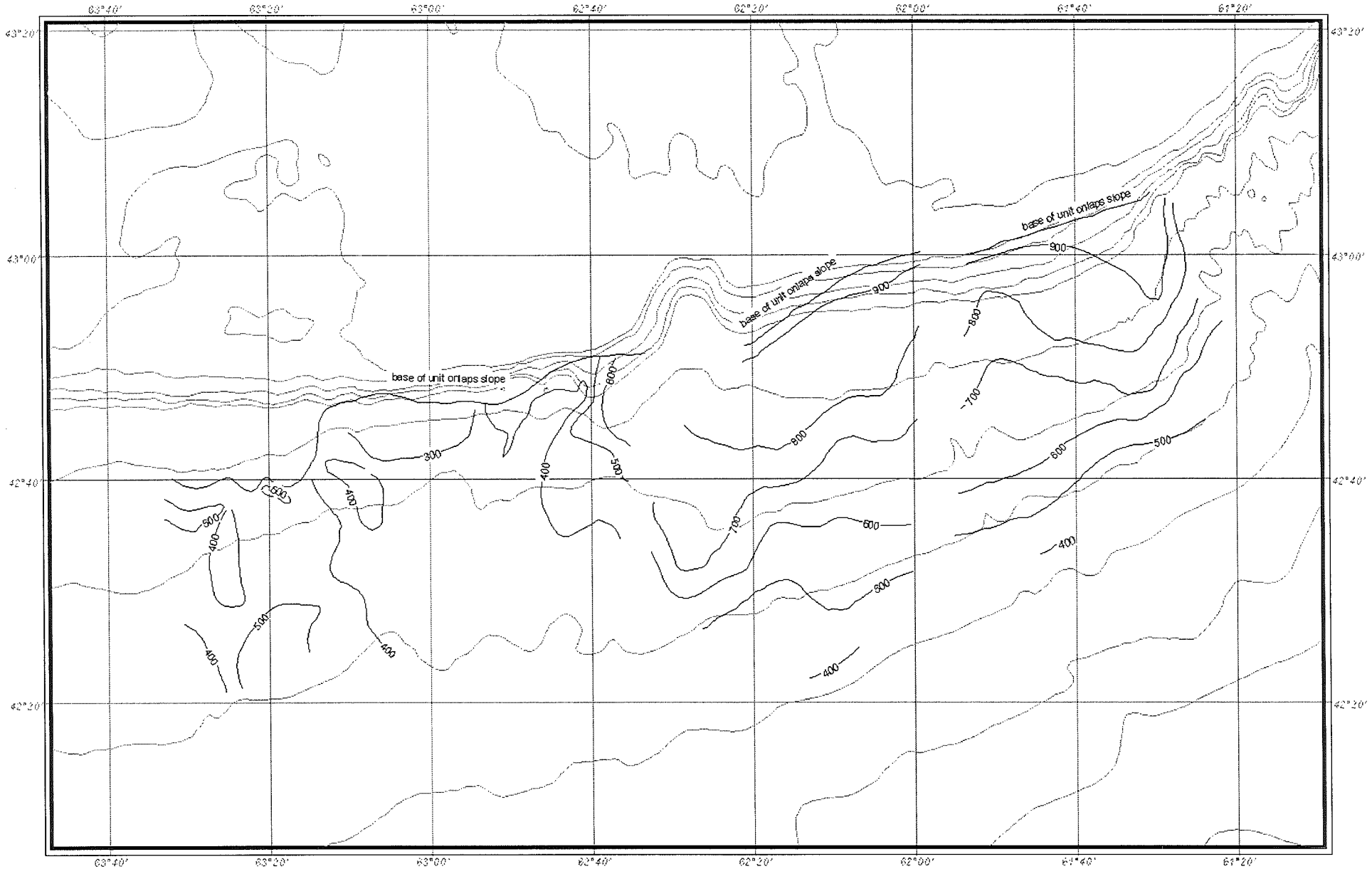

Fig. 2.5: Isopachs (in ms TWTT) of the Mid Quaternary to Mid Pliocene sequence, Shubenacadie to Shelburne wells (from Piper and Sparkes, 1990).

c:\arcview projects\geology\isopachs.apr layout Mid Quat to Mid Plio fig 2.5

Fig. 2.5

Fig 2.6

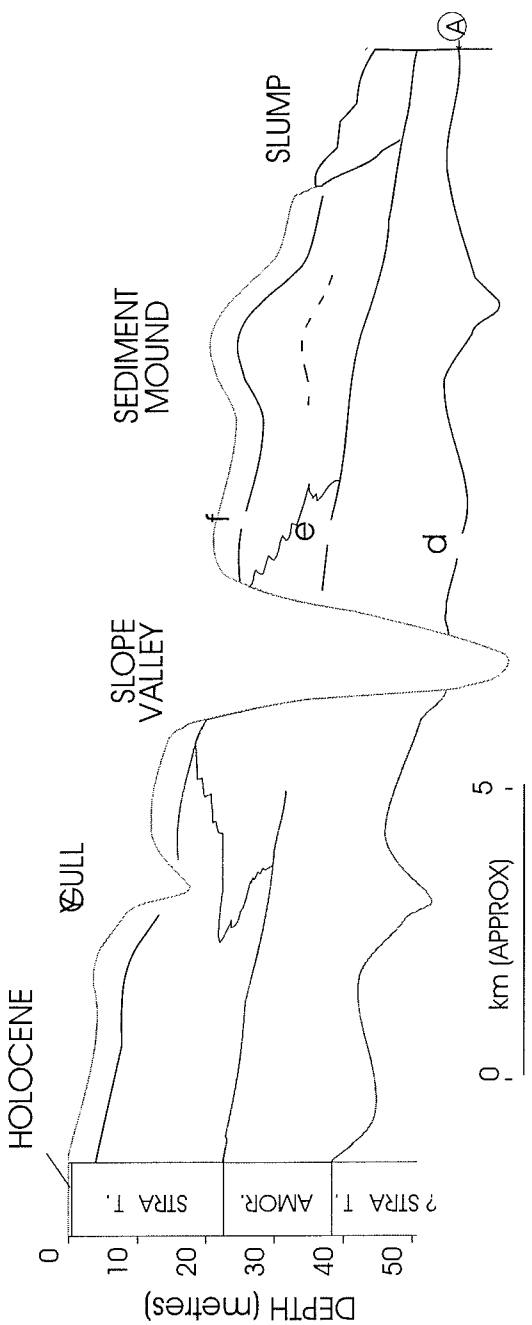

Fig. 2.6. Isopachs (in ms TWTT) of the Mid to late Pliocene sequence, Shubenacadie to Shelburne wells (from Piper and Sparkes, 1990)

C:/IErnest/revised/fig2_6.cdr

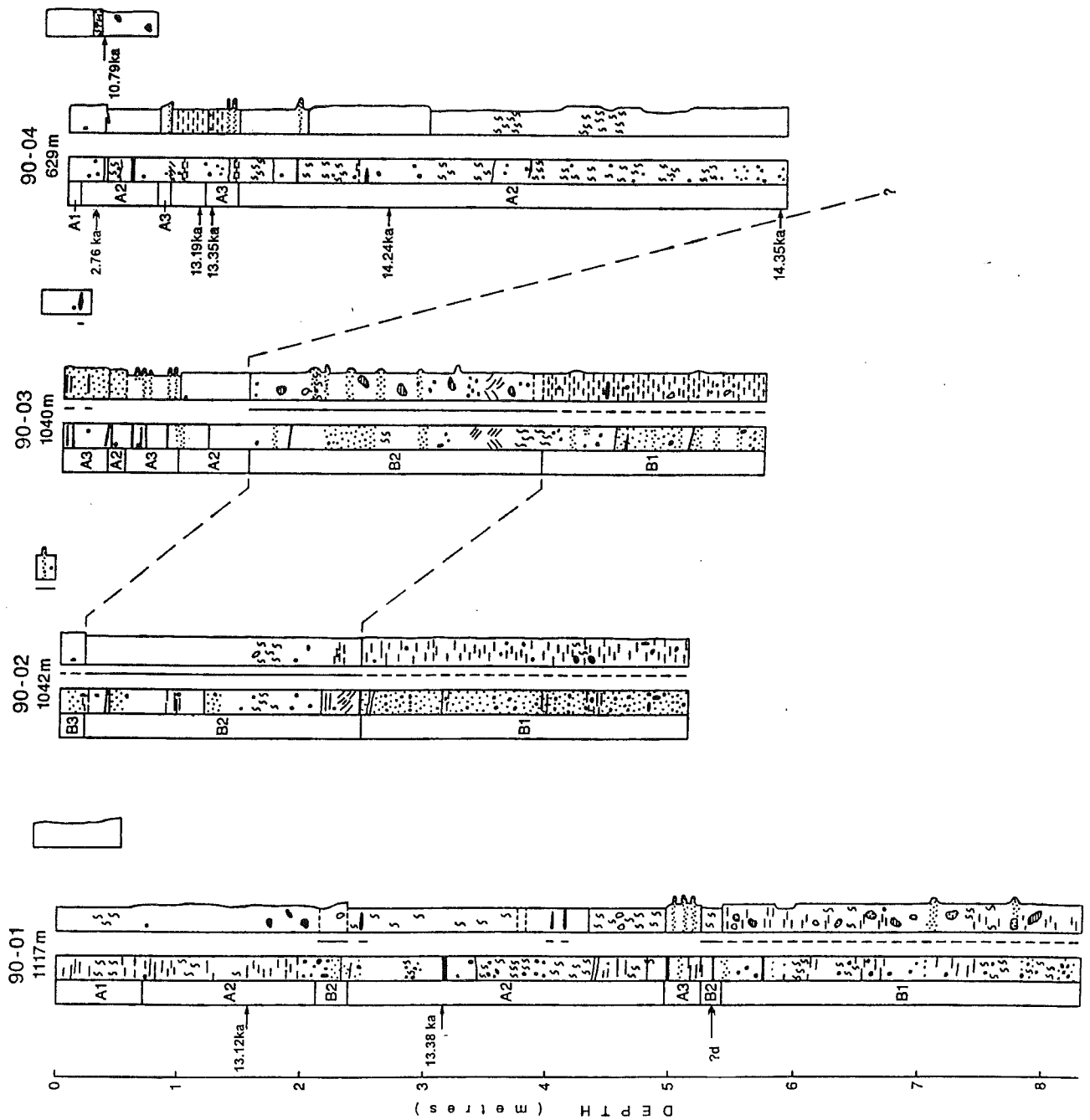

Fig. 2.7. Depth to early Miocene surface (in ms TWTT), Shubenacadie to Shelburne wells (from Piper and Sparkes, 1990).

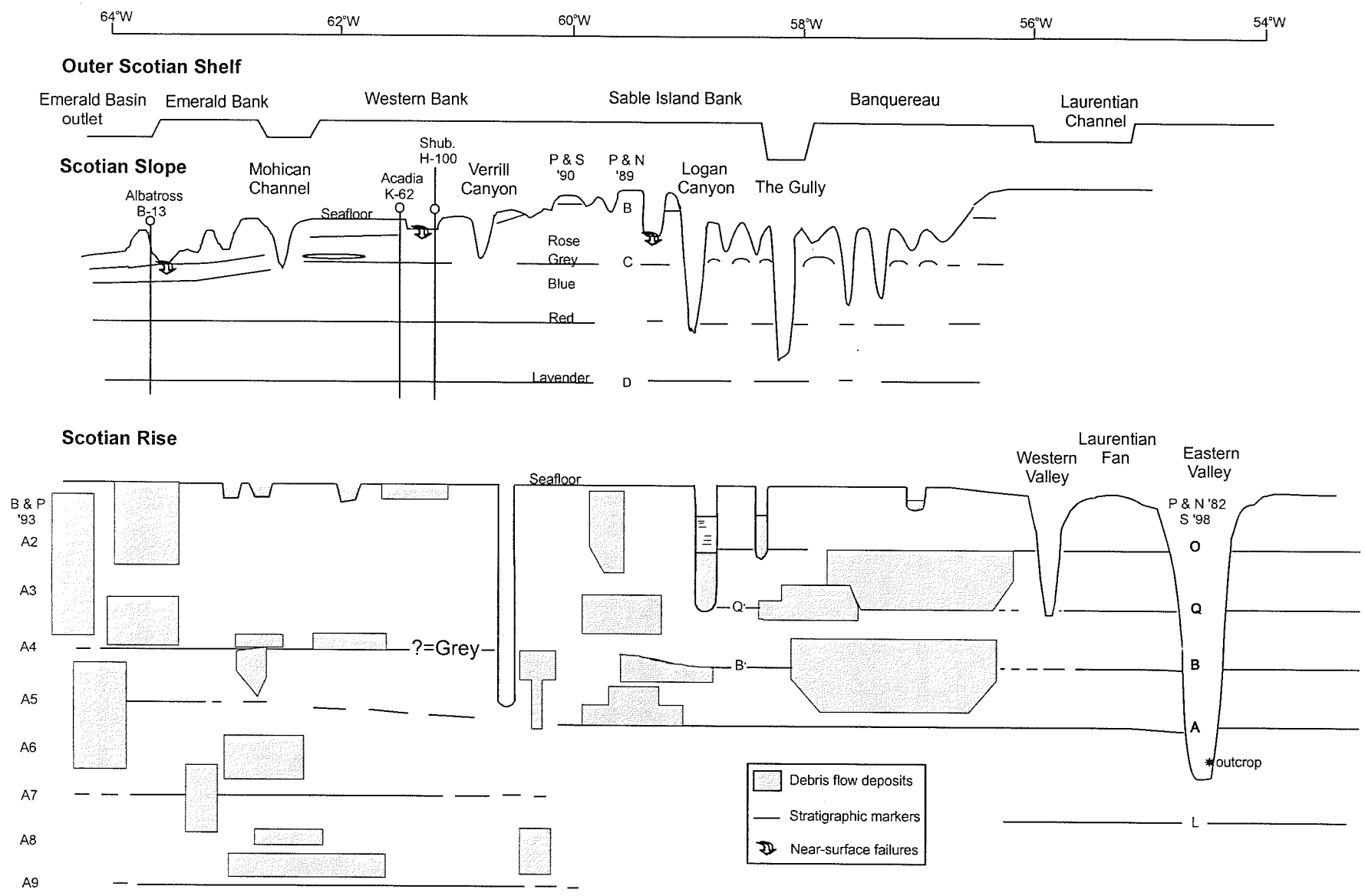

Fig. 2.8. Schematic cross section along the Scotian Rise showing age of debris flows. (Piper et al., 1999).

Fig 2.8

C:/IEmest/revised/fig2_8.cdr

3. Slope off Browns Bank

3.1 Introduction and bathymetry

The Geological Survey of Canada has relatively little data on the continental slope seaward of Browns Bank, between longitudes 64° 20'W and 65° 30'W (Fig. 3.1). Farther west, off Northeast Channel, data coverage is insufficient to make useful interpretations. Off the Canadian portion of Georges Bank, a useful synthesis of sediment instability on the continental slope is provided by O'Leary (1986). The continental rise in this sector of the margin is, in contrast, relatively well-known as a result of a 1987 GLORIA survey and a follow-up cruise on CSS Hudson in 1988 (Hughes Clarke et al. 1992).

The shelf break along this part of the margin is at about 160 mbsl; the upper slope is relatively smooth in most areas to several hundred metres depth, with the exception of two canyons that head at about 200 mbsl. Shallow channels continue across the continental slope to the continental rise (Hughes Clarke et al. 1992).

3.2 Late Cenozoic framework

Correlation to the west of the Shelburne well is based on line A3900, discussed further in Chapter 4. A tentative correlation is made on reflector character between dip lines 160 and 96, the latter intersecting A3900 near 64°15'W (sp 4200). In addition, comparison was made on reflector character with A508 and 211/20A (see Fig. 2.1). Reflectors pink and F (canary) are tentatively correlated to this area, with pink being a prominent erosional surface against which there is some onlap on the middle slope. A3900 can then be correlated with confidence to 3870, with pink and canary carried along strike. Again, this can be correlated with confidence to 3876. Thus pink and canary can be carried onto dip lines 96 and 83 (Fig. 3.2). The greatest uncertainty in all these correlations is along line A3900. Correlations were then extended westward to dip line 66 (Fig. 3.3).

No particular evidence of sediment instability, shallow diapirism or shallow faulting was found in the industry seismic examined in this region.

3.3 Late Quaternary sedimentation

High-resolution seismic data

There is little data in this area and critical airgun lines on the slope are of low quality. The shelf edge appears progradational and abrupt at about 150 mbsl. The upper slope to 375 m appears planar and acoustically hard. Below this, there appears to be a zone of failures. Stratified sediment and intervening valleys filled with debris-flow deposits are found between 600 mbsl and 1500 mbsl. Below 2000 mbsl, almost the entire seafloor consists of stacked debris flow deposits, with small intervening areas of stratified deposits. Below about 2500

mbsl, this interpretation is confirmed by the GLORIA long-range sidescan sonar imagery (Hughes Clarke et al. 1992).

Core stratigraphy

Only one piston core is available from this segment of the margin: an 8-m long core in 1117 m water depth (Figs. 3.1, 3.4). Chronology is provided by two radiocarbon ages (13.1, 13.4 ka) and recognition of brick-red markers **b** and **d**. There appears to be less than a metre of Holocene olive-grey mud, overlying about 4 m of late Pleistocene olive grey mud with ice-rafted detritus. Thin sands occur just above brick-red marker **d** and below this horizon the core penetrated 3 m of grey-brown mud with sandy patches, shell fragments and widespread evidence of bioturbation.

Geotechnical measurements

No geotechnical data is available from this sector of the Scotian margin.

3.4 **Geologic history and hazard assessment**

There is little data on which to base an assessment of the geological history of this area. Industry seismic suggests that the Pliocene - Quaternary history is much like that elsewhere on the western Scotian margin.

The surficial geology of this area appears similar to that around the Albatross well site, discussed in Chapter 5. The character of the upper slope is similar, with failures initiated at about 400 mbsl, probably at the downslope limit of till. Much of the sedimentation on the lower part of the slope appears dominated by debris flows, as is also seen in the slope off Emerald Bank. Slope stability issues are thus likely to be similar to those near the Albatross well site, where much more data is available. We have no information on pockmark distribution in the area, but sparse 3.5 kHz profiles show patchy reflectivity in stratified sediment that in other areas is associated with shallow gas.

The presence of brownish sediment in cores below the brick-red marker **d** may be a result of flux of sediment-laden meltwater out of La Have basin or may indicate direct supply of glacial sediment from ice on northern Browns Bank. Even at glacially lowered sea level, a wide area of the outer shelf would have been submerged. This suggests that sand beds and their bioturbated remnants result from storm reworking of sediment on the outer shelf.

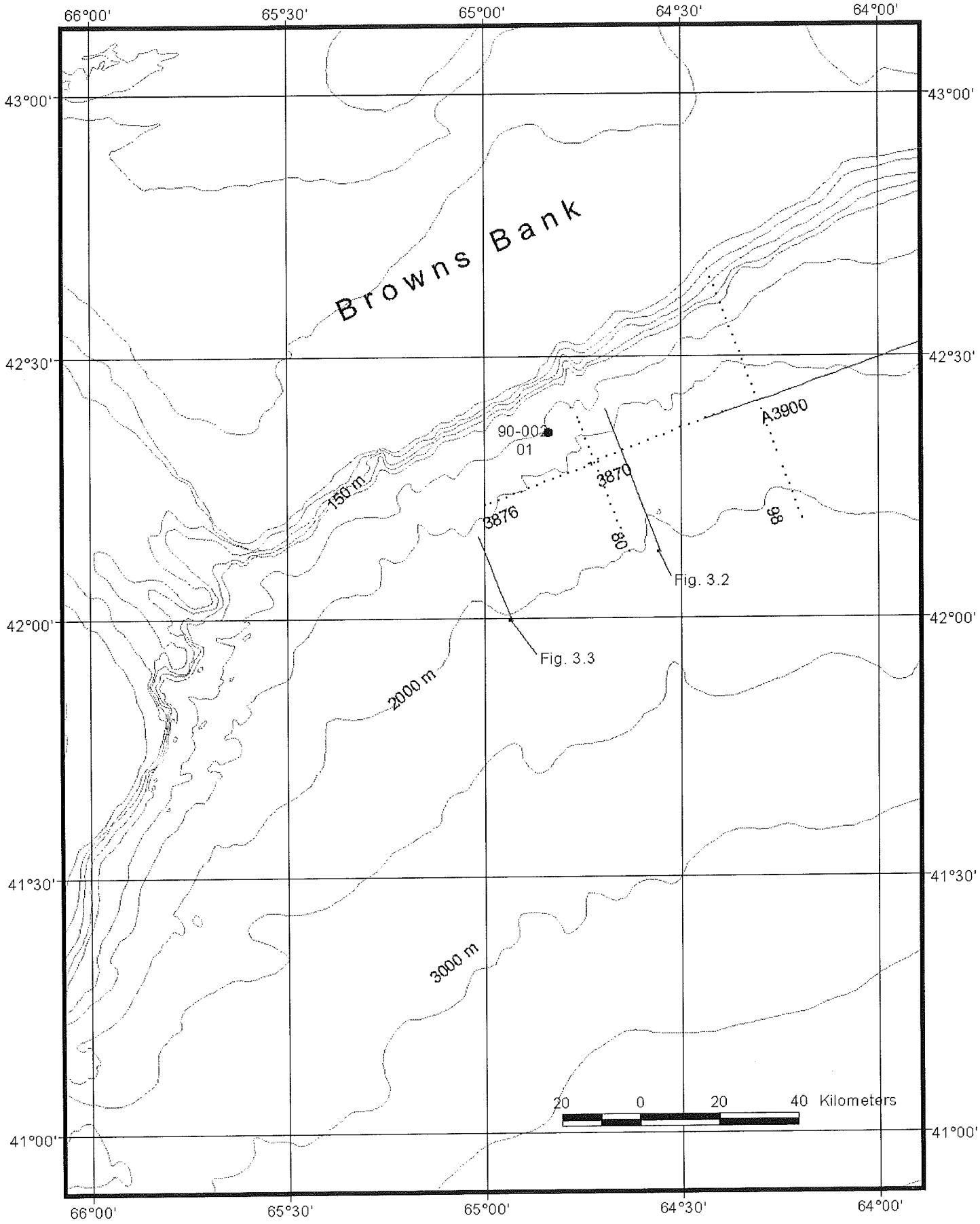

Fig. 3.1: Bathymetric map of the slope off Browns Bank.

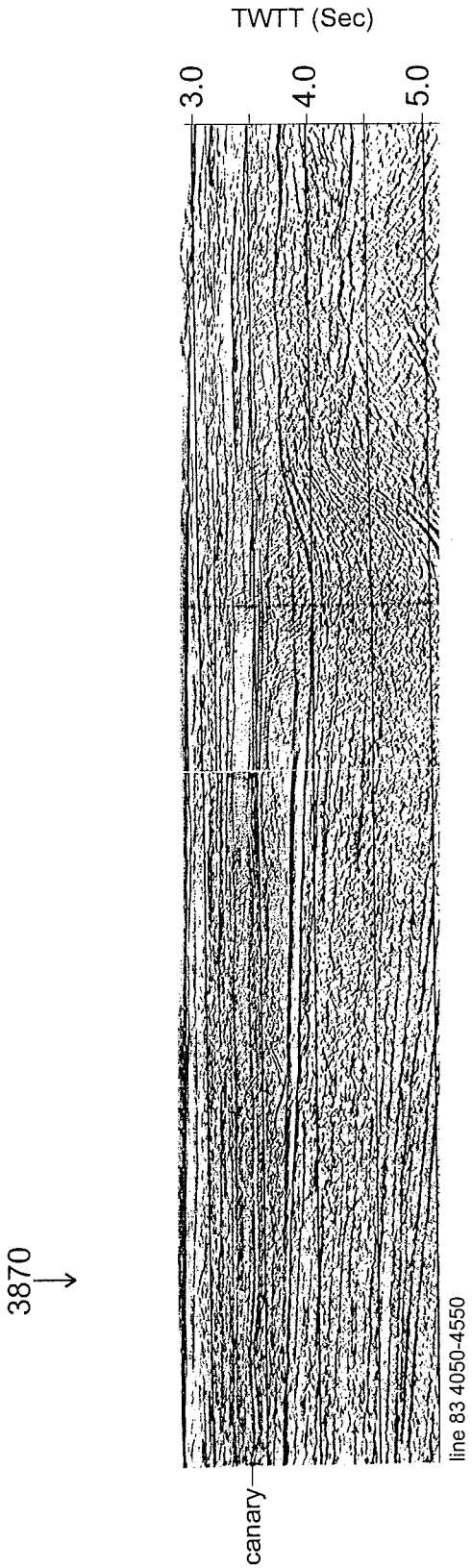

C:/IErnest/revised/fig3_2.cdr

Fig. 3.2. Seismic profile 83 illustrating the regional stratigraphy of the area off Browns Bank.

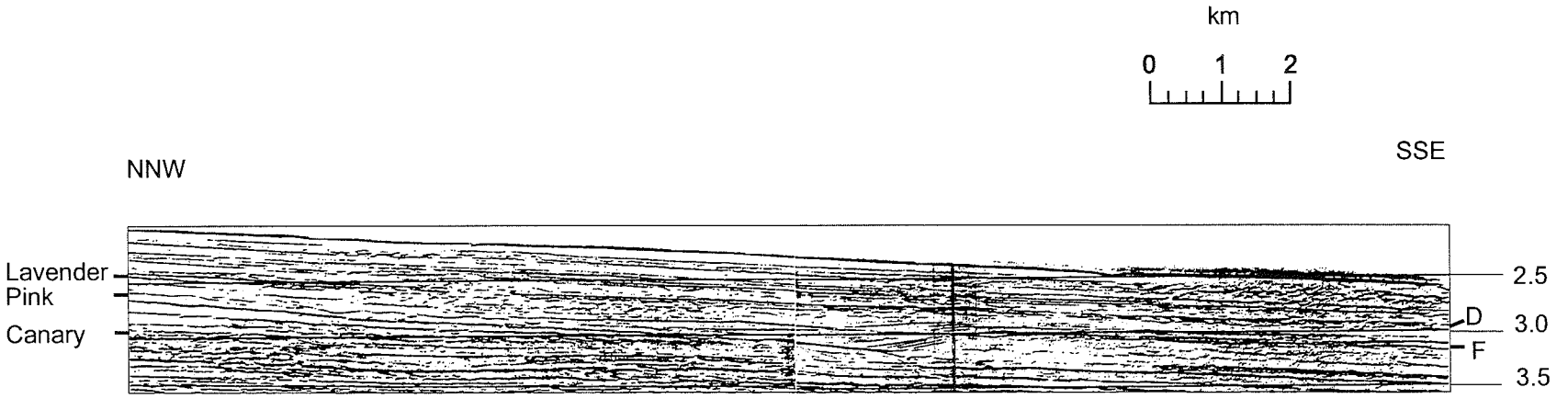

Line 66 sp 3950 - 4490

Fig.3.3. Seismic profile 66 illustrating the regional stratigraphy.

c:/lernest/revised/fig3_3.cdr

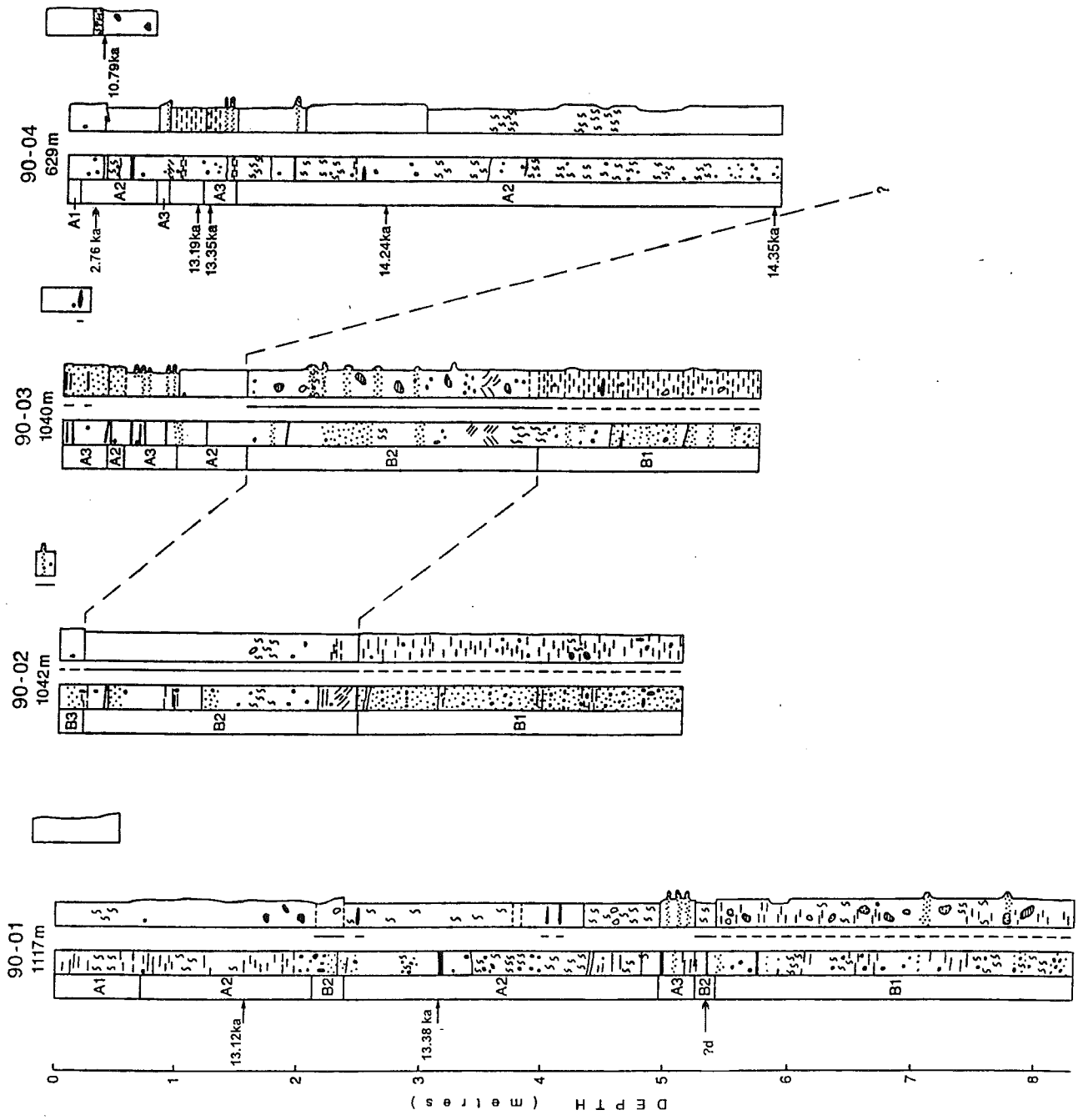

Fig. 3.4. Summary of core stratigraphy off Browns Bank and La Have Basin.

4. Slope off La Have and Emerald Basins

4.1 Introduction and bathymetry

The Scotian Slope between 63° 05'W and 64° 25'W lies seaward of two large transverse troughs on the shelf and lacks submarine canyons (Fig. 4.1). The larger trough (the "Emerald-LaHave Trough"), between Emerald and LaHave banks, leads from Emerald Basin and the main part of LaHave Basin. It is locally overdeepened on the outer shelf and reaches the shelf break in water depths of 170 m. A smaller trough (the "LaHave-Baccaro Trough"), between LaHave bank and Baccaro Bank, is only 130 m deep at the shelf break. This entire area was probably a major glacial outlet.

Off the eastern part of the Emerald-LaHave Trough, there is a large amount of seismic, sidescan and core data (Hill, 1981, 1984; Piper and Sparkes, 1987) (Fig. 4.2). Farther west, only reconnaissance data is available.

In the eastern part of the area, the slope is relatively narrow with a mean gradient of 1.9° between the shelf break and the 2500 m isobath. The slope widens westward to 64°W longitude, where the mean gradient is only 1.5°. There is a broad trough on the upper slope between 63°30'W and 63°50'W, seaward of the deepest part of the shelf break. East of this trough is the only area of detailed bathymetric coverage on the slope in this region (Fig. 4.3). The upper slope, between 200 and 600 mbsl, has a gradient of about 5°, flattening off to about 3° on the middle slope between 600 and 1200 mbsl. To the east, there is a prominent slope valley at about 63°23'W. The middle slope is cut by a series of gullies spaced 0.5 to 1 km, 100-200 m wide, and 5-10 m deep. A prominent slope valley is 400-700 m wide and in places >100 m deep (Fig. 4.4). Farther west, between 64°15'W and 64°30'W, seaward of the LaHave-Baccaro Trough, a series of canyons incise the upper slope, heading in 300 - 400 mbsl (Fig. 4.3). The bathymetric expression of these canyons dies out rapidly downslope and by 1200 mbsl, only shallow channels are visible.

4.2 Late Cenozoic framework

Miocene - Quaternary framework

Regional seismic correlation (Piper and Sparkes, 1991) can be carried from the Acadia K-62 well to the vicinity of the Shelburne G-13 well and is illustrated in Fig. 4.5. A high-resolution airgun dip profile from the outer shelf is illustrated in Fig. 4.6. This section off Emerald Basin (cf. Piper and Sparkes, 1987, Figs. 5 & 6) shows that beneath the upper slope, a thick prograded wedge of Tertiary sediment is cut by a major unconformity parallel to the slope which crops out at about 400 m water depth on the upper slope and can be traced to about 1 s subbottom depth near the 900 m isobath, where it passes downslope into lower Miocene stratified sediment (Piper and Sparkes, 1990). Shallow mud diapirs, rooted in ?Pliocene sediment, are

widespread off Emerald Basin (Piper and Sparkes, 1987, Fig. 7). The basal Quaternary reflection, grey (C), can be correlated from the Acadia wellsite to the area south and west of the mud diapirs, but it is more difficult to extend the regional stratigraphy to the mid slope and to the area off La Have Bank.

Correlation into this western area is based on lines A3900 and 115. Reflector grey is recognised on the basis of reflection character. The gold reflector can be traced to about 64°15'W where it is eroded by a channel seaward of the western outlet of LaHave Basin. Blue and lavender can be traced only to about 64°10'W before ?onlapping deeper strata. Correlation farther west is discussed above in section 3.2. Dip lines (Fig. 4.7) show progradation through the Quaternary.

Quaternary seismic correlation and facies

Airgun seismic reflection profiles have been recently interpreted by Piper (2000) as defining five zones on the upper continental slope (A to E in Fig. 4.8). A brief synopsis is presented here. Five different acoustic facies can be distinguished:

(a) Well stratified facies, characterised in airgun seismic by continuous, sub-parallel or locally mounded reflections (Fig. 4.9). The continuous sub-parallel reflections are also visible in higher resolution seismic systems, such as the Huntec DTS sparker. Piston cores show that this facies near-surface consists of stratified proglacial muds (Piper and Sparkes, 1987).

(b) Cut-and-fill facies, characterised in airgun seismic by discontinuous reflector segments commonly dipping at opposing low angles, with some more continuous reflectors. High-resolution sparker data (Fig. 4.10) show intervals of continuous parallel reflectors alternating with intervals with the seismic character of debris flows and channel-filling sands, an interpretation confirmed by cores (Hill, 1984) and sidescan sonar imagery (Piper and Sparkes, 1987).

(c) The irregular stratified facies in airgun seismic is intermediate between the two facies discussed above. It consists of some continuous planar to gently mounded reflections interbedded with intervals or areas of more discontinuous reflections (Fig. 4.11). The lithologies present are probably an alternation of those found in the two facies above.

(d) Debris-flow facies is characterised in airgun seismic by acoustically incoherent intervals with rare internal reflections, commonly a rough upper surface returning hyperbolic diffractions, and commonly a depression-filling geometry (Fig. 4.11). This facies may include debris-flow deposits *sensu stricto*, debris avalanches and rotational slumps.

(e) Till and proglacial facies, characterised in airgun seismic by incoherent reflections and short discontinuous reflections (Fig. 4.12), occurs only on the upper slope to water depths of about 600 m. This facies resembles the "incoherent wedges" recognised by Mosher et al. (1994) on the upper slope to the east and interpreted as glacial

diamict, perhaps interbedded with proglacial coarse-grained sediment. This facies passes downslope into well stratified facies (Fig. 4.12).

Five zones with differing Quaternary stratigraphies can be recognised on the continental slope between Emerald Bank and Baccaro Bank. In zone A on the middle slope (Fig. 4.11), 200 ms of shallow cut and fill facies overlies 200 ms of well stratified facies. This rests on top of a blocky debris flow unit also about 200 ms thick, overlying > 200 ms well stratified facies. The basal Quaternary marker (C) (correlated from the Acadia K-62 well: Piper and Sparkes, 1990) is near the top of this lower well-stratified facies. In about 1250 m water depth, there is an apparent slope-parallel normal fault across which the stratigraphy is offset by about 200 ms. This fault corresponds to the E-W scarp of Piper and Sparkes (1987) (Fig. 4.4). The blocky debris flow facies is developed only locally on the footwall of this fault. The debris flow and the overlying well-stratified facies overlie, probably unconformably, a somewhat deformed sequence of stratified facies that may represent substantially older sediment.

Zone B is a narrow strip of well stratified facies at least 700 ms thick, apparently fault bounded on its eastern side (Fig. 4.9), at the western end of zone A. It appears to correspond to the entire Pleistocene section to the east, including the upper cut and fill facies. Some individual reflectors appear to correlate through with small offset across the fault.

In zone C, 300-400 ms of shallow cut and fill facies overlies > 200 ms of well stratified facies (Fig. 4.13). The eastern (Fig. 4.9) and western (Fig. 4.13) margins of the zone are abrupt, apparently erosional, and persistent through time.

In zone D, seaward of LaHave Bank, the near surface sediment on the mid slope is well stratified (Fig. 4.13) and thicken westward from 200 ms in the east to 350 ms in the west. They overlie 500 ms thickness of shallow cut and fill facies interbedded with irregular stratified facies (Fig. 4.13). On the upper slope, till and proglacial facies appear to be the lateral equivalent of the upper well-stratified facies and overlie cut and fill facies (Fig. 4.14). The till and proglacial facies passes downslope into well stratified facies (Fig. 4.12), with the till bodies wedging out downslope in a manner similar to those near Verrill Canyon (Mosher et al. 1989 and Chapter 6).

The best data for zone E, seaward of the LaHave-Baccaro Trough, is on the upper slope (Fig. 4.14), where 200-250 ms of till and proglacial facies overlies 500 ms of well stratified facies that appear to be the lateral equivalent of the shallow cut and fill facies in deeper water in zone D. Several generations of partially filled gullies cut the upper slope and were interpreted by Gipp (1996) as discharge routes for subglacial meltwater. On the mid slope, rather poor quality data shows > 300 ms of irregular stratified facies.

A rather similar continental slope architecture appears to be present east of zone A, with upper slope till and proglacial facies passing downslope into stratified facies, both cut by gullies and small canyons partially

filled with cut and fill facies. An industry seismic dip line (Fig. 4.15) cuts obliquely through such a gully. The facies interpretation of the near-surface parts of this seismic profile is based on intersecting airgun seismic lines. The till and proglacial facies unconformably overlies a series of progradational shelf-edge clinoforms that pass downslope into irregular stratified facies. Seismic correlation suggests that the base of this clinoform packet is of approximately basal Quaternary age.

The prominent debris flow horizon in Figures 4.11 and 4.15 can be traced over a large area between the Shelburne and Albatross wells and in places seems to be the source layer for shallow mud diapirs. The debris flow horizon overlies a reflector between lavender and pink everywhere; in many profiles the base is as shallow as lavender and debris flow deposits are most common in the interval immediately above lavender. This incoherent unit in places appears to reach thicknesses in excess of 300 ms. In most places the nature of the margins is unclear - the unit thins gradually to less than the resolution of the seismic profiles. Locally, the unit clearly pinches out upslope.

4.3 **Late Quaternary sedimentation**

High-resolution seismic data

The surficial geology and sediment instability of the slope area near the Shelburne well was described by Piper and Sparkes (1987), based in part on earlier work by Hill (1983, 1984). Off the Emerald-LaHave trough, the depth of the shelf break is as great as 180 m and the outer continental shelf appears floored by till. Submersible investigations show that linear ridges of boulders, presumably indicating glacial supply, probably as an end moraine, occur in water depths of 330 m (Hill et al., 1983). The head of deep channels cutting the slope off the LaHave-Baccaro trough, probably cut by subglacial melt water, generally lie between 300 and 350 m water depth (Gipp, 1996). All this evidence suggests that grounded ice may have extended to more than 300 mbsl in the past.

The area studied in detail by Piper and Sparkes (1987) (Fig. 4.4), from 63°15'W to 63°35'W, has a steep upper slope from 200 to 700 mbsl, cut by gullies spaced 0.5 to 1 km apart and a larger slope valley. The upper slope is acoustically impenetrable with high-resolution systems and is probably underlain by glacial till.

On the middle slope, from 700 to 1200 mbsl, two main sediment facies are present. The main slope valley and the downslope continuations of some of the gullies are filled with sand and gravel. Intervening areas consist of well stratified muds, mostly of proglacial origin (Fig. 4.16). Within a few kilometres of the main slope valley, much of this stratified seabed has been dissected by relatively recent erosion, probably in late glacial times. Much of the seabed up to 5 km west of the main slope valley consists of shallow rotational slumps or debris flows similar to those described near the Shubenacadie H-100 well (Piper et al. 1985). In places, there are

sediment mounds at the seabed. These appear to have preferentially accumulated proglacial stratified sediment, in contrast to the surrounding seafloor (Fig. 4.9). Thin (< 50 m thick) slide or creep blocks may be present locally (Figs. 4.17, 4.18). Some mounds appear associated with faults and probably the upward diapiric movement of mud (Figs. 4.19, 4.20).

In the area near the main slope valley, three sediment units are recognised in the upper 40 m of the sediment column. Below reflector (d) of Piper and Sparkes (1987), sediment appears acoustically well stratified. Horizon (d) appears to be an irregular (? gullied) surface and is overlain by acoustically rather incoherent sediment, probably sands (Fig. 4.21). Above reflector e, the sediment is principally acoustically well stratified. This unit shows upward growth of mound-like features and thickens upslope. Near the slope valley and some smaller gullies, acoustic stratification is poorer.

Regional seismic-reflection profiles show that the lower slope comprises a complex succession of stacked debris-flow deposits, channel fill deposits and stratified muddy sediment (Fig. 4.22). The general character appears similar to the lower slope in the area of the Albatross well, discussed below. 3.5 kHz profiles suggest that debris flow deposits are common at the present seafloor.

Core stratigraphy

Hill (1983, 1984) studied a large number of short piston cores in the area from 63°15'W to 63°35'W, off the Emerald-LaHave trough. The acoustically amorphous unit between reflectors d and e corresponds to sands (e.g. cores 56, 73 of Hill, 1984). The overlying acoustically stratified unit corresponds to brown muds with both turbidite and hemipelagic origin interbedded in places with silts, sands and sandy gravelly mud of turbidite and debris flow origin (Hill, 1983, 1984). The uppermost 1-2 m of sediment are olive grey bioturbated muds, that pass upslope into silts near the 550 m isobath (Hill and Bowen, 1983).

Push core 90015-22 from the diapir crest shown in Figure 4.20 has 70 cm of winnowed Holocene silty sands overlying alternating brown and red-brown mud with some sands. A horizon at 1 mbsf may be brick-red marker **d**; a *Nucula* shell 10 cm above this level yielded an age of 14.1 ka.

Radiocarbon ages of 28.1 ka and 32.9 ka have been obtained from shell fragments in cores a short distance below reflector "f" (Fig. 4.22). If these ages are real, they demonstrate rather low sedimentation rates on this sector of the slope during the last glacial maximum, implying a lot of by-passing of sediment. They also imply that the sandy interval between reflectors "d" and "e" is either of early Wisconsinan or even Illinoian age.

The only cores from the western part of this sector are three piston cores from seaward of the LaHave-Baccaro trough (Fig. 3.4). These cores are from an area in which well-stratified sediment drapes an older gullied surface (Fig. 4.23). Age is controlled by six radiocarbon dates from core 90002-04 at 629 mbsl. The Holocene consists of less than 1 m of olive grey mud. Late Pleistocene olive grey mud (at least as old as 14.3 ka) is 5 m

thick in this upper slope core, but thins to less than 1 m thick on the middle slope at 1040 mbsl, where the Holocene section appears sandy and winnowed in cores 90002-02 and 03[1]. It overlies brownish muds with increasing amounts of sand downcore. No brick-red markers were seen in these cores, which may indicate that there was substantial outflow of meltwater from Emerald and La Have basins, diverting the regional flux along the margin of icebergs originating from the Gulf of St Lawrence.

The observed sediment section in Emerald and La Have basins is consistent with these observations on the slope cores. In Emerald Basin, the Emerald Silt consists of olive to grey coloured sediment at least down to the top of depositional sequence 2 (Gipp, 1994). Below that, some red-brown sediment occurs. The top of depositional sequence 2 is dated at 15-16 ka (Gipp and Piper, 1989). In La Have Basin, red-brown muddy debris flows have been dated to between 16 and 18 ka (Piper et al., 1990). The transition from olive grey to brownish sediment in cores 90015-22 and 90002-03 probably dates around 13.5 - 15 ka and might be diachronous.

Geotechnical measurements

Virtually no geotechnical measurements are available from this sector. Downcore physical properties have been measured on cores 93026-001 and 99036-57. In-situ cone penetrometer measurements were made at the site of core 90015-22 to subbottom depths of 2 m (HMG-10; Piper and Cochonat 1990).

4.4 **Geologic history and hazard assessment**

The regional depth of the early Miocene surface (Fig. 2.7) shows a bulge seaward of the Emerald-LaHave trough, suggesting that this area was a mid-Tertiary depocentre. The mid-Pliocene to mid-Quaternary thicknesses (Fig. 2.5) are small, particularly so in the Pliocene (Fig. 2.6). Although this might in part be the result of major failures and debris flows in the latest Pliocene-early Quaternary (Fig. 4.6), there does seem to be a depositional thinning from the area off Western Bank (e.g. Fig. 5.11) to this sector (Fig. 4.5). This suggests that deltaic sediment derived from a proto-Sackville-Shubenacadie river may have accumulated off Western Bank in the Pliocene. Mid to late Quaternary sediment, however, is particularly thick in the sector seaward of the Emerald-LaHave Trough (Fig. 2.4) and has a discernable gravity signature (Courtney and Piper, 1992).

The effects of deep-seated faults are particularly noticeable on this sector of the margin. Just east of the Shelburne well, a near-surface fault has an apparent throw of about 150 m (Fig. 4.11) and forms an E-W escarpment at the seabed (Fig. 4.4). To the east of Figure 4.11, the fault appears to split into two strands that can be followed into the industry seismic line of Figure 4.15. This profile shows that there is probably a

[1] On local highs, the Holocene section is commonly winnowed down to water depths of at least 1600 m (e.g. at the Tantallon well site, Chapter 8). On smoother areas of the upper slope, the transition from silty sands to muds occurs at 500-600 mbsl (Hill and Bowen, 1983).

corresponding deep-seated fault with a small throw, correlative with the deep-seated fault inferred from the offset in strata beneath the debris-flow horizon in Figure 4.11. However, some of the apparent motion in Figure 4.15 appears related to differential movement of sediment overlying the major debris flow. A mud diapir appears to have developed from the debris-flow horizon along the southern fault strand. A small mud diapir has also moved up a smaller fault to the northwest (Fig. 4.9), forming a small mound at the seabed (Figs. 4.19, 4.20).

In the mid to late Quaternary, three types of shelf-edge ice margin produced different styles of sediment accumulation (Piper, 2000). (1) Seaward of the Emerald-LaHave trough, ice margins of ice streams persisted for many thousands of years at the shelf edge and resulted in active sedimentation of coarse, channelled deposits and debris flows. (2) Seaward of LaHave Bank, ice advance onto the upper slope was short-lived and sedimentation was dominated by fallout from ice-margin plumes. (3) Under intermediate conditions, such as are found seaward of the LaHave-Baccaro trough, ice advance deposited upper slope till and subglacial meltwater cut gullies, but active sedimentation seaward of a broad ice front was lacking.

Little high-resolution sidescan data is available in this sector of the margin. A SAR sidescan line in 700-900 m water depth through zone A has relatively common pockmarks and gassy wipe-out features in 3.5 kHz profiles (Fig. 4.24). Pockmarks are common in the vicinity of the fault, but not on the crest of the mud diapir, illustrated in Figure 4.20.

Fig. 4.1

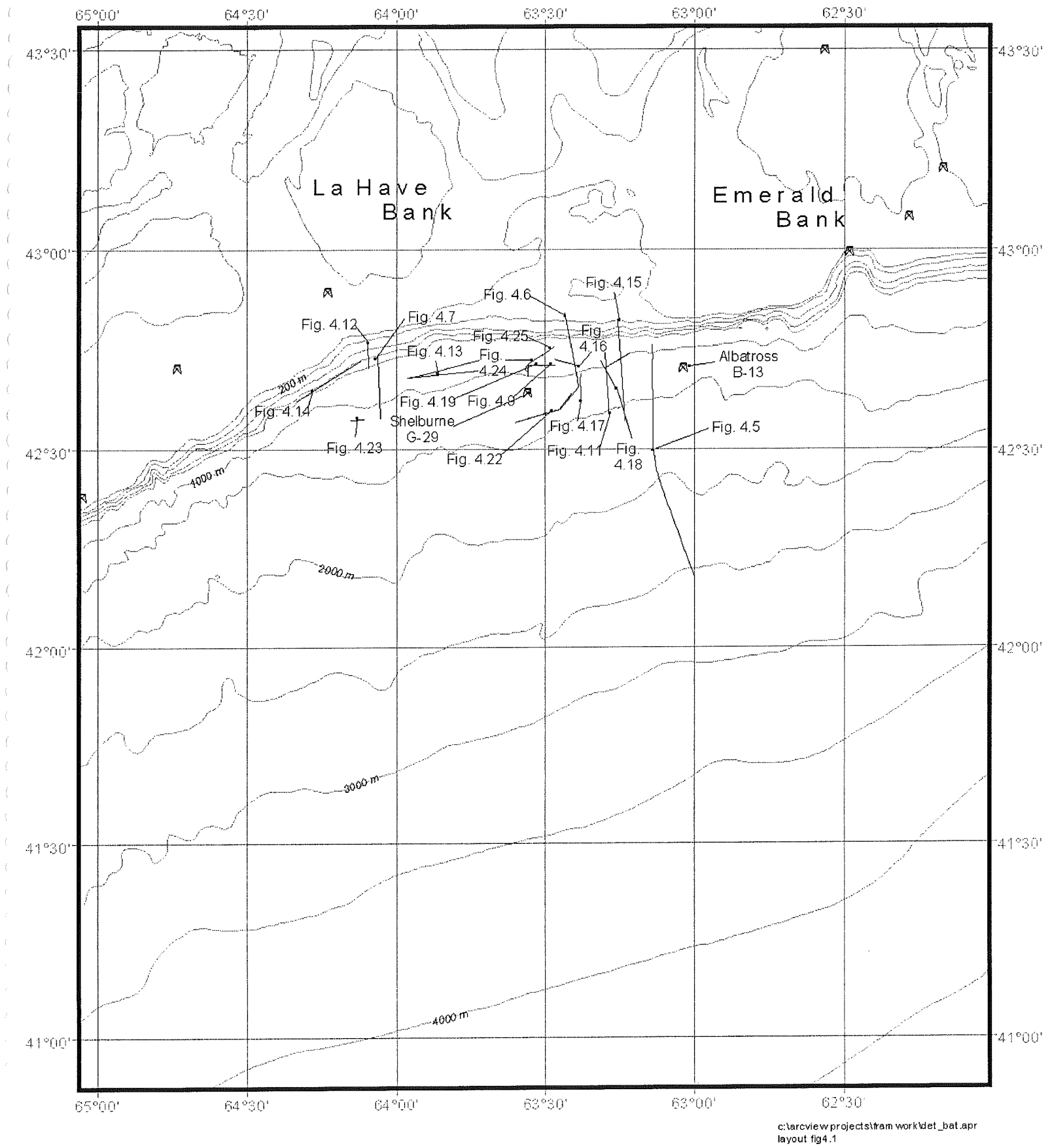

Fig. 4.1: General map of the slope off La Have and Emerald Basins.

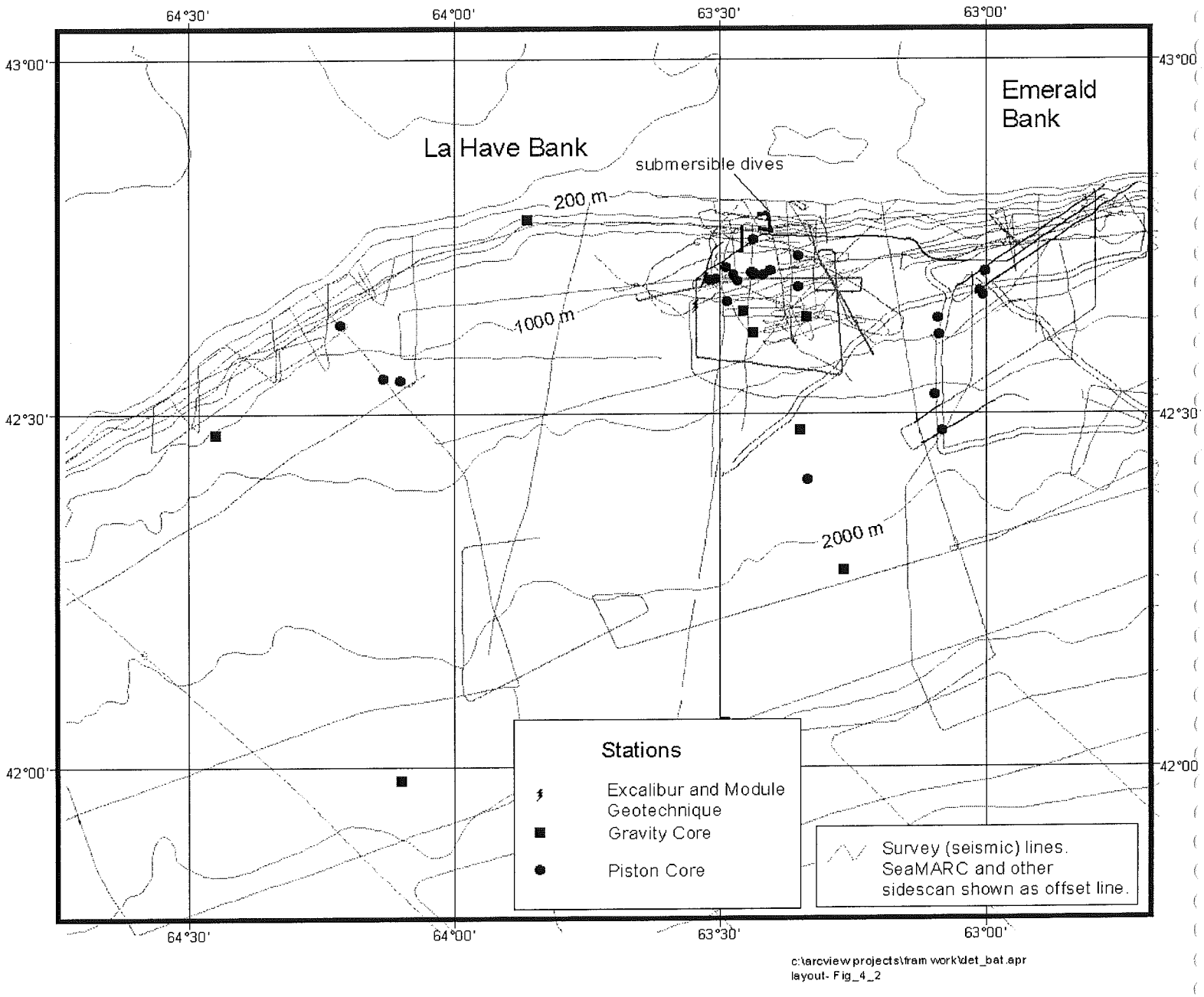

Fig. 4.2: Map showing data distributions of La Have and Emerald Basins.

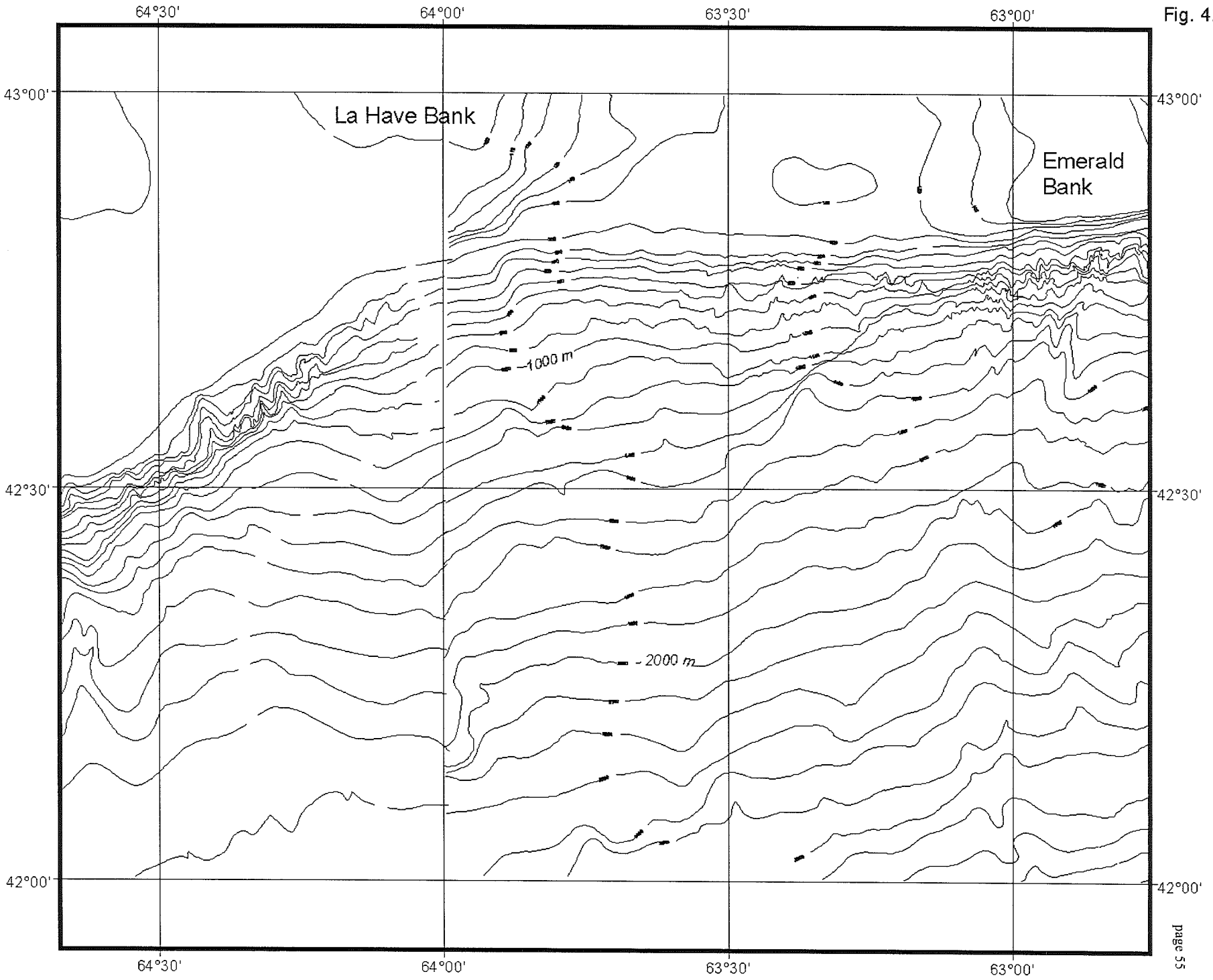

Fig. 4.3: Map showing bathymetry of upper and middle slope off La Have and Emerald Basins.

c:\arcview projects\fram work\det_bat.apr
layout- Fig_4_3

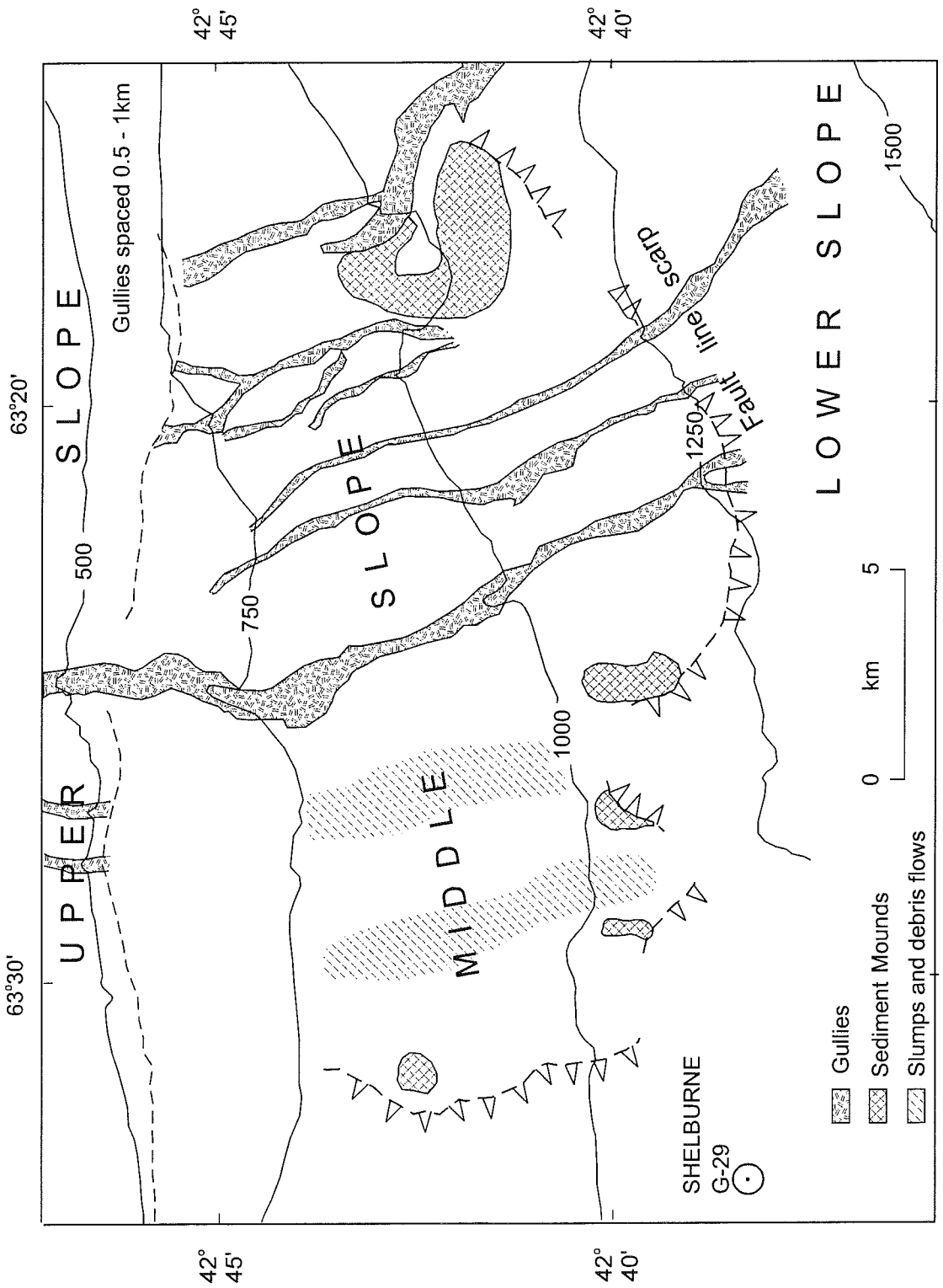

Fig 4.4. Map of seabed geomorphologic features northeast of Shelburne well.

C:/ernest/revised/fig4_4.cdr

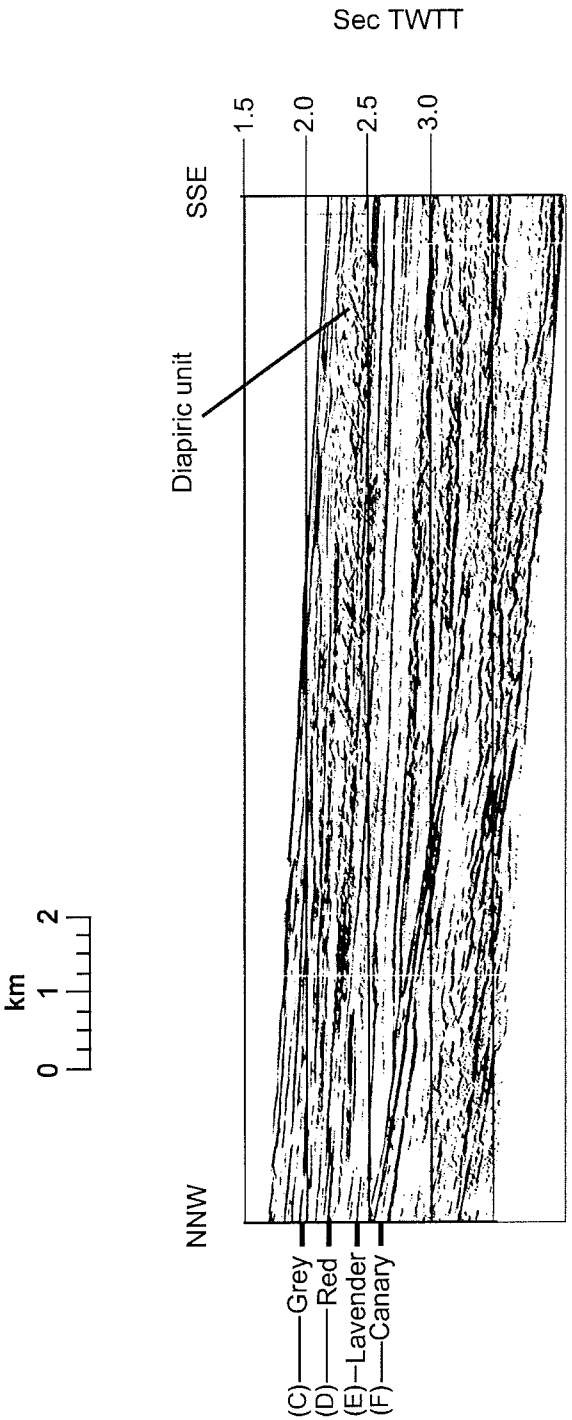

Line A160 sp 4200 - 4600

Fig. 4.5. Seismic profile 160 (sp 4200-4600) illustrating the regional stratigraphy of the Shelburne area. The correlation of reflector B is approximate. Letters represent regional reflectors.

c:/ernest/revised/fig4_5.cdr

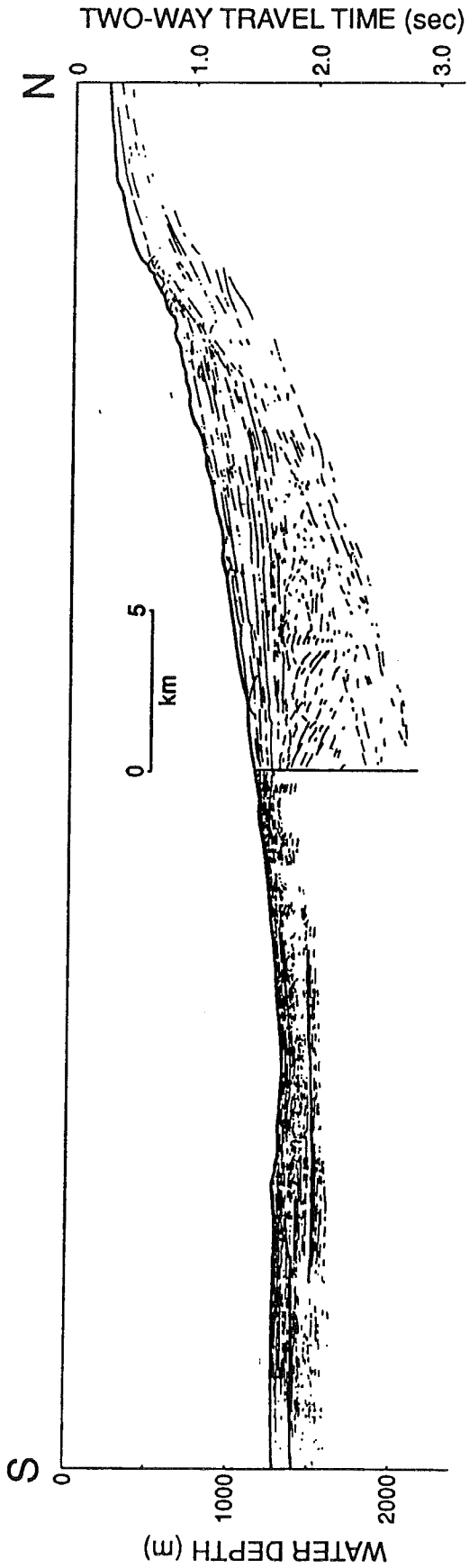

c:\campbell\framewrk\fig4_6.cdr

Figure 4.6: Line drawing of dip seismic profiles across the margin off Emerald Basin showing late Cenozoic framework. (North: profile 81044/052, original seismic record illustrated in Piper and Sparkes, 1987, Fig. 6; south - 90-002, 101/0355-0555 and 0855-0920).

Fig 4.7

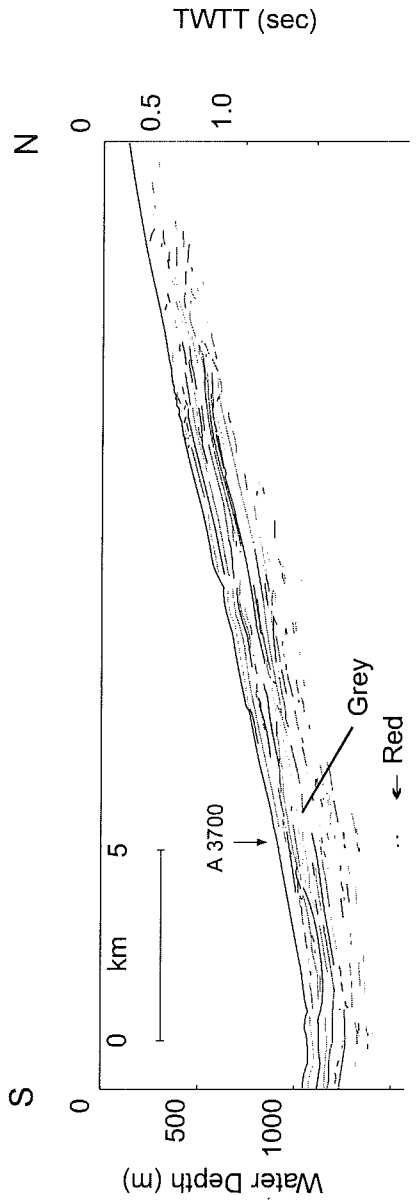

Fig. 4.7. Line drawing of dip seismic profiles across the margin off La Have Basin showing late Cenozoic framework. Depth of regional reflector D based on correlation with industry profiles A3700 and 115.

C:/fEmest/revised/fig4_7.cdr

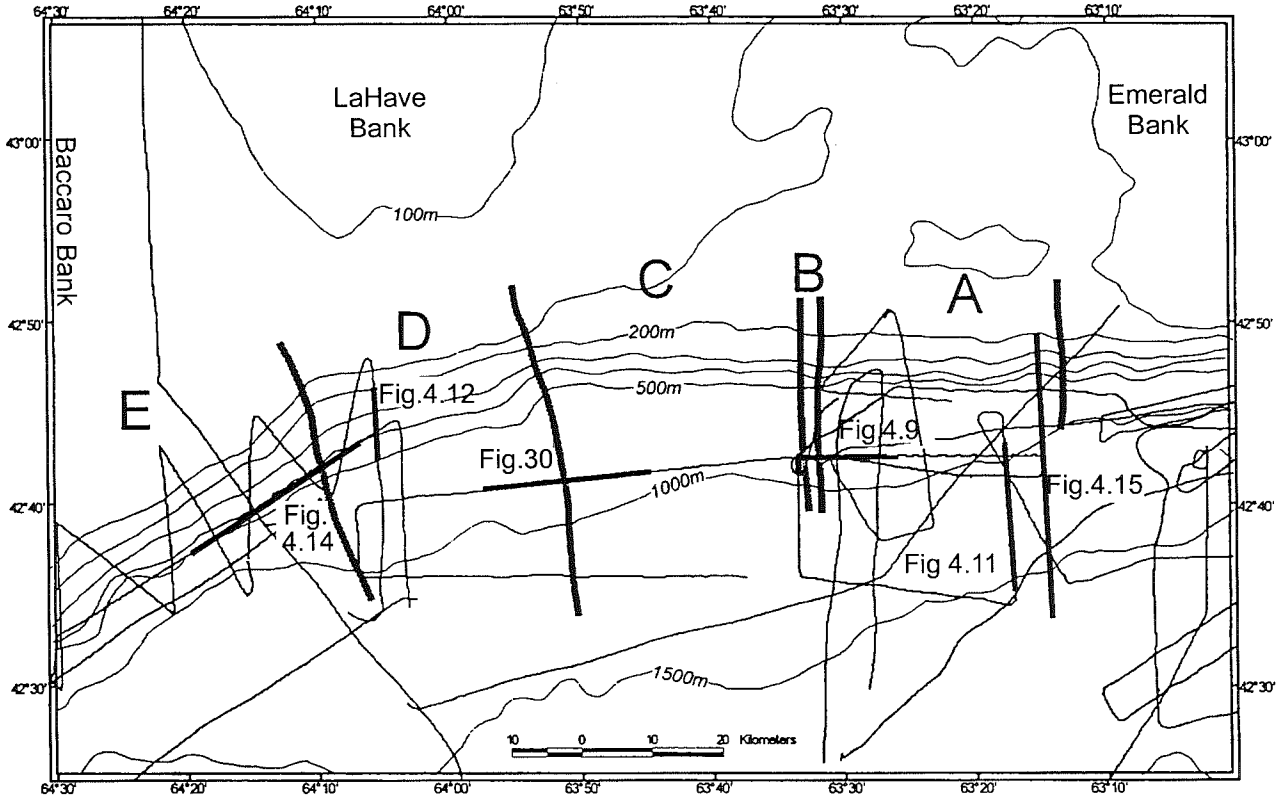

Fig. 4.8. Map of area near the Shelburne well showing zones discussed in text and illustrated in seismic profiles.

C:/IErnest/revised/fig4_8.cdr

Fig 4.8

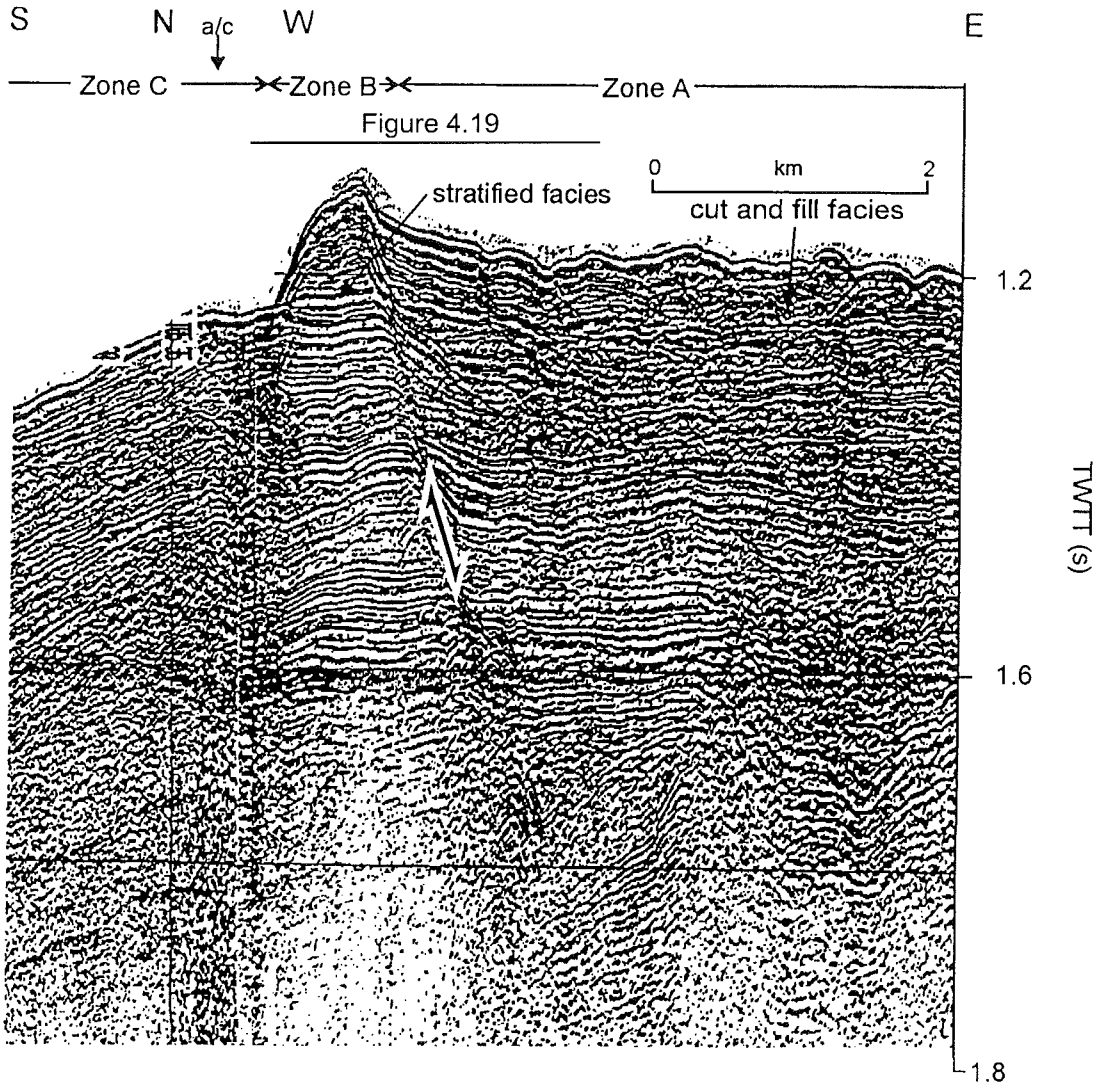

Fig. 4.9. Seismic reflection profile along strike in 900 m water depth north of the Shelburne well, in zones A-C showing facies, stratigraphy and faulting. Two 40 cu. in. sleevegun source, cruise 99-036.

C:/!Ernest/revised/fig4_9.cdr

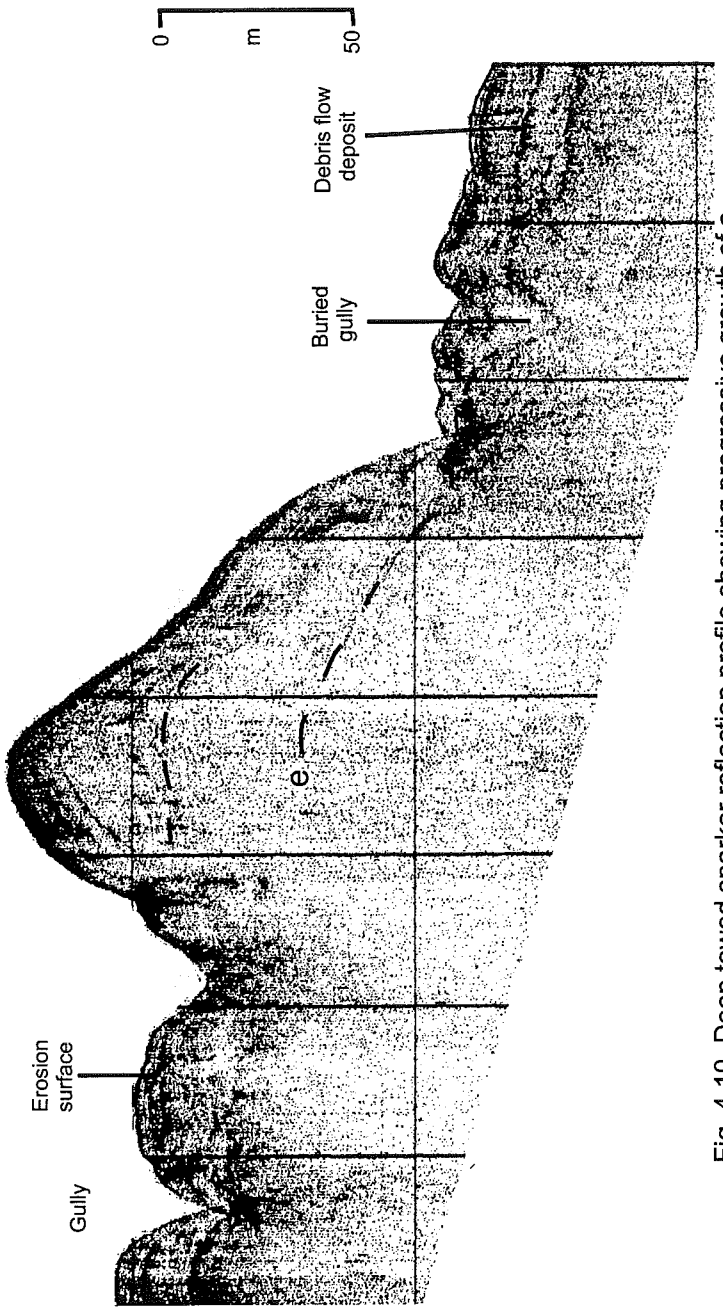

Fig. 4.10. Deep towed sparker reflection profile showing progressive growth of a sediment mound above reflector "e". East of Shelburne G-29 well.

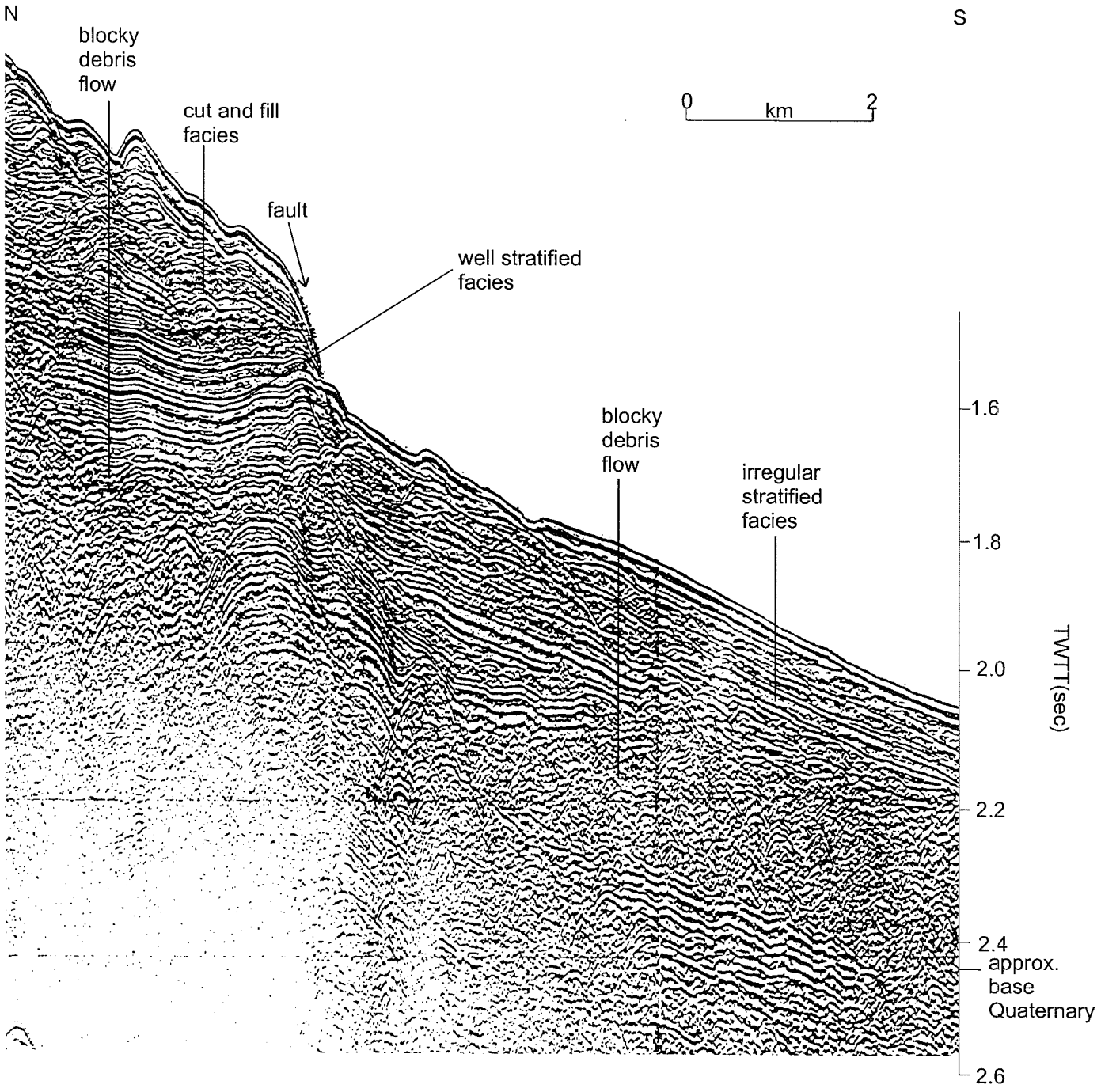

Fig.4.11. Seismic reflection profile down dip east of the Shelburne well in zone A, showing facies, stratigraphy and faulting. Two 40 cu. in. sleevegun source, cruise 99036.

Fig 4.11

c:\Ernest/revised/fig4_11.cdr

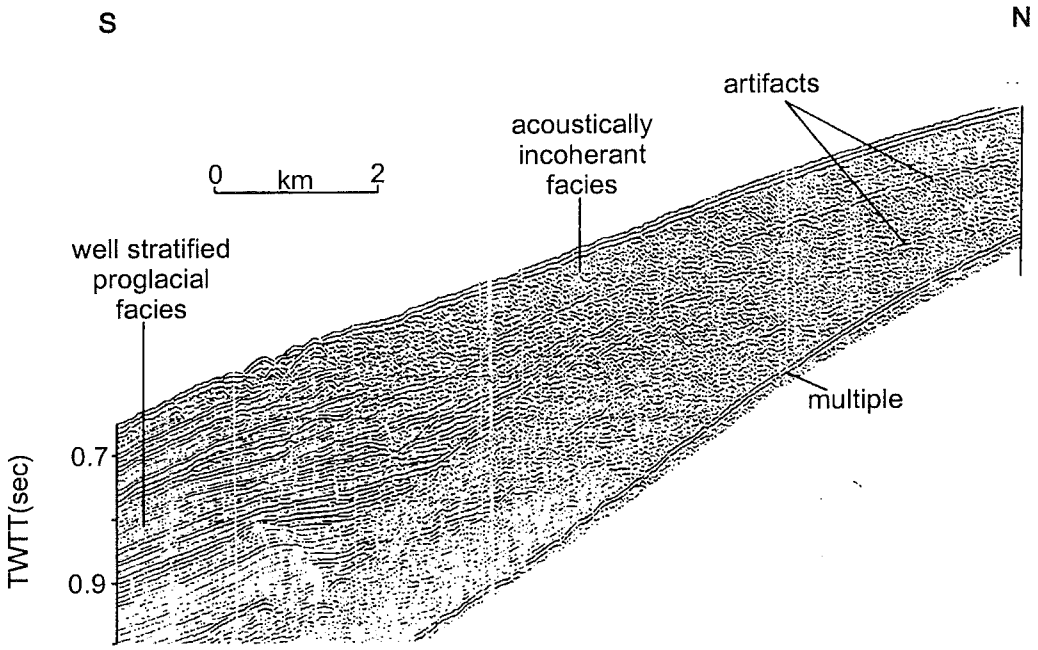

Fig.4.12. Seismic reflection profile down dip of the Shelburne well, in zone D, showing incoherent acoustic facies corresponding to till passing down slope into well stratified acoustic facies, corresponding to proglacial plume fall-out deposits. One 40 cu. in. airgun source, cruise 90002.

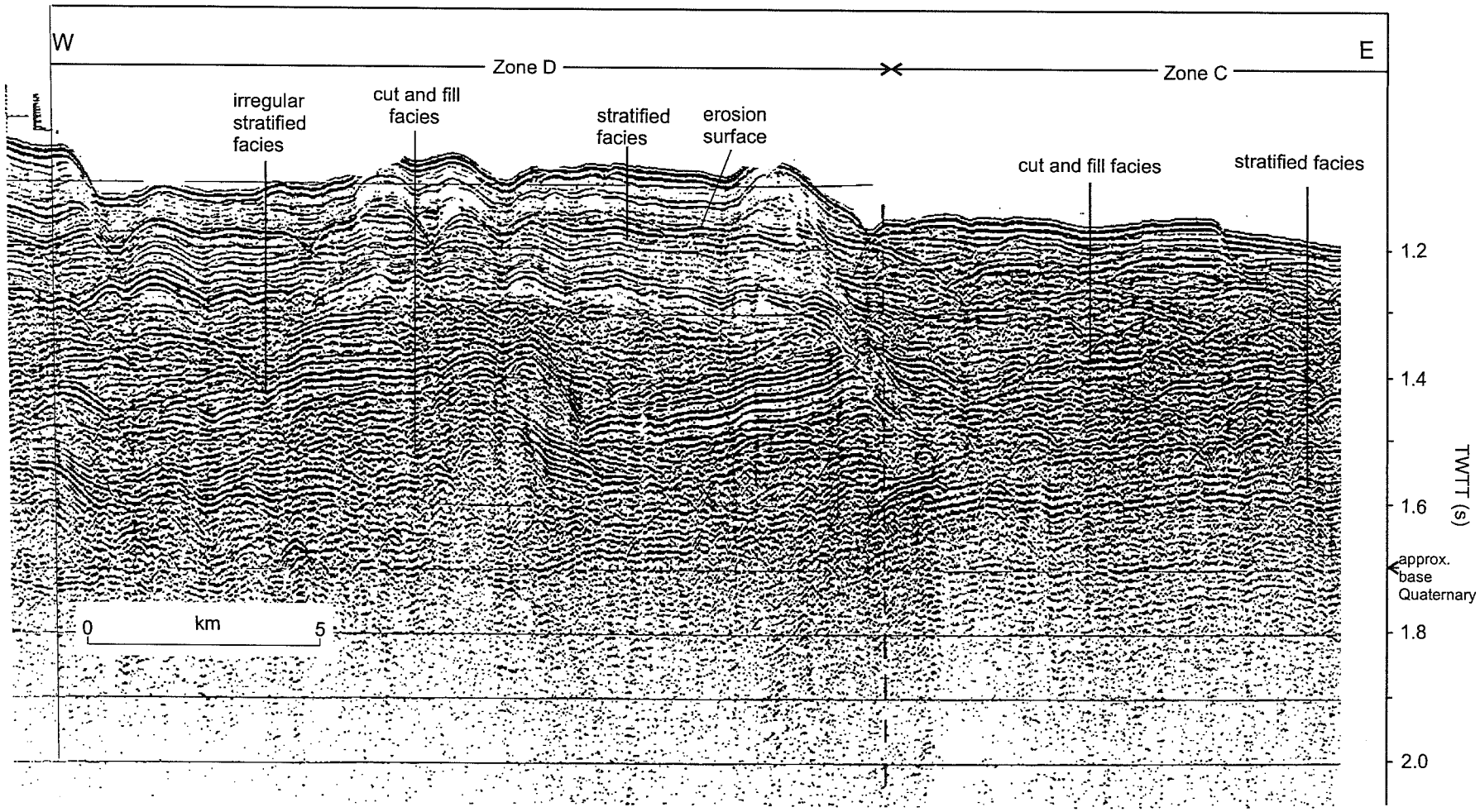

Fig. 4.13. Seismic reflection profile along strike west of the Shelburne well in 900 m water depth in zones C and D showing facies and stratigraphy. One 40 cu. in. sleevegun source, cruise 90-015.

90015
Airgun
st:312T0145
ed:312T0350

C:/!Ernest/revised/fig4_13.cdr

Fig 4.13

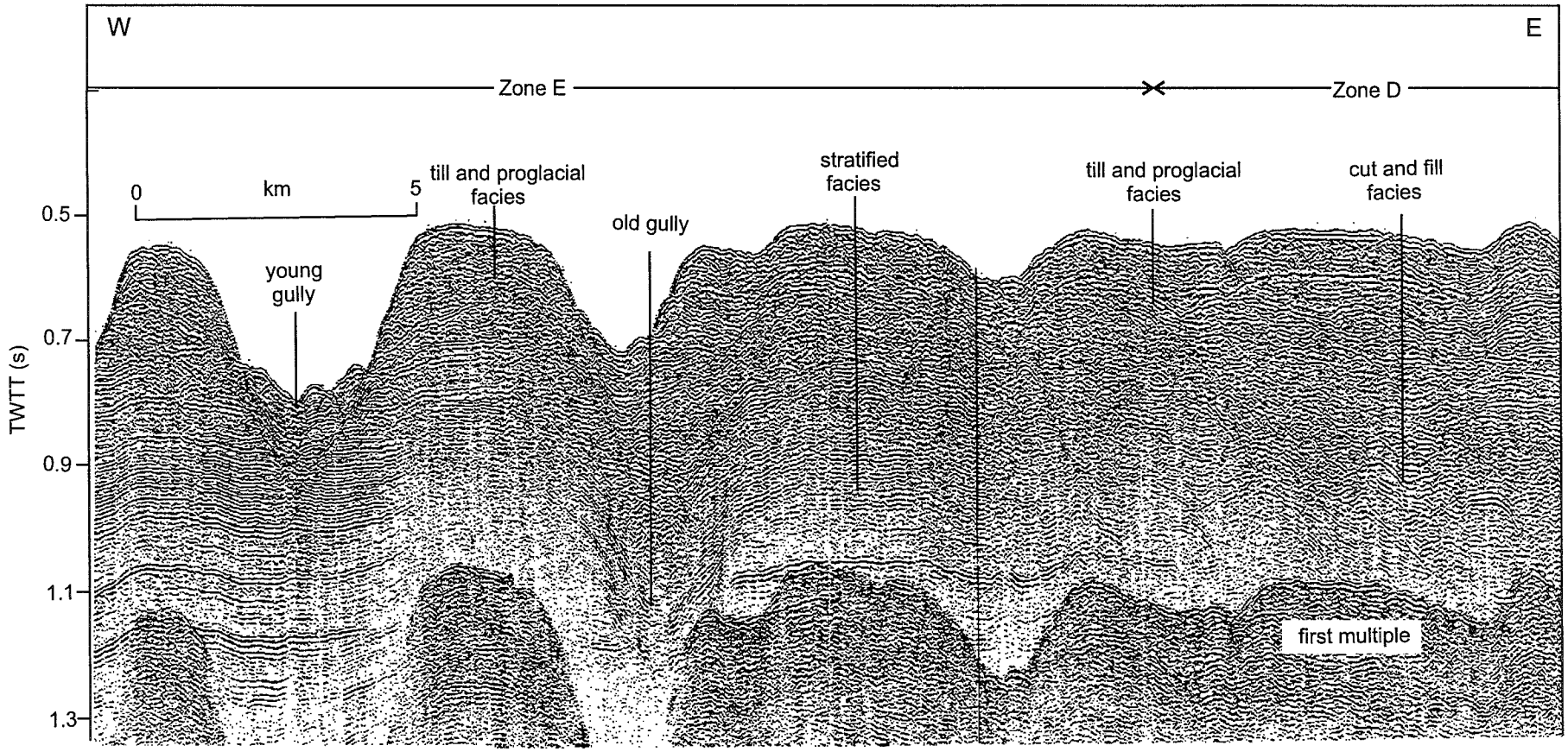

Fig. 4.14 Seismic reflection profile along strike in 400 m water depth west of the Shelburne well in zones D and E, showing gullies cutting and proglacial facies overlying well stratified facies in zone E whereas in zone D, till and proglacial facies lack gullies and overlie cut and fill facies. One 40 cu. in. airgun source, cruise 90-002.

90002
Airgun
st:100T1905
ed:100T2100

C:/!Ernest/revised/fig4_14.cdr

Fig 4.14

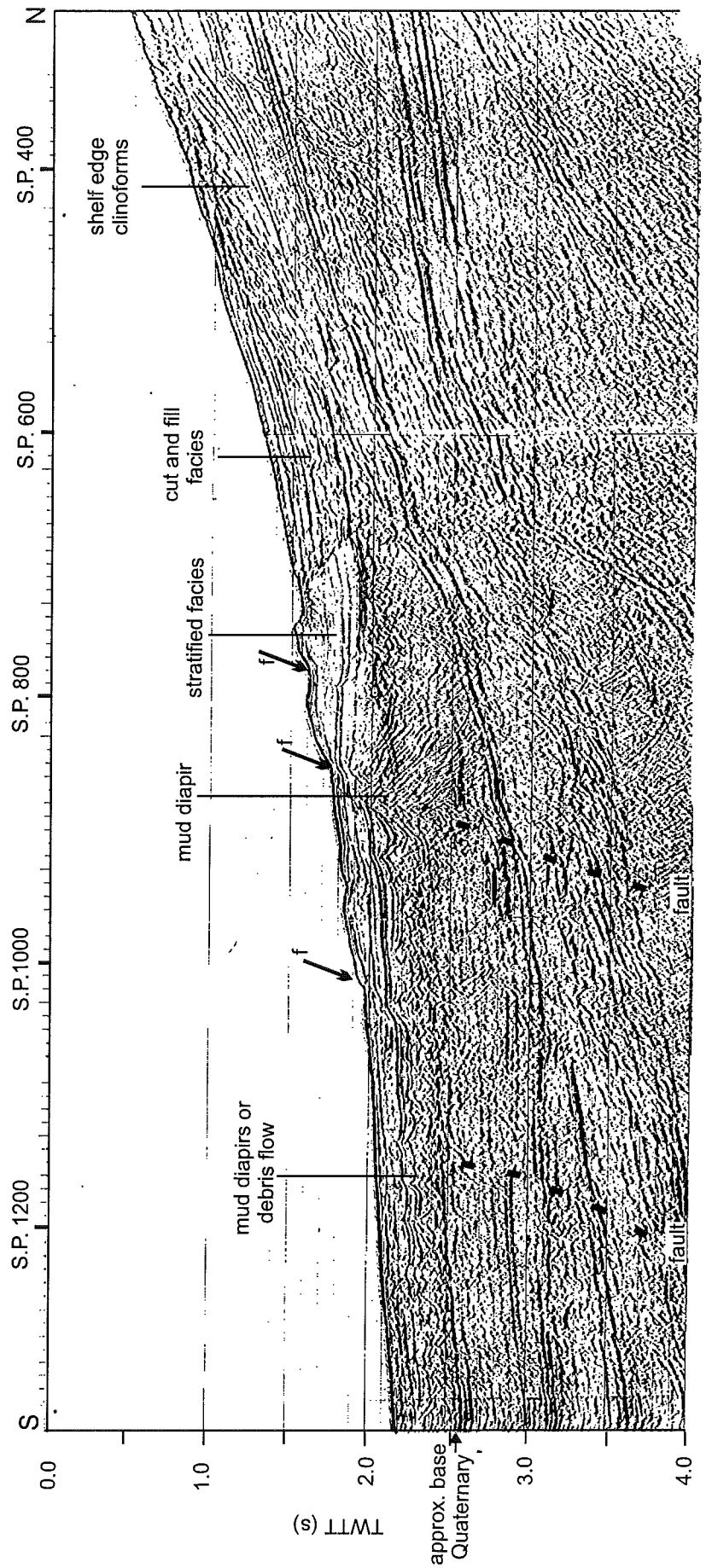

Fig. 4.15. Industry multichannel seismic reflection profile down dip from the eastern end of zone A, east of the Shelburne well, showing late Cenozoic stratigraphy and facies. PetroCanada line 3416-82P courtesy Canada Nova Scotia Offshore Petroleum Board.

C:/IEmest/revised/fig4_15.cdr

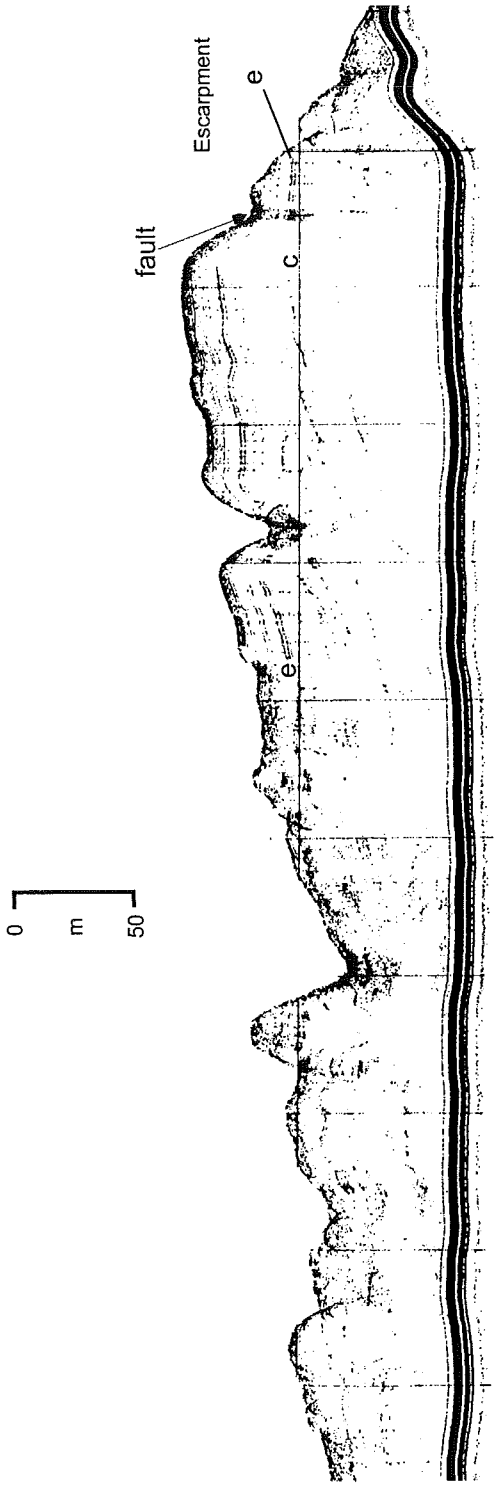

Fig.4.16. Deep towed sparker reflection profile showing western marginal escarpment and near-surface slumps and debris-flow deposits. East of Shelburne G-29 well.

C:/IErnest/revised/fig4_16.cdr

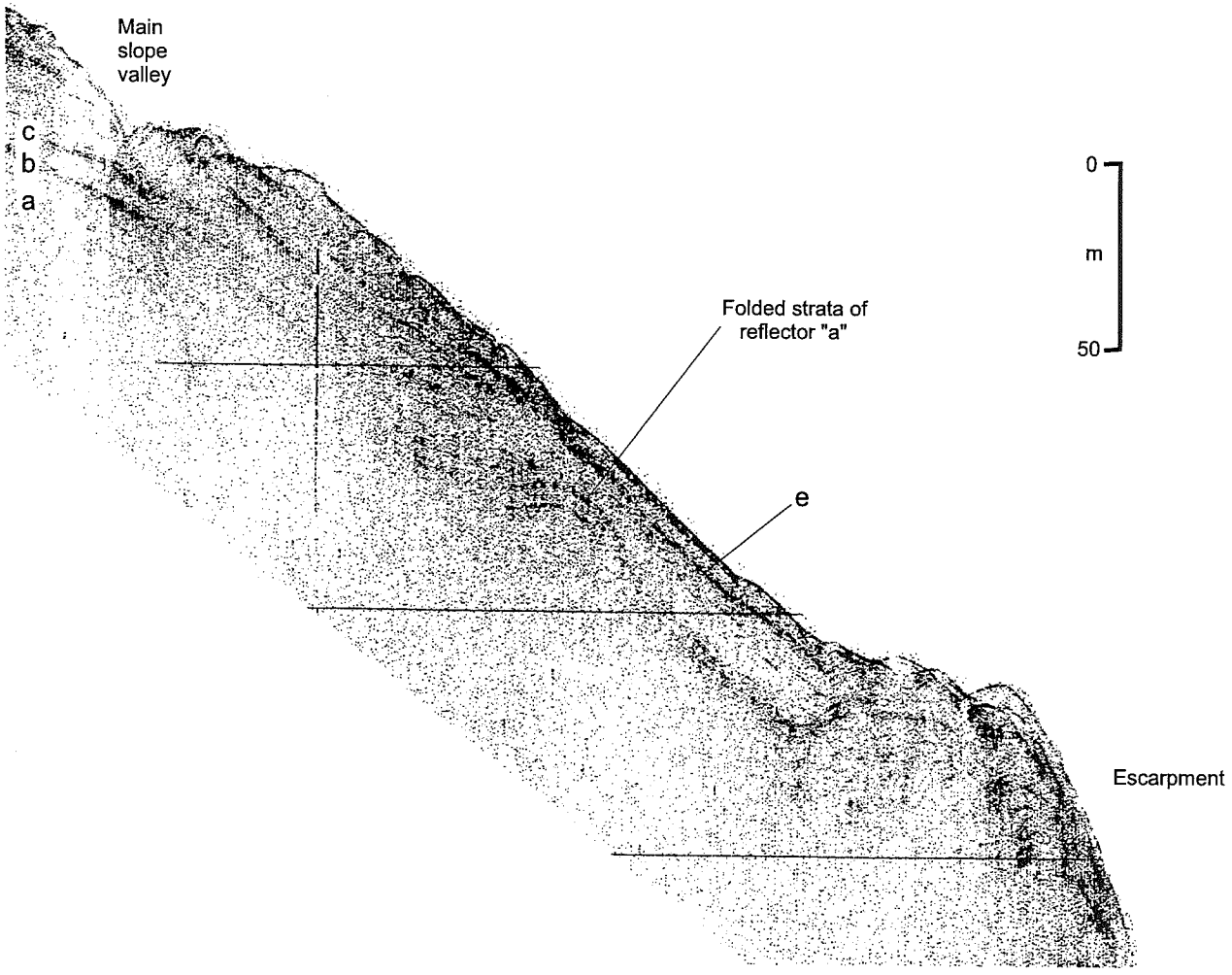

Fig.4.17. Deep towed sparker reflection profile showing deformation of near-surface sediments and escarpment at toe of possible thick slide or creep block. East of Shelburne G-29 well.

Fig 4.17

C:/!Ernest/revised/fig4_17.cdr

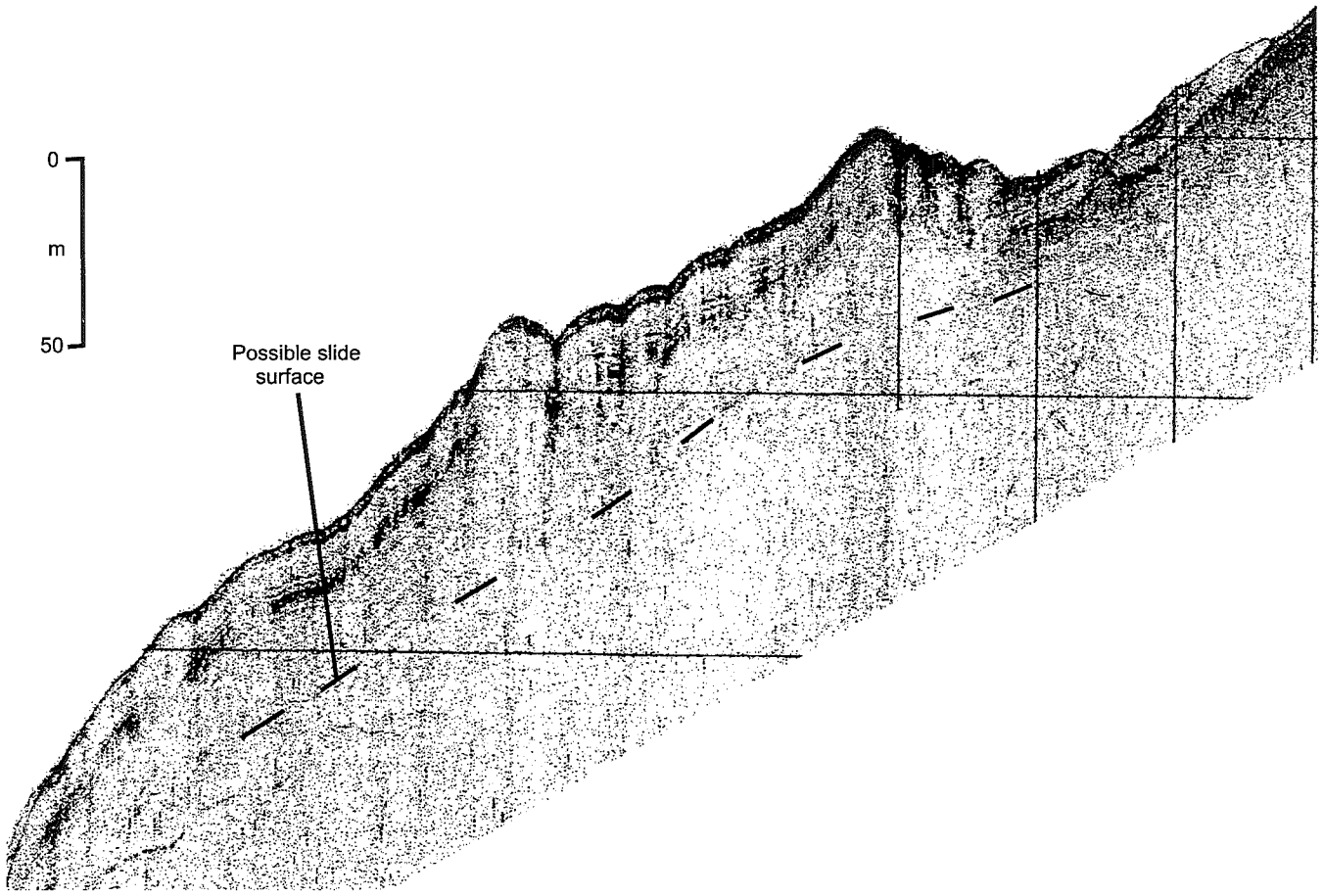

Fig.4.18. Deep towed sparker reflection profile showing slide or creep block about 50m thick.`
East of Shelburne G-29 well.

Fig 4.18

C:/Ernest/revised/fig4_18.cdr

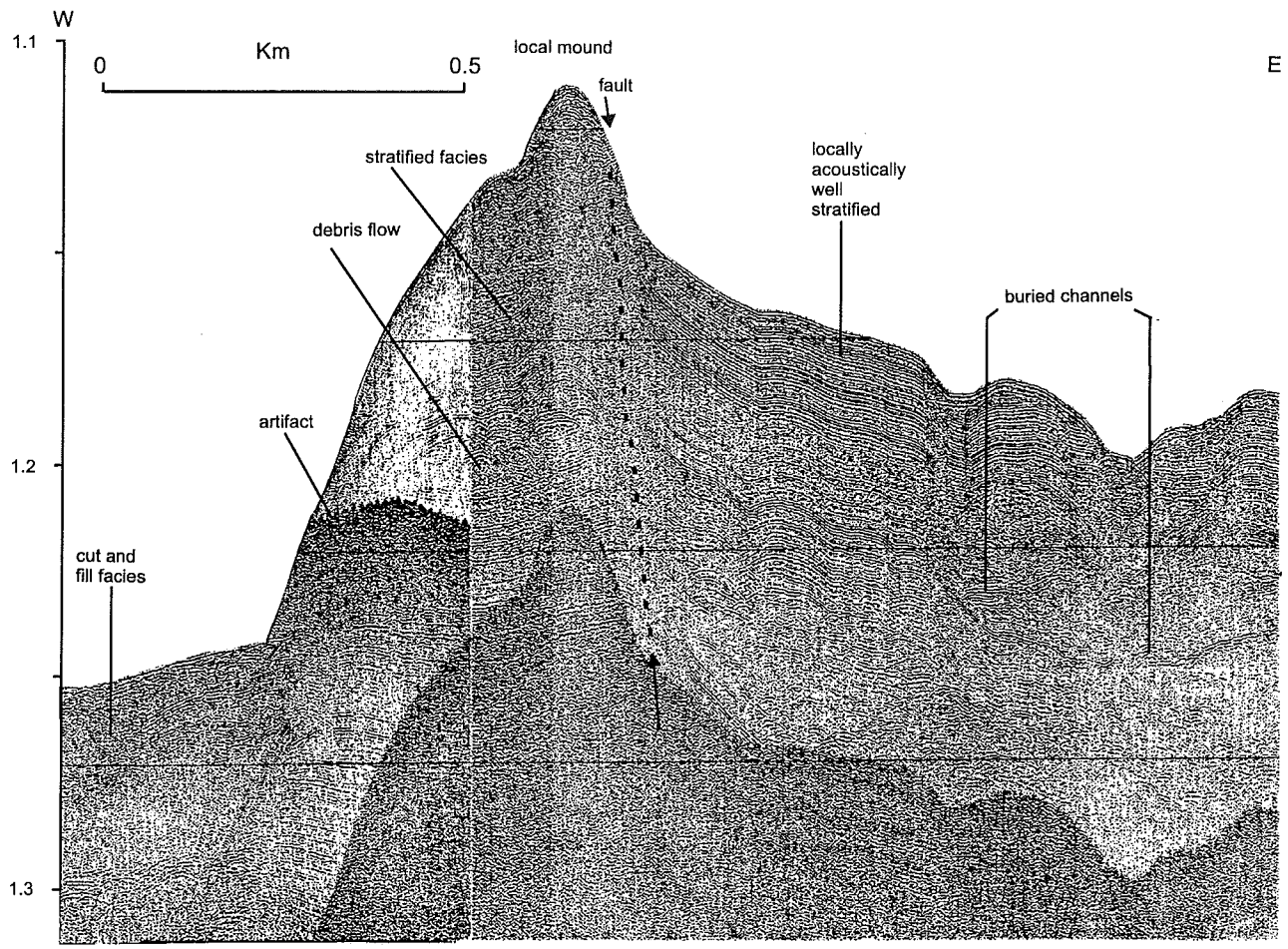

Fig. 4.19. Deep-towed sparker profile showing mud mound developed along fault north Shelburne G-29 well.

99-036
Huntec
st:250T0545
ed:250T0605

C:/IErnest/revised/fig4_19.cdr

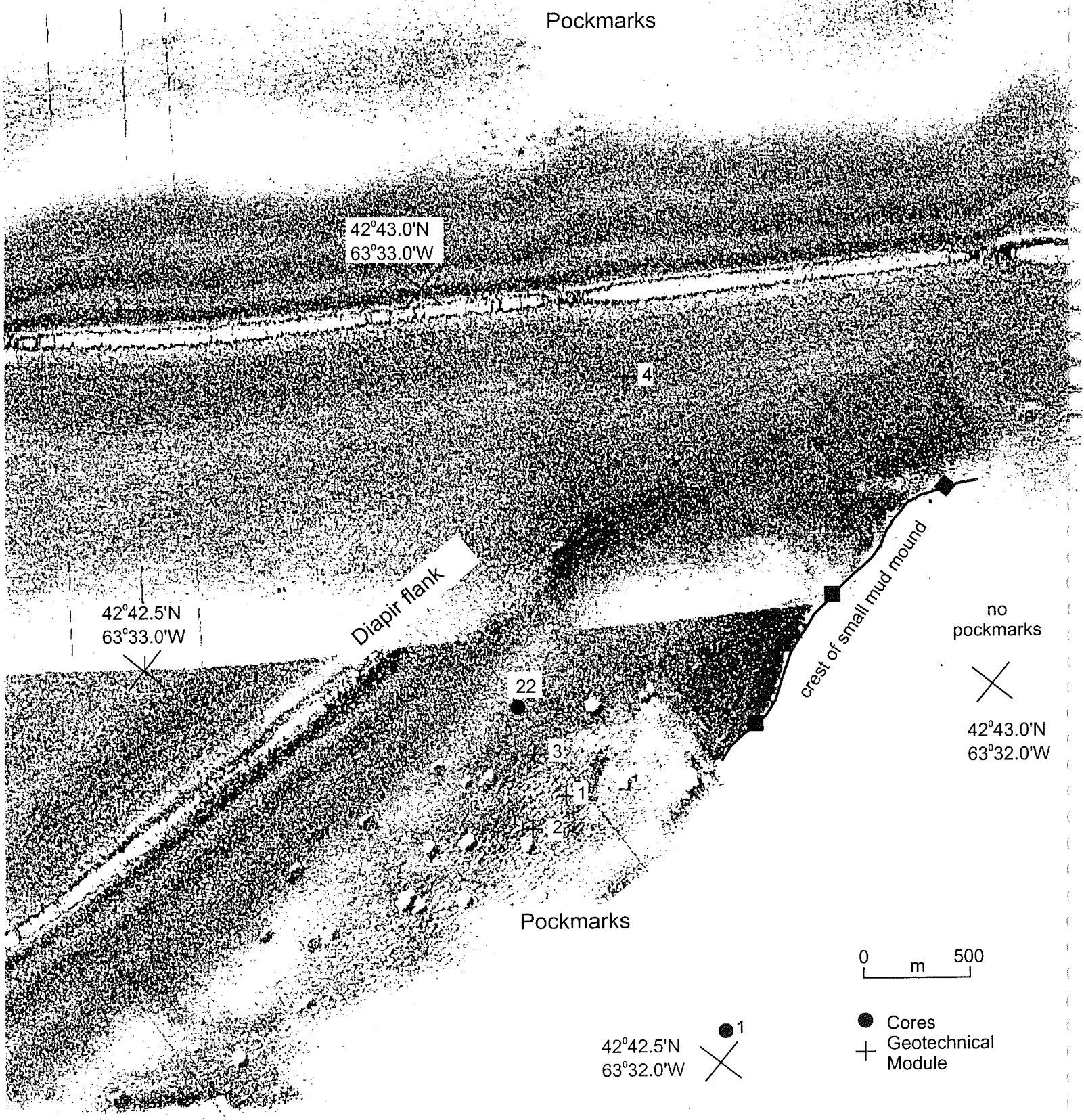

Fig. 4.20. SAR 1 km swath sidescan showing pockmarks over a mud diapir, north of Shelburne G-29 well.

C:/!Ernest/revised/fig4_20.cdr

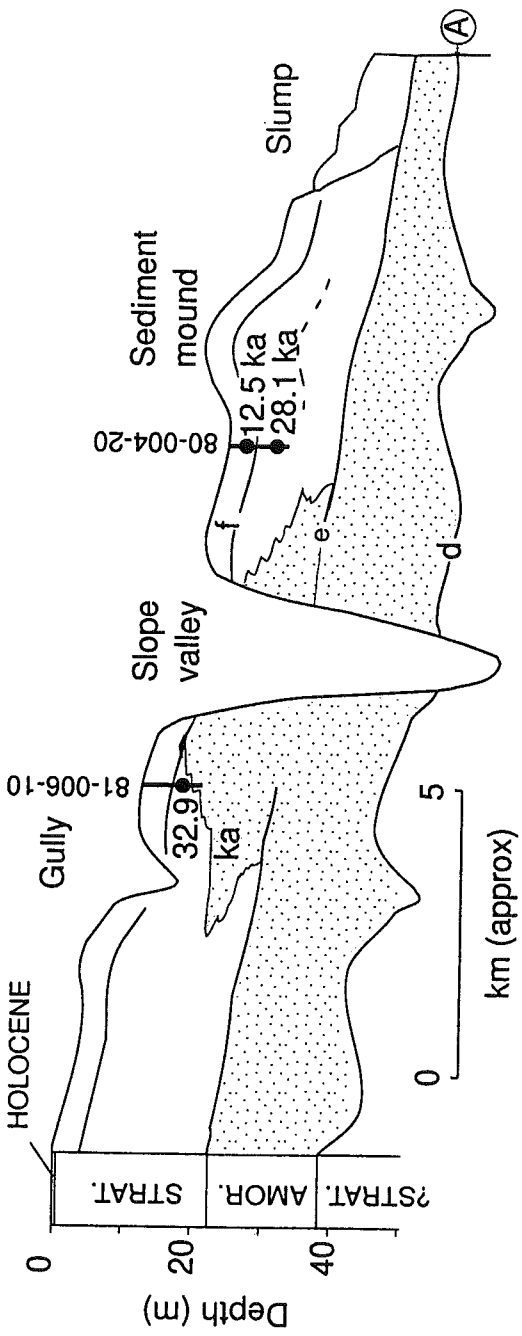

C:/IEmest/revised/fig4_21.cdr

Fig. 4.21. Near-surface acoustic stratigraphy of the eastern part of the transect (based on Piper and Sparkes, 1987 and Hill, 1984).

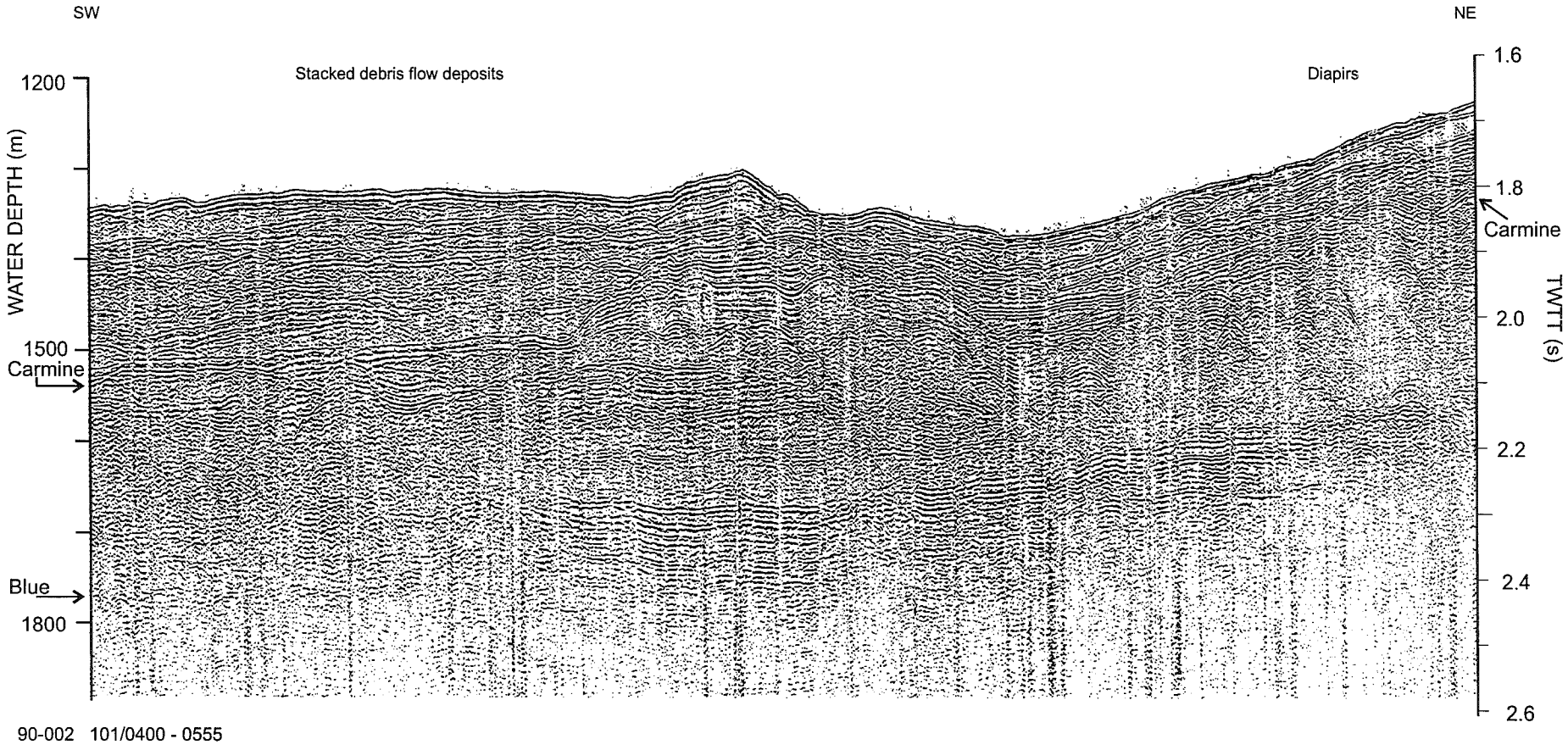

Fig. 4.22. Seismic reflection profile (40 cu in airgun, single channel) across the lower slope south of the Shelburne G-29 well showing mud diapirs in the northeast and stacked debris flow deposits in the southwest.

C:\Ernest/revised/Fig4_22.cdr

Fig 4.22

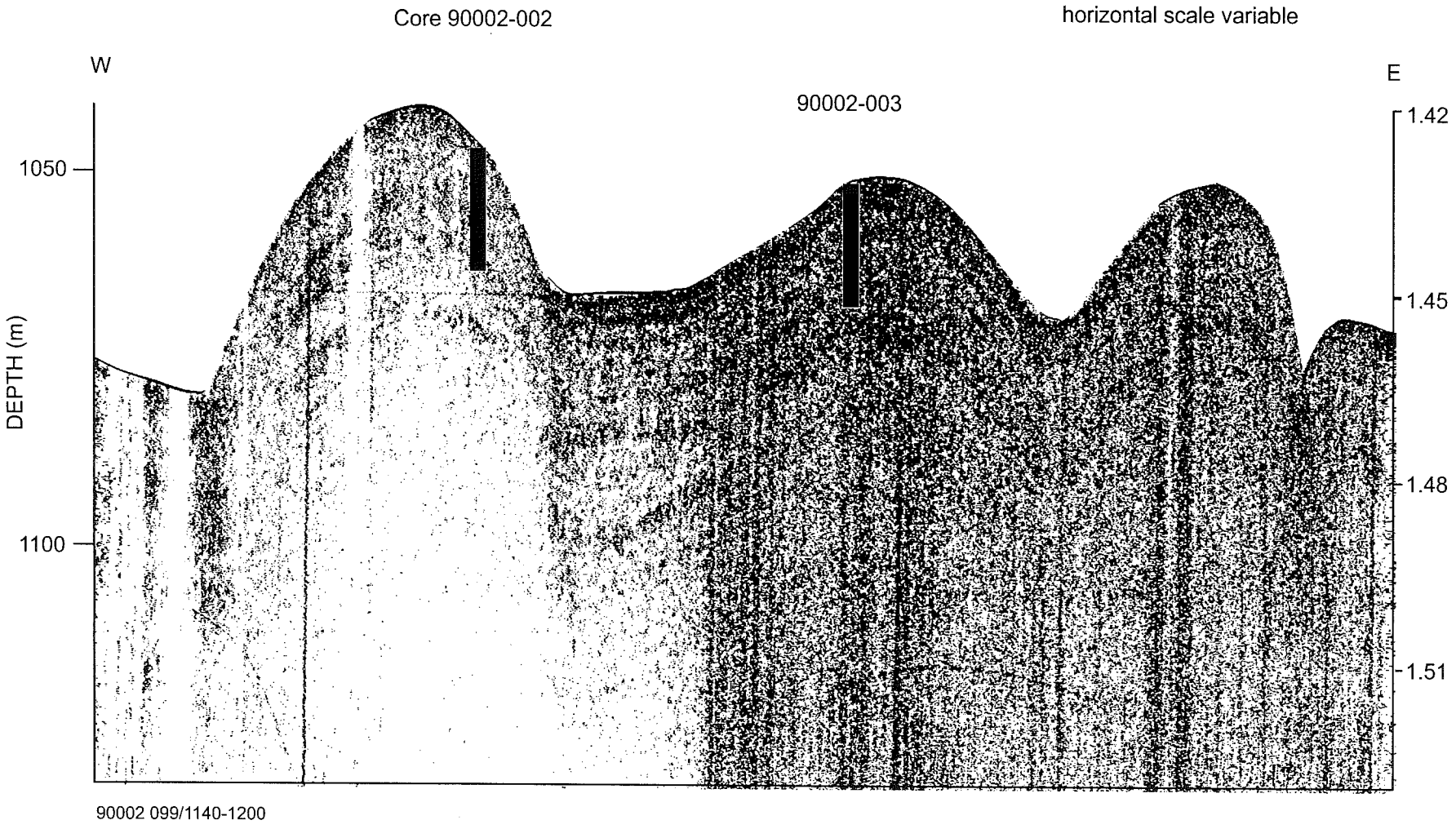

Fig. 4.23. 3.5 kHz profile showing location of cores 90002-002 and 003(cf. Fig.3.4) on low levees adjacent to filled slope channels.

C:/IErnest/revised/fig4_23.cdr

Fig 4.23

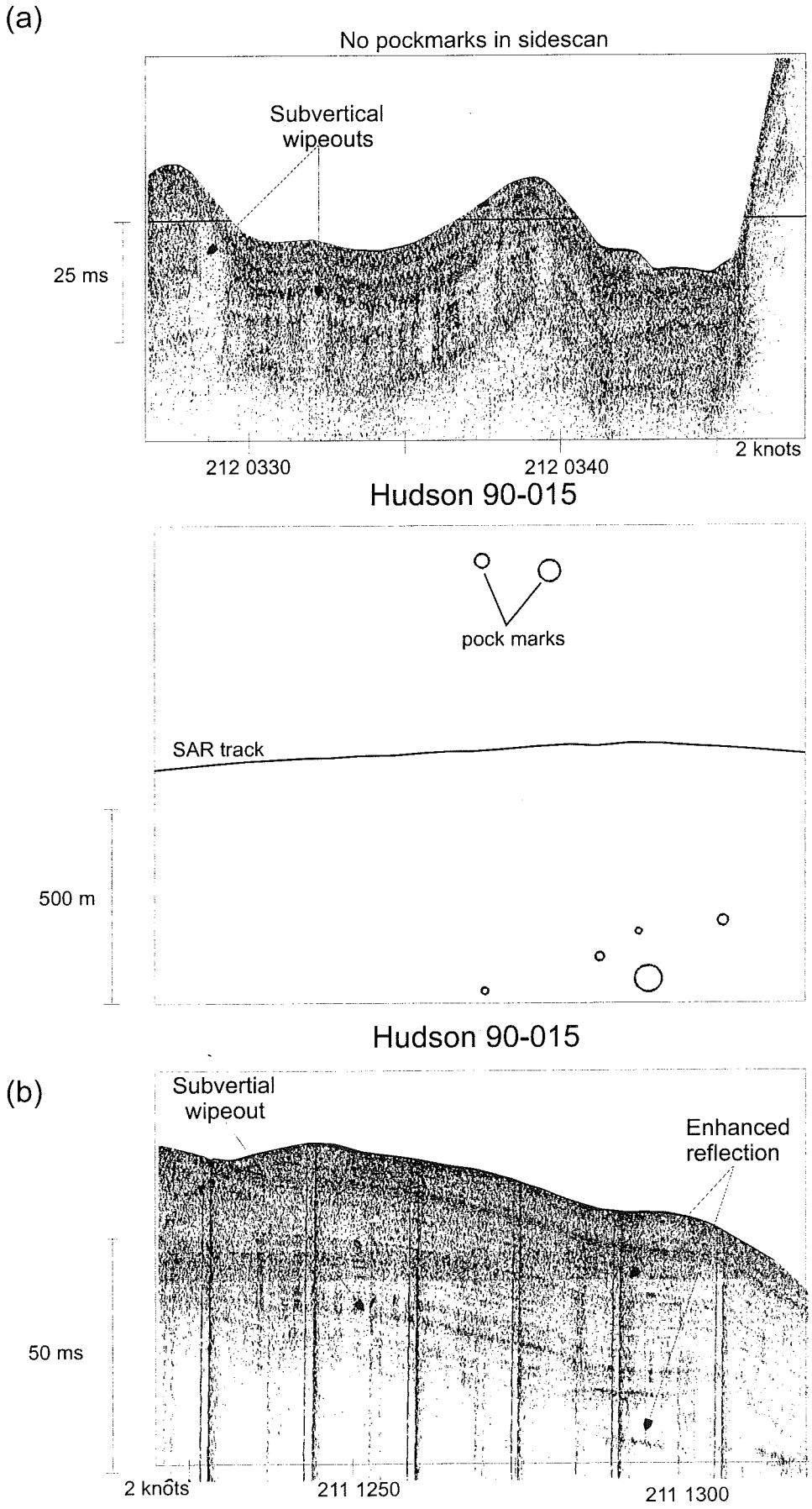

Fig 4.24. 3.5 kHz profiles and corresponding pockmark distribution on upper slope in zone A.

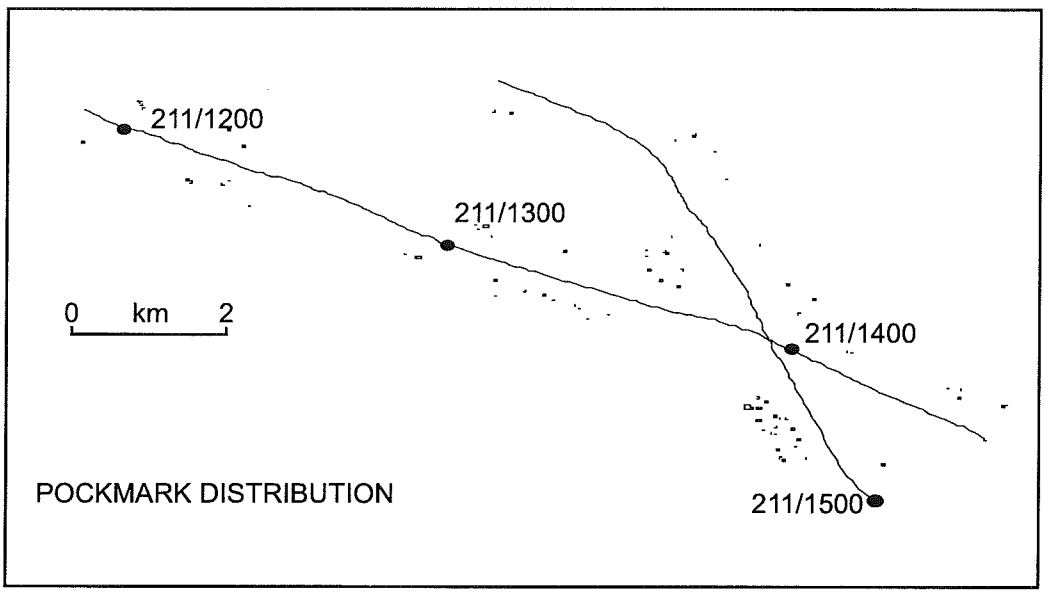

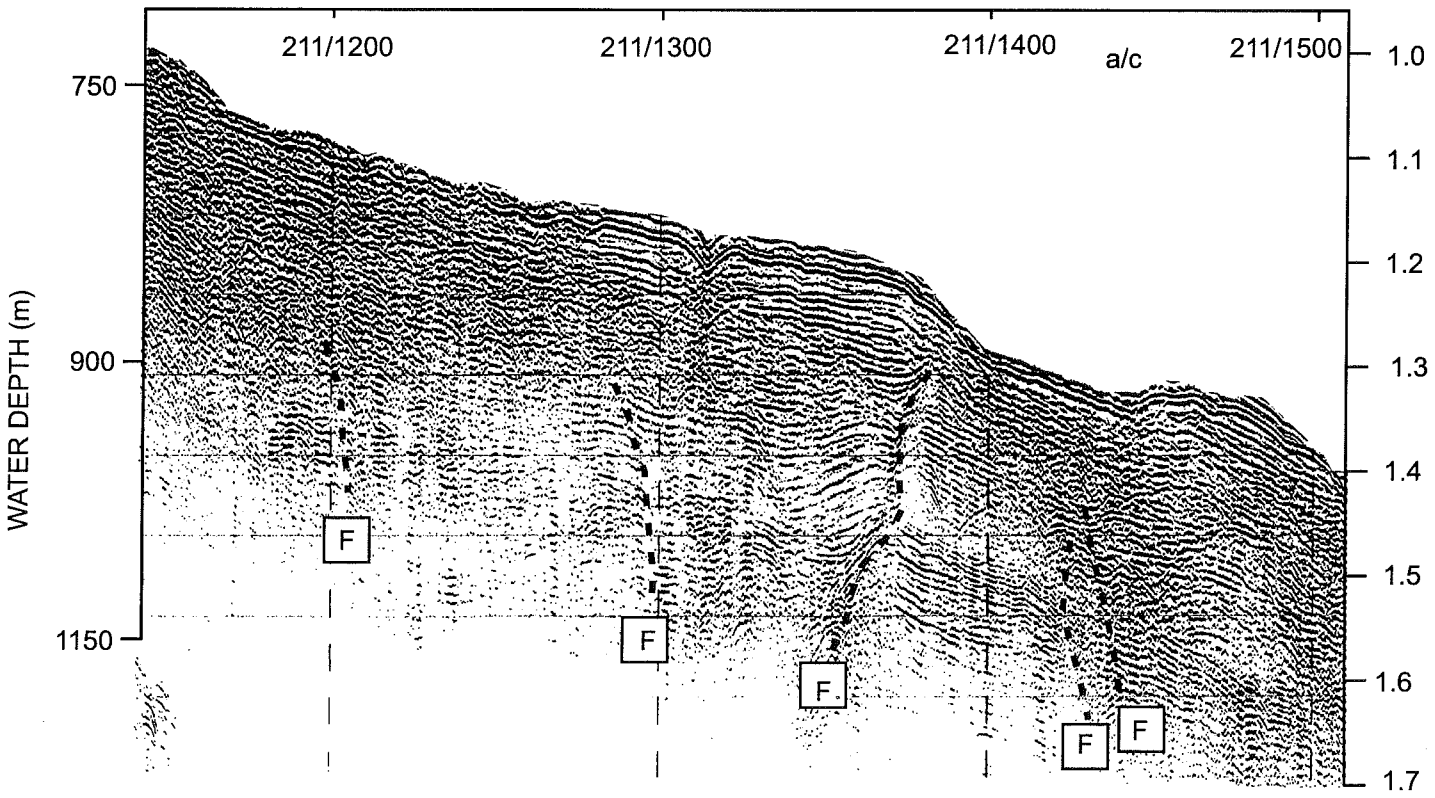

Fig. 4.25. Seismic reflection profile showing faults and corresponding distribution of pockmarks.

C:/!Ernest/revised/fig4_25.cdr

5. Slope off Emerald Bank

5.1 **Introduction and bathymetry**

The shelf break off Emerald Bank lacks deeply incised submarine canyons, other than the U-shaped trough of Mohican Valley (Fig. 5.1). Small submarine canyons are developed west of Mohican Valley, above the Albatross well site.

Detailed studies using seismic, sidescan and cores have been carried out in the area around the Albatross well site (Shor and Piper, 1989). The prominent debris flow that extends from near the Albatross well site to the continental rise has been the subject of detailed investigation (Berry, 1992; Mulder et al., 1997). The Late Cenozoic seismic stratigraphy of the entire area has been synthesized by Piper and Sparkes (1990).

The shelf break throughout this sector is at 120-140 mbsl. In the area near the Albatross well, the upper slope is smooth down to 450-550 mbsl and the mid slope between 500 and 1000-1200 m is dissected by small submarine canyons. Sidescan data shows that the upper parts of the canyons display pinnate gully patterns and complex tributary patterns. Canyons pass downslope into a few major slope valleys, partly obscured by the late Pleistocene Albatross debris flow (Shor and Piper, 1989). Mohican Channel is a major valley seaward of the central part of Emerald Bank. It differs from most canyons in having a 10 km wide flat floor and lacks a pinnate network of feeder canyons.

5.2 **Late Cenozoic framework**

Mohican Channel

Because the type section of the late Cenozoic section lies to the east (Table 1.1), we first describe the seismic framework around Mohican Channel and then extend correlations westward to the Albatross well site area. In water depths of 1300 - 1900 m there is a grid of exploration seismic lines shot for Shell that cross Mohican Channel obliquely. The canary reflector extends beneath the modern Mohican Channel area without significant relief. The character of canary is clearly shown on dip lines, for example line 190 (Fig. 5.3). Down-dip, canary appears to be a conformable reflector about 0.4 secs above a regional planar unconformity (Oligocene unconformity). Updip, canary abruptly becomes a high-amplitude reflection that is unconformable on underlying mounded high-amplitude reflections. Further updip, this surface is marked by lower amplitude reflections and it eventually onlaps the Oligocene unconformity in about 1300 m water depth (Figs. 5.3, 5.4). This discontinuous planar character of canary is similar to the character described by Swift (1987) for his CS2 unconformity, which he interpreted as resulting from bottom current erosion.

Strata above canary are generally conformable in deeper water, but downlap in mid-slope areas (in present water depths of less than 1200 m). The 0.5 secs of strata between canary and the next prominent reflector, orange, are characterised by well stratified low-amplitude reflectors, which increase in amplitude upwards. The orange reflector is generally planar and unconformable.

The lavender reflector is likewise a planar unconformable surface. Downslope it cuts down to the orange reflector, and locally shows shallow channel cutting. The 0.2 secs above lavender consist in many places of cut and fill structures with local mound deposition. Overlying this irregular seismic facies with a planar unconformity is a series of parallel, sharp but low amplitude reflections (Fig. 5.4) 0.1 to 0.2 secs thick. This package locally (Fig. 5.5, sp 4500 - 4600) shows downlap on the basal unconformity and possible levee-type growth. Regional correlation places this sequence immediately below the red reflector. The seismic character of this sequence is very similar to the parallel reflectors below the red reflector recognised in high-resolution multichannel profiles in the Acadia-Shubenacadie region (Piper et al., 1987).

Two prominent channelling erosional surfaces are recognised above this package of parallel reflectors and are correlated regionally with the red and blue reflectors. In many places, the red reflector appears to have been cut out by deeper erosion of the blue reflector. Erosion is deepest just east of the modern Mohican Channel (Fig. 5.6).

Irregular cut and fill deposition, the details of which cannot be resolved, continue upwards to a prominent change in reflector character that is correlated approximately with the carmine reflector (although the problems of correlating near-surface reflectors on industry exploration seismic means that the reflector might correlate as deep as gold or as shallow as brown). On the eastern flank of the buried Mohican Channel, this reflector is unconformable over stratified channel margin sediment (Fig. 5.5). Above this reflector, reflectors appear continuous and draped.

Albatross area

A grid of dip and strike industry profiles is available west of the Mohican Channel. An independent stratigraphic scheme was originally erected for this area, but was subsequently correlated with the type section near the Acadia well.

In strike line A3900 (Fig. 5.6), the orange reflector is continuous beneath Mohican Channel, and the lavender reflector is only just cut, so that there is no doubt as to its continuity to the west. Shallower reflectors cannot be traced across Mohican Channel. Furthermore, shallow diapirism in the Albatross to Shelburne area hinders correlation both along strike and down dip. The lavender reflector is the deepest reflector normally visible in single channel air gun profiles from the Albatross area, described below. Reflector continuity in these higher resolution profiles has been used to confirm correlations made on the lower resolution industry profiles.

The uppermost acoustic unit consists of subparallel low amplitude reflections, and thins rapidly seawards. The basal reflection can be seen on profile 178 (not illustrated) to be locally erosive and here can be correlated with carmine on the eastern side of Mohican Channel. West of Albatross, carmine rests apparently unconformably on an acoustically incoherent unit characterised by numerous hyperbolic diffractions in industry seismic lines (Fig. 4.5). The base of this package is in places a horizon correlated approximately with blue in the type area, and in places a shallower horizon which may correlate approximately with grey. East of Albatross, well stratified sediment underlies carmine (Fig. 5.7). One erosional horizon is correlated (on the basis of its apparent stratigraphic level) with the erosion surface just below grey in the type area.

A more prominent erosion surface, with local channelling and deposition of acoustically reflective facies, can be traced throughout most of the area west of Mohican Channel. This surface is approximately at the same stratigraphic level as the blue reflector in the type area, although no certain correlation is possible. It overlies a thick well stratified package on the mid slope (Fig. 5.7), which is truncated by a relatively planar erosional surface (Figs 5.7; also Fig. 4.5): this surface may be tentatively correlated with red in the type area. Beneath this surface is a package of well stratified reflectors overlying and locally downlapping (Fig. 4.5) onto an erosional horizon which can be traced along strike into the lavender reflector east of Mohican Channel.

Beneath lavender, there is another package of stratified sediment overlying an erosional horizon correlated by reflector continuity with orange in the type area. Canary shows the same character as in the Shubenacadie area: it forms a high-amplitude planar reflector which ends abruptly both up and down-dip (Fig. 5.7).

Detailed studies of upper Mohican Channel and the slope to the east

High-resolution multichannel seismic sections (Fig. 5.8) through Mohican Channel show a complex history of cut and fill. Immediately east of Mohican Channel, the section below grey (C) is evenly stratified and probably represents highstand slope sedimentation. Between grey and rose, a series of shallow channels and intervening stratified sediment is visible. Some of the channel fill may be debris flows. At about the rose reflector, there is a major erosion surface and a channel is developed immediately east of modern Mohican Channel, with complex onlapping fill up to the flesh reflector and a levee-like deposit to the east. Above the flesh reflector, well stratified sediment drapes the underlying topography. Small failures are recognised at three horizons (a, b, c), the shallowest at the seabed and partially filled with a debris flow or rotational slump.

Beneath Mohican Channel, the oldest erosion surface cuts down to below the red reflector. This erosion surface appears to date from the grey to rose interval, although it is possible that it is younger. The nature of the deeper fill is unclear. Higher in the section, intervals of incoherent reflections are followed by stratified fill. At least four distinct horizons of incoherent reflections are recognised, the last being close to the seafloor. This

youngest incoherent fill appears to correlate with the multiple debris flows that fill the channel in deeper water (Fig. 5.18). Incoherent fills 1 and 2 appear to be younger than the brown reflector and may thus correlate with the two till tongues above brown illustrated in Figure 6.7.

East of Mohican Channel, an incoherent unit just above grey is imaged in well-site survey quality multichannel seismic profiles from cruise 81044 (Fig. 5.9). It is not clear whether this unit is a buried blocky debris flow (as suggested by the overlying high amplitude ?channel-fill reflections) or whether it represents interstratal deformation (with a possible sideswipe of a small diapiric structure). Immediately above grey at the eastern end of line 47 of 81044 (Fig. 5.8), apparent channel fill deposits and stratified sediment are cut by a major erosion surface and do not continue laterally. This geometric relationship is more consistent with a debris-flow origin than interstratal deformation. This debris flow is at the same stratigraphic horizon as the flow near Shelburne that appears to show mud diapirism and Quaternary fault offsets on overlying strata (Fig 4.11).

Detailed studies near the Albatross well

High-quality single channel airgun profiles were obtained in the vicinity of the Albatross well (Fig. 5.10) during a SeaMARC I deep-water sidescan survey, run at 2 knots. This data is supplemented by later single-channel airgun profiles run at 5 - 6 knots. The outer shelf shows a series of stacked deltas (Fig. 5.11), overlain by a thin acoustically incoherent section, leading to a generally progradational continental slope. On the upper slope (Fig. 5.12), two seismic sequences are visible above the Miocene (F) unconformity. The lower sequence (from B to F) consists of evenly prograded stratified sediment cut by a few shallow valleys (100-200 msecs deep). These include ancestral valleys near the site of the present Tern, Puffin and Egret valleys, but also two valleys that have no marked expression at the present surface. All of these valleys lack prominent levees.

The style of sedimentation above the B reflector is totally different. The major valleys, such as Tern and Puffin, have complex cut and fill sequences and are separated by high levees (Fig. 5.12a). Smaller gullies are developed, particularly west of Puffin Valley, again separated by high levees. Many gullies have persisted to the present seabed; some are present only at certain stratigraphic horizons and have subsequently been filled.

On the mid slope (Fig. 5.13), the same two-fold division can be recognised. In the sequence below B, ancestral Skua Valley (Fig. 5.13b) was a broad shallow valley, wider than the modern valley, but with lower levees, which extended over a broad area west of the valley. To the west, beneath modern Puffin Valley, there are irregular alternations of well stratified reflector packages with zones of incoherent reflectors, generally with relief of less than 50 msecs. This incoherent facies is interpreted as aggrading debris flow deposits, locally cut by sandy channel deposits. Westward, beneath modern Heron and Egret valleys (Fig. 5.13a), this facies passes up gradually into more laterally extensive stratified reflector packets, interpreted as intervalley muds, with the development of levee-like mounds close to channels. At an interval near the blue reflector, a broad valley

underlies the modern Albatross Ridge (Fig. 5.13a).

In the mid to late Pleistocene (corresponding to above B), this stratified sequence was partially reworked by erosion in modern Egret Valley. To the west of Egret Valley, the Albatross Ridge appears to have become a progressively more elevated relief feature as a result of mound-like deposition above the B reflector. A body of acoustically incoherent material up to 100 ms thick fills modern Puffin Valley (Fig. 5.13b) and corresponds to the debris flow deposit recognised in sidescan sonographs. Unlike the more deeply buried incoherent facies, which probably include considerable amounts of channel-fill facies, this facies does not have laterally equivalent levee deposits.

Diapirism is widespread in water depths of 1000 to 1500 m ("DI" in Fig. 5.10), mostly affecting Tertiary sediment immediately below the lavender reflector. Some diapirs are developed below grey and cut the B reflector. Both our data and exploration seismic profiles indicate that these diapirs are shallow-rooted, as also noted by Piper and Sparkes (1987) 30 km to the east, but we have insufficient acoustic penetration to define their character in detail. They are developed in areas of alternating coarser and finer sediment packages, and may result from overloading of rapidly deposited muds by coarse sandy deposits or debris flows.

On the lower slope (Fig. 5.10), above reflector orange, zones of acoustically incoherent sediment alternate with zones of well stratified sediment (Fig. 5.14). The incoherent sequence below lavender is up to 0.4 secs thick beneath Tern Valley (Fig. 5.14), thinning to less than 0.2 secs to the east, where it appears more stratified, although incoherent seismic facies and hyperbolic reflections (probably indicating shallow valleys in thin debris-flow deposits) remain widespread, particularly in the lower part of the interval.

The lavender reflector is a fairly continuous, prominent reflector (Fig. 5.14), marked by shallow channel-like morphology in two places, one beneath Tern Valley and the other 15-20 km to the west. The section immediately above lavender is more stratified than the underlying sequence. Incoherent facies fills two channel-like features, one just west of Tern Valley (Fig. 5.14a) and the other 10-15 km to the west. The overlying sediment package is generally incoherent, with local discontinuous reflectors. The top of this package is marked by a prominent irregular reflecting surface that in places is marked by hyperbolic reflections corresponding approximately to grey. This incoherent package is thin (0.05 secs) beneath Tern Valley in the east and Egret Valley in the west, and thickens (0.2 secs) immediately west of Tern Valley. The overall convex-up morphology of this unit and its rough upper surface indicate that it is most probably an old debris flow deposit. The prominent upper reflector may mark the impedance contrast between a blocky debris flow with well lithified blocks and overlying unconsolidated muds. The debris flow was largely removed by subsequent erosion from the valleys. Above reflector grey, sediment is more stratified, with local development of incoherent facies. The sequence shows the same trend as the underlying strata of progressive eastward thickening towards Tern Valley; but substantial thicknesses of sediment (up to 0.4 secs) have been removed by subsequent erosion in Tern and

Puffin Valleys (Fig. 5.14b).

Tern Valley has persisted as a distinct morphological feature throughout the entire sequence from just below lavender. Sediment sequences appear condensed within the valley, but particularly thick sequences have been deposited on the western levee. A smaller valley persisted through the interval around lavender, with slight lateral migration, beneath the lower part of the modern Puffin-Heron valley system. This was blocked by a major sediment deposit between grey and lavender, but the contemporary seabed once again appears predominantly erosional, with at least 0.2 secs of sediment present on the levee between Puffin and Tern valleys that is absent within Puffin Valley. What may have been an original north - south downslope trend of Puffin-Heron valley has been blocked by a diapir, which appears to have diverted the valley westwards (Fig. 5.13a).

Although Egret Valley continues downslope as a distinct morphologic feature (Fig. 5.10), its geologic history is quite different from Tern Valley. Egret Valley crosses a broad area with a persistent low sedimentation rate in which major erosional features are lacking, although shallow channels are visible through much of the sequences above lavender.

5.3 **Late Quaternary sedimentation**

High-resolution seismic data

In the Albatross area, the upper slope from 140 to 550 mbsl is relatively flat and has a gradient of about 7°. This seabed is floored by sand. Huntec boomer and 40 cu. in. airgun profiles[1] suggest that the upper slope is a constructional sandy deposit, overlying a sloping till ramp that outcrops at about 220 mbsl. Other overconsolidated surfaces may outcrop in deeper water, although the overall form of the upper slope is progradational. On the outermost shelf, the till ramp overlies principally prograding deltaic deposits (Fig. 5.11) similar to those found off Sable Island Bank (MacLaren, 1988). A series of slope canyons head in 550 to 700 m water depth and have been imaged both by SeaMARC 5-km swath sidescan (Fig. 5.15) and by SAR 1 km swath sidescan, illustrated in Baltzer et al. (1994). These canyons lead downslope into a series of valleys, which are partly filled by several large debris flows that cover the lower slope (Figs. 5.13, 5.14) and continental rise (Fig. 5.16) below the Albatross well. The flows on the rise were studied in an M.Sc. thesis by Berry (1992).

The flows near the Albatross well and their putative source areas on the upper slope were imaged by 5 km swath SeaMARC (Shor and Piper, 1989) (Fig. 5.15) and 1 km swath SAR sidescan (Baltzer et al., 1994). Mulder et al. (1997) distinguished two near-surface debris flows (DF1 and DF2) that were together termed the Albatross Debris Flow in the older literature. DF1 generally appears rough whereas DF2 is smooth (Fig. 5.17). The mapped distribution of the surficial debris flows suggests that they originated on the continental slope

[1] HU86034, JD317, 0900-1200Z

between Albatross Ridge and Tern Valley (Fig. 5.10). SeaMARC 5-km swath sidescan imagery shows that much of the middle slope, from 550 - 1000 m water depth, is cut by canyons and gullies. Part of this area has a rough "ridge and gully" topography characterized by pinnate patterns of small gullies. A large area, however, appears smoother in the sidescan imagery with only the larger canyons and gullies visible (Fig. 5.15). In the few areas where acoustic returns are coherent, the 3.5 kHz profiles show weak reflectivity in the area of small pinnate gullies but a harder prolonged return in the smooth area, which also returns more energy with small airgun seismic. One module géotechnique penetration in this smooth area (HMG9-1) reached a cone resistance of > 1000 kPa (shear strength ~ 65 kPa) at about 70 cm depth whereas penetrations in the area of small pinnate gullies showed normal consolidation with cone resistance of about 100 kPa at 2 m depth (Baltzer et al., 1994). As best can be seen from the sidescan data, the source area for the Albatross debris flows terminates upslope in a series of scarps in water depths of 550 - 700 m that mark the heads of the submarine canyons on this sector of the slope.

A small amount of high-resolution Huntec DTS sparker data is available from lower Mohican Channel (Fig. 5.18). It shows a series of at least five relatively transparent debris flows overlying well stratified sediment. The acoustic transparency of the debris flows suggests that they were derived from failure of muddy slope sediment, rather than being ice-margin mass flows including coarser sediment.

Core stratigraphy

A preliminary interpretation of late Quaternary sedimentation near the Albatross wellsite was provided by Shor and Piper (1989): this is summarised here and amplified with new data. Available cores are from three main settings. The longest stratigraphic section is from the muddy Albatross Ridge (a levee like feature), where core 88010-23 recovered 7 m of bioturbated sediment with scattered ice-rafted detritus (Fig. 5.19). A brick red mud horizon (probably **b**) occurs at 30 cm depth, suggesting that the Holocene section is thin. A few thin fine sand beds, presumably of turbidite origin, interbed with the bioturbated muds.

Core 86034-41 (Fig. 5.19) is from the depositional turbidite plain on the lower slope west of Albatross Ridge (Fig. 5.10). The Holocene olive grey mud is about 2 m thick and overlies 0.5 m of brown mud with abundant clasts of both mud and rock pebbles, together with rare shell fragments and a scaphopod that yielded a 13.2 ka date. This interval is interpreted as a debris flow deposit. It overlies 40 cm of red brown mud that might represent a diluted brick-red sandy mud interval (?bed **d**). In nearby core 86034-39, both brick red sandy mud beds **b** and **d** appear to be present. The debris flow deposit in 86034-41 is tentatively correlated with regional debris flow 1 (Fig. 5.22). The abundance of rock pebbles suggests a source on the upper slope. This debris flow overlies several metres of muds with sand beds of various thicknesses, with a date of 16.05 ka near the base of the core. The upper part of this section is red brown, the lower part dark brown. Similar sections are

seen in other cores in this area (Fig. 5.20), one of which includes a date of 18.7 ka (approximately the last glacial maximum) near its base.

A core downslope from the Albatross area on a low levee on the continental rise (Fig. 5.21) was described briefly by Berry and Piper (1993). It consists of late Holocene foraminiferal ooze overlying early Holocene olive grey muds and late Pleistocene brown mud turbidites. A few thin debris flow deposits and sands interbed with the mud turbidites. The shallowest debris flow deposit is muddy and overlain by brick-red sandy mud b; it may correlate with debris flow 2 in the Albatross area. A radiocarbon age of 20.9 ka was obtained from foraminifera near the base of the core.

Cores from the blocky Late Pleistocene debris flow (e.g. 86034-35, Fig. 5.20) show mud clast conglomerate overlain by a few thin sand to mud turbidites and then olive grey mud. A core from the smoother area (86034-36) shows two debris flows. The upper one has the coarse sand, mud clasts, shell fragments rock clasts typical of debris flow 1 in core 86034-31. A shell near the top of the debris flow yielded an age of 14.3 ka, providing a maximum age for the debris flow. Furthermore, the similar debris flow deposit in core 86034-41 contains a shell of 13.3 ka and a probably correlative debris flow on the slope east of Mohican Channel in core 78005-77 contained a 13.0 ka shell (TO-2455) and was overlain by a 11.35 ka shell (TO-2453) (Piper and Skene, 1998). This upper debris flow in 86034-36 overlies fine sand and bioturbated brownish mud that in turn overlies a blocky mud-clast conglomerate, interpreted as regional debris flow 2. A proximal debris flow of mud clasts, resembling debris flow 2, in core 90015-19 is bracketed by radiocarbon ages on shells of 12.5 ka (TO-2084)[1] above and 13.35 ka (TO-2086) below in core 90015-19. This chronology then suggests that the debris flows date from around 13 to 13.3 ka. Brick-red sandy mud markers are not readily recognisable in cores containing debris flow deposits, except that bed **b** appears to be substantially above debris flow 2 but is perhaps older than debris flow 1 (Fig. 5.22).

Preliminary results from a core collected in August 1999 from lower Mohican Channel show that the last debris flow down the channel occurred at about 14 ka and one 10 cm thick sand bed was deposited at about 12 ka. One or more thin sand beds have been deposited in the past thousand years or so, suggesting that storm transport of sand on the shelf may occasionally initiate small turbidity currents that flow down the slope (as inferred by Baltzer et al. 1994 north of the Albatross well).

Geotechnical measurements of the Albatross debris flow

In a series of papers, Mulder and colleagues (Mulder et al., 1997, 1999) reported geotechnical

[1] note that the age of 13.4 ka (13.0 ka reservoir corrected) reported by Piper and Skene (1998) is an error (the date was determined on another core, but a typographic error was made in the lab report).

measurements on the debris flow and explore mechanisms by which it may have been initiated. In samples from the Albatross debris flow, Mulder et al. (1997) used the downcore variation of shear strength with depth to distinguish four groups of sediment on the basis of degree of consolidation:

(a) underconsolidated (Fig. 5.23):

88010-28	muddy debris flow
88-010-29	thick muddy debris flow

(b) normally consolidated (apart from some surface overconsolidation) (Fig. 5.23):

91020-9	proglacial muds
91020-13	proglacial muds, thin debris flows
91020-14	proglacial muds, thin debris flows
91020-24	proglacial muds
91020-3	debris flow matrix
91020-11	debris flow matrix

(c) overconsolidated

91020-7	eroded seabed over diapir
91020-10	blocky debris flow
91020-11	block in debris flow

(d) very overconsolidated

91020-25	blocky debris flow
91020-27	blocky debris flow

Most blocks in the Albatross Debris Flows are very over consolidated and their undrained shear resistance measured using the miniature vane shear device was as high as 70 kPa for sediment located at only 3 to 5 mbsf (Mulder et al., 1997). These high values coincide with low water content values (40 to 60%). The thickness of sediment involved in the failure at source was estimated from the undrained strength of the blocks transported by the debris and by comparison with the *Su* value if the sediment was normally consolidated (cf. Mulder et al., 1992). The estimates vary from 15 to more than 56 metres, which represents a minimum value of the depth below the seafloor of the original failure. This thickness suggests that failures occurred at large depths below the seafloor, i.e. depth greater than 50 mbsf.

Surface overconsolidation in the upper few metres is a consequence of biological cementation, as documented by Christian et al. (1991) and Baltzer et al. (1994). In normally consolidated proglacial stratified muds, the strength ratio is about 0.3 (Fig. 5.23). The underconsolidated sediments, with a strength ratio of about 0.2, are all muddy debris flows.

5.4 **Geological history and hazard assessment**

Synopsis of geological history

Late Cenozoic geological history is broadly similar to that in the better known area to the east off Western Bank. Mud diapirs of probable Pliocene age occur, similar to those to the west near the Shelburne well. Mohican Channel and the major valleys of the Albatross area appear to have been the site of broad slope channels throughout much of the late Pliocene and Quaternary. At some stratigraphic intervals, they appear filled with sands; at others with debris flows.

Upper slope progradation is of a quite different style above the B (carmine, or possibly flesh) reflector, as noted in other parts of the margin. This probably reflects the effects of shelf-crossing glaciation and proglacial plumes issuing through Mohican Channel. We have insufficient upper slope data to determine the limits of till deposition; west of the Albatross well, the outer shelf appears to be largely deltaic, like that south of Sable Island.

Distribution of shallow gas

The available SAR data near the Albatross well site shows pockmarks more abundant in 500 to 1000 m water depth than in deeper water (Fig. 5.24). This pattern is similar to that observed near the Shubenacadie well. It is not known if there is any relationship to deeper structures.

The risk of failure

Cores from the Albatross area show no evidence for any widespread debris flow deposits younger than about 11 ka. The possibility of local failure on steep headwalls of canyons later than that time cannot be excluded.

The failures above the Albatross well head in the same water depth (Figs. 5.10, 5.15) as those near the Shubenacadie well (Fig. 6.13) and those on St Pierre Slope (Piper et al., 1999), despite the rather different geological setting and gradients. The presence of undisturbed seabed down to 700 mbsl in places, before the onset of failure, indicates that bearing capacity failure from an ice load on the shelf (Mulder and Moran, 1996) is unlikely to be a cause of the observed failure. Failures in this water depth are also difficult to account for by excess pore pressure due to ice-loading (Mulder and Moran, 1996; Mulder et al. 1999), which is unlikely to be significant in water depths of more than 250 m. Melting of gas hydrates appears to be the most probable cause of excess pore-pressure leading to failure: this interpretation is discussed more fully in Chapter 10.2.

The risk from storm-driven sediment transport

Studies in this sector of the continental margin have shown the effect of large storms on transport of sand on the continental slope. Hill and Bowen (1983) showed that sorted sands and silts mantle the upper slope to water depths of 450-600 m. These are apparently derived from the outer continental shelf and remobilised by storm-driven, contour parallel currents.

North of the Albatross well, 1-km-swath SAR sidescan imagery showed a dendritic network of small middle-slope gullies (Baltzer et al., 1994, their Fig. 10). A push core on the floor of one such channel recovered 1.5 m of silty sand, with a 9.6 ka mollusc shell at 0.9 m. The sand occurred in beds 10-20 cm thick. These dendritic channels therefore appear to accumulate sand occasionally during the Holocene and may provide evidence of down-slope transport of sediment suspended on the outer shelf.

Storm-driven sediment transport is an issue to be considered in the development of any production facilities, but is not on a scale that would directly impact any exploration procedures.

Mohican Channel and boulder beds

The deep incision of Mohican Channel continues beneath the outer Scotian Shelf. The Mohican I-100 well at the edge of the continental shelf contains 950 m thickness of glacial Quaternary deposits. The channel is probably inherited from an Oligocene canyon. The rather flat floor of the Quaternary features suggests that it might be a jokulhlaup channel similar to the canyons on the eastern Scotian Slope and may therefore contain buried boulder beds.

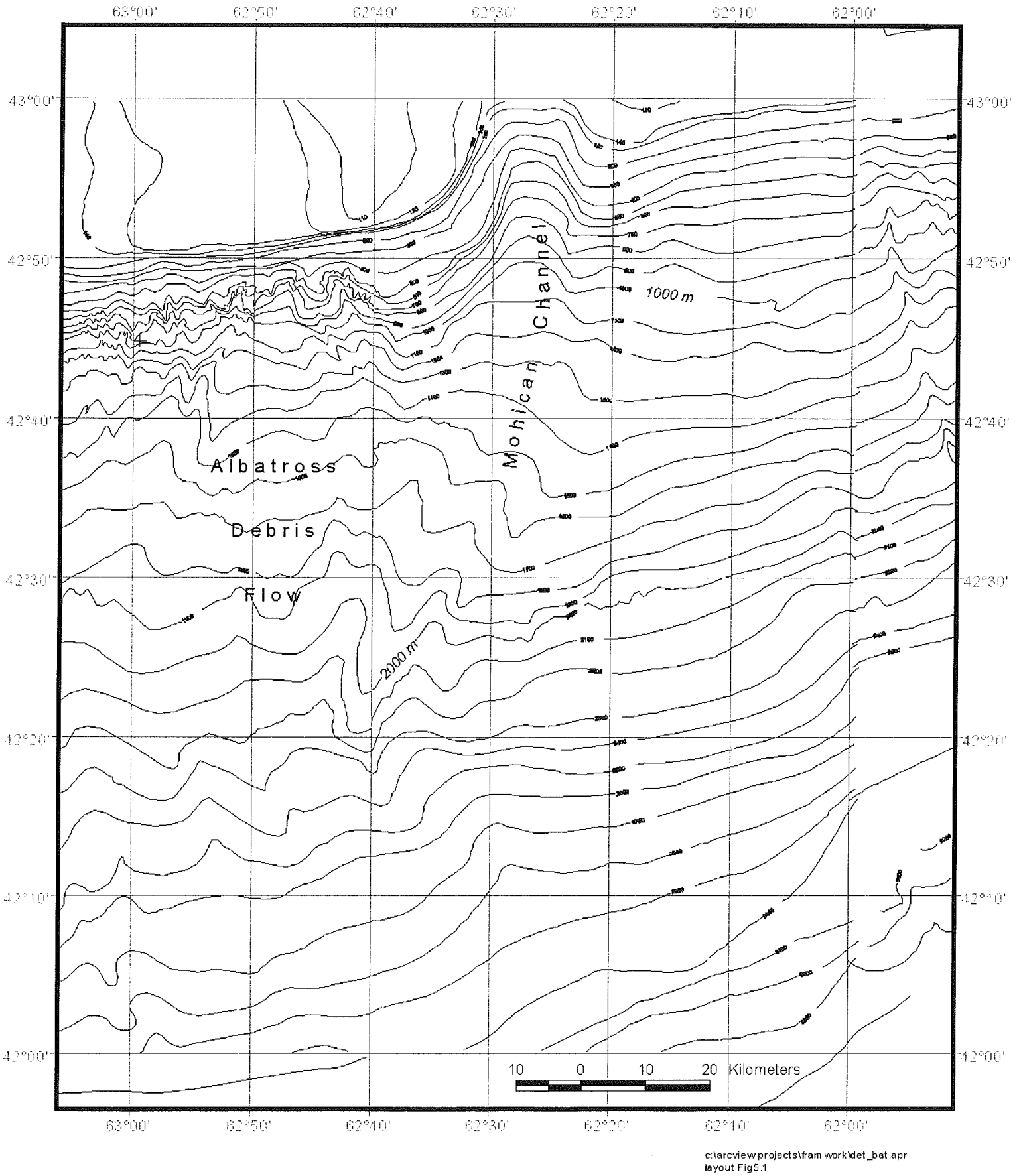

Fig. 5.1: General map showing the slope off Emerald Bank.

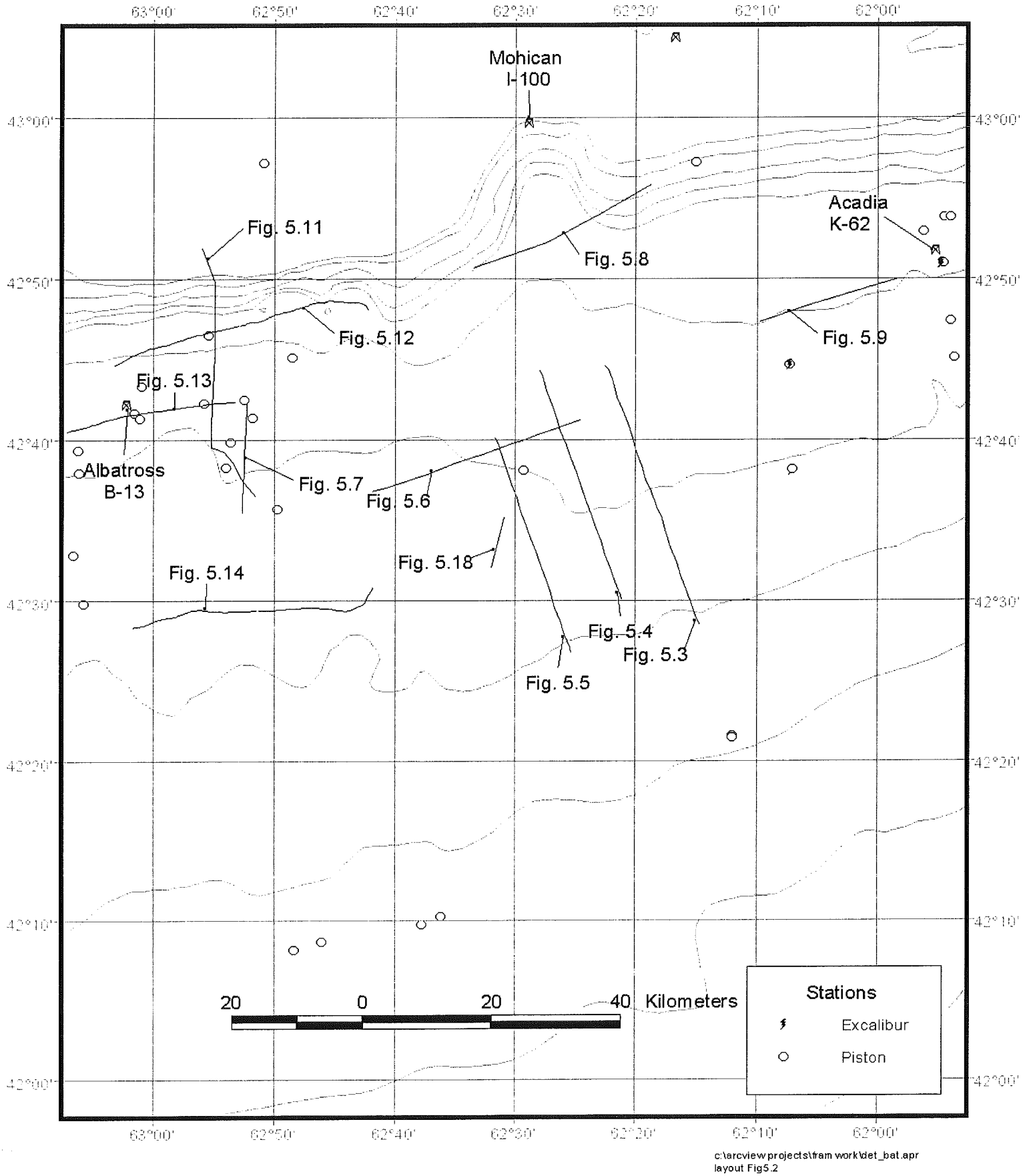

Fig. 5.2: Map showing data distribution off Emerald Bank.

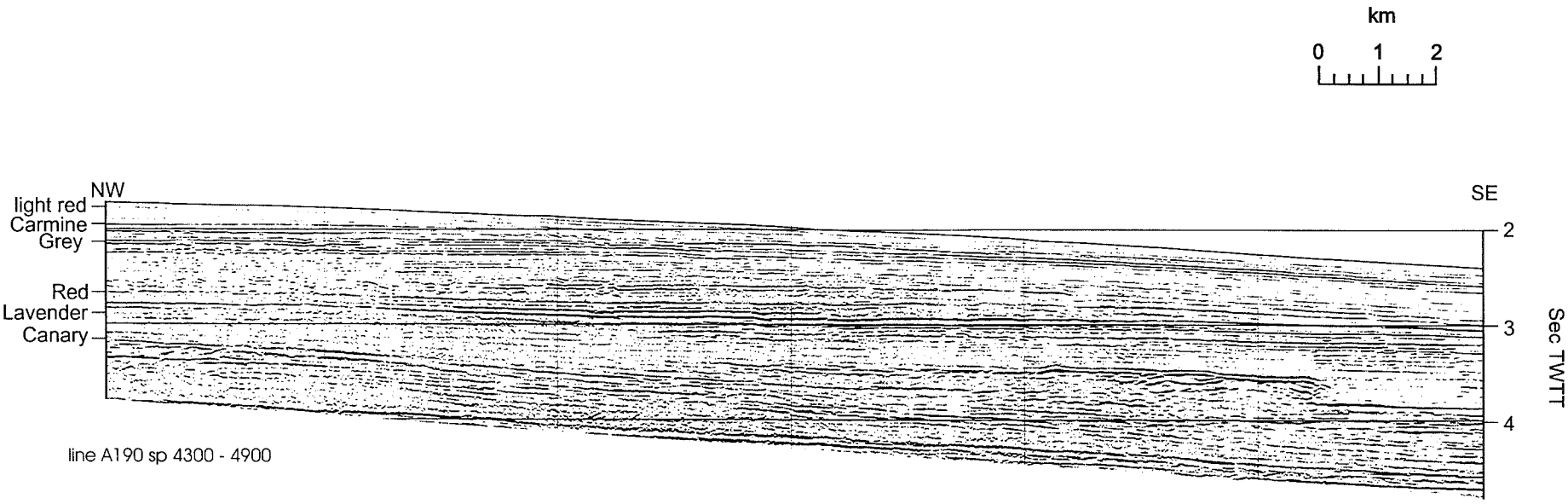

Fig.5.3. Seismic profile showing character of canary reflector and its underlying unconformity in the Mohican Channel area. (line 190, sp 4300-4900).

C:/!Ernest/revised/fig5_3.cdr

Fig. 5.3

Fig 5.4

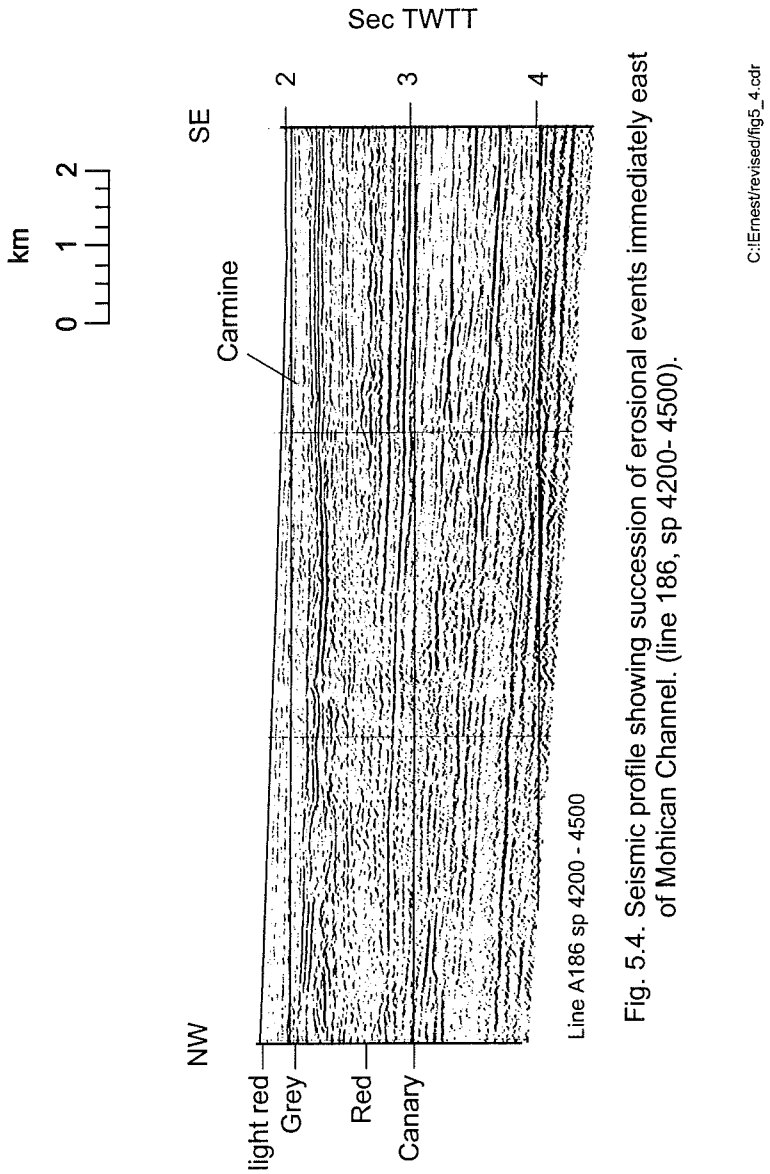

Fig. 5.4. Seismic profile showing succession of erosional events immediately east of Mohican Channel. (line 186, sp 4200- 4500).

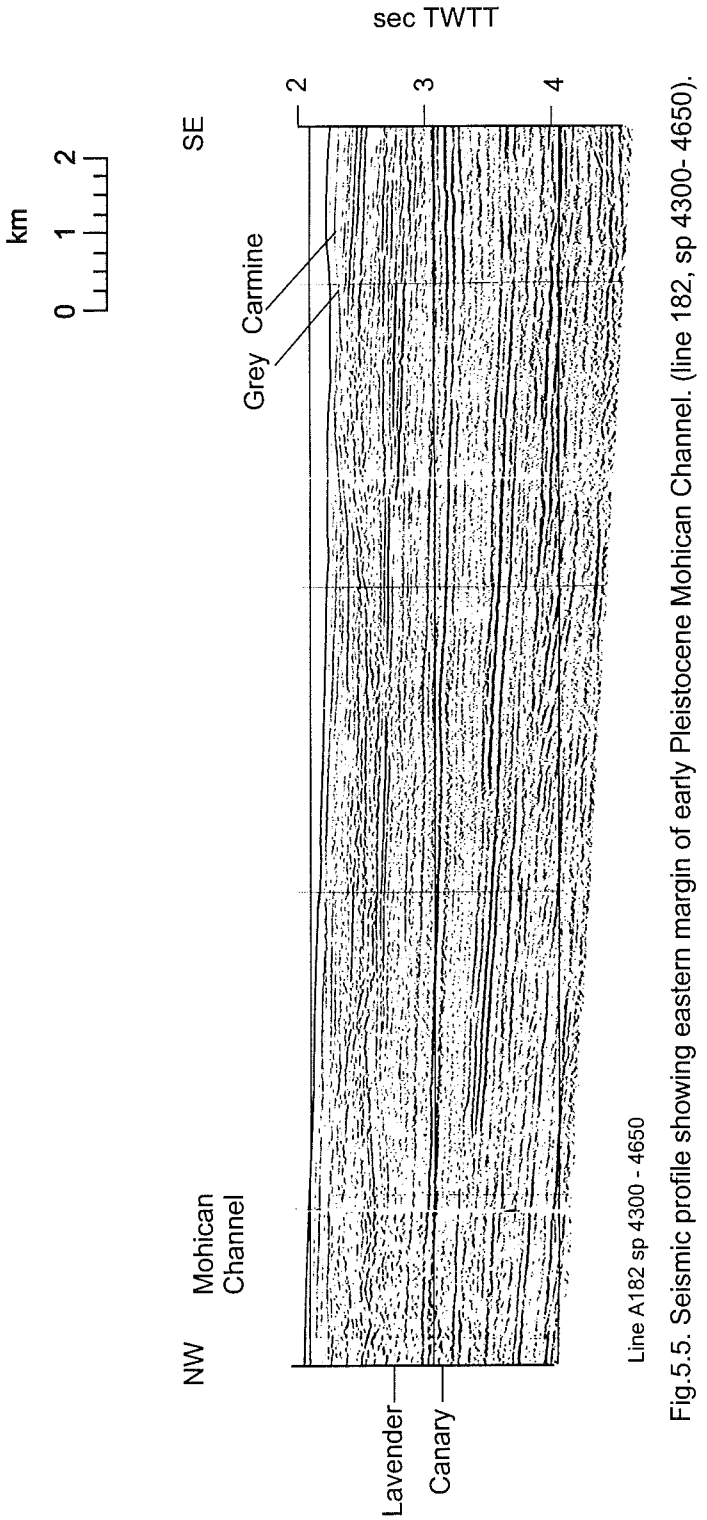

Fig.5.5. Seismic profile showing eastern margin of early Pleistocene Mohican Channel. (line 182, sp 4300- 4650).

C:/IErnest/revised/fig5_5.cdr

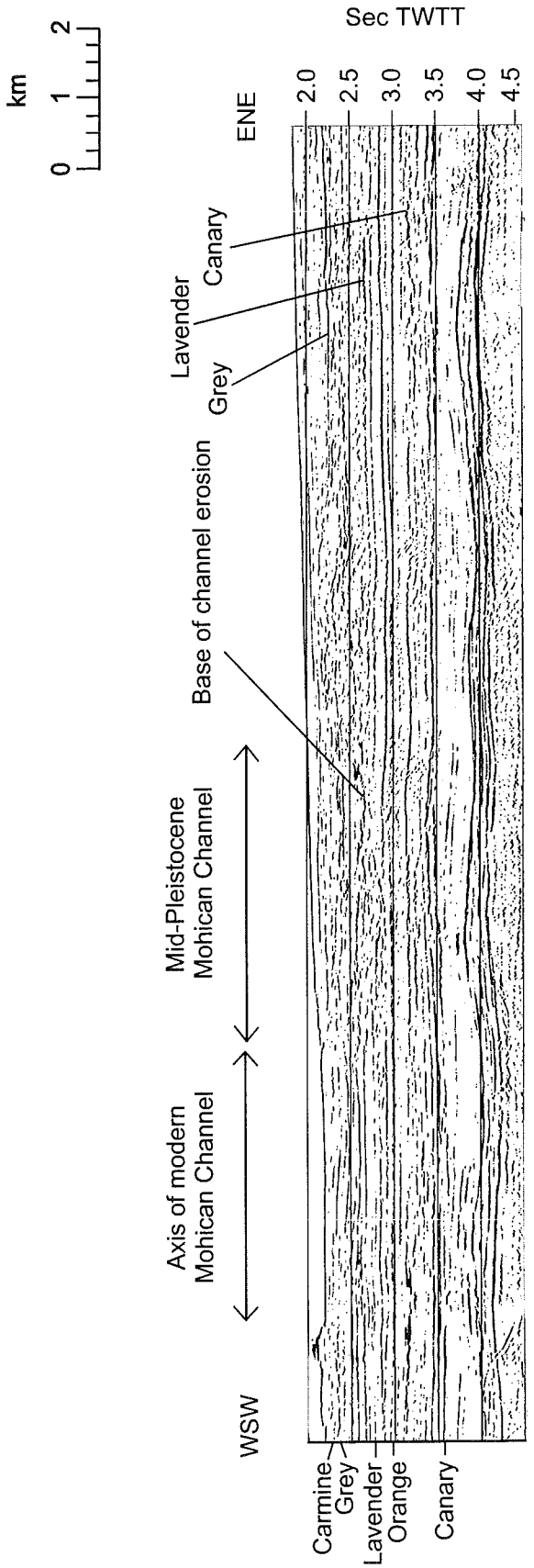

Fig.5.6. Seismic section across the Mohican Channel showing westward migration of channel in the Pleistocene.

Line A3900 sp 8650 - 9400

C:\Ernest\revised\fig5_6.cdr

Fig 5.7

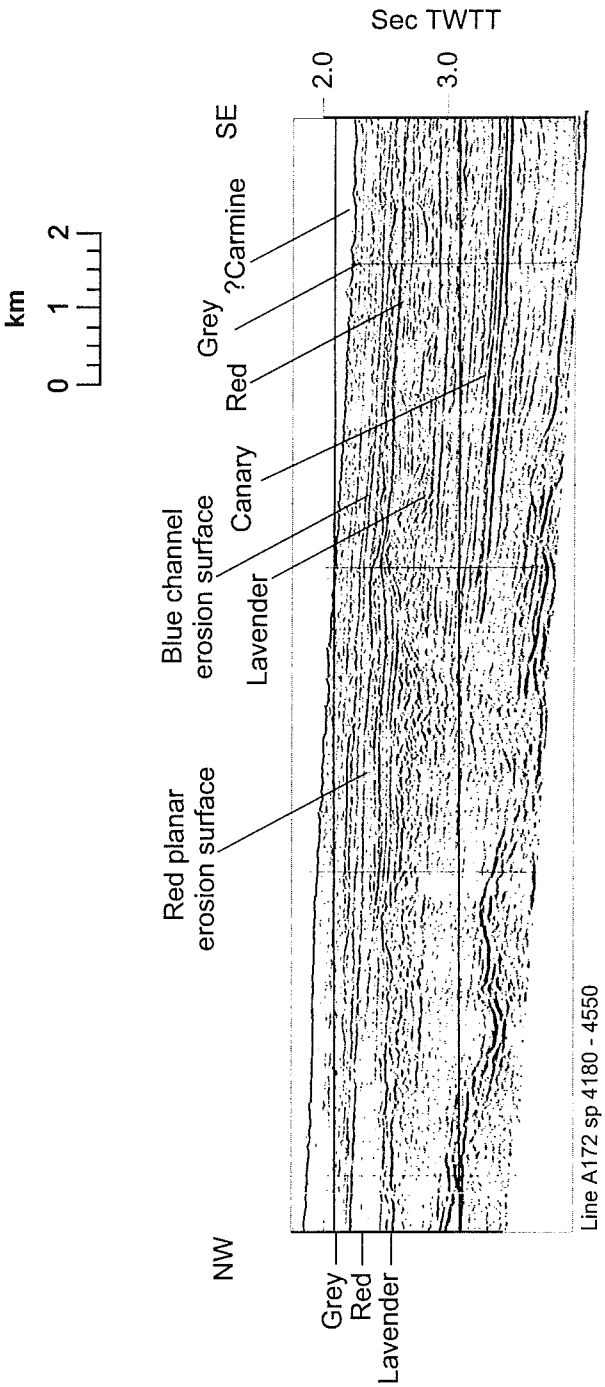

Fig.5.7. Seismic profile 172 (sp 4180- 4450) illustrating the regional stratigraphy in the Albatross area.

C:/IErnest/revised/fig5_7.cdr

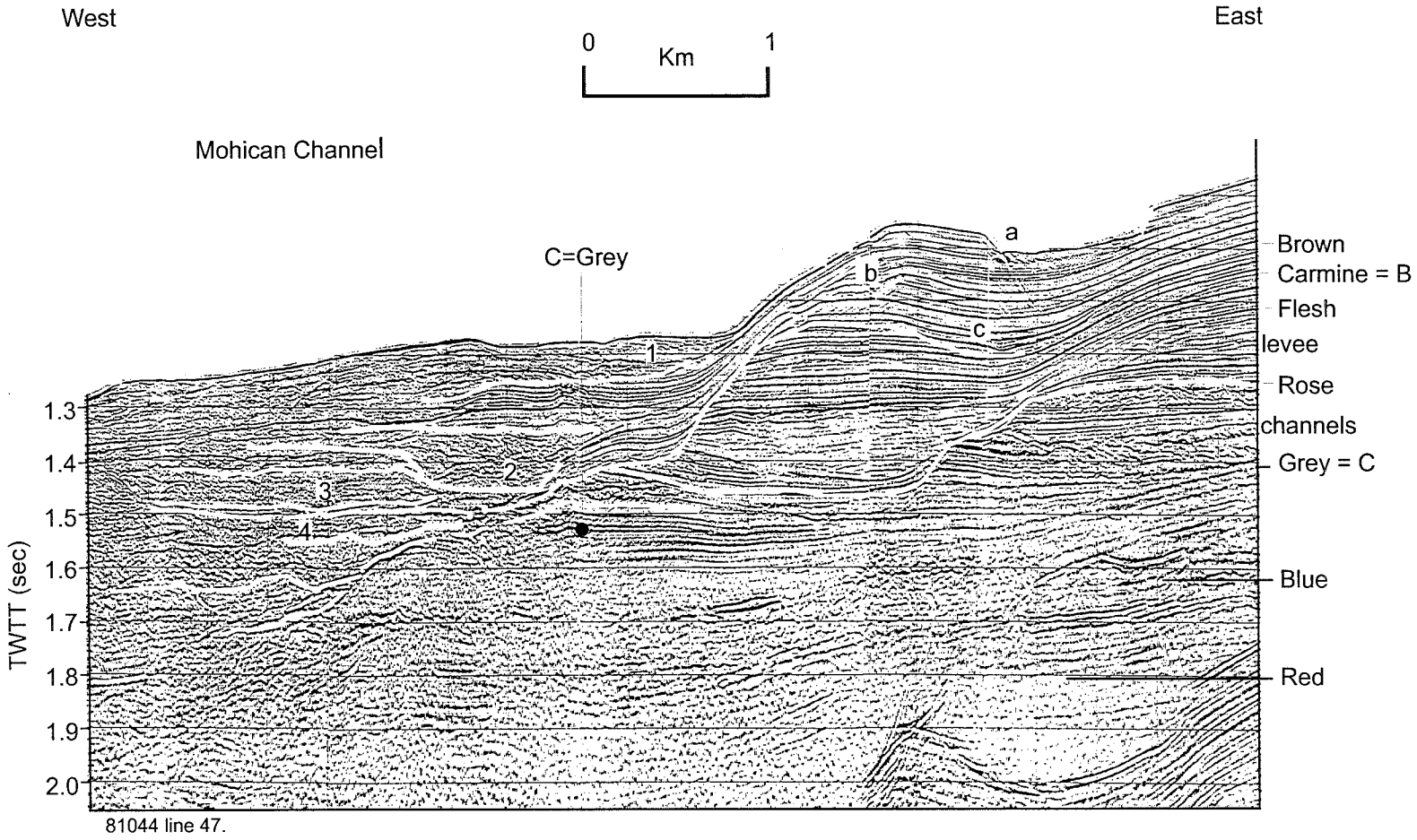

Fig.5.8. High-resolution multichannel seismic line across the eastern margin of Mohican Channel showing erosion surfaces and nature of channel fill. Small failures are shown as a, b, and c.

C:/!Ernest/revised/fig5_8.cdr

Fig 5.8

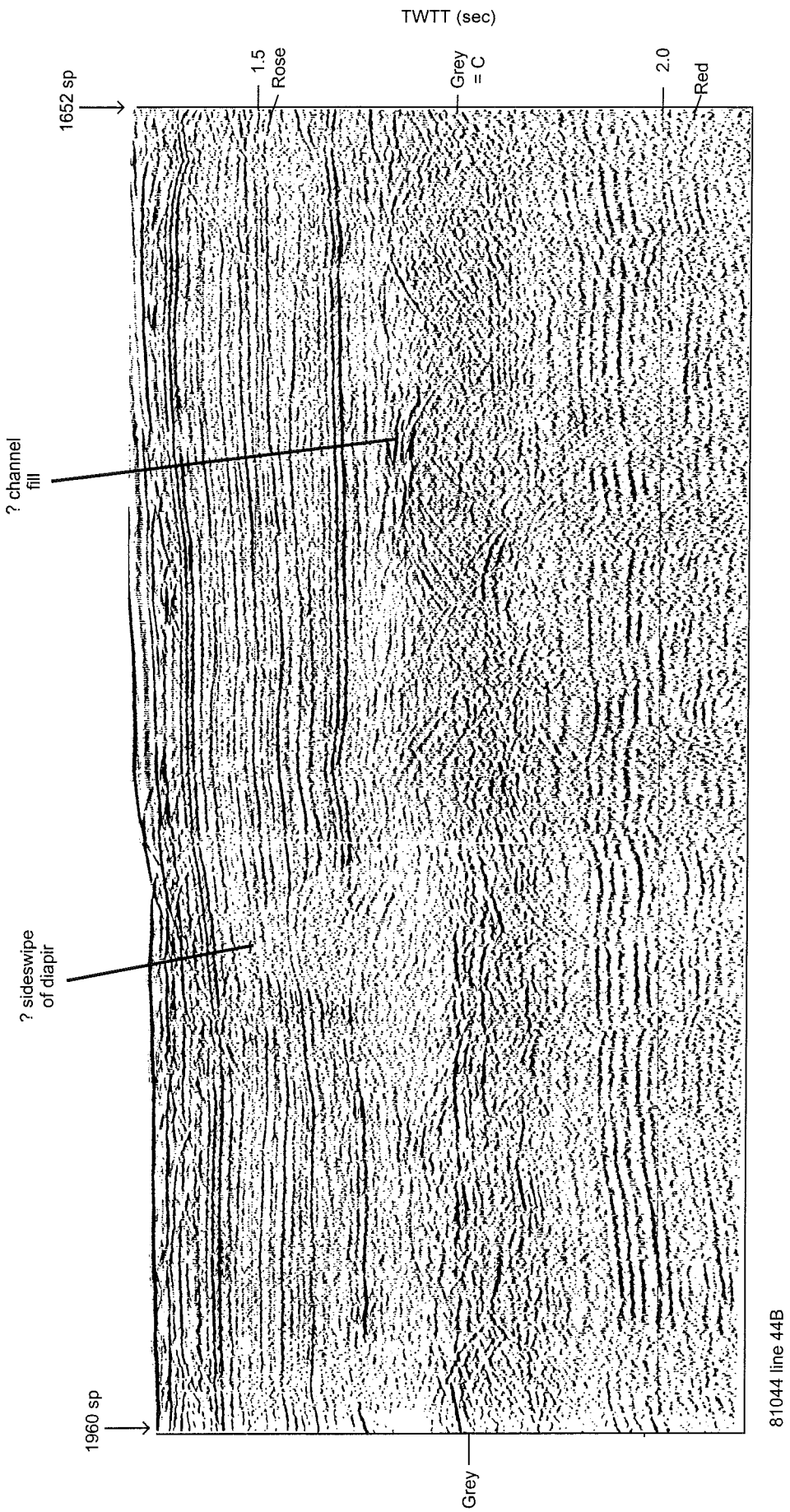

Fig.5.9. High resolution multichannel seismic line from east of Mohican Channel showing disturbed horizon above grey (C).

C:/Ernest/revised/fig5_9.cdr

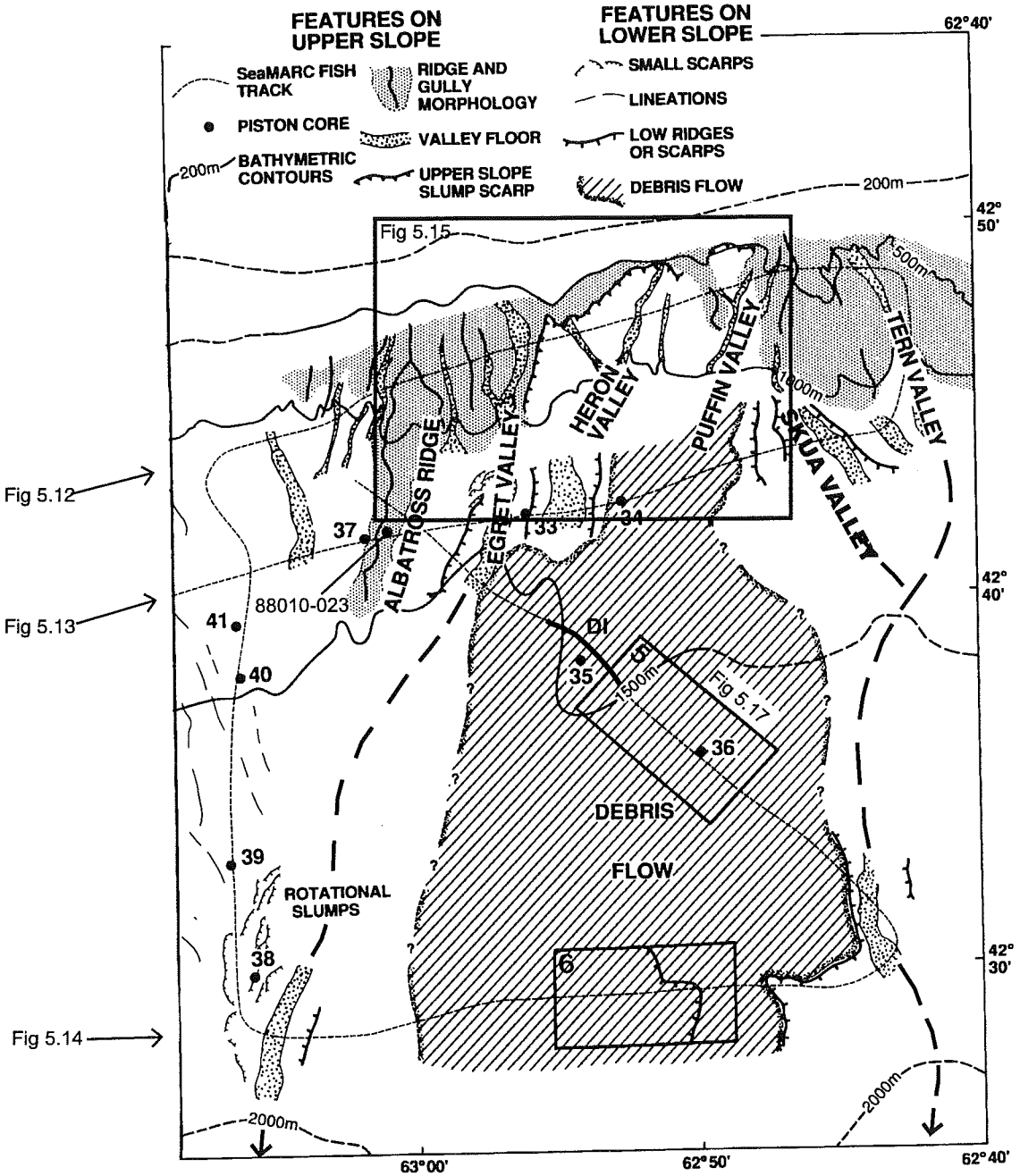

Fig. 5.10. Map showing principal shallow subsurface features seen in seismic profiles in the Albatross area, and location of more detailed figures. DI = shallow diapir.

C:/IErnest/revised/fig5_10.cdr

Fig 5.11

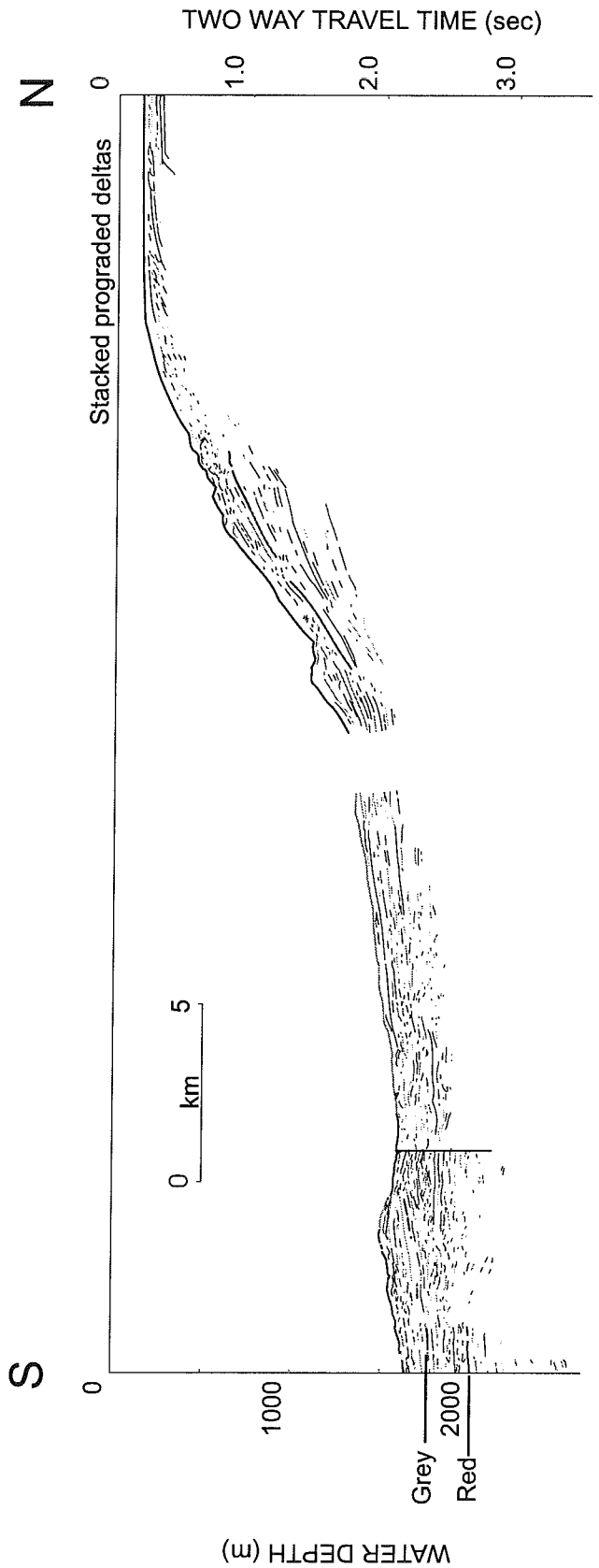

Fig. 5.11. Seismic section off Emerald Bank. (profiles 86-034 (north) and 84-040 (south)). Note stacked deltas on outer shelf.

C:/IErnest/revised/fig5_11.cdr

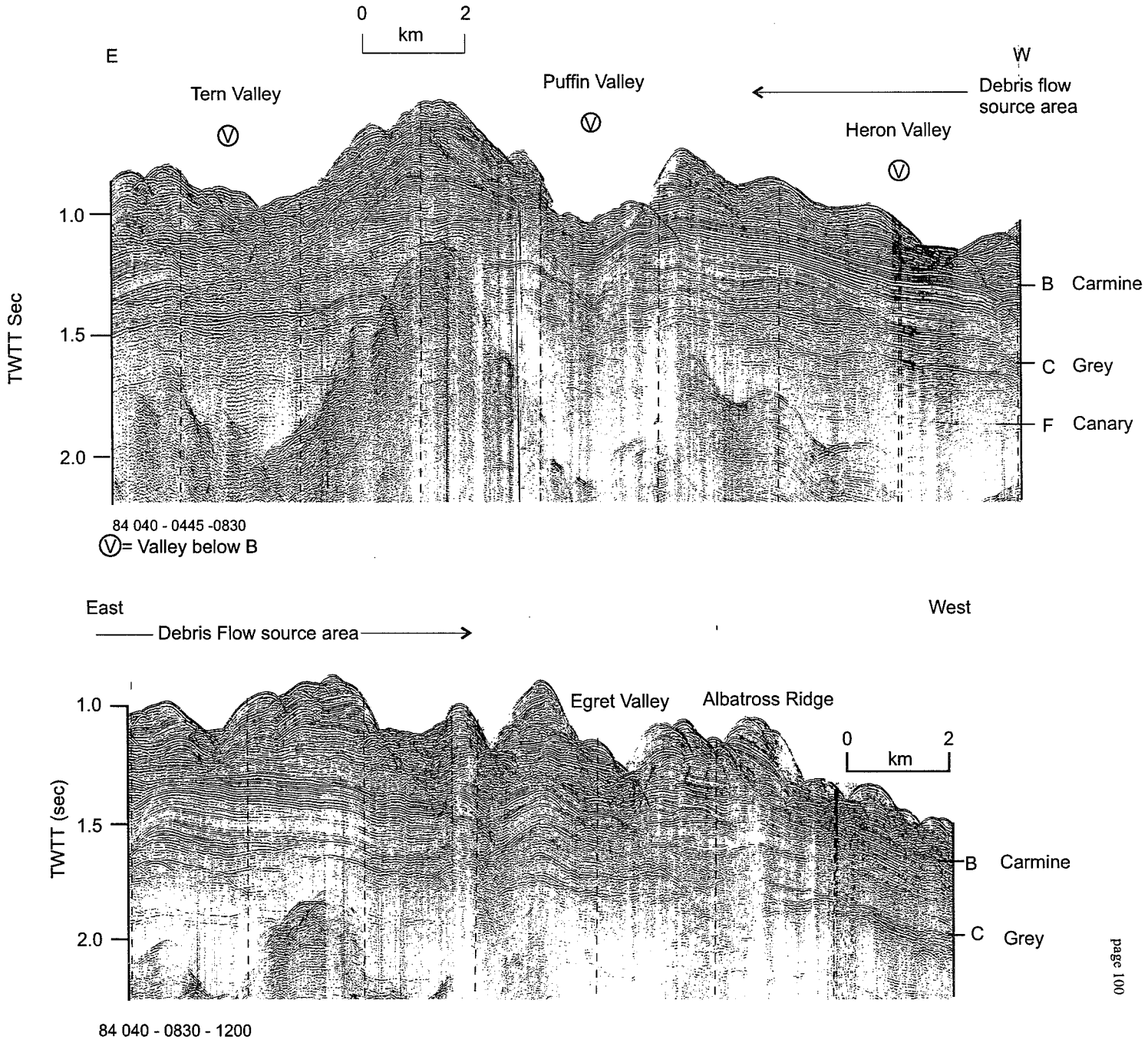

Fig. 5.12. High-resolution single channel airgun profile from middle slope above the Albatross well. (84-040, 0445-1200). cf. SHor and Piper (1989).

C:/!Ernest/revised/fig5_12.cdr

Fig.5.12

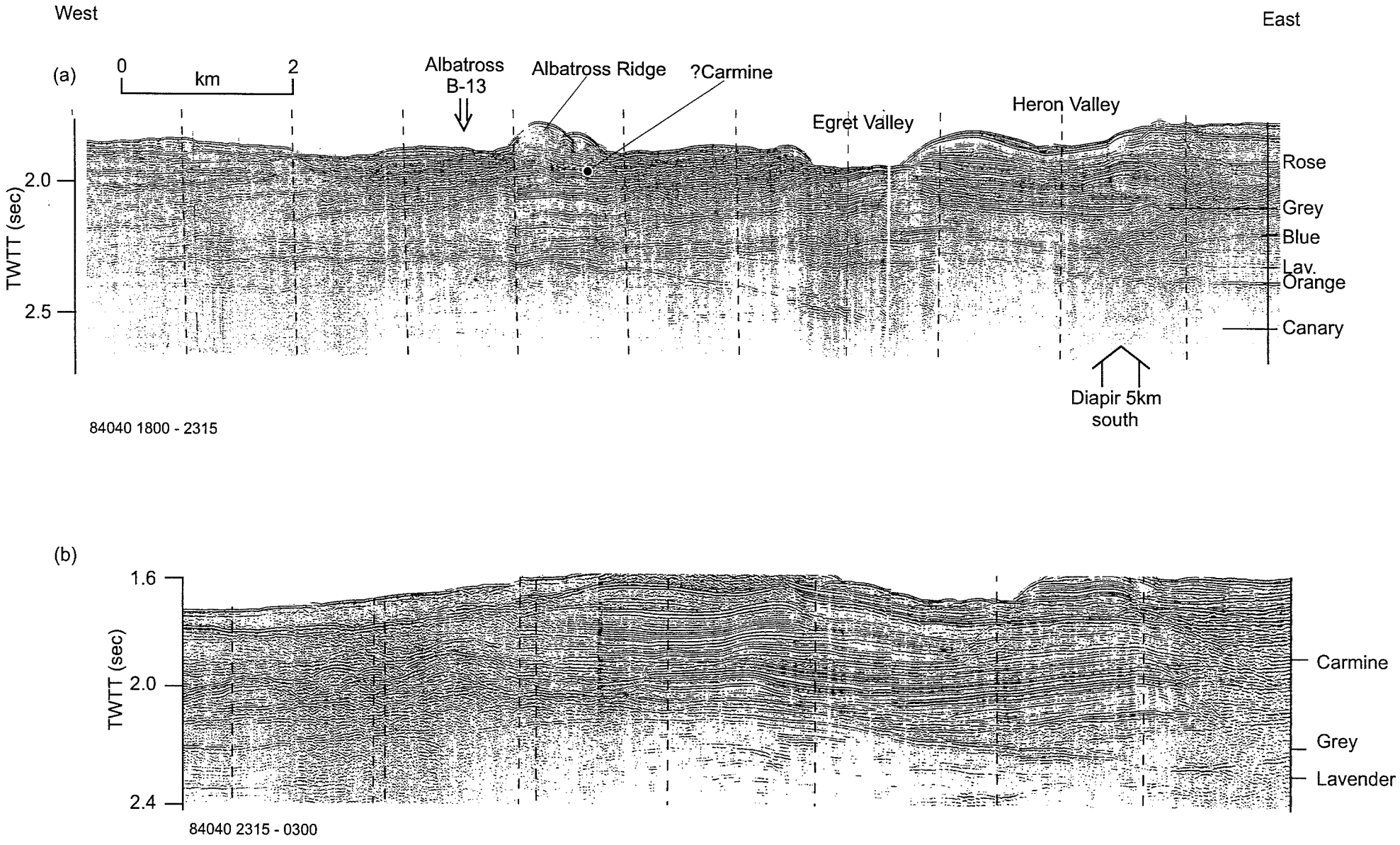

Fig. 5.13. East-west airgun seismic reflection profile at about 1200 m water depth through the Albatross well showing key stratigraphic markers. For explanation, see text.

Fig 5.13

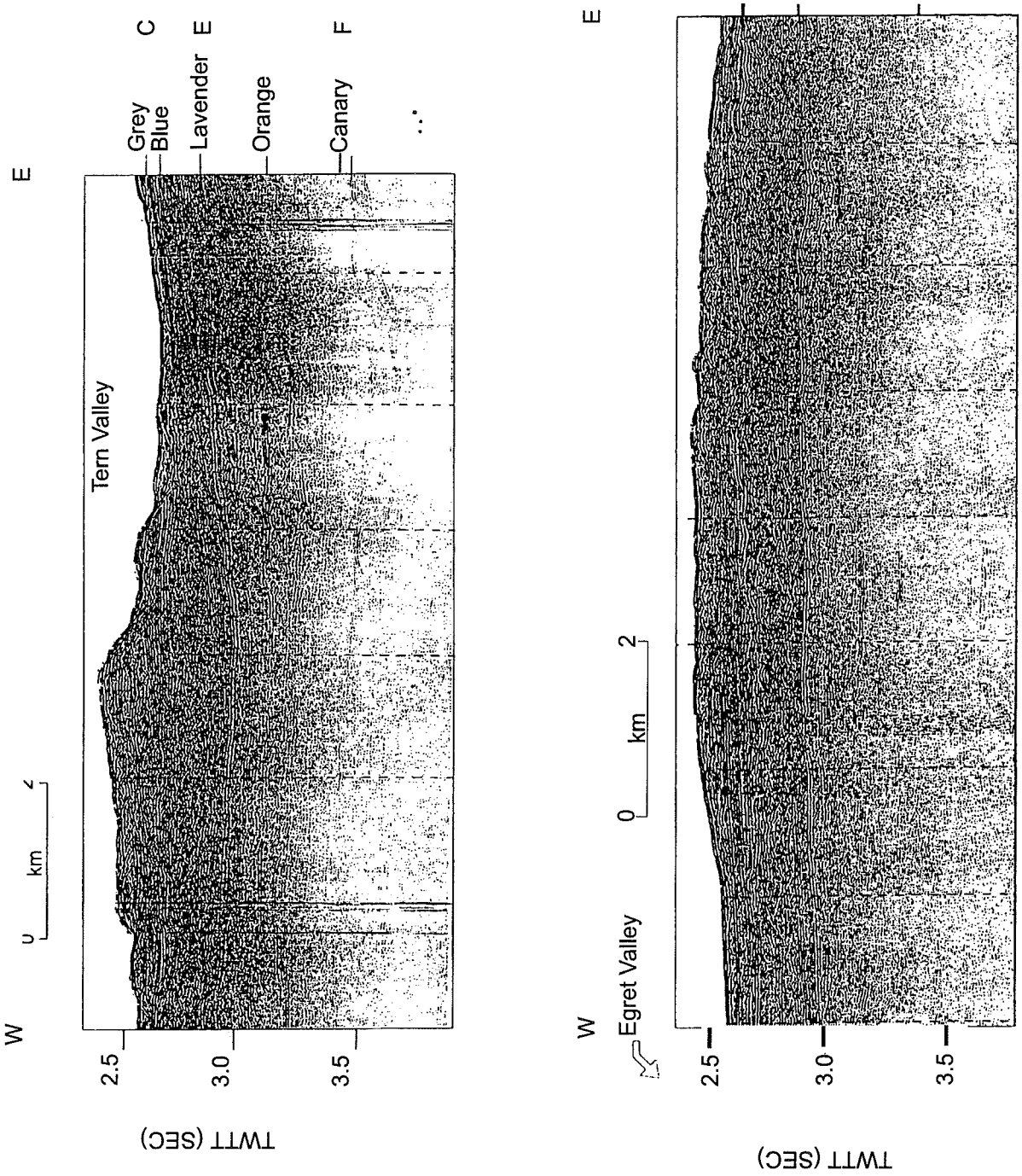

Fig. 5.14. East-west airgun seismic reflection profile at about 1900 m water depth south of the Albatross well.

C:/IErnest/revised/fig5_14.cdr

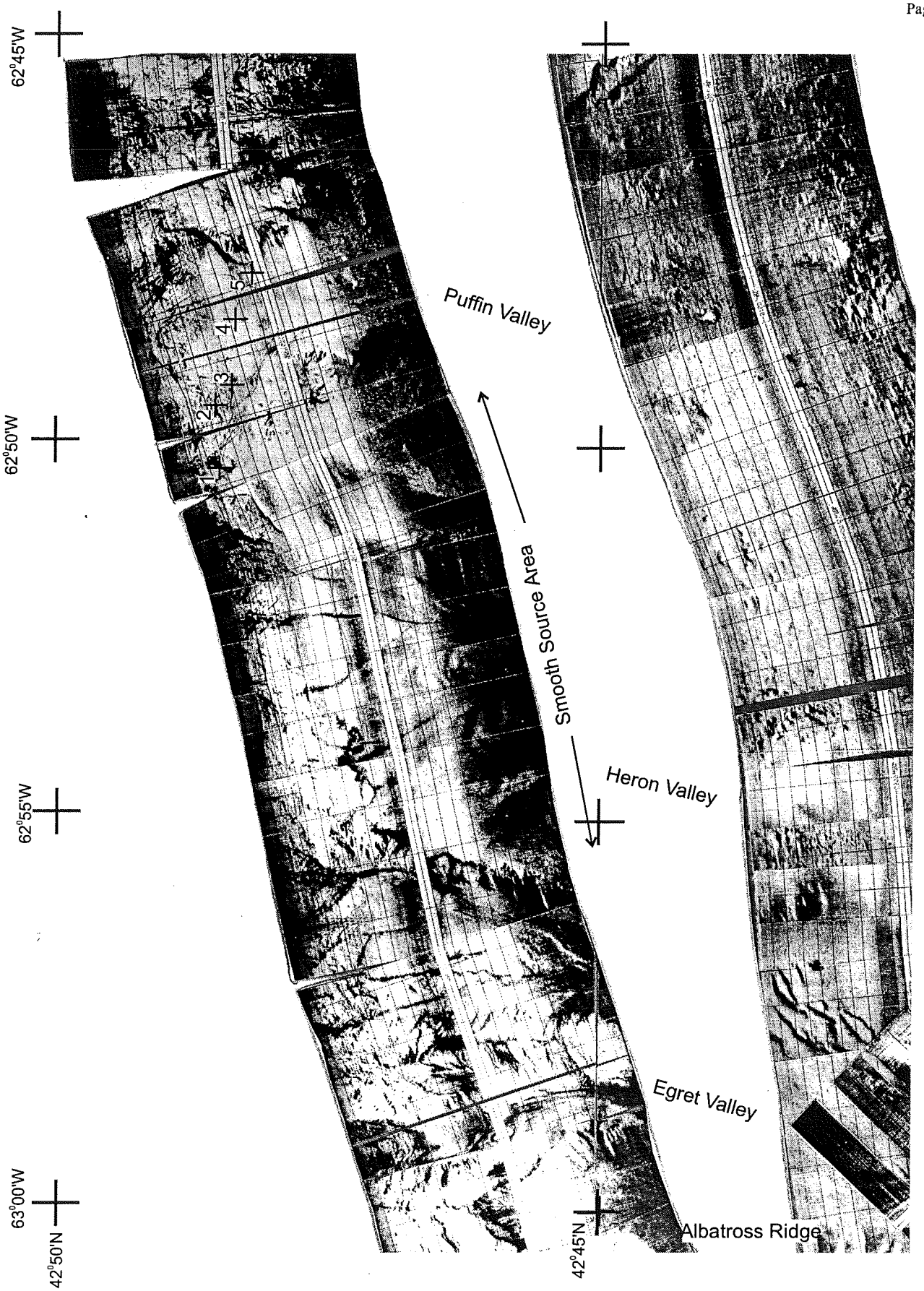

Fig. 5.15. SeaMARC 5-km swath sidescan image of the slope above the Albatross well showing the location of the source area for the Albatross debris flow.

C:/!Ernest/revised/fig5_15.cdr

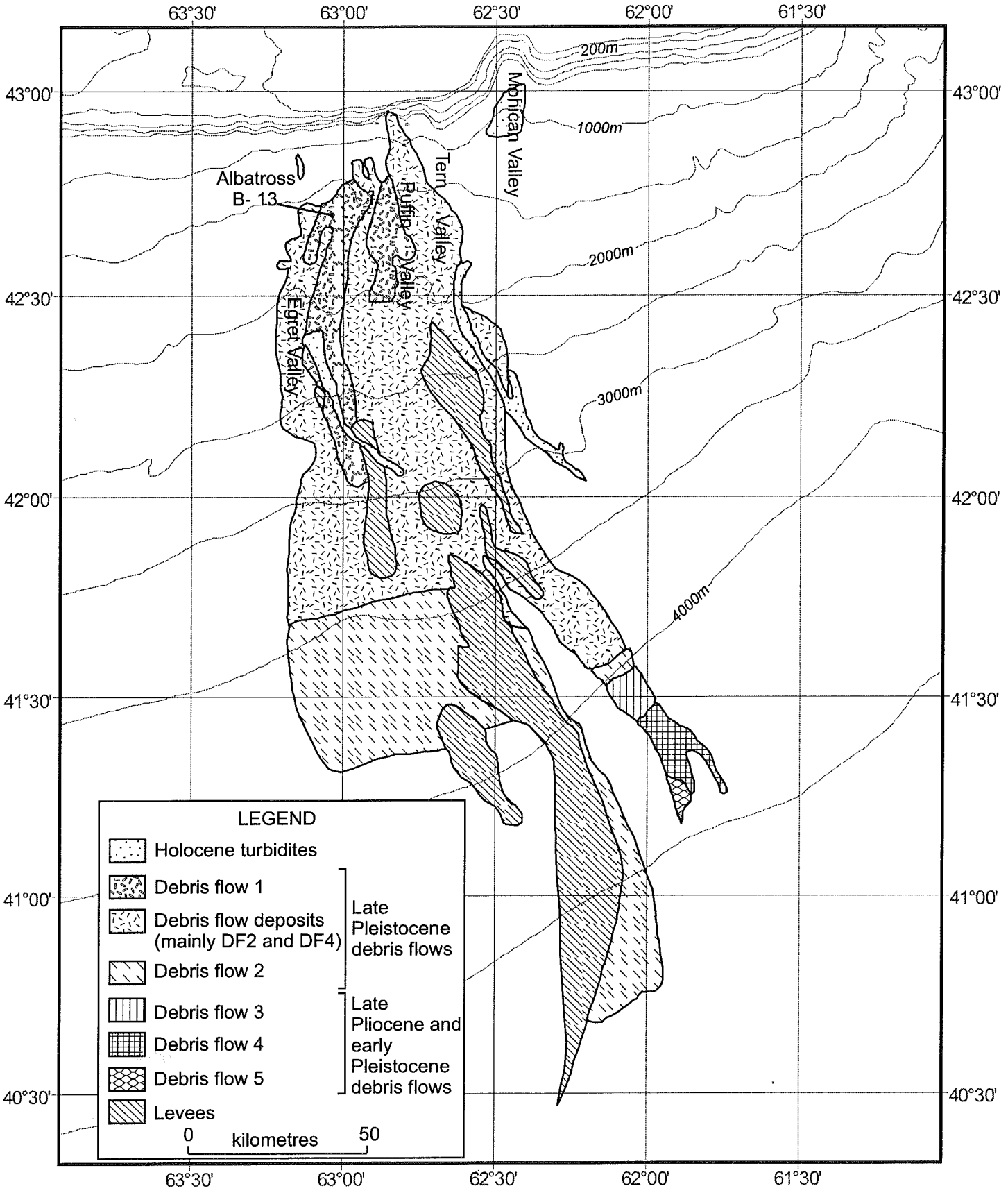

Fig. 5.16. Map showing distribution of the Albatross debris flow on the Scotian Rise (from Mulder et al., 1997).

C:/!Ernest/revised/fig5_16.cdr

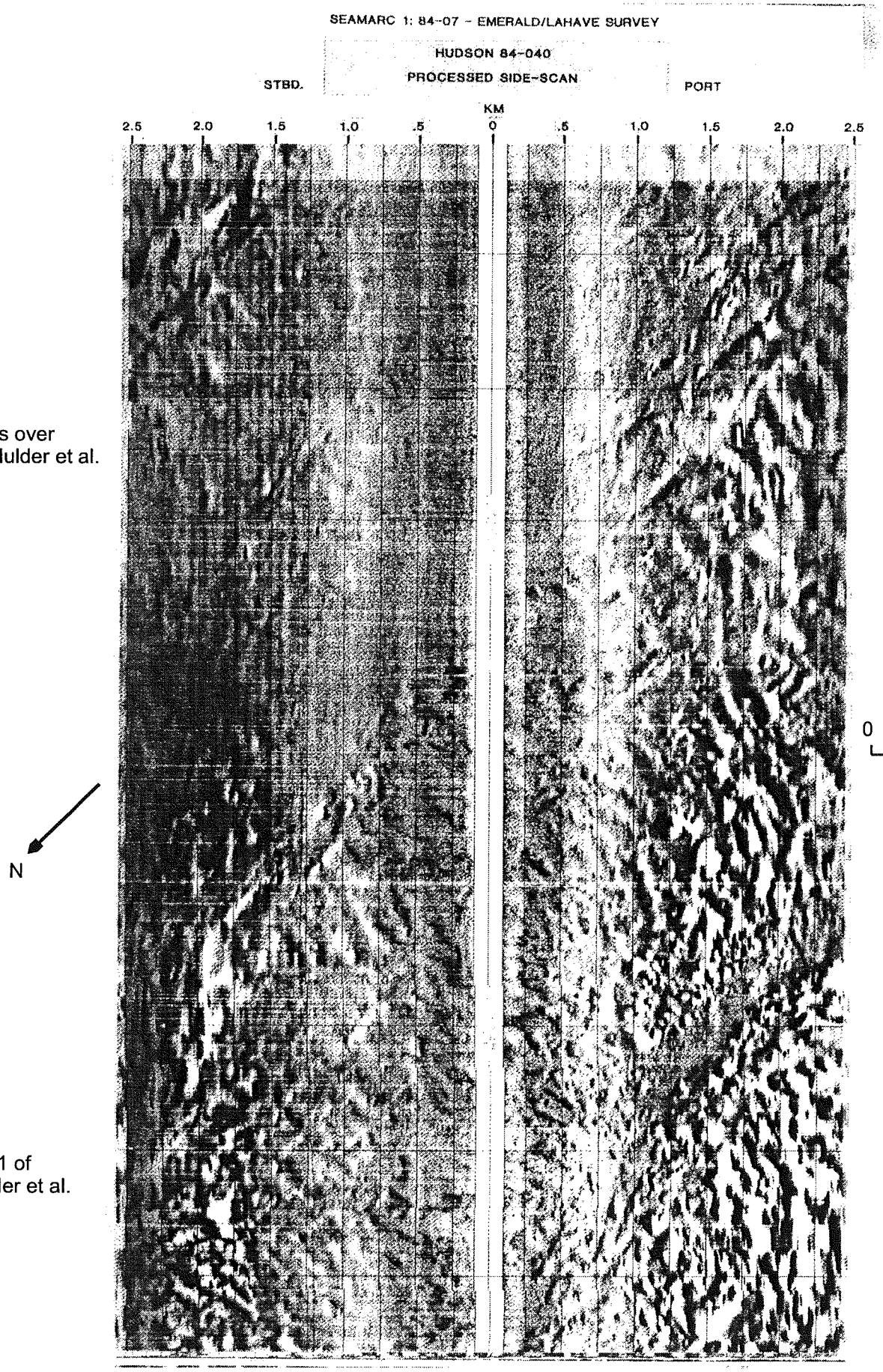

Fig. 5.17. SeaMARC 5-km swath sidescan images showing the rough Albatross DF1 and smooth Albatross DF2 debris flows. (location shown in figure 5.10).

C:/IErnest/revised/fig5_17.cdr

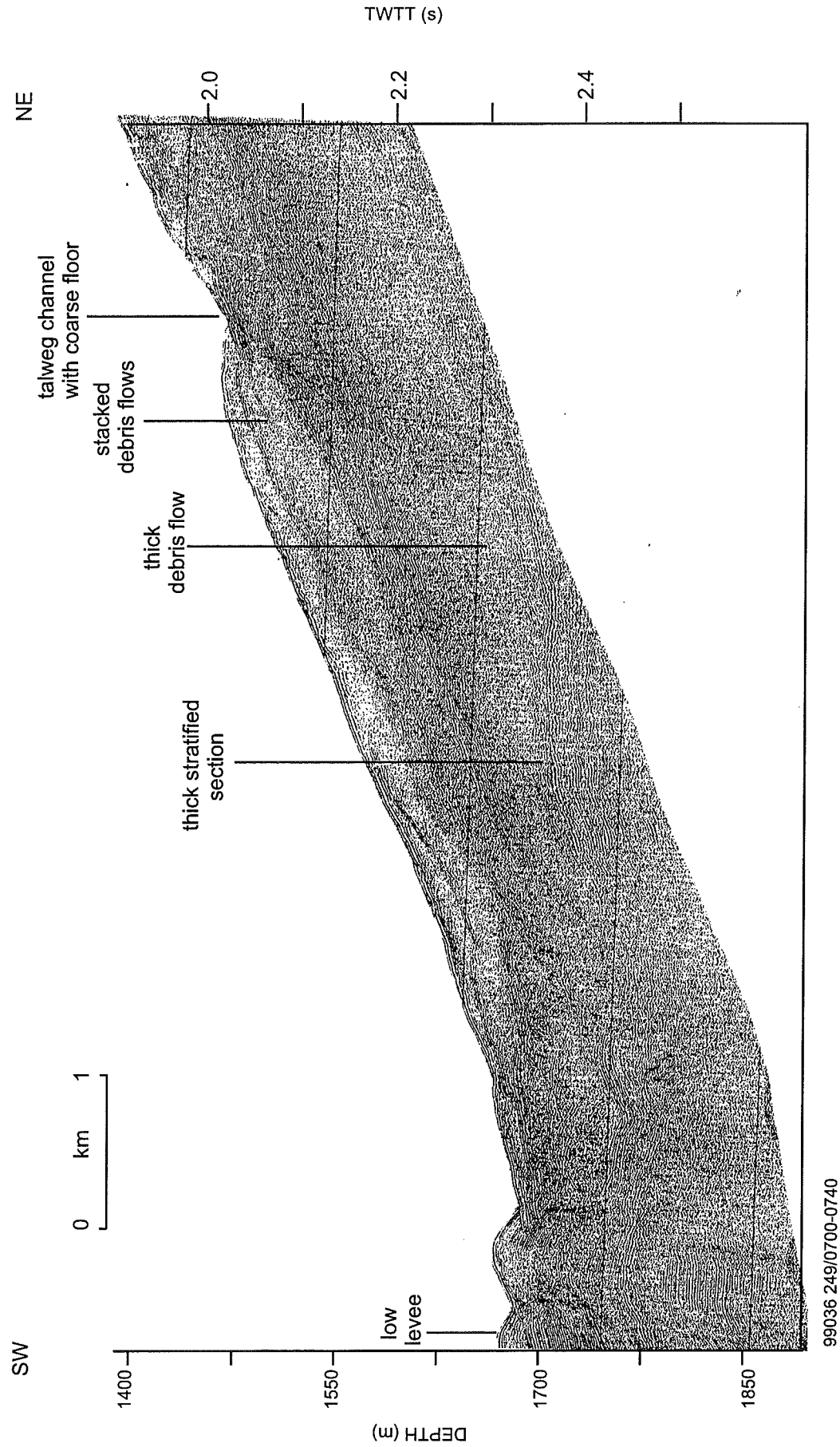

Fig. 5.18. Huntec DTS sparker showing debris flow deposits in Mohican Channel

C:/fErnest/revised/fig5_18.cdr

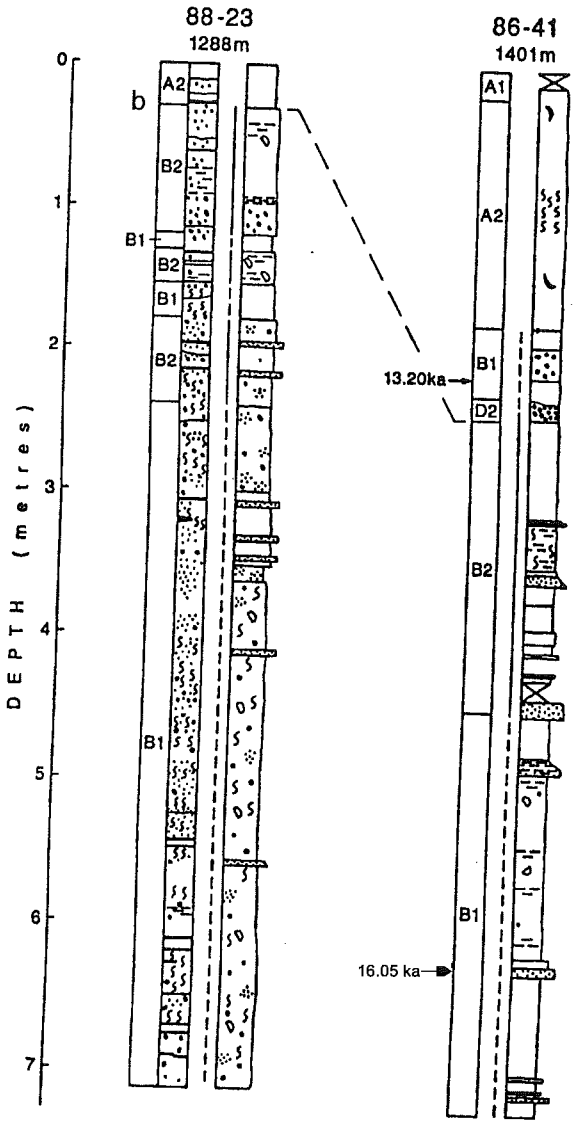

Fig. 5.19. Lithologic summary of two selected cores from Albatross area. Legend in figure 1.5.

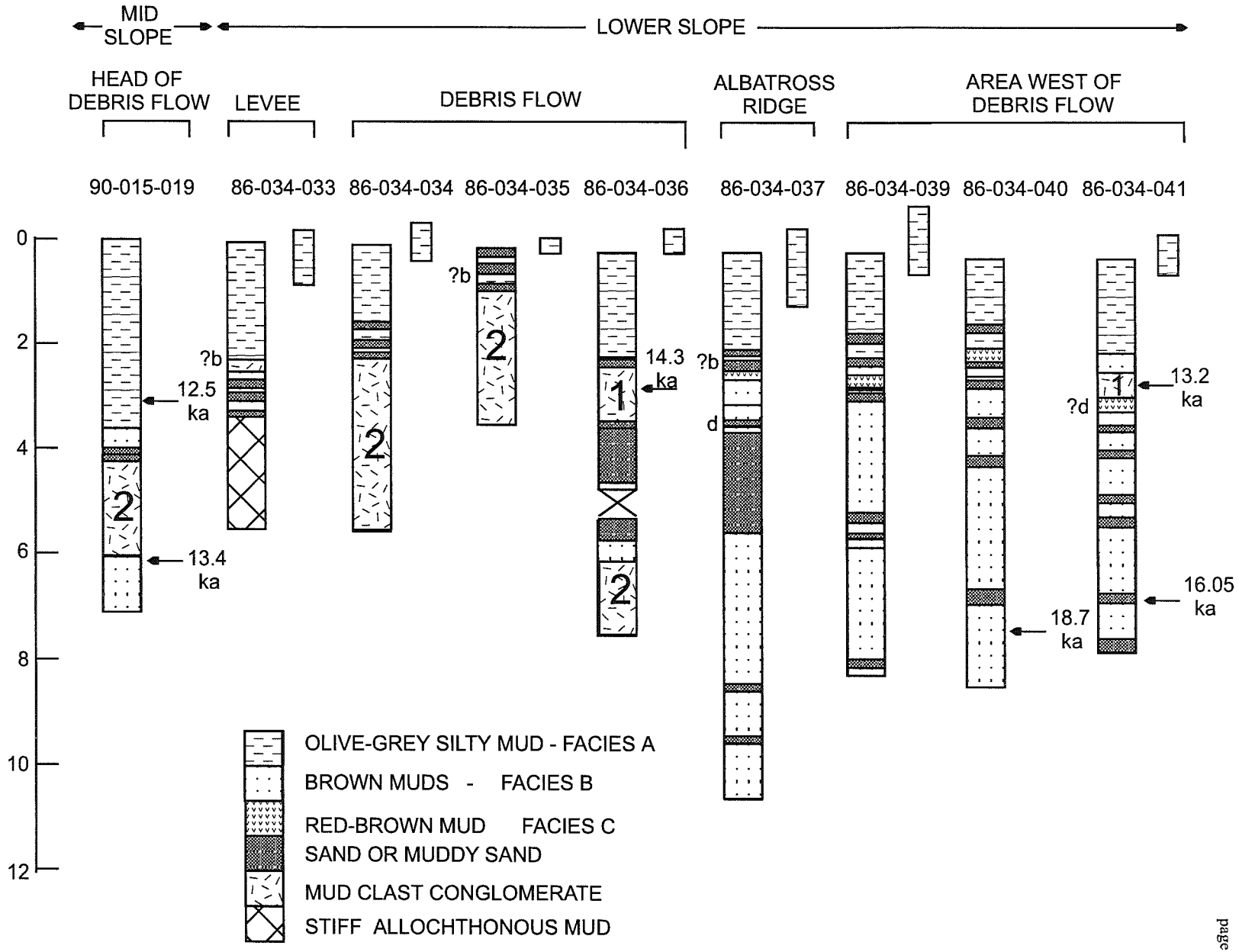

Fig. 5.20. Summary of all the cores from the Albatross area showing facies development

C:/!Ernest/revised/fig5_20.cdr

Fig 5.20

91020-013 west Scotian Rise

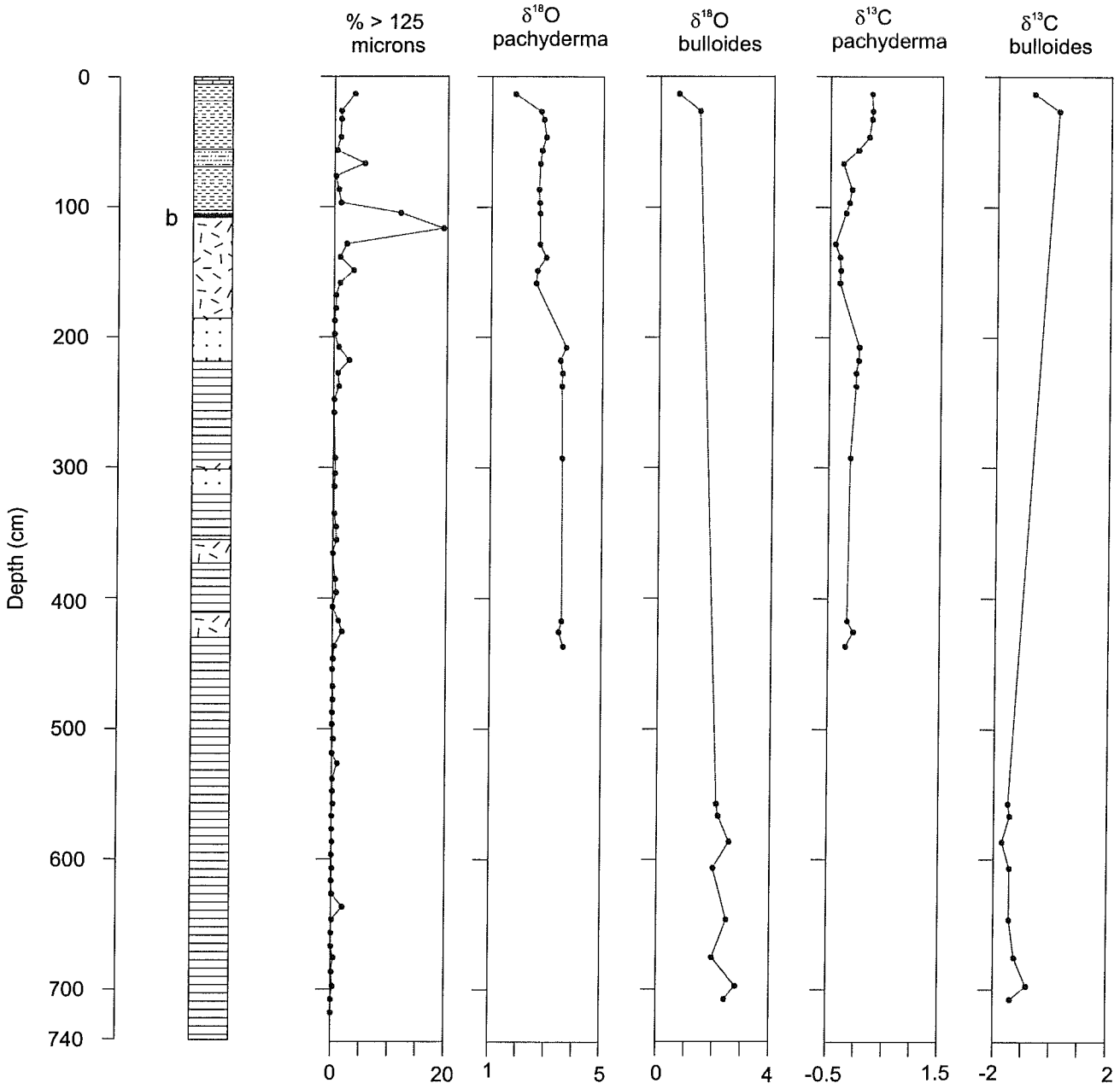

Fig. 5.21. Lithology and isotope stratigraphy of core 91020-013, Scotian Rise.

C:/lErnest/revised/fig5_21.cdr

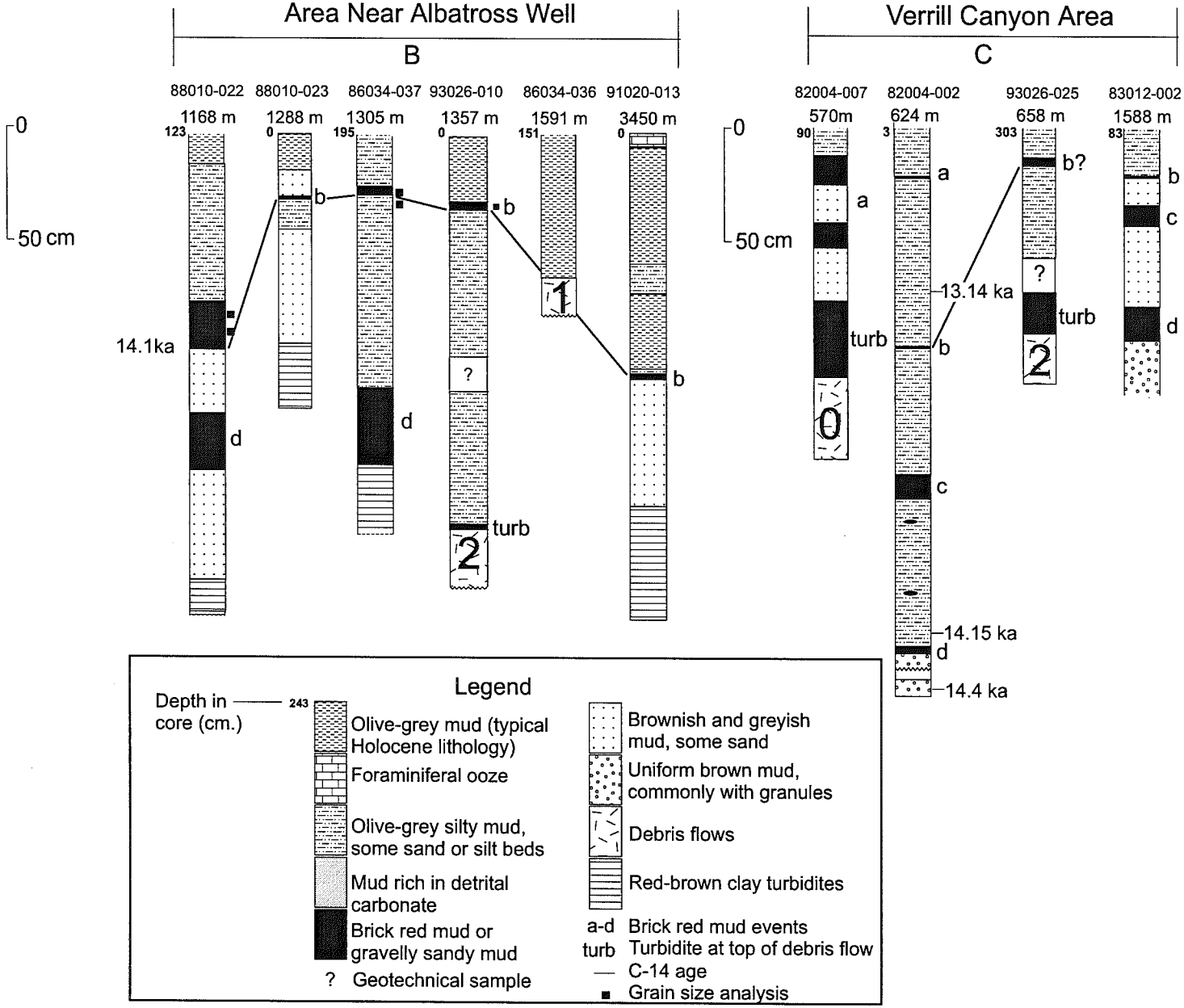

Fig. 5.22. Stratigraphy and dating control of debris-flow deposits near the Albatross well.

Fig 5.22

C:/!Ernest/revised/fig5_22.cdr

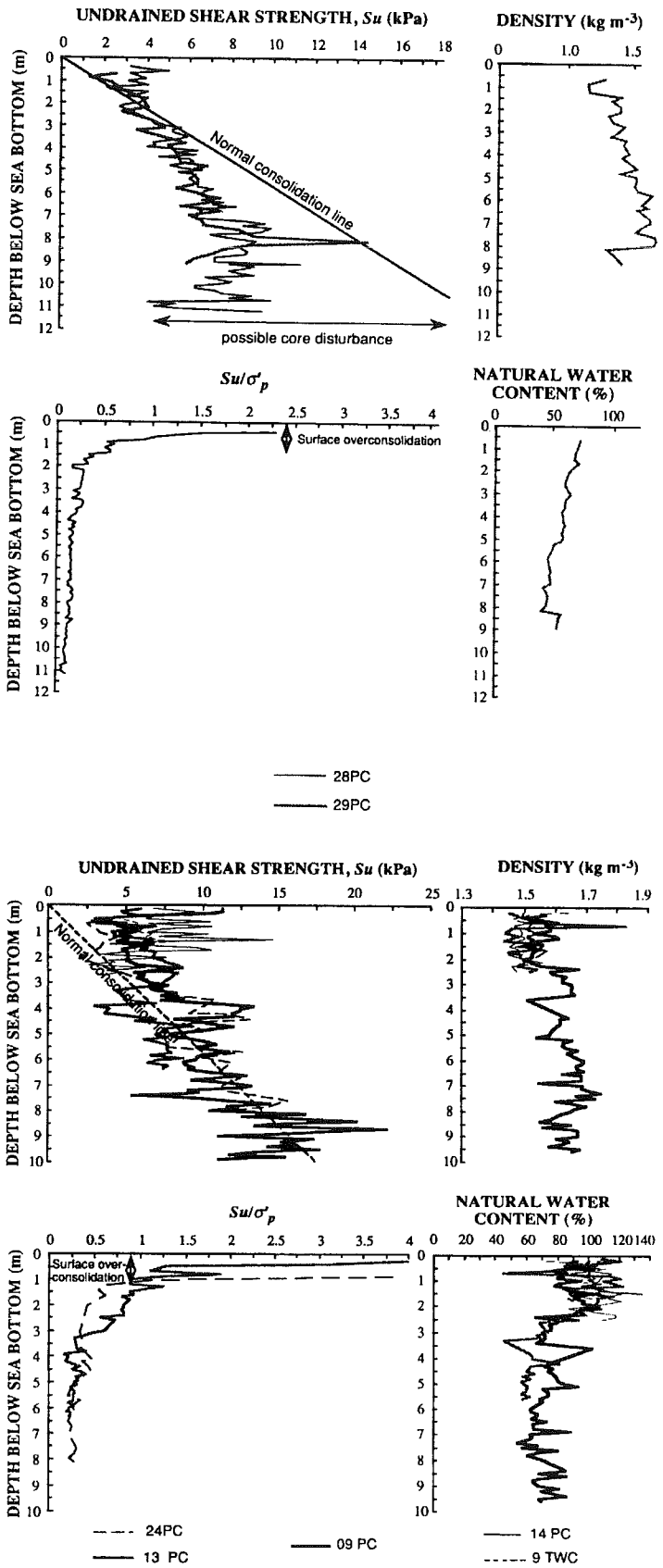

Fig. 5.23. Plots from Mulder et al. (1997) of downcore variation in shear strength ratio in cores from stratified sediments south of the Albatross well.

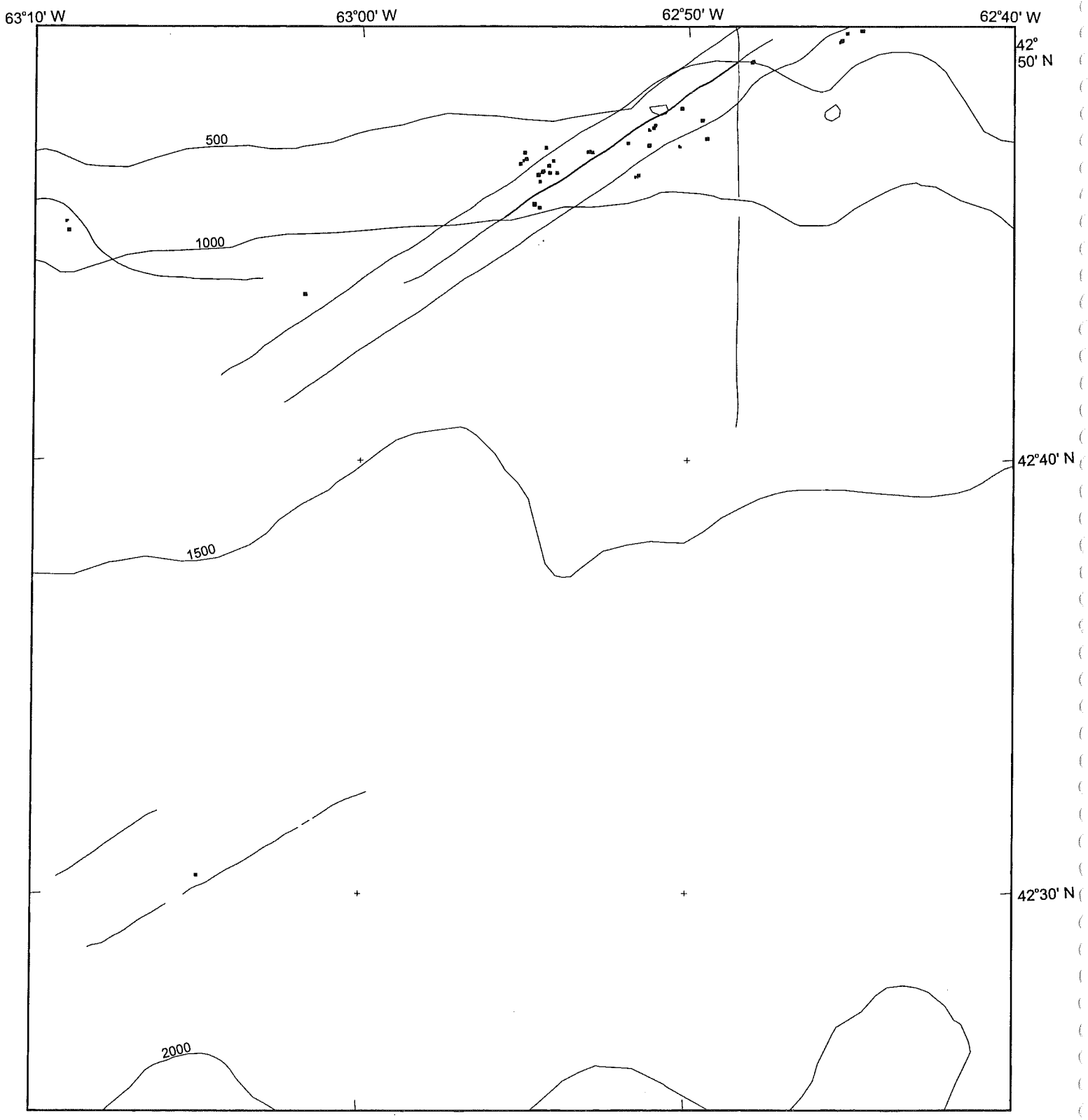

Fig. 5.24. Map of pockmarks in the area near the Albatross well. Lines indicate 1 km swath sidescan survey lines, each pockmark is shown by a dot.

C:/IErnest/revised/fig5_24.cdr

6. Slope off Western Bank

6.1 Introduction and bathymetry

The slope off Western Bank, as far east as Verrill Canyon, is generally smooth, or marked by only shallow gullies (Fig. 6.1). This area appears to have progressively prograded during the late Cenozoic (Fig. 6.2) and was a major Pliocene depocentre (Fig. 2.6). Two deep-water wells, Acadia K-62 and Shubenacadie H-100 were drilled in this sector of the slope.

Detailed studies using seismic, sidescan and cores have focussed on the area between the Shubenacadie and Acadia wells (Fig. 6.3), just west of Verrill Canyon (Piper et al., 1985; Piper et al., 1987; Mosher, 1987; Dodds and Fader, 1987; Mosher et al., 1989). In the area off Western Bank immediately east of Mohican Channel, Hill (1981) made detailed studies of cores.

A detailed bathymetric compilation by Piper and Sparkes (1990) was based on numerous BIO tracklines together with some sidescan imagery (Fig. 6.4). The shelf break shoals eastward from 120 mbsl to 100 mbsl. The generally smooth slope has a mean gradient of 3° to the 1000 m isobath and 2.2° to 2500 m. Two small slope valleys, East and West Acadia valleys, extend upslope to near the 500 m isobath. The upper slope in the area east of the Acadia wellsite has relict iceberg furrows down to depths of 600 m and is cut by shallow gullies (20 m deep, 500 m wide: Mosher, 1987). Rotational slumps on the mid-slope head at low scarps in water depths of 500 - 600 m (Piper et al., 1985). Larger rotational failures occur at the base of the mid slope, near the 2100 m isobath.

6.2 Late Cenozoic framework

A Pliocene - Quaternary seismic stratigraphy for the area near the Shubenacadie well was proposed by Piper et al. (1987) using high-resolution multichannel airgun data tied to biostratigraphic picks in the Acadia K-62 and Shubenacadie H-100 wells, summarized in Chapter 2.2. This work was extended by Piper and Sparkes (1990) to include a grid of industry multichannel seismic data back to the Miocene "canary" marker. Piper et al. (1987) recognised four phases of development of the continental margin recognisable in strike lines in the area from the Acadia K-62 well to Verrill canyon (Fig. 6.5). Mid Tertiary slope sediment appears to have accumulated without significant channelling. A broad valley was then cut in the mid to late Pliocene. Widespread shallow gullies were cut in the latest Pliocene or early Pleistocene and these developed into deeper canyons through the Pleistocene.

This late Cenozoic evolution is illustrated in the industry strike profile in Figure 6.6 and high-resolution dip profiles illustrated in Figures 6.2 and 6.7. Between the seabed and the carmine reflector, reflectors are

subparallel and continuous along strike, but the unit thins to 40% between 650 and 1700 m water depth. The subparallel reflectors interfinger upslope with wedge-shaped bodies of incoherent reflections that pinch out downslope at depths of 400 to 550 mbsl and upslope pass into glacial till deposits on the continental shelf (Fig. 6.7b). These wedge-shaped bodies have been informally referred to as "till tongues". The interval from carmine to grey is also characterised by parallel continuous reflectors on the mid to lower slope, but upslope the till tongues appear to be absent. This unit shows a reduction to only 75% of upslope thickness over the same depth range. Immediately below grey, but above magenta is a series of shallow erosive gullies, well defined on single channel 40 cu. in. airgun data as channels 40 ms deep and up to 4 km wide (Fig. 6.8b). This erosional surface and the overlying drape of the reflectors around grey is seen in line 524 (Fig. 6.9) to extend into the western edge of Verrill Canyon.

The interval from grey to red is characterised by high amplitude continuous parallel reflectors (Fig. 6.6). Other than the gullies between grey and magenta, no gullying or erosion is visible west of Verrill Canyon. The erosional surface below grey caps a thin channel floor facies sequence at the western margin of Verrill Canyon (Fig. 6.9) that appears equivalent to the entire sequence from red to magenta. This profile also shows that the sequence from red to blue appears to drape and fill the main channel of Verrill Canyon further to the east (the "ancestral valley" of Piper et al., 1987); this main channel is eroded down to the level of the pink reflector. West of Verrill Canyon, the interval between grey and red thins only slightly away from Verrill Canyon (from 0.37 secs at the edge of Verrill Canyon in 1500 m water depth to 0.33 secs in line 501, Fig. 6.10): it is not clear whether it can be regarded as a levee sequence, although there is a substantial thickening at the very edge of Verrill Canyon.

Immediately below the red reflector are weak continuous reflections, but most of the sequence down to lavender consists of short, discontinuous, shingled or scour-and-fill type reflectors. This irregular reflector character may in places extend down to the orange reflector. West of Shubenacadie H-100, reflectors become particularly discontinuous between red and lavender and fill the floor of a local depression: this appears to be a channel (Fig. 6.12).

In the area near the Shubenacadie well, within the interval immediately above lavender, normal faults are common (Figs. 6.10, 6.11). Most dip basinwards; a few dip upslope. These faults have offsets of up to 20 msecs; measured apparent dips are frequently rather low, in the range of 40° to 60°. Above the "magenta" reflector, faults are draped by younger sediment, or have offsets that cannot be resolved. No faults extend with certainty below the "orange" reflector, although locally possible offsets down to between pink and canary are visible[1]. The canary (F) reflector everywhere continues unbroken below the faults. These faults, therefore, are not

[1] e.g., line 501, sp 4370 (not illustrated)

basement-related or deep growth faults: rather they are shallow features that must be rooted in low angle displacement planes. They resemble polygonal faults described by Cartwright and Dewhurst (1998). It is possible that some of the reflector irregularity associated with the horizon at and above lavender is the result of displacements subparallel to bedding. In places, this faulted interval passes laterally from acoustically stratified to an interval of short discontinuous dipping reflections (Fig. 6.11) suggesting a more broken up character. The extreme top of the uncased well section at Shubenacadie H-100 intersects this interval with normal faulting above reflector lavender. Standard logs were not run in this interval, but the mud log showed high background gas between 2140 and 2340 m (Baroid mud log report), corresponding to the interval above lavender.

Over much of the area, the interval between orange and canary consists of fairly continuous subparallel reflectors. More detailed examination, however, shows that there is substantial variation in reflector amplitude, both along strike and down dip. In many areas of higher amplitude, the reflector is clearly a planar unconformity surface, with local toplap. The behaviour of canary is particularly regular: it is a high-amplitude reflection from where it onlaps the Miocene/Eocene unconformity downdip for about 10 km, where it abruptly decreases in amplitude. West of Shubenacadie, there is a large channel at or immediately below the orange reflector that cuts out pink. The margin of this channel appears to have prograded westwards (Fig. 6.12).

Swift (1987) interpreted the canary disconformity in the vicinity of the Shubenacadie well as resulting from bottom current erosion. The Late Miocene to Early Pliocene age of the canary, pink and orange disconformities corresponds to a time of strong bottom current erosion and redeposition on the continental margin of Eastern North America (Tucholke and Mountain, 1985; Myers and Piper, 1989). It is therefore possible that the "channel" features described above might be related to bottom current erosion. The location of erosion in dip lines at the orange reflector close to the break in paleoslope where orange onlaps the mid-Tertiary unconformity is a feature that would be expected from bottom current erosion. However, the steepness of the channel margin seen in line 521 suggests that the channel erosion was due to downslope processes, although subsequent filling might be the result of bottom current sediment deposition. Downslope channels cut winnowed bottom current deposits in several places on the Canadian margin: for example, on the Labrador Slope (Carter and Schafer, 1983; Myers and Piper, 1989) and at Titanic Canyon (Savoye et al., 1990). However, no constructional features related to bottom current deposition have been recognised in the seismic reflection profiles.

6.3 **Late Quaternary sedimentation**

High-resolution seismic data

On the upper continental slope, seismic reflection profiles show wedge-shaped bodies of incoherent reflections that pinch out downslope at depths of 400 to 550 mbsl (Fig. 6.7b). These bodies have been informally

referred to as "till tongues" because of their acoustic similarity to glacial till on the continental shelf.

Two large shallow failures on the continental slope between the Acadia and Shubenacadie wells (the eastern and western "disturbed zones") (Fig. 6.13) were first reported by Piper et al. (1985b) on the basis of SeaMARC 5 km swath sidescan, piston cores and NSRF V-fin deep-towed sparker profiles. These failures head in low scarps in 500-700 m of water, just downslope from the limit of the till tongues, and appear to be rotational slumps overlain by thin debris-flow deposits. Scours downslope from the slumps suggests that the debris flows may have evolved into an erosive turbidity current.

Detailed studies of these features are also presented in an M.Sc. thesis by Mosher (1986) and in Open File reports by Piper and Wilson (1983) and Piper et al. (1983). Additional sidescan and boomer data collected in 1985 is reported by Hutchins et al. (1985). SAR 1 km swath sidescan collected in 1990, together with in situ geotechnical data collected with the IFREMER module géotechnique are reported by Baltzer et al. (1994). Mosher et al. (1994) presented other new acoustic and core evidence for the style of failure. They showed that slabs of surficial sediment slid over disrupted horizons 5-20 m subbottom (Mosher et al., 1994, their Fig. 3).

In Huntec boomer, 3.5 kHz and other high resolution seismic profiles, a regular succession of reflectors is recognised (defined in Piper et al. 1983 and summarised in Figure 6.14). Note that the correlation of brown by Mosher (1987) to the lower slope is questionable. Furthermore, the (French) colour scheme used by Baltzer (1994) does not precisely correspond after translation to this standard. The youngest till tongue corresponds to an interval just below the green high resolution reflector (Mosher et al. 1989).

High-resolution sidescan data (principally the IFREMER SAR system) shows that pockmarks are common on the continental slope. Pockmarks are generally interpreted as gas escape craters and this interpretation is supported by the presence of gas in piston cores in areas of pockmarks. Pockmarks are most readily formed and preserved in muddy substrates. They are most easily recognised in sidescan data in areas of smooth seabed. Pockmarks were first recognised in the Acadia K-62 area using the Canadian SEAMOR sidescan system by Hutchins et al. (1985) (Fig. 6.13). Mapping of pockmarks using the 1 km swath SAR system in the Acadia-Shubenacadie area shows that they are most abundant in water depths of 500-900 m although they are present in all water depths to 2200 m (Fig. 6.15).

South of the main rotational slumps (particularly the western failure) in the Shubenacadie - Acadia area, Piper et al. (1985a) described widespread erosion. Although, in places, flute-like scours were observed, much of this erosion was down to particular bedding planes and was interpreted to result from sliding along planes of weakness and removal of the overlying failed sediment. Some surfaces corresponded to planes at the base of the rotational slumps (Piper and Wilson, 1983; Baltzer 1994).

In this same zone south of the rotational slumps, the SeaMARC I survey showed some large slump scars with headwalls up to 75 m high (Mosher et al., 1994, their figure 4) in 2000 m water depth. The presence of

these features has been confirmed by seismic reflection profiling (Fig. 6.8a). Below the depth of core penetration, we have attempted to correlate failure surfaces with the sequence of till tongues on the upper slope (Fig. 6.7b). The deepest recognisable till tongue occurs between carmine and flesh. A widespread failure surface south of East Acadia Valley occurs below flesh, in sediment of unknown character. The base of the large slump scar in Mosher et al. (Fig. 6.8a) is a short distance above carmine and could well correlate with till tongue (4).

In the eastern part of the slope sector off Western Bank, near surface sediment is relatively uniform over large areas and shallow slumps and/or debris flows are relatively uncommon. However, locally in channels multiple stacked debris flows are present and a few of these flows extend outside of the channels (Fig. 6.16). In places, deep-seated faults extend almost to the seabed (Fig. 6.17) and appear to have an influence on seabed morphology.

Core stratigraphy

Hill (1981) described the stratigraphic section off the western part of Western Bank. He distinguished two main units (Fig. 6.18). Unit 2 consists mainly of olive grey mud of facies A: the top of this unit (2d) is sandy or silty on the upper slope. In many cores there was an intercalation of browner mud (10YR 4/2, "yellowish brown" of Hill, 1981) (2c and 2a) over and underlying the lower unit of olive muddy silt (2b). Below this, unit 1 consists principally of brown muds, with ice rafted detritus and some sand beds. The upper part (1b) is principally red brown mud, the lower part (1a) principally brown. A brick-red marker, correlated with **b** of Piper and Skene (1998), is present but marker **d** was not seen (Fig. 6.18). Hill's only dating control was several TOC conventional radiocarbon dates (with corrections for dead carbon) and one conventional radiocarbon date on a small mollusc (unreliable because of the small size of the sample). New AMS radiocarbon dates from core 78-77 provide the following interpolated chronology. A date of 8.87 ka was obtained near the base of unit 2c, and a date of 10.3 ka from near the top of unit 2b. A shell at the base of unit 2b gave an age of 10.5 ka. The base of unit 2a lies between 11.5 and 13.0 ka. Ages on units 2a and 2b can be based only on extrapolated ages, which require assumptions as to sedimentation rates in silty sediment and in mud. The base of unit 2a has an extrapolated age of about 6.0 ka assuming constant sedimentation rates in units 2a and 2b; the base of unit 2b lies between 9.3 and 10.25 ka. In core 90015-18, a shell at 90 cm within unit 2b yielded an age of 9.6 ka. The changes from silty sand (2b) to silty mud (2c) to silty sand (2d) suggest fluctuations in the strength of storm driven currents along the upper slope. The diminution in current strengths between 6 ka and 9.3 ka corresponds to the period of early Holocene warming.

The most complete late Quaternary section is in the Acadia-Shubenacadie area described by Piper and Wilson (1985), Mosher (1987) and Mosher et al. (1989). Piper and Wilson (1985) described four lithofacies, using 82004-05 as a type section (Fig. 6.19). Unit 1 consists of olive grey mud, with interbedded red brown mud

in a few cores, and reached a thickness of 3.9 m in core 82004-09. Unit 2 is a variable sequence of muds and gravelly sandy muds of a generally brownish colour, including several brick red sandy mud horizons. In core 82004-02, four such horizons are recognised (Fig. 5.22). Unit 3 consists of rather monotonous dark brown mud with dispersed sand and gravel. Unit 4 consists of dark olive grey mud with some bioturbation and scattered granules.

We have used core 88010-18 (Fig. 6.20), from 1342 mbsl in the undisturbed area between the two failure zones, as a reference core in which measurements of O and C isotopes and organic carbon were made (Fig. 6.21). Less than 1 m of Holocene olive grey muds (Unit 1) overlie a condensed sequence with two brick-red sandy mud horizons (Unit 2) over 1.5 m of brownish muds with dispersed sands and granules (Unit 3). Beneath this is about 2 m of olive grey and dark grey muds (Unit 4), locally bioturbated, with their base corresponding to the brown high-resolution reflector. Organic carbon is relatively abundant in the lower part of this lithofacies. This interval appears to have failed locally at the western edge of the eastern disturbed zone (cf. Campbell 2000). Beneath this grey interval are at least 5 m of brownish muds with thin sand beds. The orange and green high-resolution reflectors fall in this lithofacies. A shell sample from near the orange reflector has been submitted for radiocarbon dating.

Cores 83012-04 and 83012-06, taken in areas where failures have removed surficial sediment, sample the section between high-resolution reflectors yellow and pink (Fig. 6.23). They sampled principally brownish muds with ice-rafted sand and granules. A radiocarbon date of 36.4 ka was obtained from the base of core 83012-06.

The chronology of the stratigraphic succession in this area is constrained by several reasonable consistent radiocarbon dates. Correlation between cores 82004-1 and 82004-2 suggests that the two dates in 82004-1 are too old. These two dates were the first two AMS dates every obtained for this study and we suspect there may have been some analytical error. Otherwise, the available dates suggest that the top of unit 4 dates from about 18.3 ka. Core 90015-17 sampled a debris flow resting on brown muds with granules; the base of the debris flow deposits corresponds approximately to the yellow high-resolution reflector. A radiocarbon date of 20.8 ka from near this boundary was originally interpreted as being from sediment underlying the debris flow, but is now considered to represent material within the debris flow. High-resolution reflector pink is dated at 36.4 ka. The youngest till tongue is rather older than the 18.3 ka date and is thus probably equivalent to the last glacial maximum. Attempts at coring the "till tongues" have recovered only short cores of overconsolidated sediment[1], but whether the overconsolidation was due to loading by grounded ice or by icebergs is unclear. We believe that

[1] 88010-20 recovered stiff silty mud, but all washed out; 90015-003 penetrated similar material on St Pierre slope and recovered 36 cm of alternating consolidated sands and muds.

the deposits are of overconsolidated till, but alternatively they might represent pro-glacial debris flows.

Cores in the failure zones generally penetrate lithofacies 1, 2 and in some cases 3, which rest unconformably on tilted blocks of grey mud (lithofacies 4) (Figs. 6.19, 6.24). In the distal part of the Western Disturbed Zone, debris flow deposits consisting of mud clast conglomerate rest unconformably on a slide scar and in core 83012-08 are overlain by a sorted coarse sand.

The age of the failures between the Acadia and Shubenacadie wells is constrained by radiocarbon dating of molluscs. A small debris flow (identified as DF0) in core 82004-7, at the head of the eastern failure, contained a gastropod dating at 10.8 ka (TO-5077) thus providing a maximum age. The main failure sediments in the eastern zone in core 82004-2 are overlain by a shell dating from 15.1 ka (Beta 10987) and sediment immediately overlying the failure (probably deposited during the same event) includes mollusc fragments dating from 15.8 ka (TO-5078). This core also shows a brick-red gravelly sandy mud, most likely bed **d** of Piper and Skene (1998) at 51-53 cm and a possible higher brick red gravelly sandy mud (?bed **b**) at 40-43 cm. In contrast, sediment overlying the western failure contains no brick-red sandy mud beds, but rather has a section of typical Holocene olive-grey muds overlying the failed sediment. In core 82004-11, in the northwestern part of the western failure near its upslope limit, failed sediment is immediately overlain by a gastropod with a date of 12.3 ka (TO-5568), rather younger than the 13.2 ka age of bed **b** (Piper and Skene, 1998). In summary, the main failure in the Eastern Disturbed Zone (DF3) is bracketed by dates of 15.1 and 15.8 ka and is overlain by a small failure (DF0) that is younger than 10.8 ka. The Western Disturbed Zone (DF1) dates from about 12 ka.

Geotechnical measurements

In cores from near the Shubenacadie well, Mosher et al. (1994) reported downcore measurements of shear strength, bulk density and water content (Fig. 6.25) and evaluated slope stability using infinite slope analysis (Fig. 6.26). On the regional 2° slopes, surficial sediment is stable. They considered and rejected triggering mechanisms such as storm wave loading and excess pore pressure due to shallow gas. Excess pore pressures of 6 - 11 kPa would be required for failure: note that excess pore pressures of 2.5 Kpa in gassy sediment and 6.7 kPa in debris flows have been measured on St Pierre Slope. They concluded that failure was probably seismically triggered. Sediment in this area is less silty than on St Pierre Slope, although regrettably no Atterberg limit determinations are available. Downcore variation in shear strength implies a strength ratio of about 0.33. This may indicate some slight cementation by early diagenetic iron monosulphides. Clay minerals are dominantly illite, with minor kaolinite and chlorite and large amounts of rock flour of quartz and feldspar.

Campbell (2000) has correlated the observed failure planes beneath the rotational slumps and in the bedding plane slides with sediment recovered in cores from areas of undisturbed seabed (Fig. 6.23). This analysis shows that failures seem to be localised at horizons with abundant sand beds.

6.4 **Geologic history and hazard assessment**

Geological history

Through the Pliocene, there is evidence of shallow channels throughout this sector of the slope, which regionally appears to have been an important Pliocene depocentre. Widespread gullying took place at the base of the Quaternary, but most of the lower to middle Quaternary section consists of draped presumably muddy sediment.

Above carmine (perhaps above flesh), the style of sedimentation changed and upper slope till tongues record advances of ice across the shelf. Gullies appear to have been maintained downslope from these ice margins. The last ice advance only affected the eastern part of the area (Mosher et al 1989).

Distribution of shallow gas

Pockmarks are most abundant in water depths of 500-900 m although they are present in all water depths to 2200 m (Fig. 6.15). The relationship of pockmarks to deeper structures is not known. The significance of these observations is discussed in section 10.2.

The risk of sediment failure

The available core stratigraphic data suggests that, as in the area off Emerald Bank, Holocene sediment failures are not found. The age of the two major rotational slumps in the east of the area is ca. 15 ka and ca. 12 ka.

Mulder and Moran (1995) examined the possible influence on strength properties of ice loading on the outer shelf and upper slope, assuming shelf-edge late Wisconsinan ice thicknesses of 175 - 250 m, permitting direct ice loading to 200 - 400 m during the last glacial maximum sea level lowstand that would cause excess pore pressures. Additional excess pore pressures would be created by deposition of the distal parts of "till tongues" beyond the ice limit, but this effect would have been unimportant in water depths of more than 600 m. Dissipation of excess pore pressure could take up to 8000 yr. Bearing capacity analysis showed that the loading of the outer shelf by ice could cause failures in water depths in excess of 1000 m, but these failures would also involve large areas of the outer shelf. This analysis, then, does not account for the observed styles of thin-skinned failure in water depths of 600 - 2000 m.

It seems likely that earthquakes are the trigger for the thin-skinned failures (Piper et al. 1985a). The failures are quite widespread and show a range of structures similar to those associated with the 1929 Grand Banks earthquake on St Pierre Slope (Piper et al. 1999). The analysis of Mosher et al. (1994) suggests that

excess pore pressures would also promote failure. Such excess pore pressure might result from rapid deposition of proglacial sediment or might be associated with the melting of gas hydrates as bottom waters warmed up after glaciation.

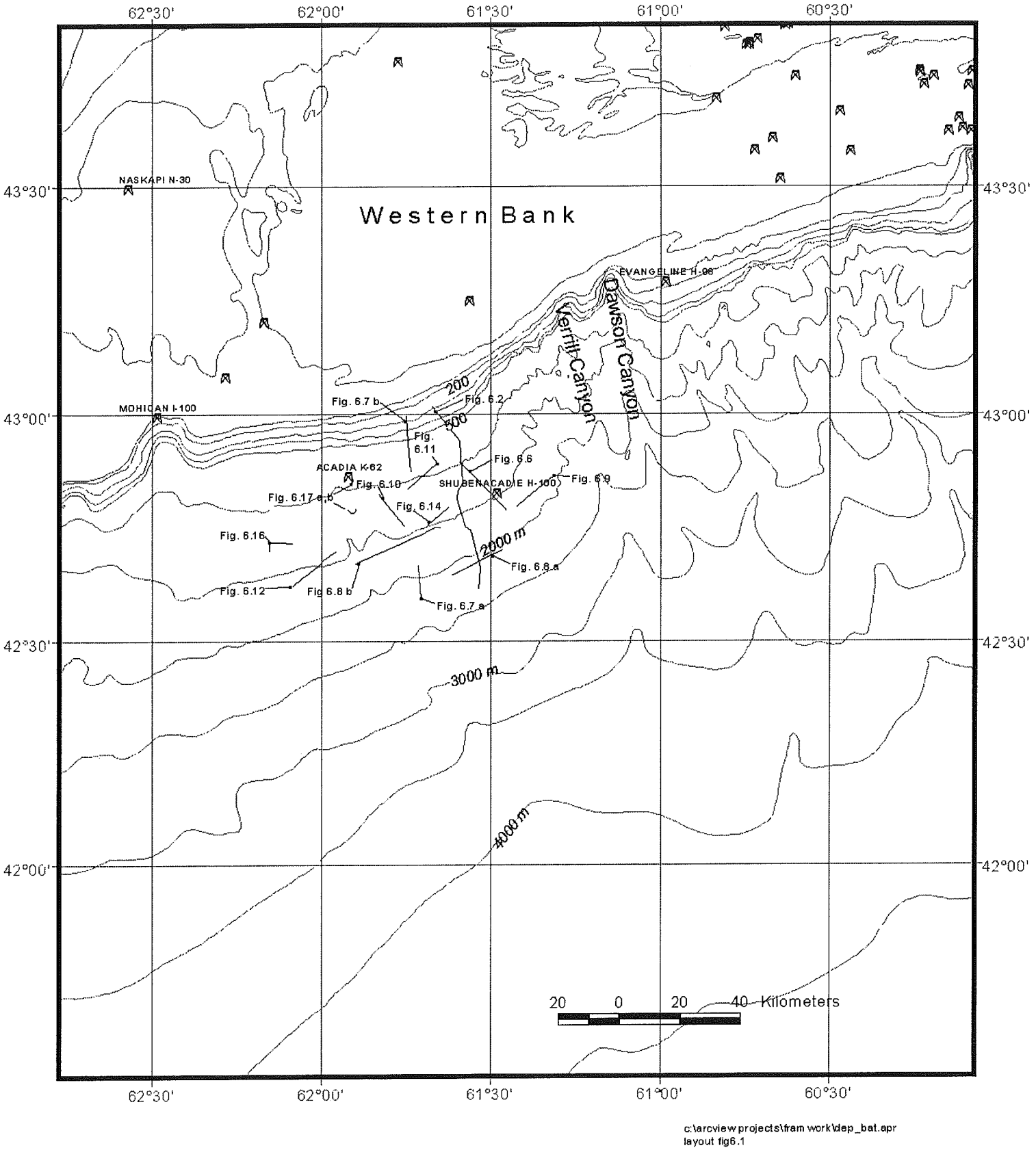

Fig. 6.1: General map showing the slope off Western Bank.

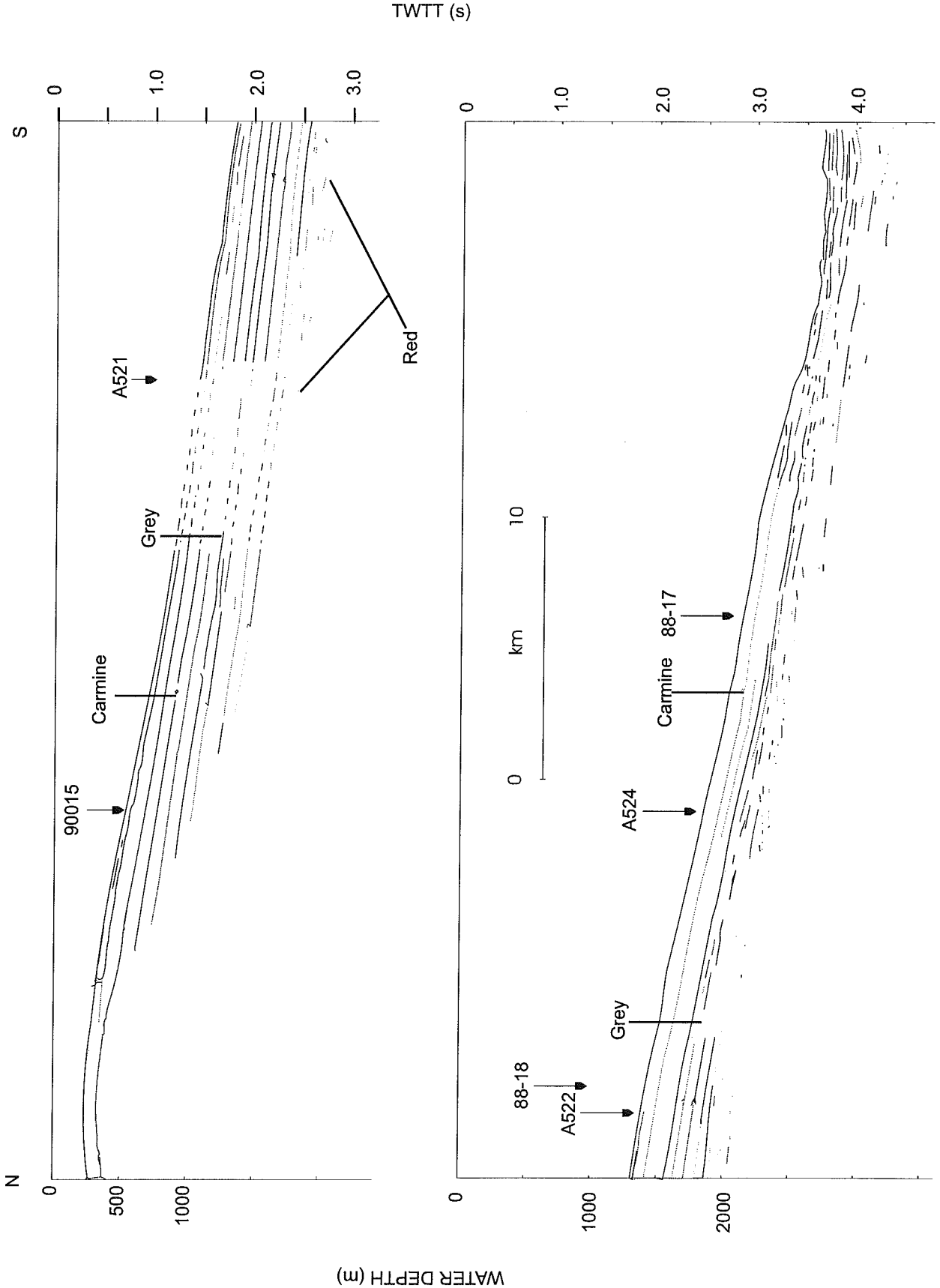

Fig. 6.2. Line drawing of seismic section off Western Bank near the Shubenacadie well to show the general progradational character of the continental slope. (profile 85001; part of original record illustrated in Mosher et al., 1989).

C:/IErnest/revised/fig6_2.cdr

Fig. 6.3: Map showing data coverage on the slope off Western Bank.

c:\arcview projects\fram work\det_bat.apr
layout fig 6.3

Fig. 6.4

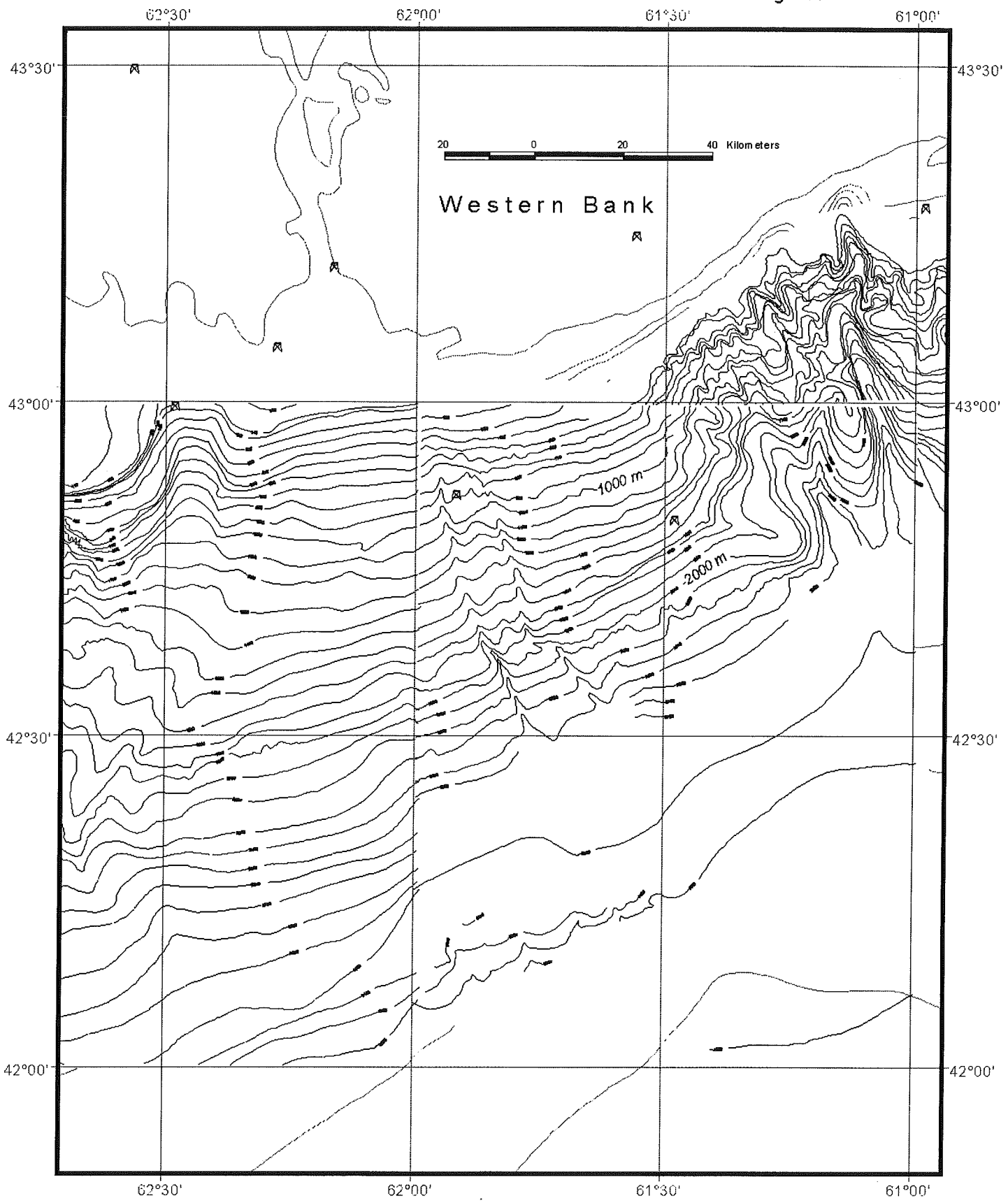

Fig. 6.4: Detailed bathymetry of the slope off Western Bank.

c:\arcview projects\fram work\det_bat.apr
layout fig 6.4

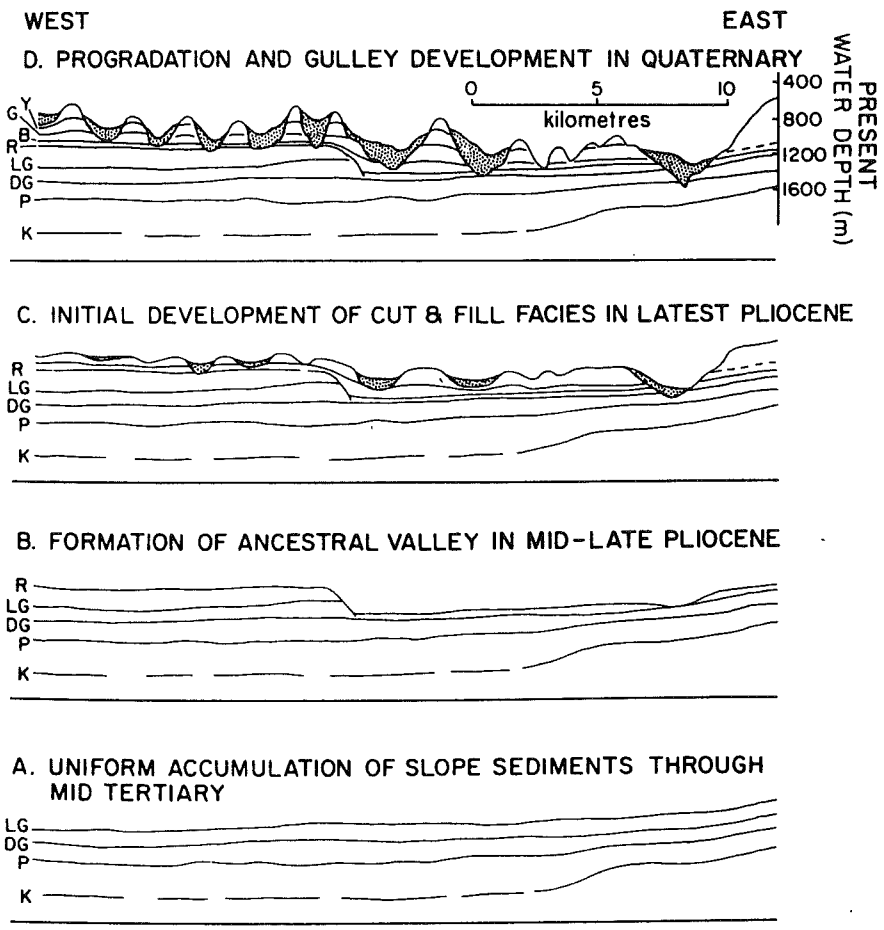

Fig. 6.5. Schematic strike sections showing evolution of the late Cenozoic stratigraphic sequence in the vicinity of the Shubenacadie H-100 well (from Piper et al. 1987).

C:/IErnest/revised/fig6_5.cdr

Fig 6.6

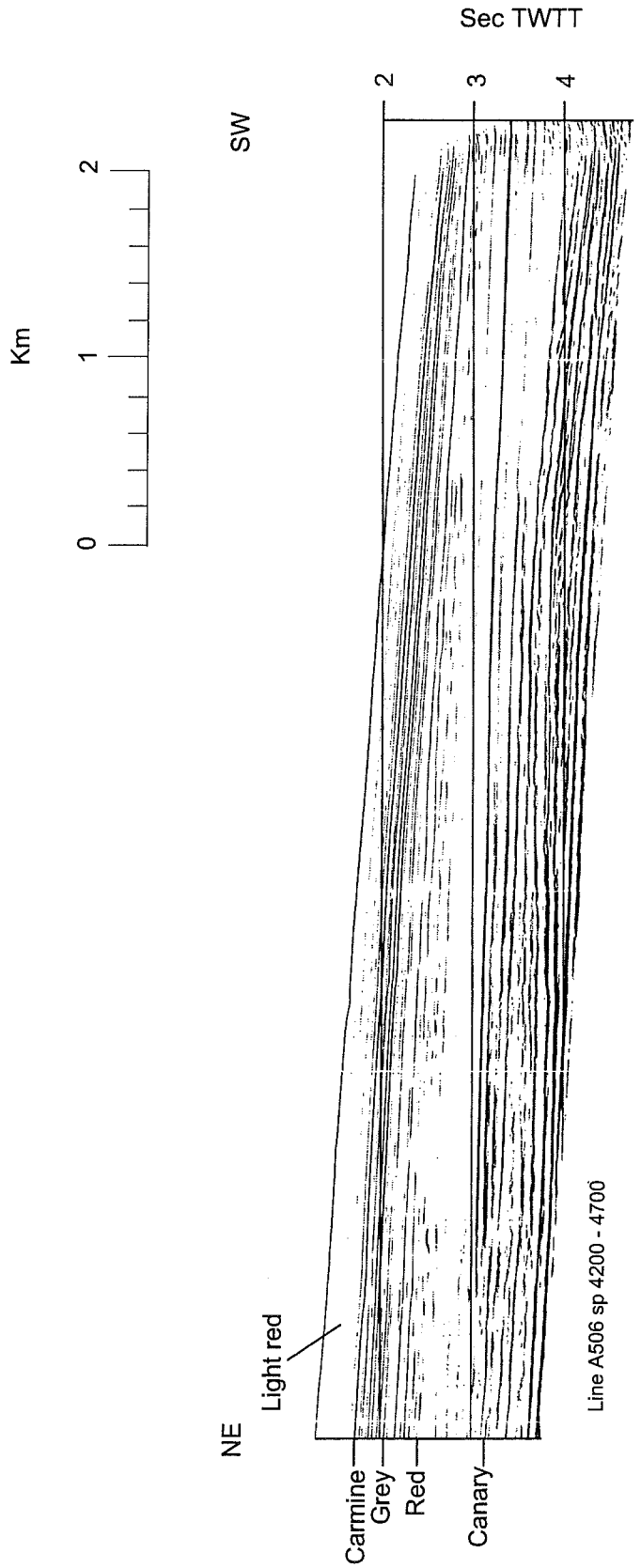

fig. 6.6. Seismic profile 506 illustrating regional stratigraphy of the Shubenacadie H-100 area.

C:/IErnest/revised/fig6_6.cdr

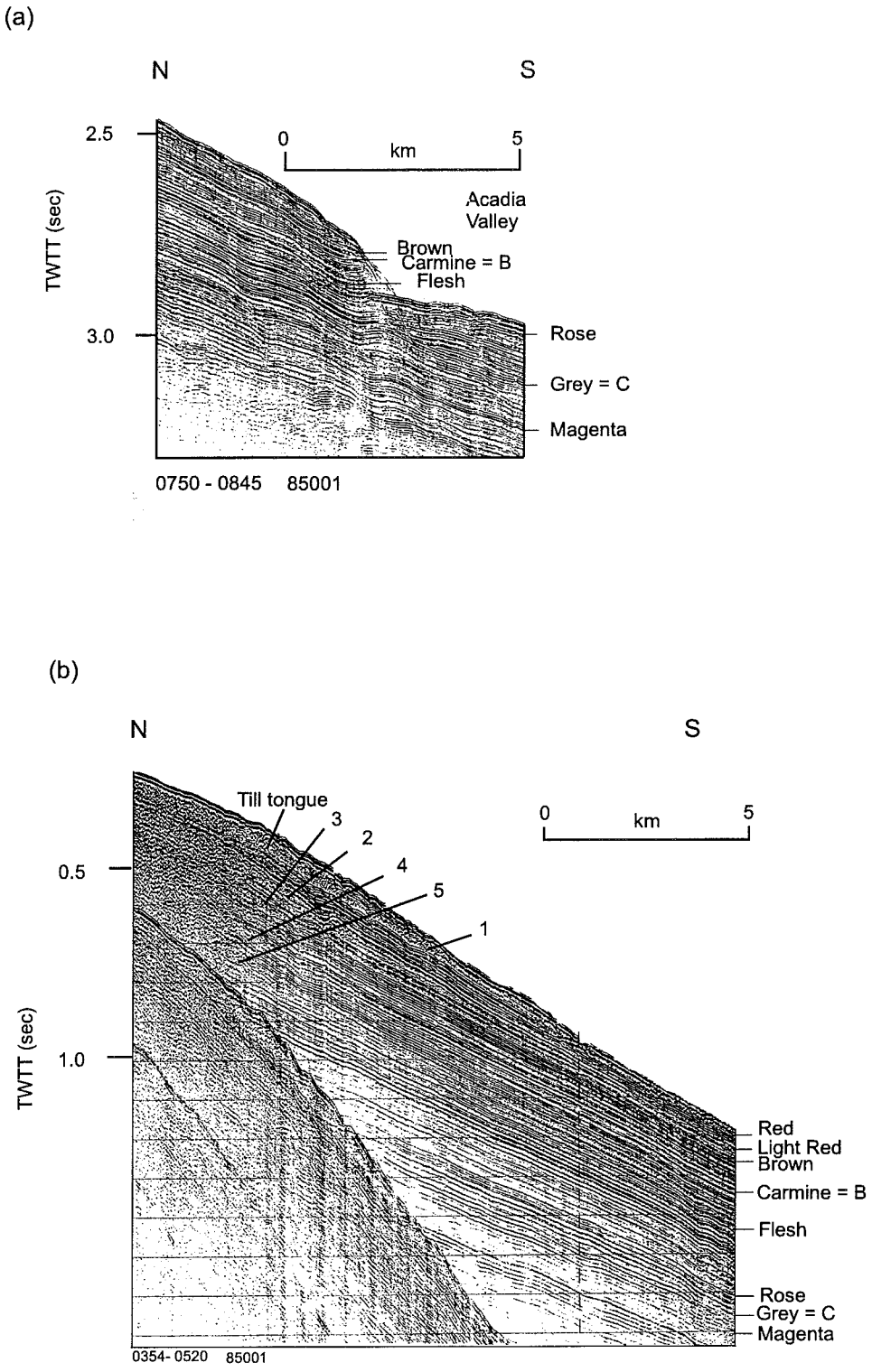

Fig.6.7. Single channel sleeve gun seismic profiles near the Shubenacadie well showing upper slope till-tongues (numbered 1-5) and correlation of reflectors into Acadia valley. Reflector names as in Table 1.4.

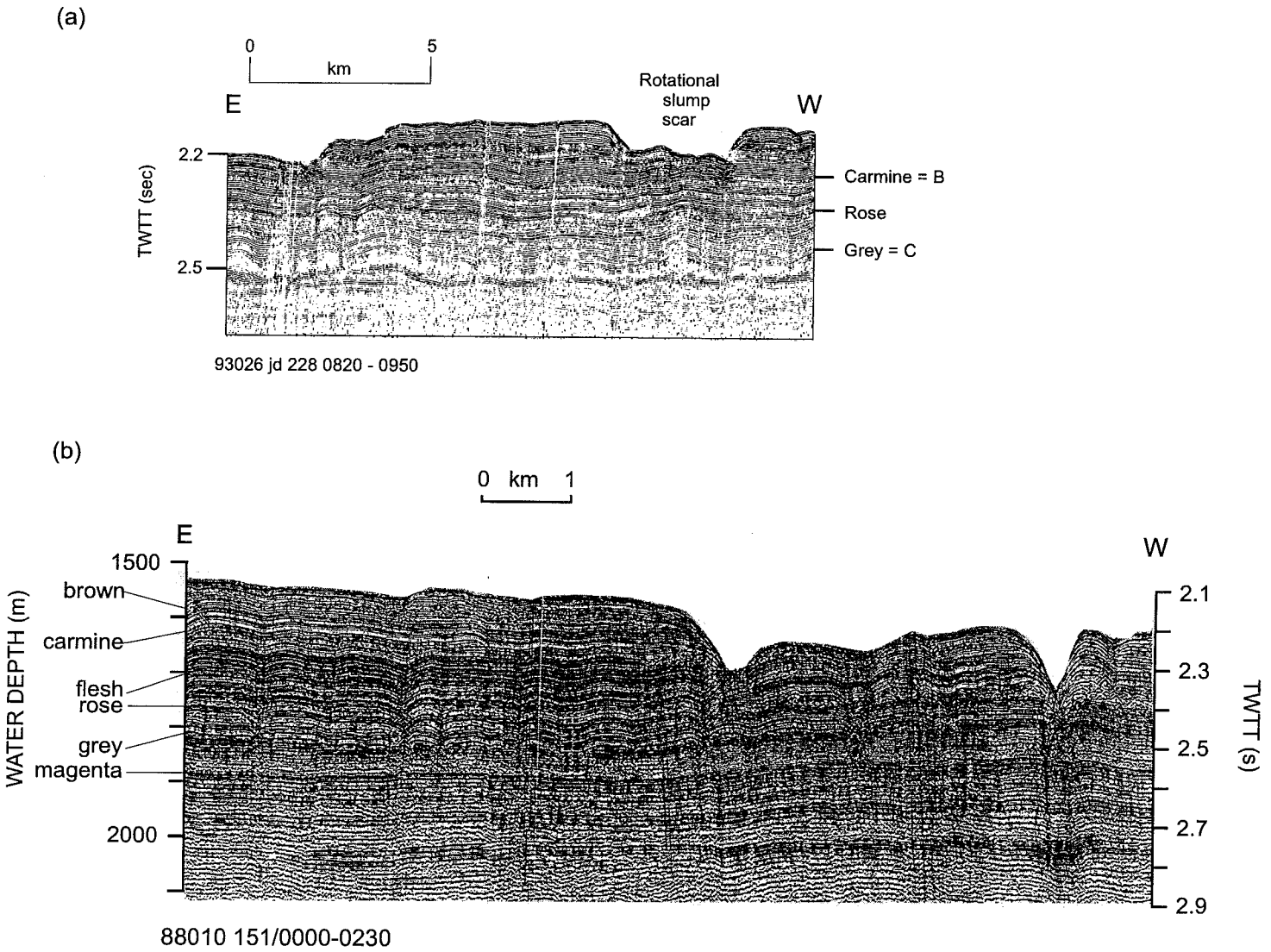

Fig. 6.8. Single channel sleeve-gun seismic profiles near the Shubenacadie well. (a) Stratigraphic control on deep water rotational slump. (b) Gullies at the grey (C) reflector.

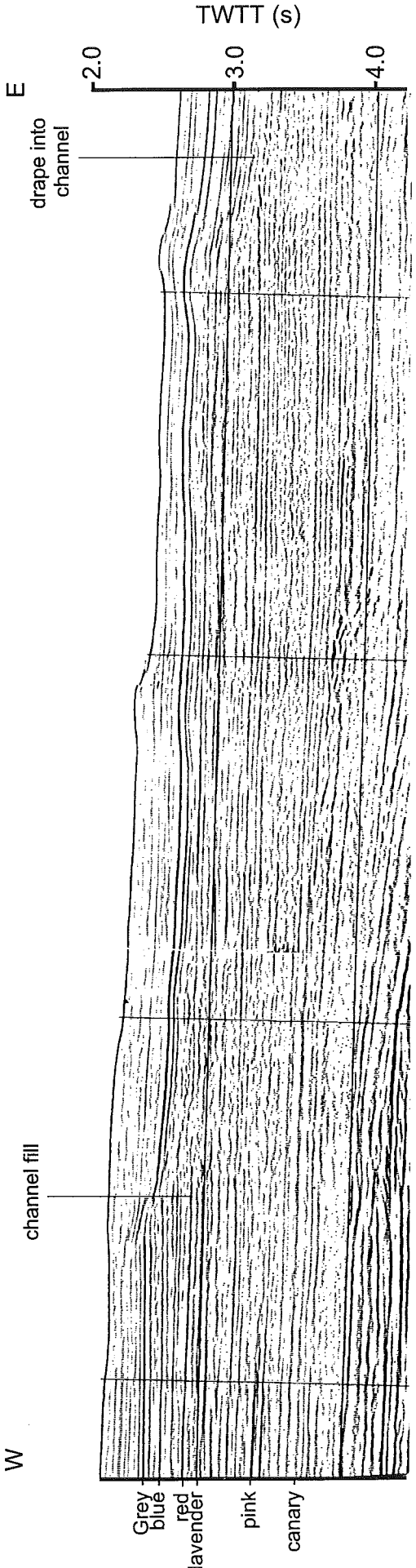

Fig. 6.9. Seismic profile at the edge of Verrill Canyon showing occurrence of channel fill deposits in the late Pliocene.

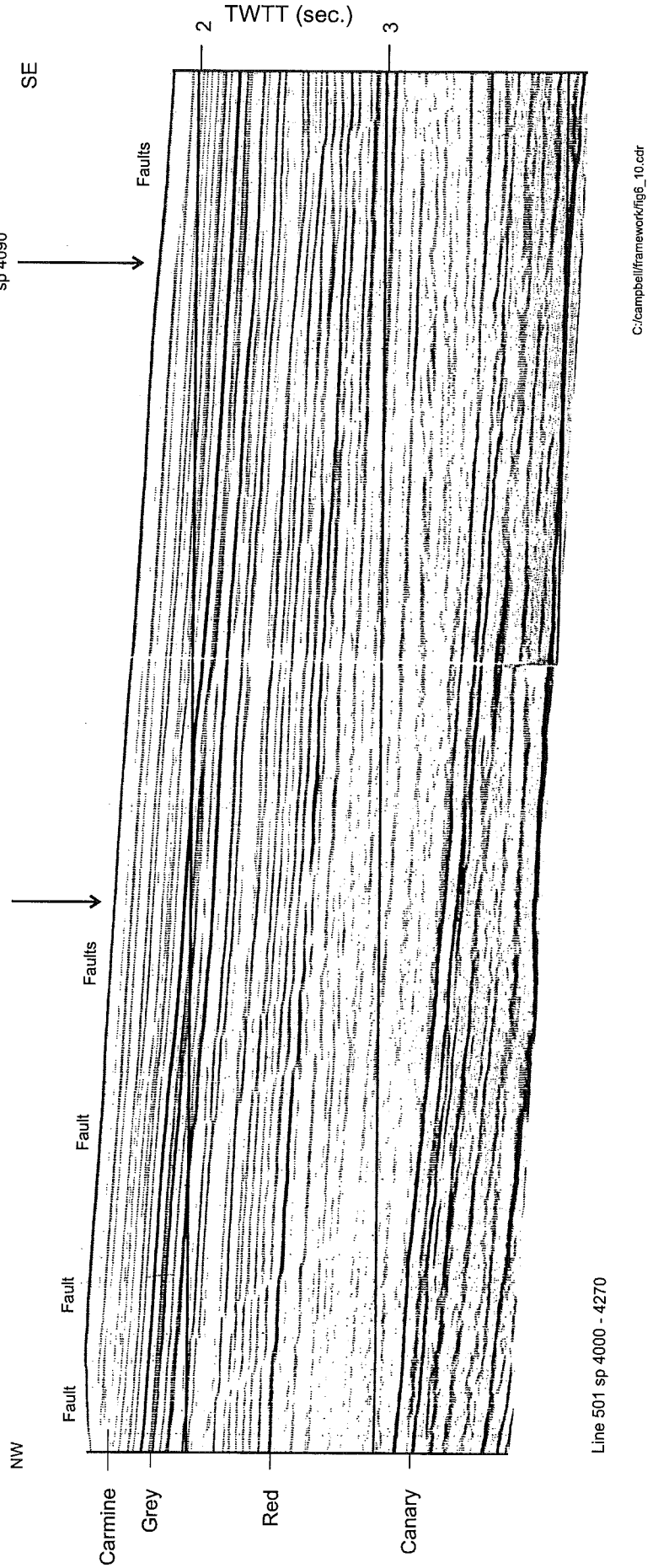

Fig. 6.10: Seismic profile showing interstratal faulting near the Shubenacadie H-100 well site.

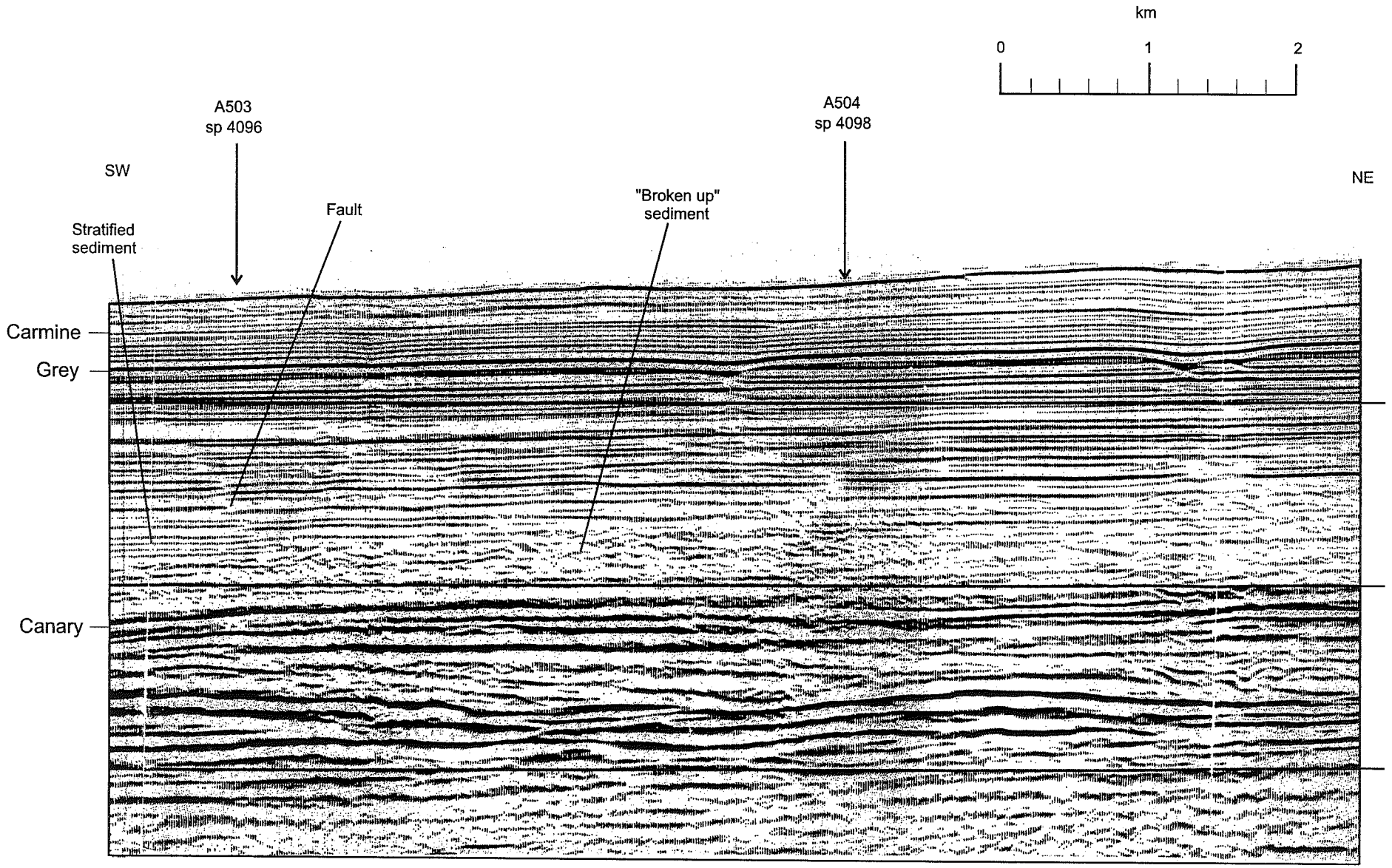

Line A520 sp 5010 - 5270

Fig. 6.11. Seismic profile showing interstratal "break-up"near the Shubenacadie well site.

Fig 6.11

C:/!Ernest/revised/fig6_11.cdr

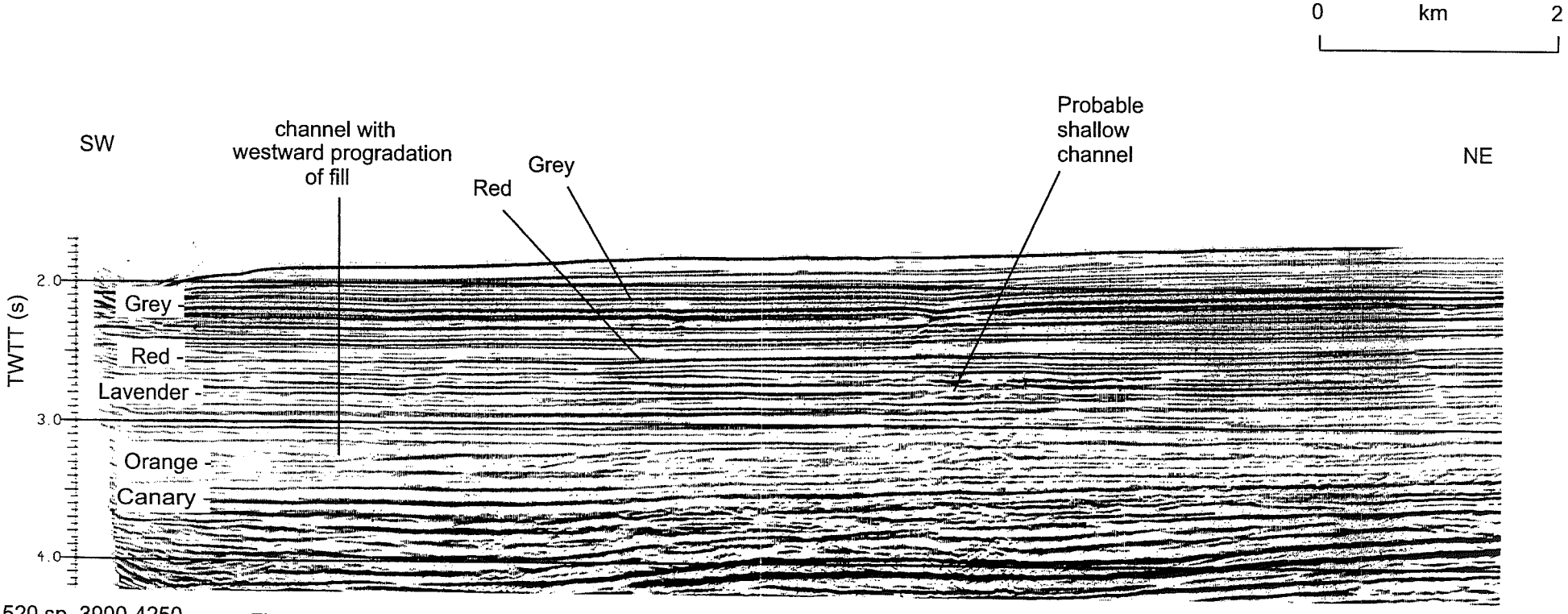

520 sp. 3900-4250

Fig. 6.12. Seismic profile showing middle Pliocene channel with westward progradation of fill, near the Shubenacadie H-100 well.

C:!Ernest/revised/fig6_12.cdr

Fig 6.12

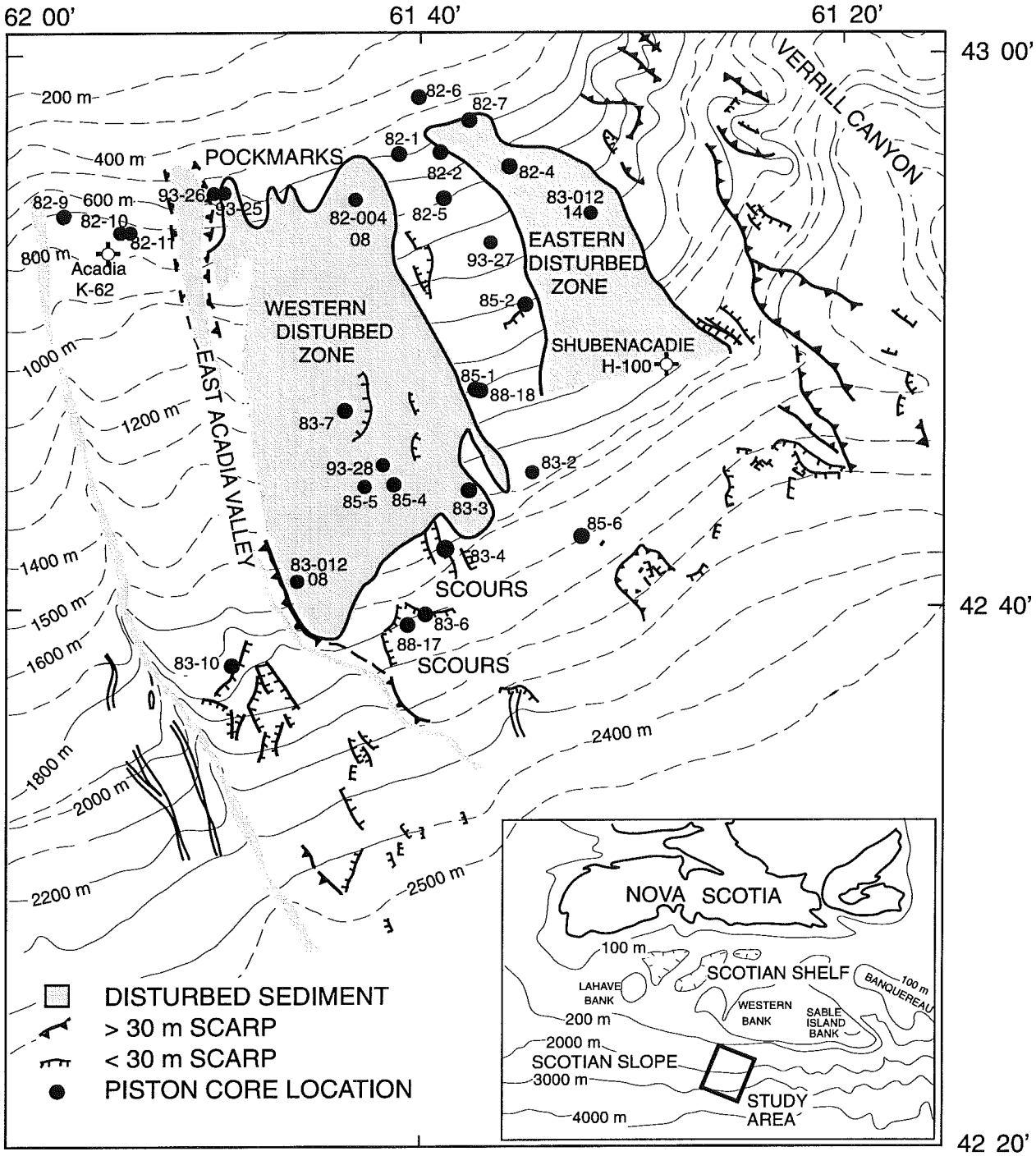

Fig. 6.13. Sediment instability features near the Acadia and Shubenacadie wells (modified from Piper et al., 1985 and Mosher et al., 1994), showing location of piston cores.

C:/IErnest/revised/fig6_13.cdr

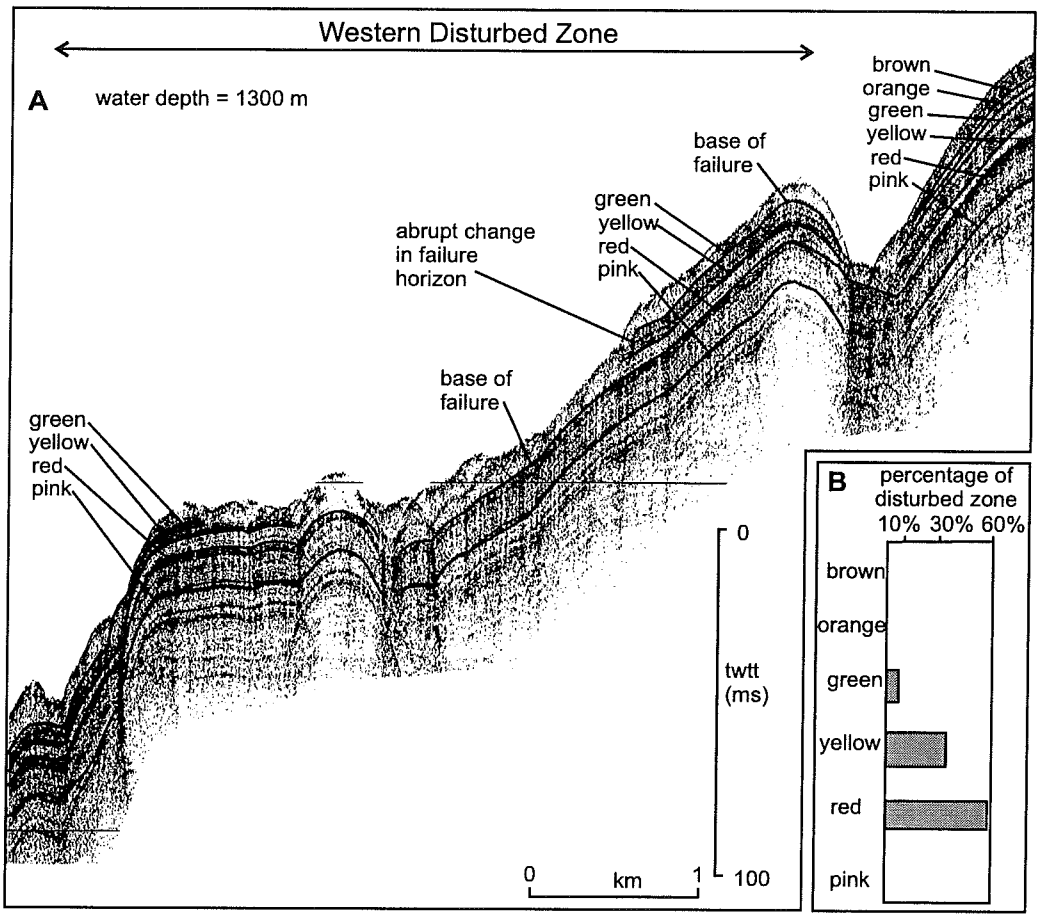

Fig. 6.14. High resolution seismic nomenclature. (Campbell,2000).

C:/!Ernest/revised/fig6_14.cdr

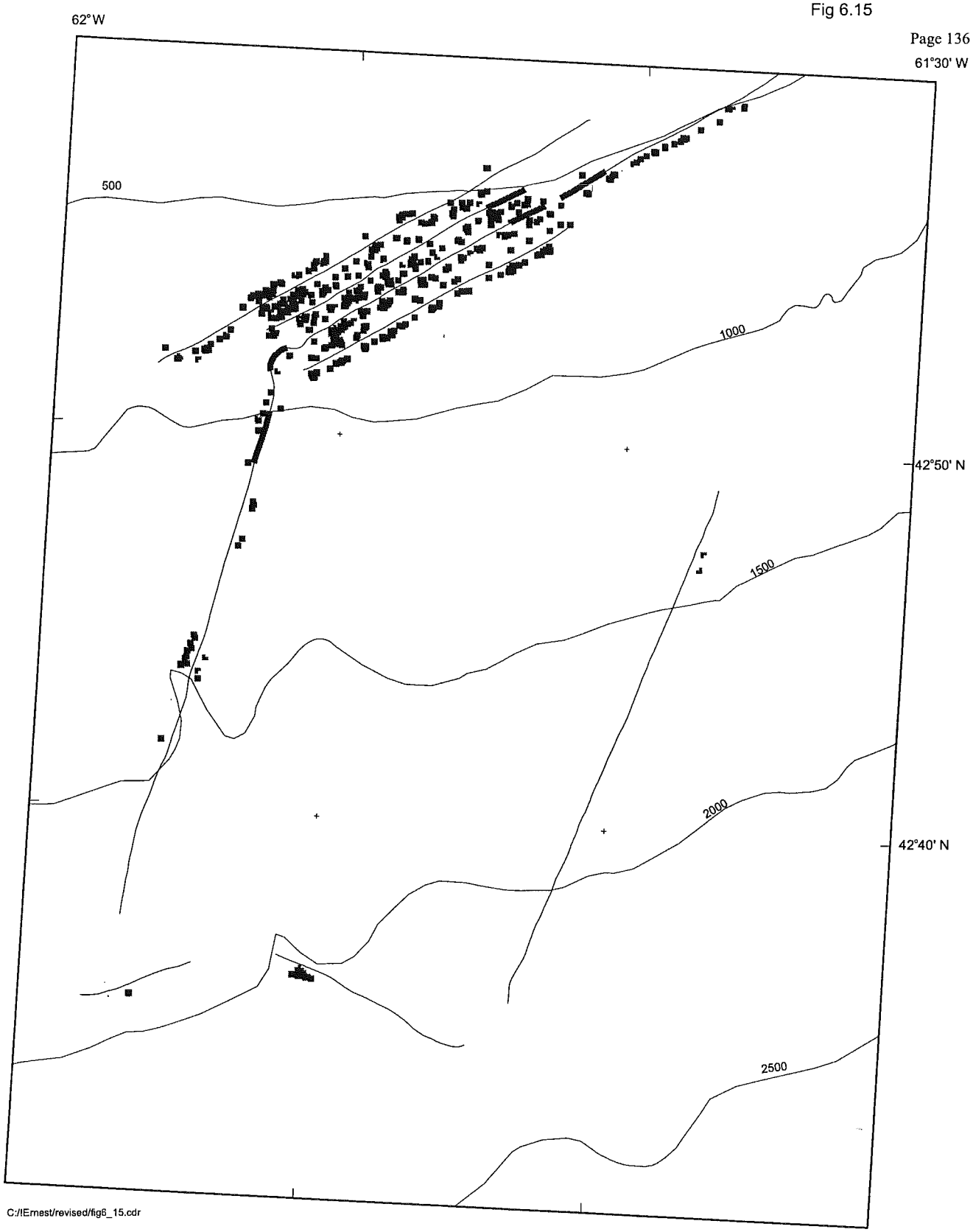

Fig. 6.15. Map of pockmarks in the area between the Subenacadie and Acadia wells. Lines indicate 1 km swath sidescan survey lines, each pockmark is shown by a dot.

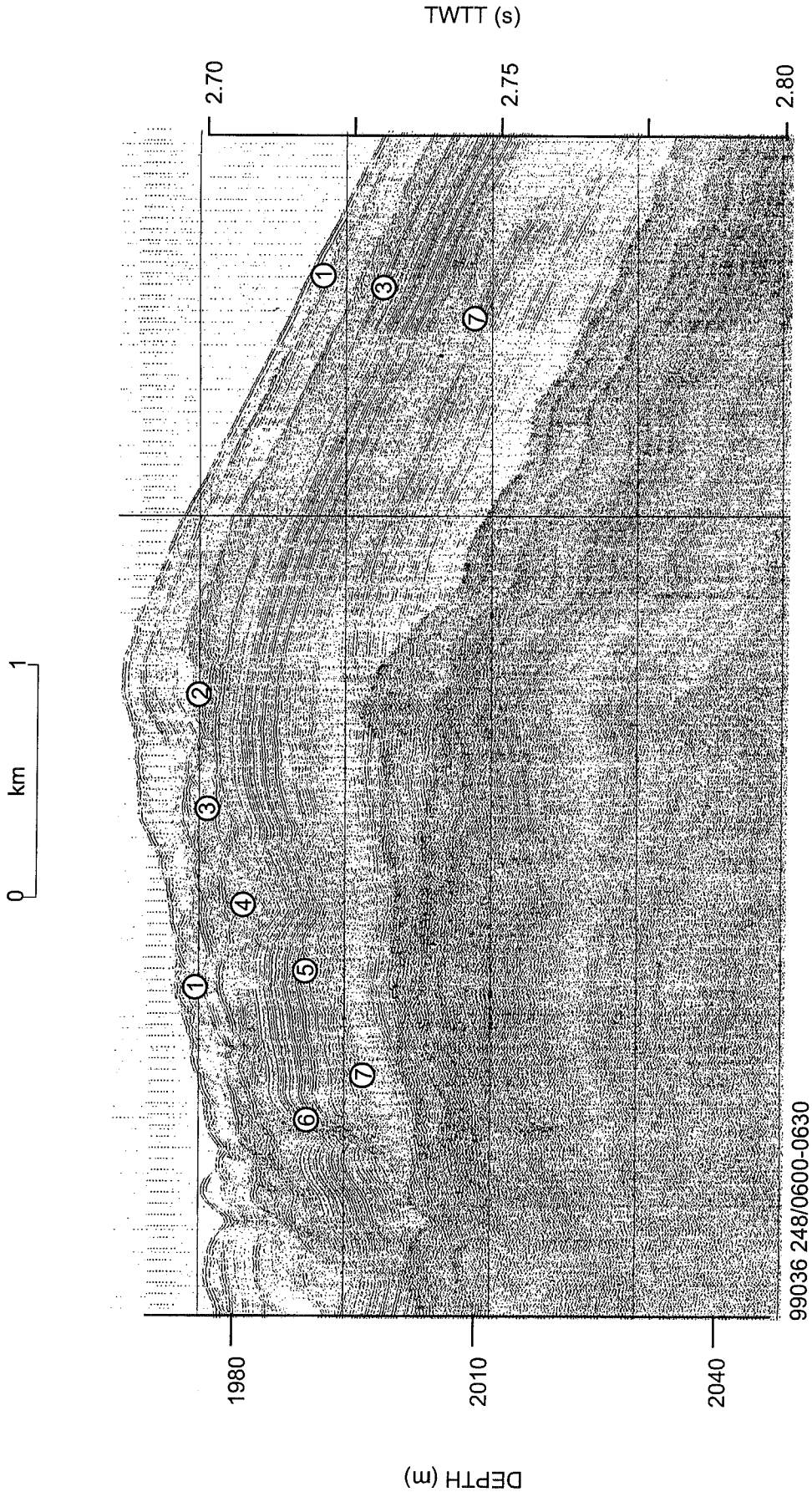

Fig. 6.16. Huntec DTS profile showing shallow failures and debris flows southwest of the Acadia K-62 well.

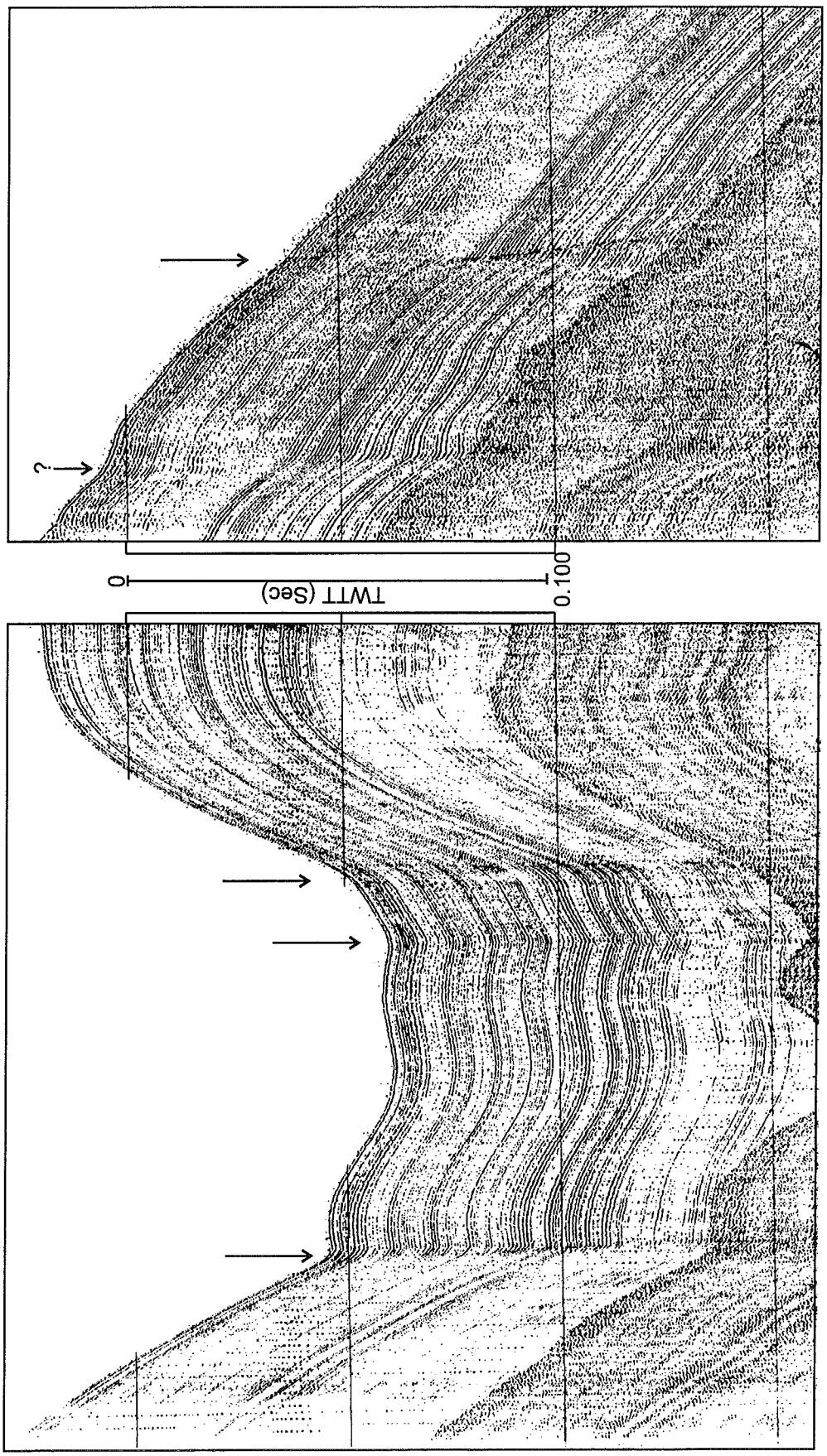

Fig. 6.17. Examples of faults breaking the surface in Huntec high-resolution sparker profiles. Cruise 99036.

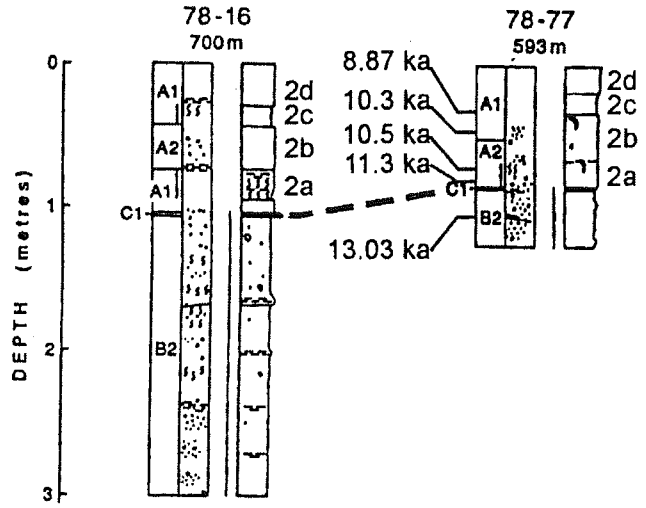

Fig. 6.18. Summary stratigraphy of cores from Western Bank (from Hill, 1981). Vertical bars within the facies column denote slightly browner intervals of olive grey mud. 2a-2d are lithostratigraphic unit designations of Hill (1981).

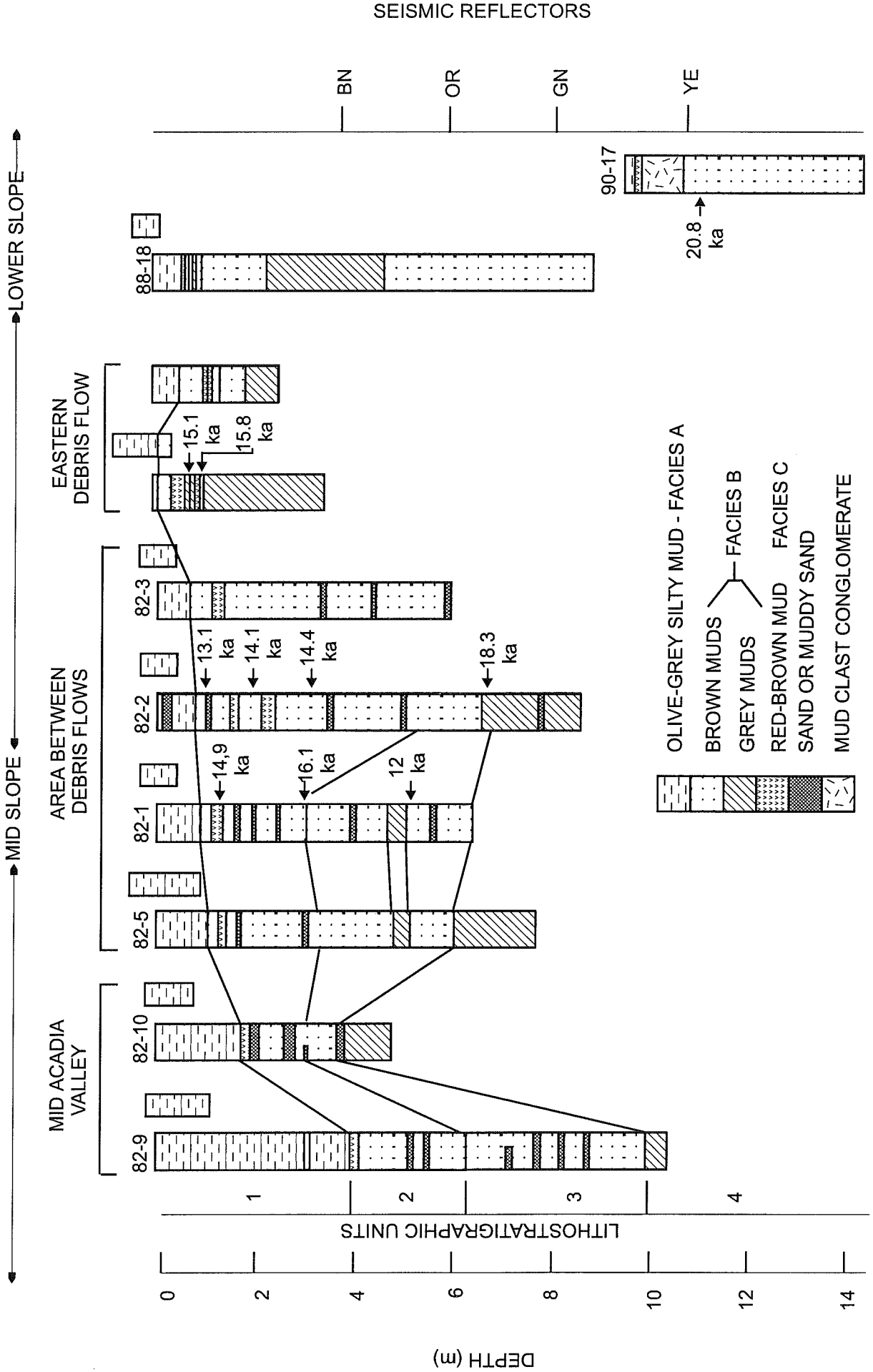

Fig. 6.19. Summary of the stratigraphy of the Verrill Canyon area (based on Piper and Wilson, 1985, with some data from Mosher et al., 1989).

C:/IEmest/revised/fig6_19.cdr

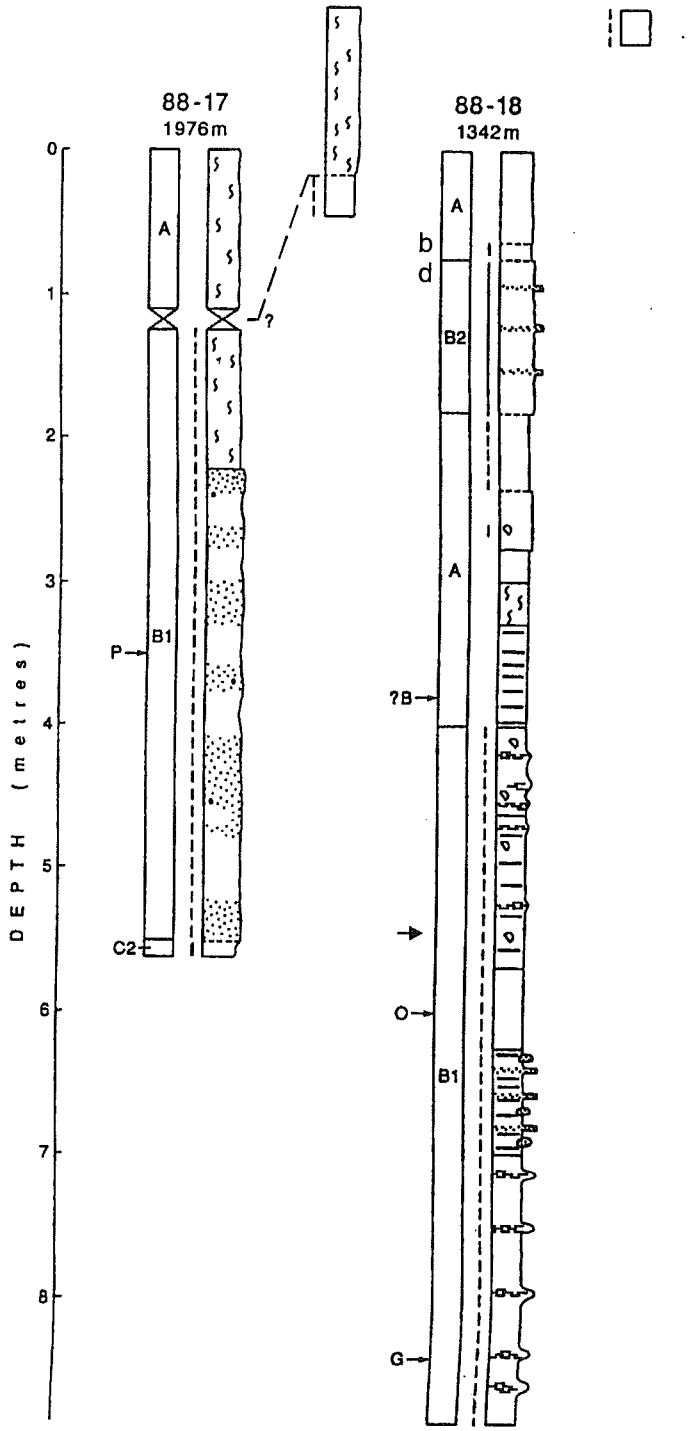

Fig. 6.20. Composite core profile of cores 88010-017 and 018, showing lithologies, seismic markers and ages. Legend in figure 1.5.

C:/IErnest/revised/fig6_20.cdr

88-010-18 Verill Canyon

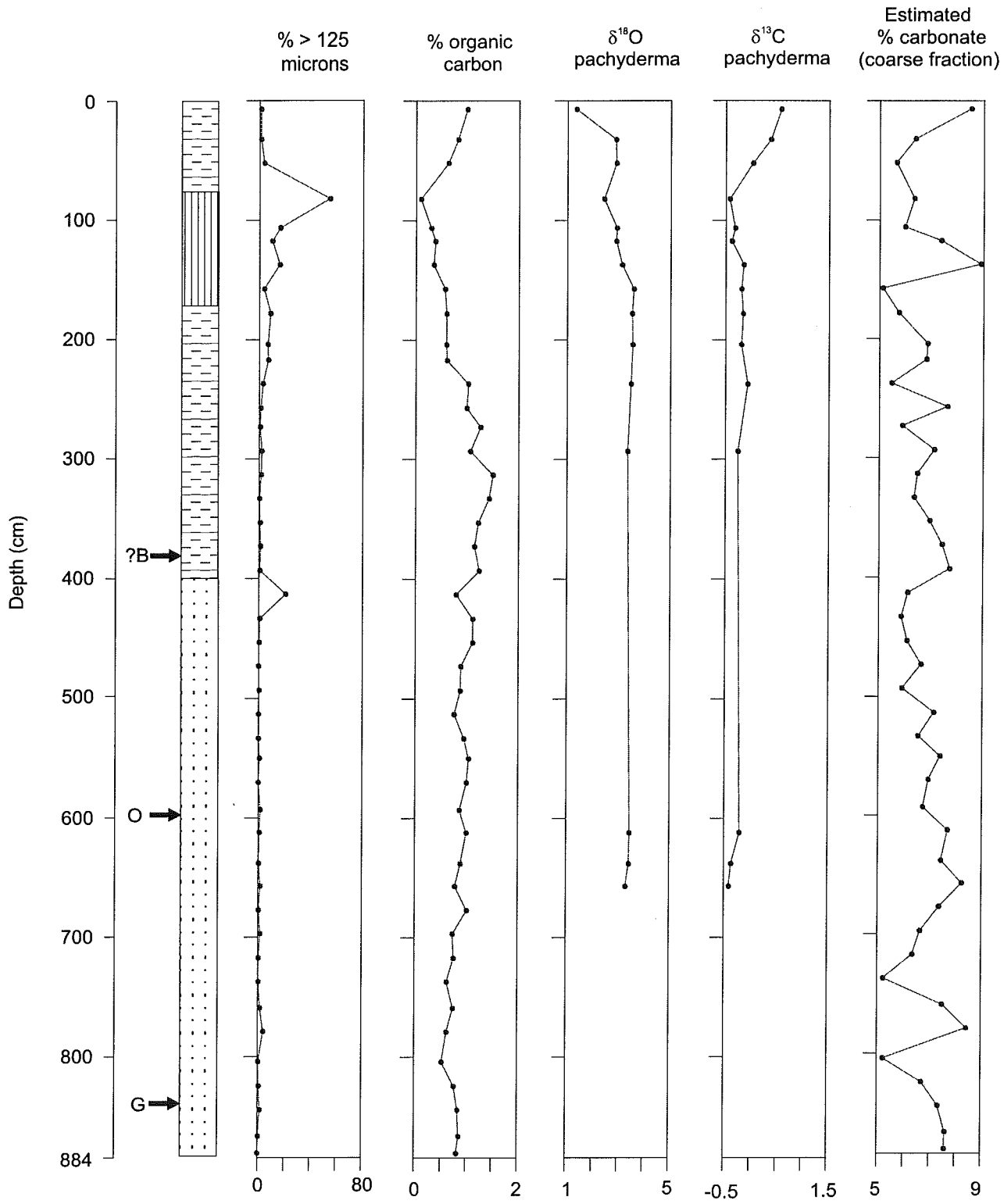

Fig. 6.21. Isotope stratigraphy of core 88010-018.

C:/!Ernest/revised/fig6_21.cdr

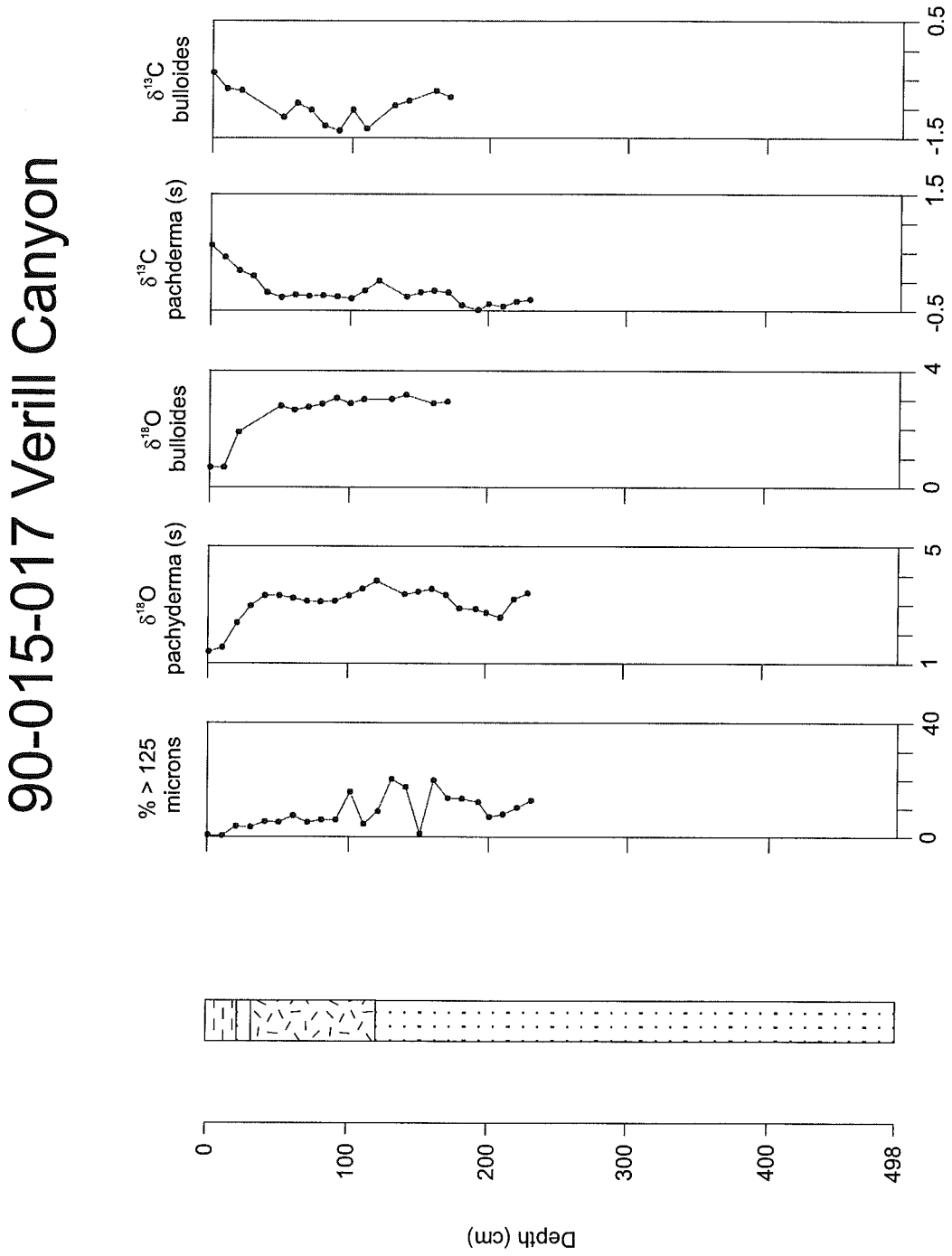

Fig. 6.22. Isotope stratigraphy of core 90015-017.

C:/IEmest/revised/fig6_22.cdr

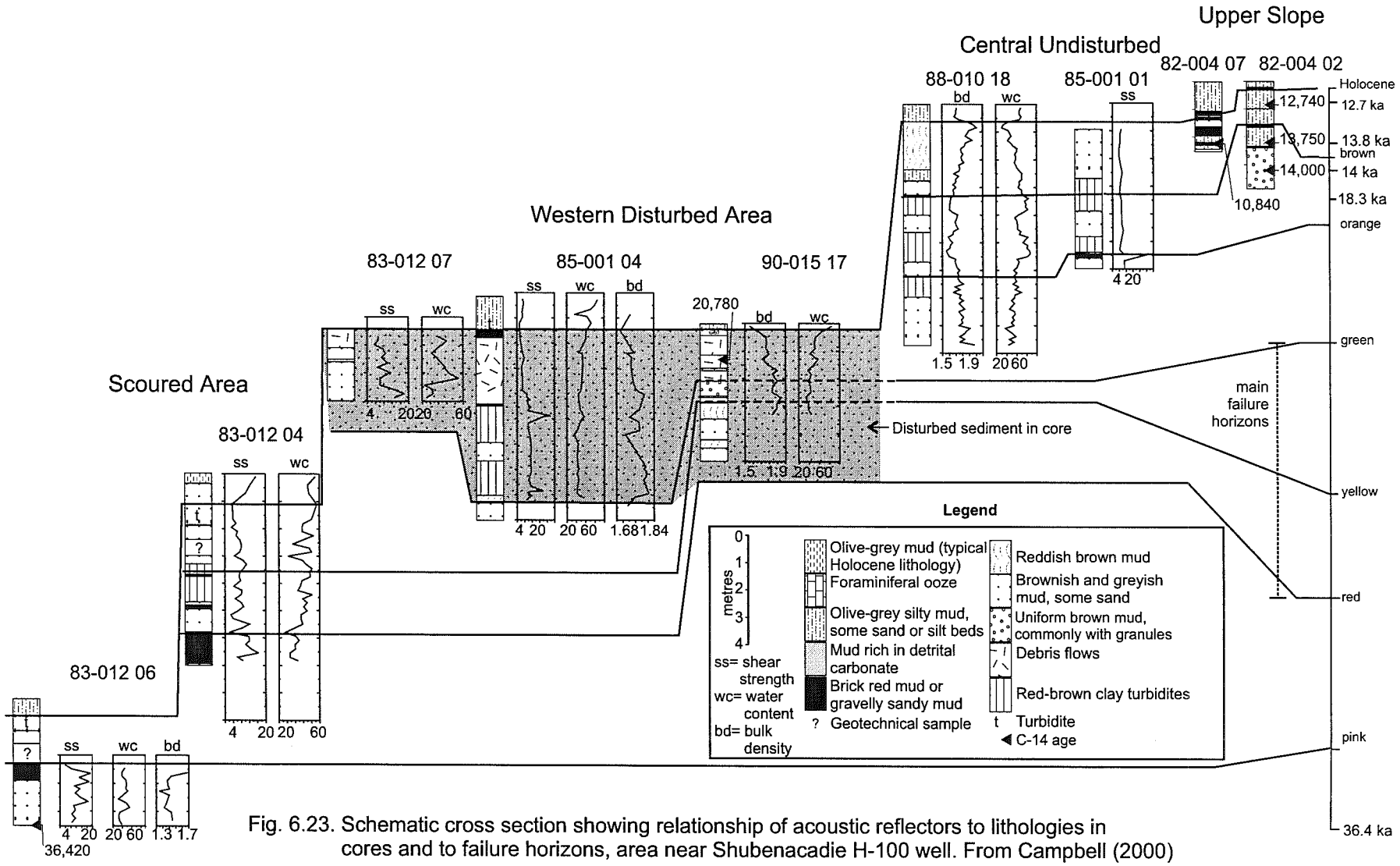

Fig. 6.23. Schematic cross section showing relationship of acoustic reflectors to lithologies in cores and to failure horizons, area near Shubenacadie H-100 well. From Campbell (2000)

C:/!Ernest/revised/fig6_23.cdr

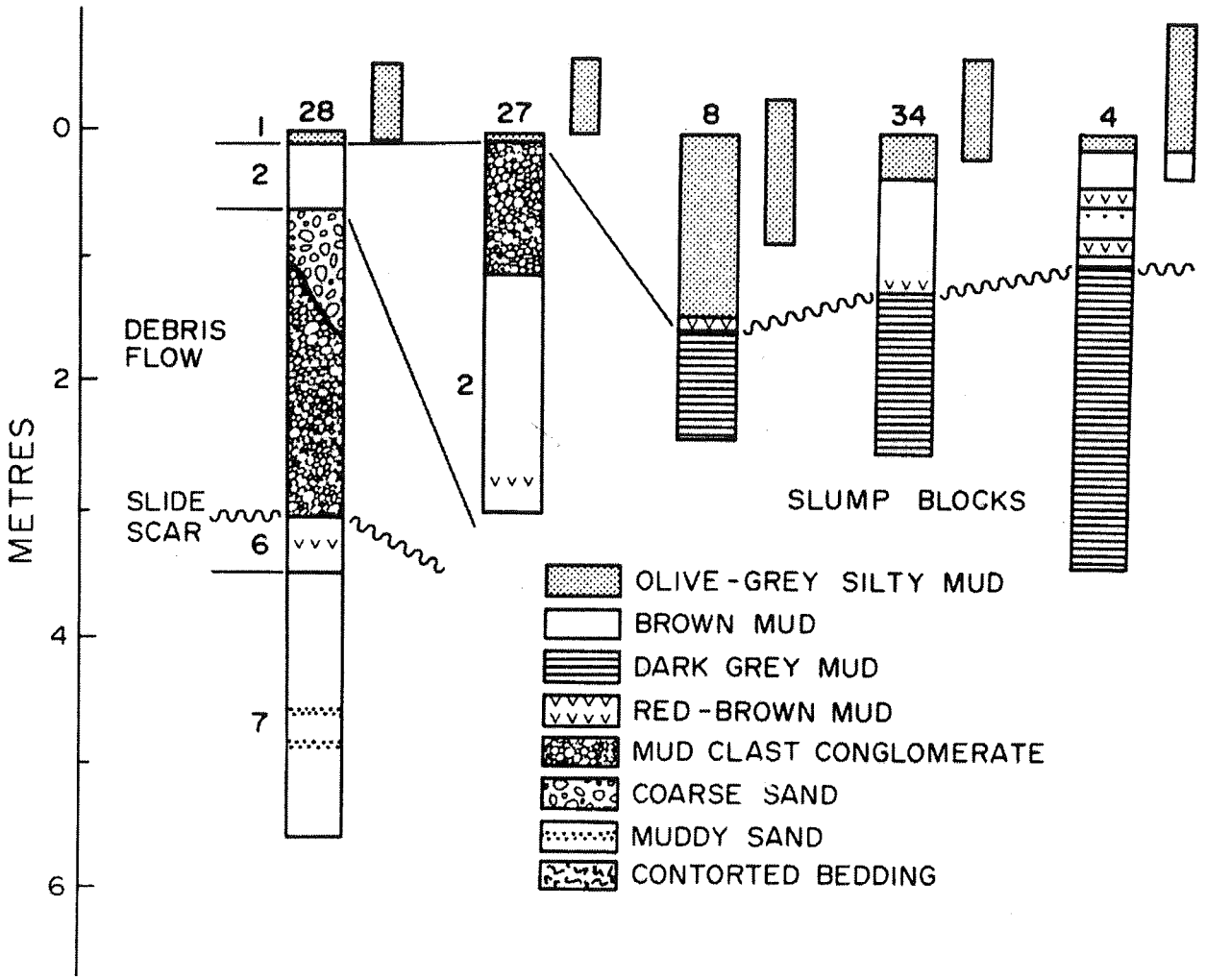

Fig. 6.24. Stratigraphy of cores in the failure zones. Modified from Piper et al. (1985).

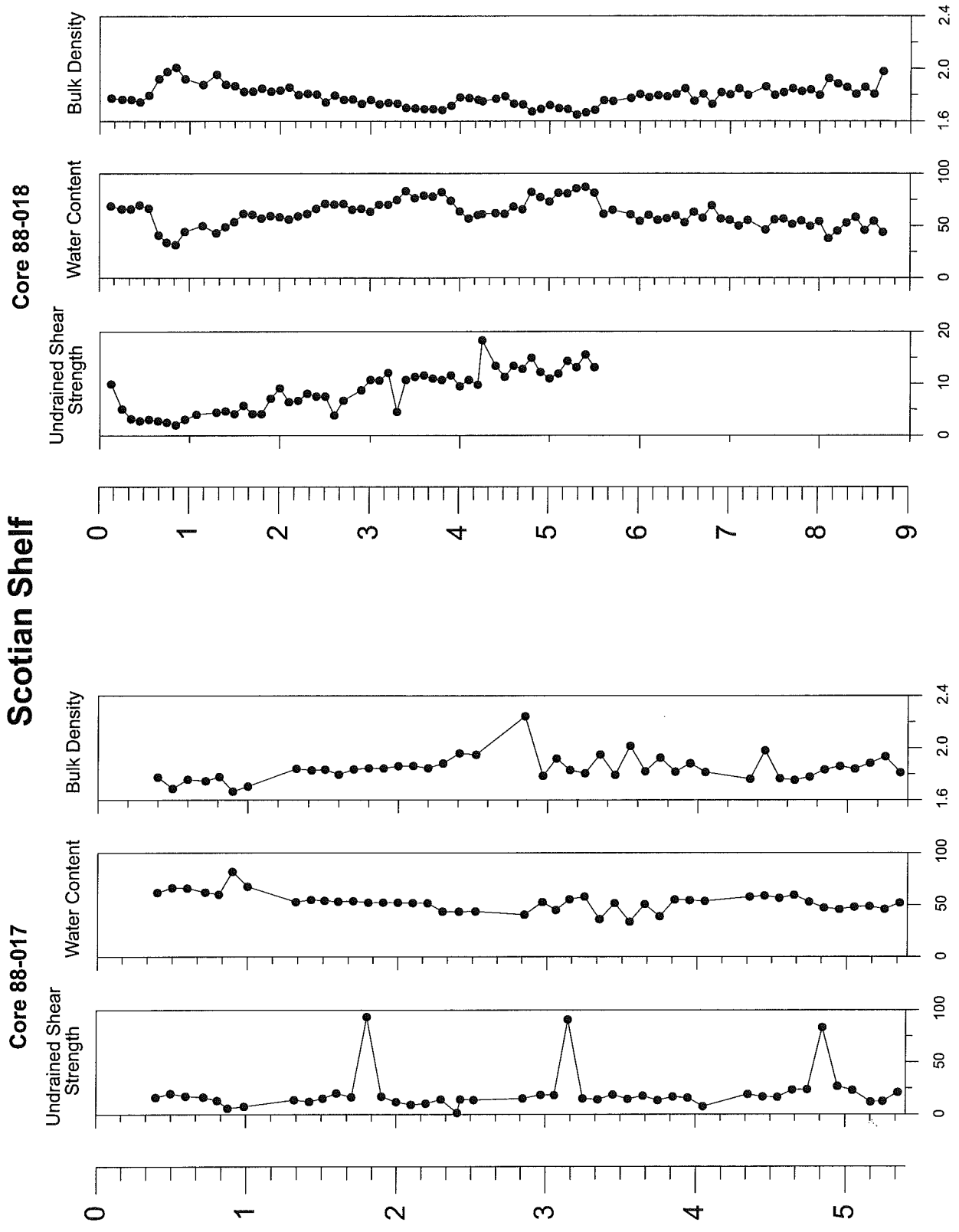

Fig. 6.25. Downcore plots of geotechnical properties for cores 88-017 and 88-018 near the Acadia and Shubenacadie well sites. Mosher et al., (1994) used the data from 88-018 for their infinite slope analysis summarised in fig. 6.26.

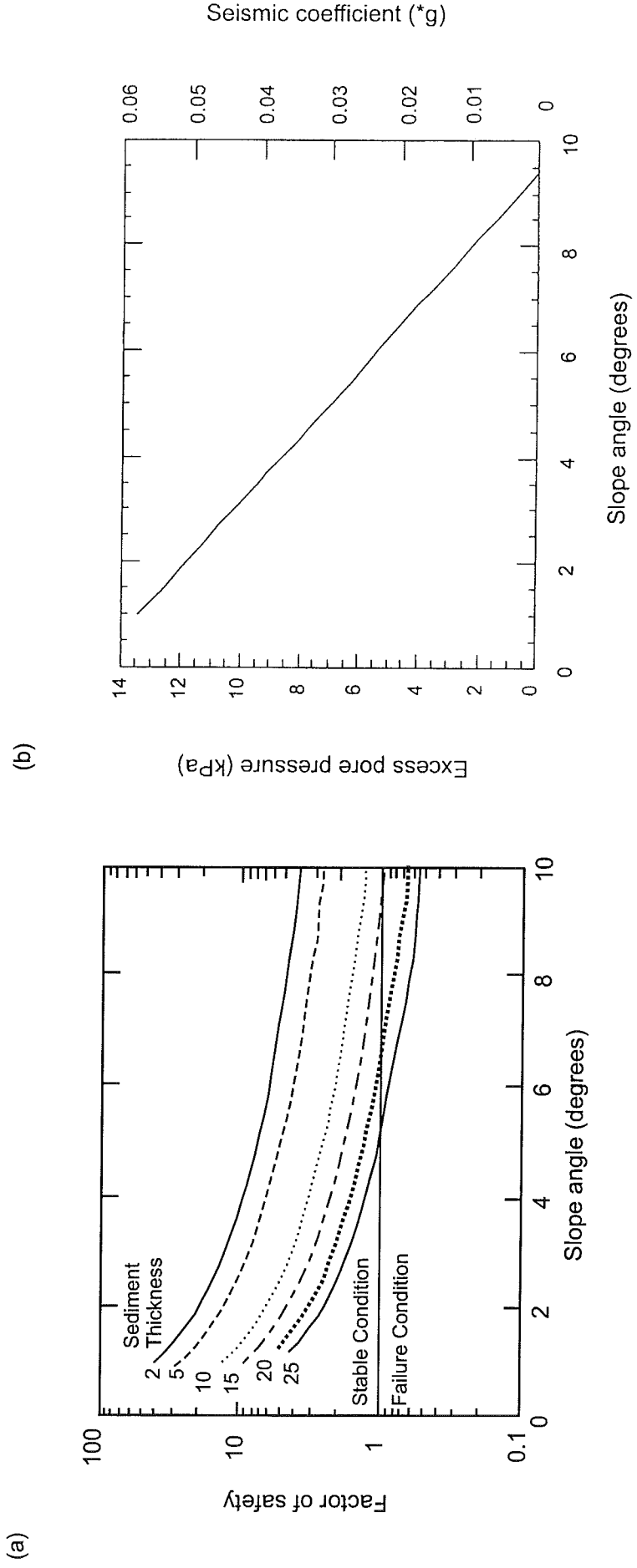

Fig. 6.26. Slope stability analysis of the slumps near the Acadia and Shubenacadie well sites (from Mosher et al., 1994). (a) factor of safety versus seafloor slope angle, for various sediment thicknesses. (b) excess pore pressure and seismic coefficient for the seafloor slope angle for the condition of instability for a 15m sediment thickness.

C:/IEmest/revised/fig6_26.cdr

7. Slope off Sable Island Bank

7.1 Introduction and bathymetry

In this section, we consider the continental slope that is cut by numerous canyons between Verrill Canyon in the west and The Gully in the east.

The Quaternary geology of Sable Island Bank is well known (McLaren, 1988; Boyd et al., 1988). The outer shelf shows a series of stacked late Quaternary deltas, the top of which is cut by the Holocene transgression surface. Tunnel valleys occur at three stratigraphic horizons. Seismic profiles and boreholes show no evidence that ice reached the outer part of Sable Island Bank in the past 30 ka. Four regional reflectors are identified on Sable Island Bank: R_0 is the Holocene transgression; R_1 a stage 3 transgression younger than a 37.2 ka date in the SAB85 borehole (Boyd et al., 1988) that reached >-55 m; R_2 an older transgressive surface that truncates the main set of tunnel valleys; and R_3 which is an unconformity between Tertiary and Quaternary strata (Boyd et al., 1988).

The slope off Sable Island Bank has been studied in most detail near Logan Canyon (Fig. 7.1). Logan Canyon is one of the largest canyons on the Scotian Margin and like Mohican Channel and The Gulley, indents the shelf edge. East of Logan Canyon, the outer shelf gradually steepens seawards, with an abrupt break in slope at 350 to 450 m water depth, corresponding to the heads of a series of small submarine canyons. By the 1000 m regional isobath, these canyons have spacings averaging 2 km and are typically 200 to 500 m deep. West of Logan Canyon, canyons are deeper and more widely spaced, but again head in about 400 mbsl, except for Dawson and Verrill Canyons, which indent the shelf break (Fig. 7.2).

7.2 Late Cenozoic framework

One high-resolution multichannel seismic strike profile is available through the region, close to the 1000 m isobath (Figs. 7.3, 7.4, 7.5). This was interpreted by Clifford (1988) and Piper and Normark (1990), by a low-resolution industry seismic tie to the Triumph P-50 well and by comparison of reflection character with the Shubenacadie-Acadia area. They recognised a mid-Pliocene erosional event; rather uniform sediment aggradation during the late Pliocene; followed by canyon cutting through the Quaternary, with some sediment aggradation on inter-canyon ridges.

The mid-Pliocene and base-Quaternary markers can be identified on dip airgun lines (Fig. 7.6). Below the base Quaternary marker C, continuous sub-parallel reflections predominate. Above C, the outer shelf to upper slope is underlain by discontinuous or incoherent reflectors; several indistinct clinoforms may record paleo-shelf breaks. The Quaternary reflectors underlying the middle slope canyon topography tend to be short

and discontinuous, giving the impression of alternating transparent and acoustically well-stratified reflectors (Fig. 7.7).

In many dip lines, faults are visible that reach to the seabed (Fig. 7.8). Some of these growth faults sole out at depth. Many show a surface bathymetric expression and clearly offset Quaternary strata. There is presumably potential for further motion on these faults.

7.3 **Late Quaternary sedimentation**

High-resolution seismic data

The upper part of the stratigraphic section west of Logan Canyon has the signature of glacial till in Huntec DTS boomer records (Fig. 7.9): this till extends downslope to water depths of about 500 m. It is overlain by about 5 m of stratified sediment, suggesting that the till is of late Wisconsinan age.

The question as to whether glacial till extends to the shelf edge south of Sable Island is controversial. Huntec DTS records on the outer shelf to upper slope (Fig. 7.10) show a highly reflective ("hard-bottom") sea bed which has probable iceberg scours to water depths of at least 300 m. Boyd (in McLaren, 1988; also figure 12 of Stea et al. 1998) interpreted the southern edge of Sable Island Bank as a series of stacked deltas. Boreholes at Sable Island (Boyd et al. 1988), Panuke and Cohasset (Amos and Miller, 1990) show an alternating succession of bedded sands and glaciomarine silts, cut by erosional surfaces. At the shelf edge, sparse seismic data (Figs. 7.10, 7.11) show thick acoustically incoherent sections below the R2 reflector of Boyd that resemble shelf-edge till elsewhere on the Scotian margin, but might represent thick sands. At the shelf edge, only thin sandy deposits appear to overlie R2. Reflector R2 is dated at about 30 ka (Amos and Miller 1990) and interpreted to result from a low stand of sealevel at this time (although evidence globally for a low stand of sea level at this time is lacking). A higher regional unconformity, R1, is characterized by an overconsolidated clay layer interpreted as inter-tidal and dated at about 11 ka. A deeper regional unconformity, R3, cuts apparent pre-glacial (early Pleistocene) sediment and was interpreted as dating from about 75 ka by Amos and Miller (1990). There is clearly a long history on Sable Island Bank from R3 to the time of the earliest shelf-crossing glaciation at about 0.5 Ma and sediment from that history accumulated on the uppermost slope. The difference in morphology between the slope areas off Sable Island Bank west and east of Logan Canyon may be a consequence of glacial ice not reaching the shelf break after R2 (30 ka) east of Logan Canyon, probably because of a vigorous ice stream in The Gully, but likely being present at the late Wisconsinan maximum (18 ka) or younger west of Logan Canyon. There are similar uncertainties with the extent of glacial deposits on the shelf edge of Banquereau (Amos and Knoll, 1987).

West of Logan Canyon, a series of apparent sediment failures head in about 400 m water depth and lead downslope into a major debris flow corridor (Fig. 7.12, 7.13). Debris flow deposits also fill smaller gullies and

valleys (Fig. 7.14). On intervening high areas, well stratified sediment has accumulated (Fig. 7.15), with thicker sediment on levees adjacent to erosional channels (Fig. 7.15). Sediment thickness decreases by 50% passing downslope from 900 to 1350 m water depth.

Core stratigraphy

Core 87-07 shows a stratigraphic sequence that is similar to that defined by Hill (1981) off Western Bank. The upper 5 m of the piston core shows an alternation of olive green and slightly browner intervals, which may correspond to units 2a-d of Hill; three brick-red horizons occur at the base of unit 2a. The base of the upper brown unit (possibly equivalent to 2c) is dated by the shell at 341 cm as 10.35 ka, considerably older than unit 2c off Western Bank. The age of the brick red horizons is poorly constrained by two radiocarbon dates of 10.77 ka above and 14.63 ka below.

Below 523 cm, three lithologic units are distinguished: 1) coarse grained graded beds with varying amounts of mud (facies C), interpreted as proximal turbidites; 2) red-brown muds with abundant clay clasts, sporadic pebbles and some sandy laminae (facies B2), interpreted as an ice-rafted or debris flow facies; and, 3) bioturbated greenish brown silty mud with scattered stones (facies B1), interpreted as glacially-influenced hemipelagic sediment. Facies C probably represents spillover of coarse turbidites from the channel.

Using velocity and bulk density to predict reflections, core 87-07 can be correlated with the Huntec record (Fig. 7.15). Note that the TWC does not correlate in its physical properties with the piston core, suggesting that the top of the sediment column was not recovered in the piston core. Three acoustic units are distinguished in the upper 15 ms, bounded by local reflectors LR1 and LR2. An upper transparent unit corresponds to facies A1. The acoustically well-stratified unit beneath corresponds to Facies A2 and B1, with prominent reflection LR2 corresponding to a marked impedance contrast at 5-6 m. The underlying unit with more incoherent reflections, but occasional high-amplitude reflections, correlates to the interbedding of facies B1, B2, and C. The upper debris flows in the gully illustrated in Fig. 7.14 corresponds approximately to reflector LR2.

Four cores were collected in Verrill and Dawson canyons in 1999 (Fig. 7.17). Two closely spaced cores were taken in the central part of Dawson Canyon at about the 2500 m isobath. The one from the channel floor (30) recovered normal Holocene olive grey muds, with some interbedded sand deeper in the core, overlying a thick massive sand below 2 m. No brick-red sandy mud marker is present in this core. A nearby core (29) on a narrow terrace 60 m above the channel floor recovered a thin Holocene olive grey mud overlying a varve-like sequence of sand to mud turbidites, each typically a few centimetres thick. Intervals of brick-red coloured mud and mud rich in detrital carbonate are correlated with brick-red sandy mud markers **b** and **d** and with Heinrich event H1 (Fig. 7.17). The varve like facies reflects the passage of numerous large turbidity currents down the canyon, the last one being responsible for the thick sand bed in core 30. We suspect that these turbidity currents

may have been generated at an ice margin at the shelf edge, but more work is required to confirm this. Higher up Dawson Canyon, near the 2000 m isobath, the Holocene sequence in core 32 is thicker than in core 30. The corer was stopped at about 6 m penetration and no sediment was recovered in the core catcher, suggesting that the corer hit a thick sand bed, probably correlative with the bed at the base of core 30. In a tributary canyon leading from the gullied area west of Verrill Canyon, core 31 recovered about 3 m of Holocene olive grey mud, sandy near the base, overlying a thick muddy debris flow deposit. No brick-red marker beds were found in this core, but the character of the overlying Holocene sediment suggests that the debris-flow deposit is unlikely to be younger than 8 ka.

7.4 **Geological history and hazard assessment**

Geological history

The Late Pliocene and early Quaternary history of the continental slope off Sable Island Bank appears similar to that farther west, with relatively well-stratified sediment accumulation and a few horizons at which gullies or small slope canyons are present. The later Quaternary section west of Logan Canyon is probably similar to that farther west, with abundant upper slope till and slope valleys developing from failures developed at the downslope limit of till.

East of Logan Canyon, the style of sedimentation is rather different and erosion is more widespread. Evidence of thick till on the upper slope is lacking, although thin tills may be present. The abundance of shallow gullies may be a consequence of the frequent development of a fluvioglacial outwash plain at times of glacially lowered sea level, with hyperpycnal flow of cold, sediment-laden water down gullies and canyons. We are currently analysing the stratigraphic relationship between eastern Sable Island Bank and the continental slope in more detail to better understand the geological history.

Canyon stability

Relatively little is known about the stability of canyon walls, largely because of the difficulty of imaging steep slopes with surface acoustic equipment. The best known area is Verrill Canyon, the edge of which was imaged by SeaMARC I 5-km swath sidescan. It shows classical pinnate "ridge and gully" topography on the western edge of Verrill Canyon (Fig. 7.18) that has also been imaged in US Atlantic canyons and on upper Laurentian Fan (illustrated on the west side of Fig. 3 of Piper et al. 1985b). Such topography has been investigated by submersible on Laurentian Fan (Hughes Clarke et al. 1989) and appears to be generally stable. This is confirmed by the core evidence discussed above that debris flow deposits are lacking in the past 10 000 years. The relative distribution of debris flow deposits and sands suggests that the debris flows were small and

did not completely transit the canyon.

The role of major faults in the canyoned areas is uncertain. Such faults may act as planes of weakness along which failures might occur. Mapping of near-surface faults in areas with steep canyon walls will be necessary to assess seabed stability.

Logan Canyon debris flow corridor

In the area southwest of Logan Canyon, a series of near surface debris flows on the Rise can be traced upslope into a major slump scar more than 300 m deep (Fig. 7.12). A narrow ridge has been preserved between the debris flow corridor and the deep Logan Canyon, probably because the canyon permitted drainage of excess pore pressures along permeable horizons. Debris-flow deposits on the Rise date back to at least the early Quaternary. This feature was investigated on the recent cruise 99036 (Piper, 1999) and interpretation is not yet complete. What is clear is that there have been several near surface debris flows (Fig. 7.13). Cores were collected to date these flows and preliminary results suggest that none are of Holocene age.

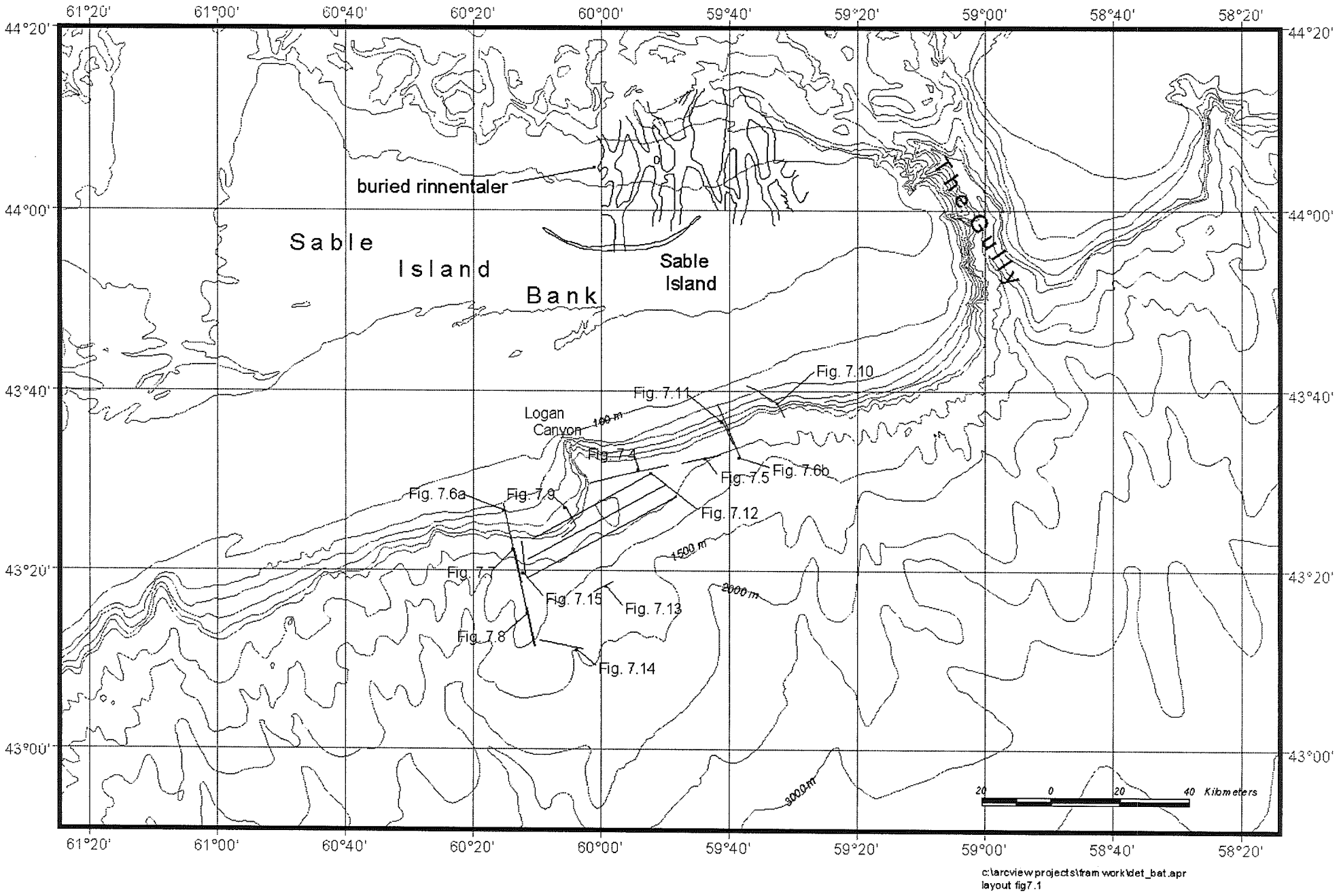

Fig. 7.1: General map of the slope off Sable Island Bank. Buried Rinnentaler on shelf from Boyd et al. (1988).

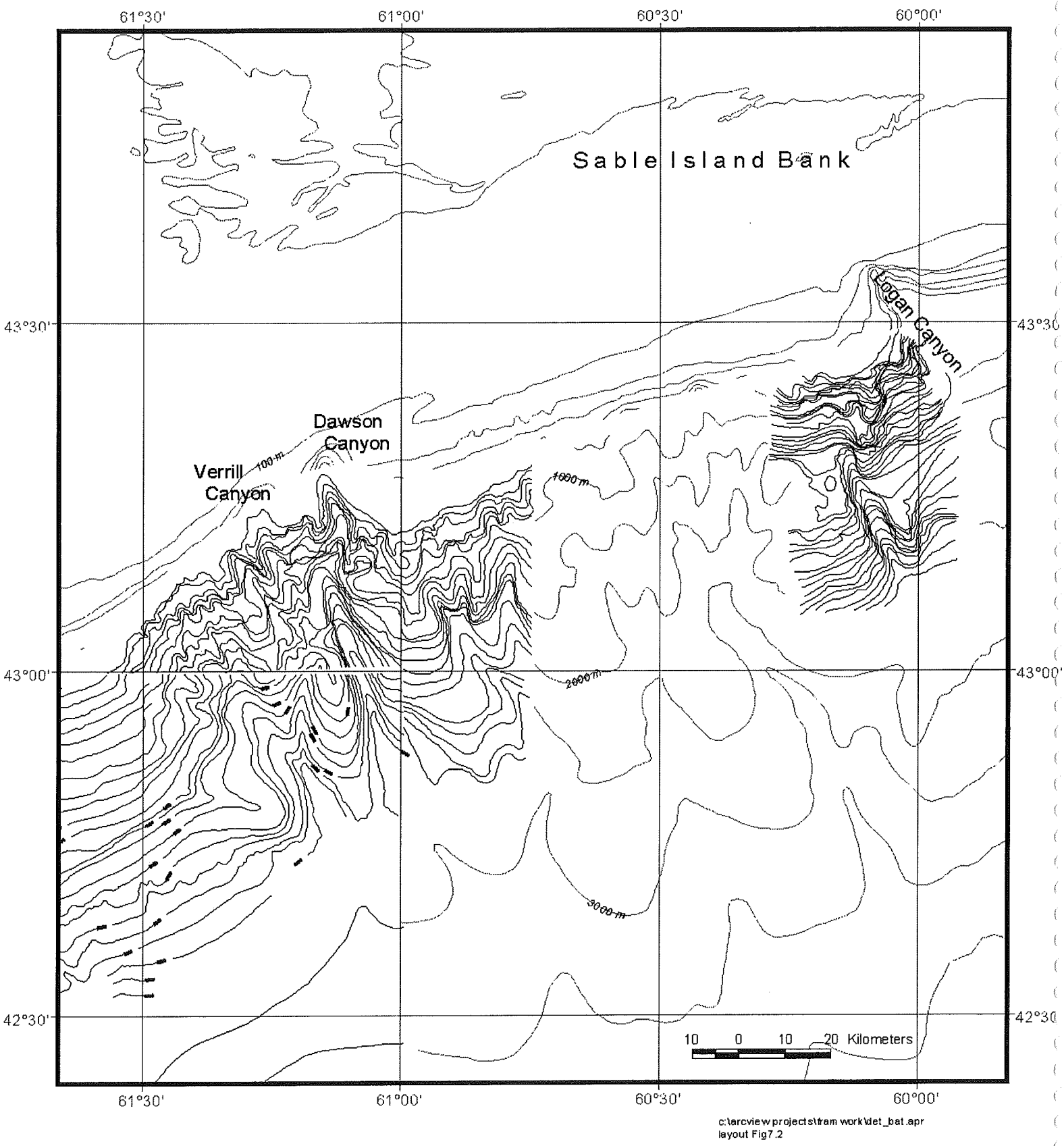

Fig. 7.2: Map showing detailed bathymetry of the areas near Verrill Canyon and Logan Canyon

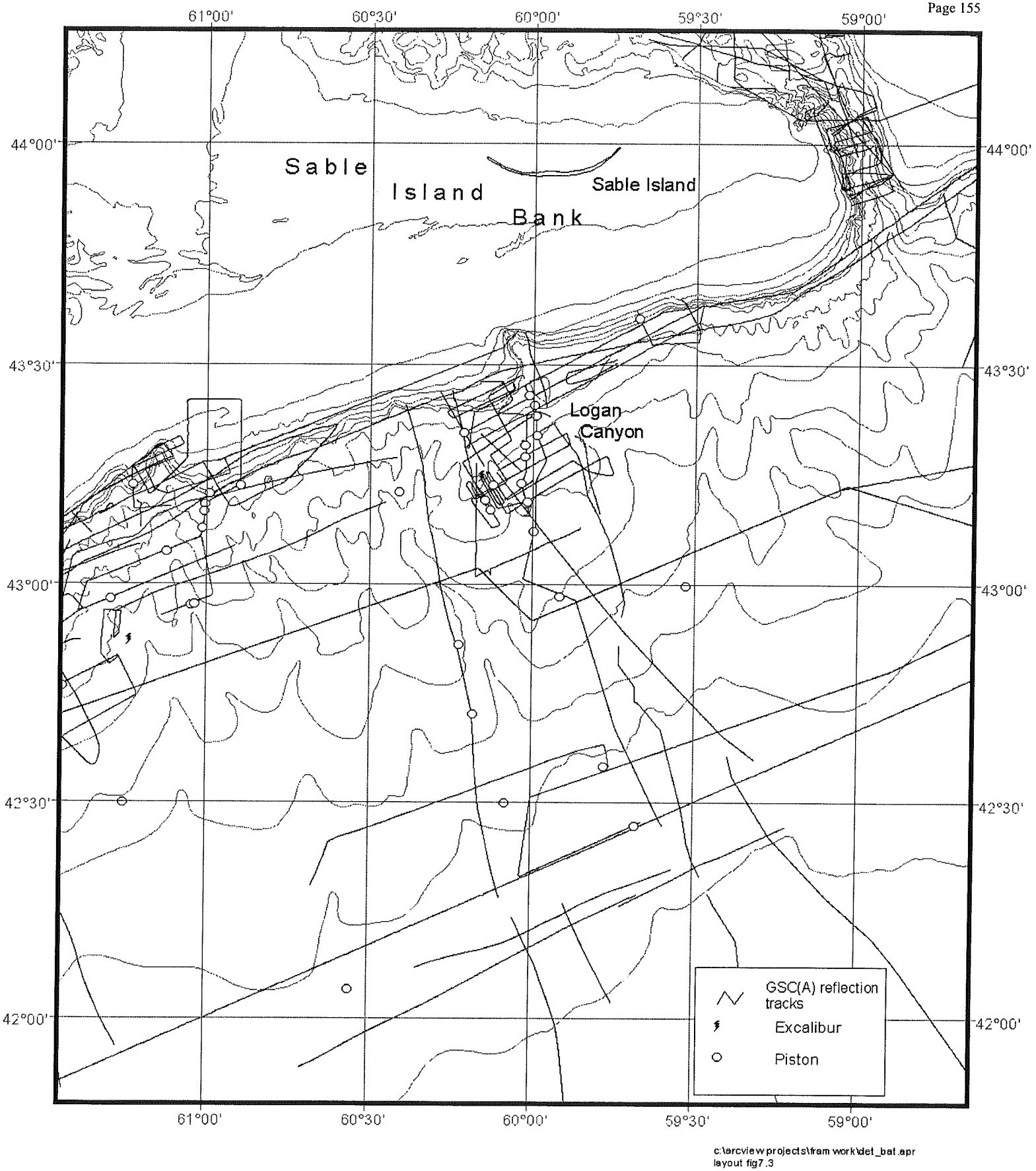

Fig. 7.3: Map showing data distribution on the slope off Sable Island Bank.

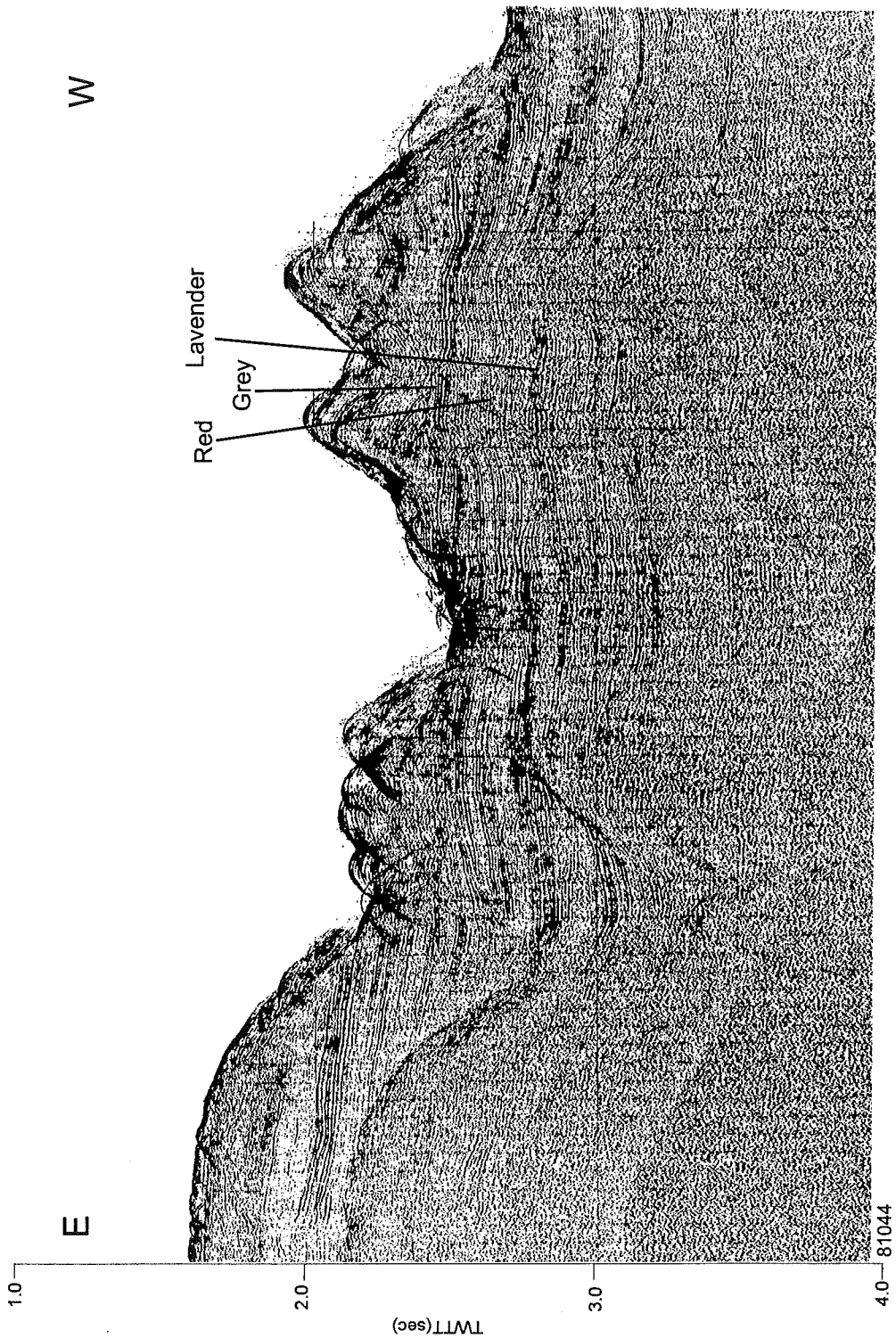

Fig. 7.4. High-resolution multichannel sparker line (cruise 81044) from east of Logan Canyon.

C:/Ernest/revised/fig7_4.cdr

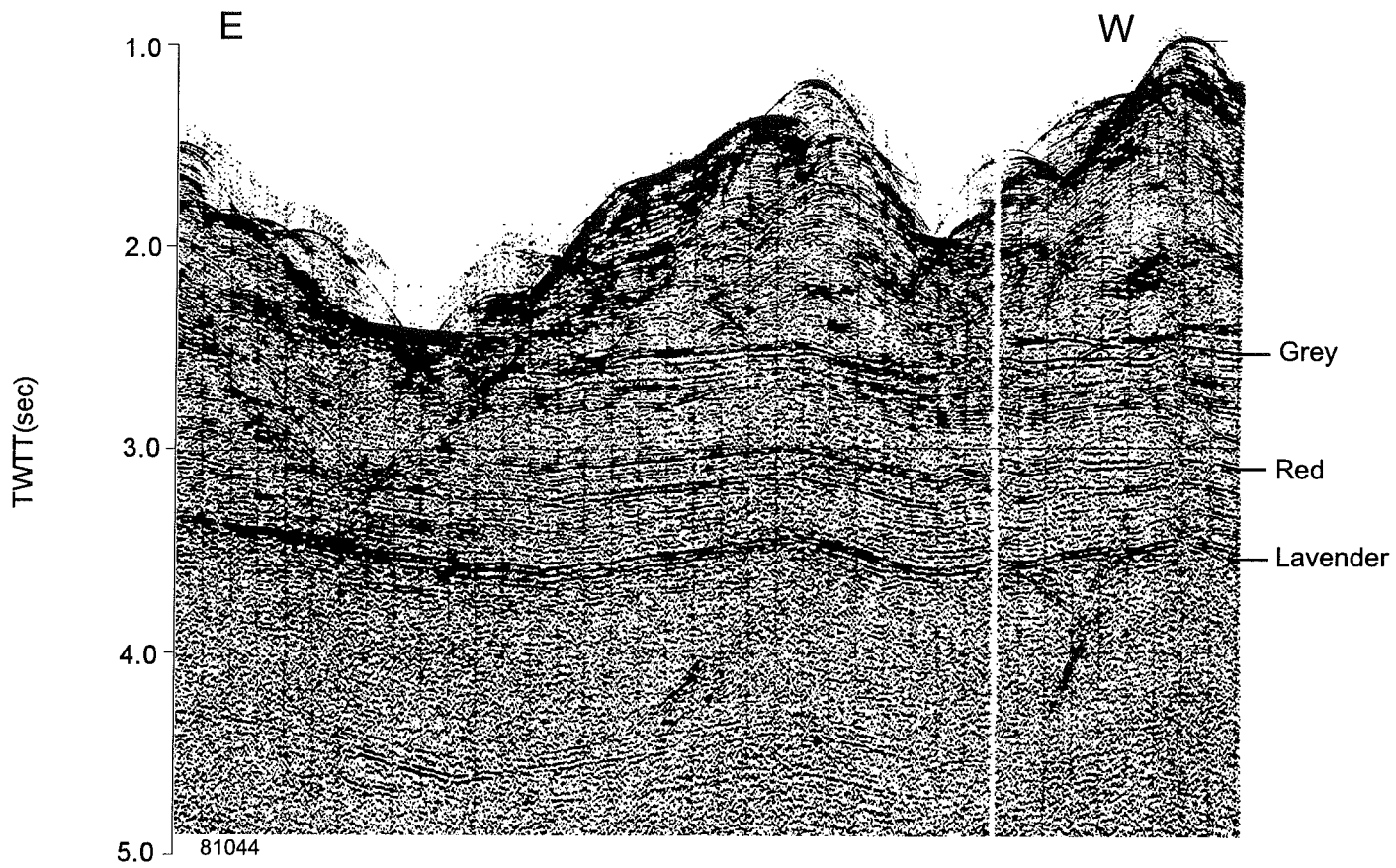

Fig.7.5. High-resolution multichannel sparker line (cruise 81044) from east of Logan Canyon.

C:/!Ernest/revised/fig7_5.cdr

c:\campbell\marathon report\figures\marfig34.cdr

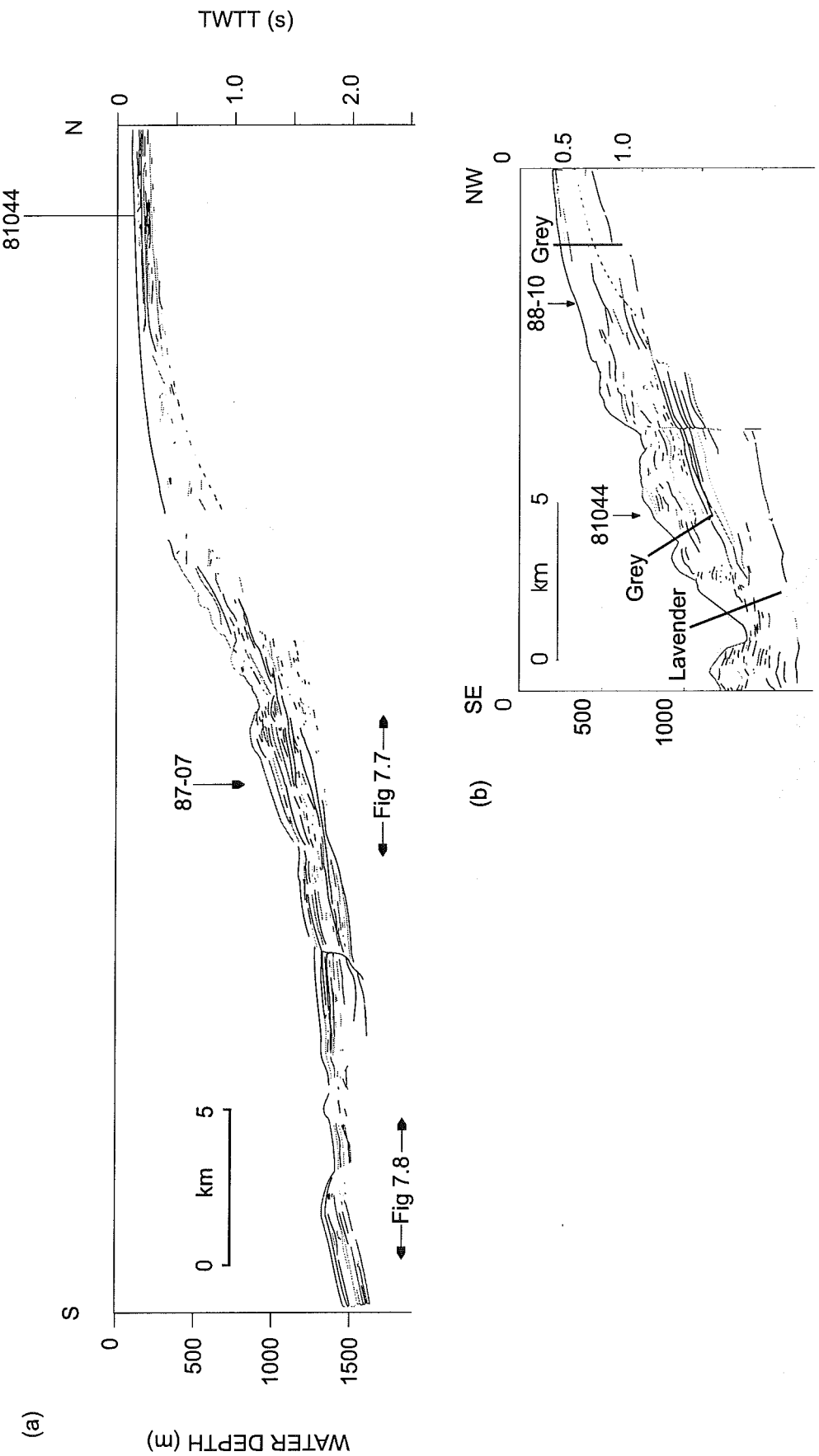

Fig. 7.6. Line drawing of two dip seismic profiles across the margin showing late Cenozoic framework. (a: 87003; b: 88010).

C:/IEmest/revised/fig7_6ab.cdr

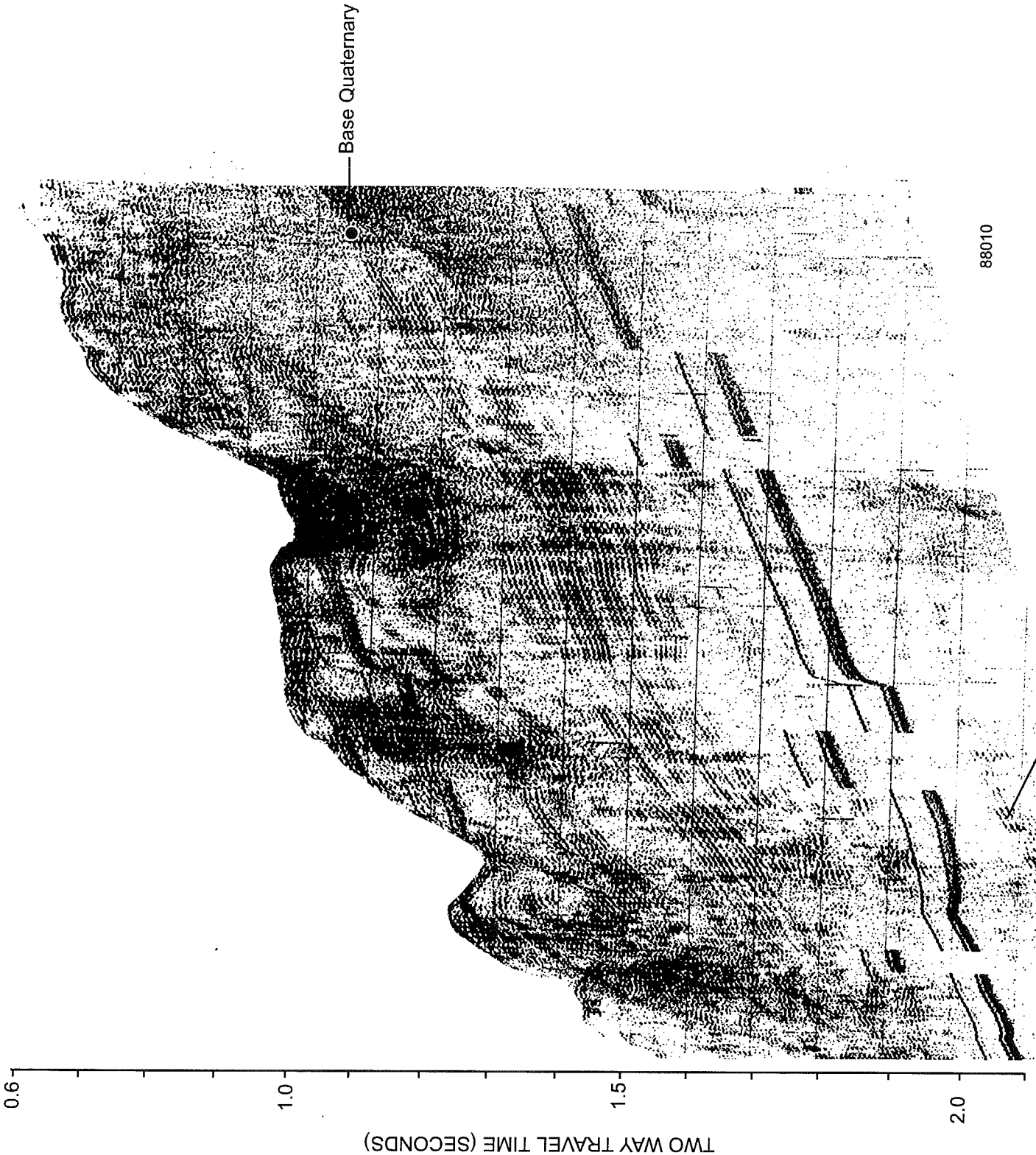

Fig. 7.7. Airgun dip line east of Logan Canyon showing Pliocene- Quaternary stratigraphy and facies.

C:/IErnest/revised/fig7_7.cdr

Fig. 7.8

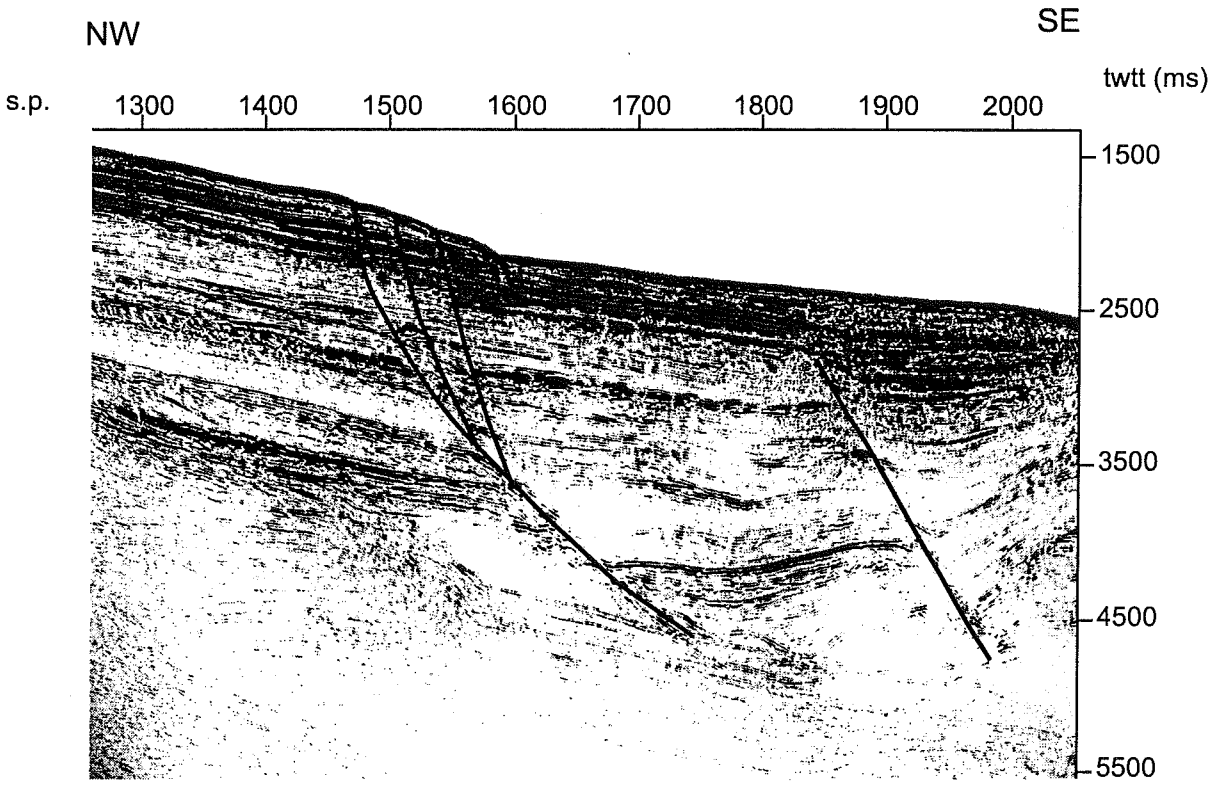

Fig. 7.8. Major faults near Logan Canyon.

C:/IErnest/revised/fig7_8.cdr

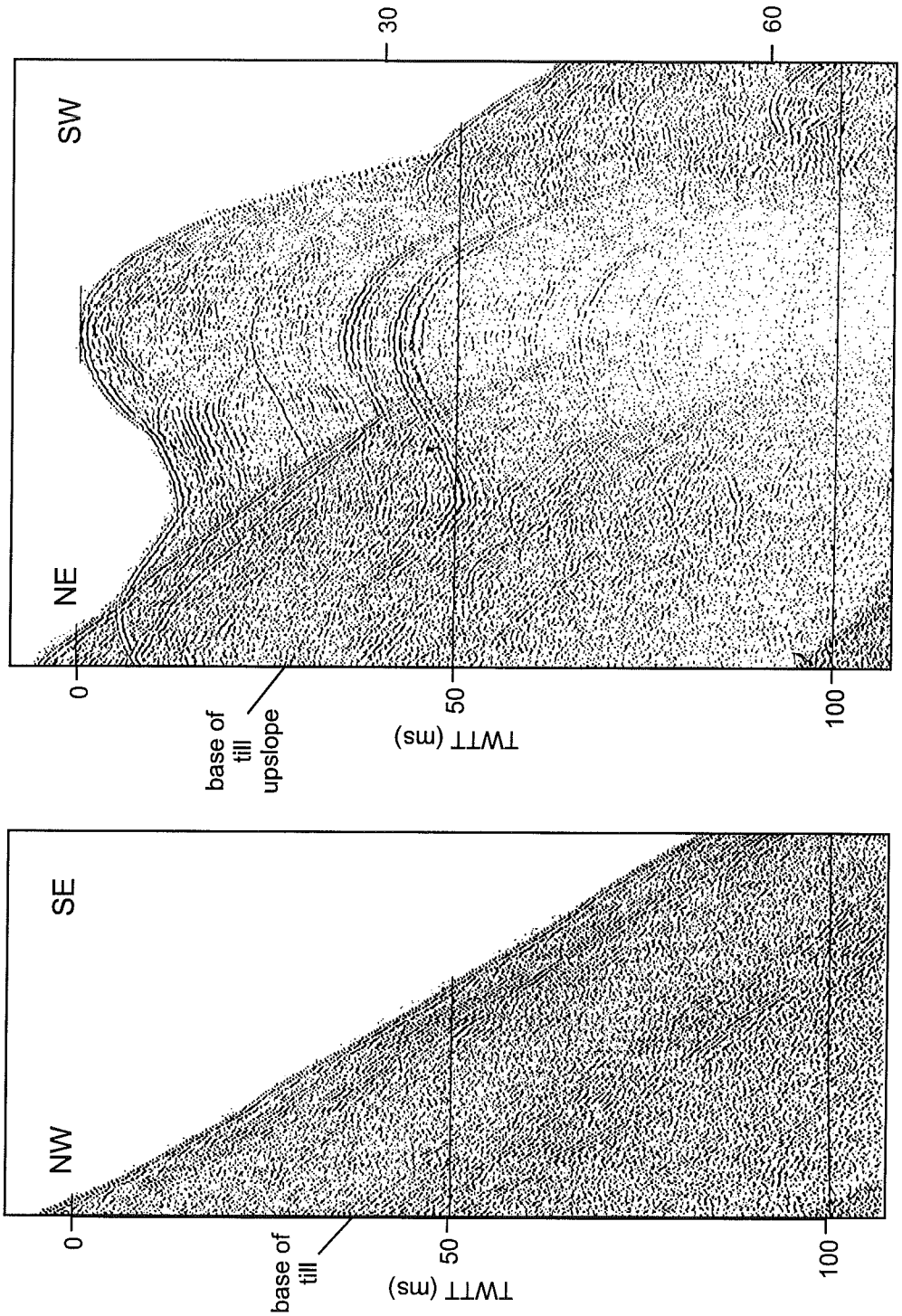

Fig. 7.9. Huntec sparker high-resolution profile down upper slope immediately west of Logan Canyon showing probable till passing downslope into stratified sediment.

C:/IErnest/revised/fig7_9.cdr

Fig 7.10

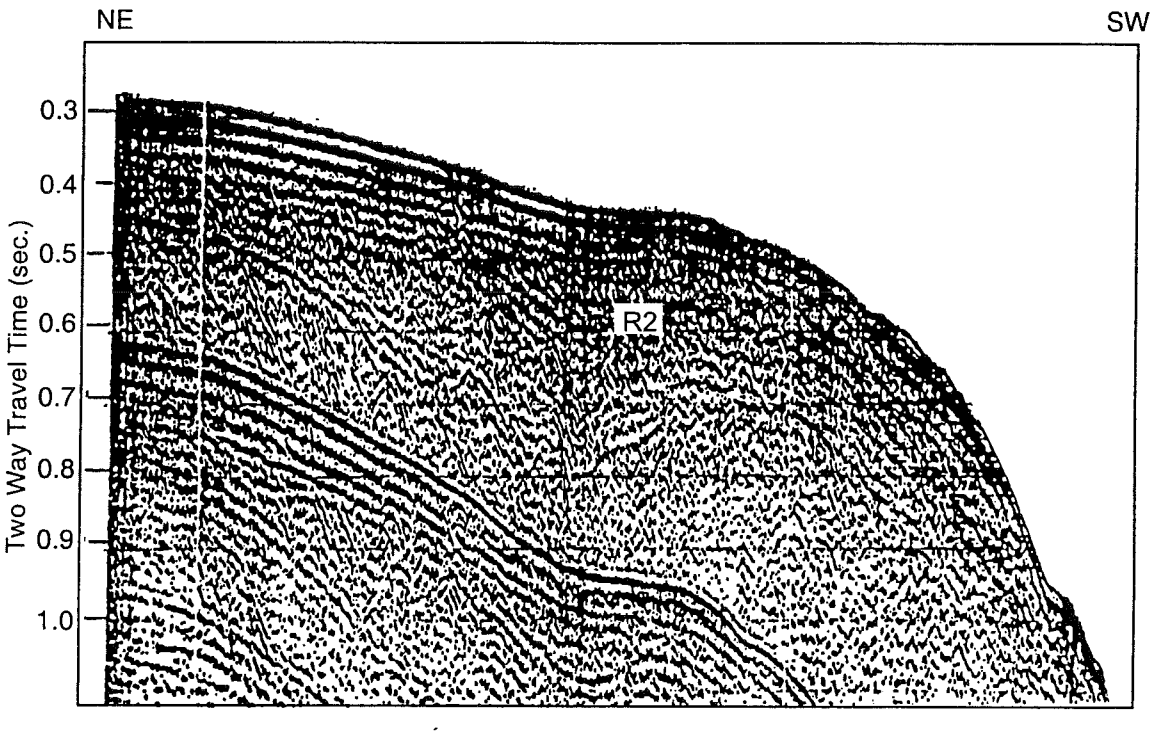

Fig. 7.10. Outer shelf and upper slope east of Logan Canyon, showing acoustically incoherent character suggesting coarse grained sediment. Reflector R2 is correlated with Boyd's stratigraphic scheme (Fig. 12 of Stea et al. 1998). Single airgun, 88010 138/1330-1510.

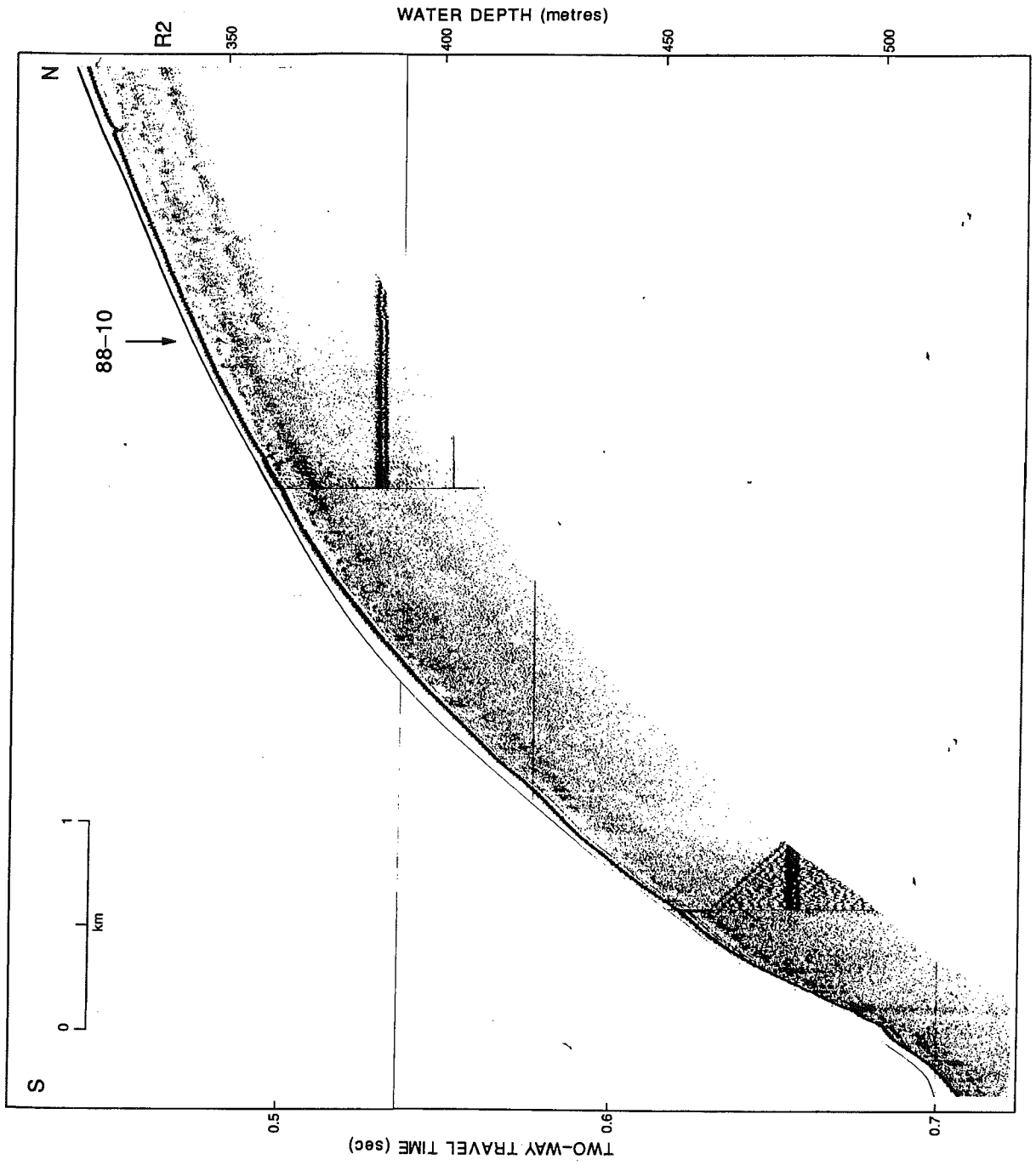

Fig. 7.11. Huntec boomer profile east of Logan Canyon showing acoustic character of outer shelf and correlation with reflrctor R2. Cruise 88010.

C:/IEmest/revised/fig7_11.cdr

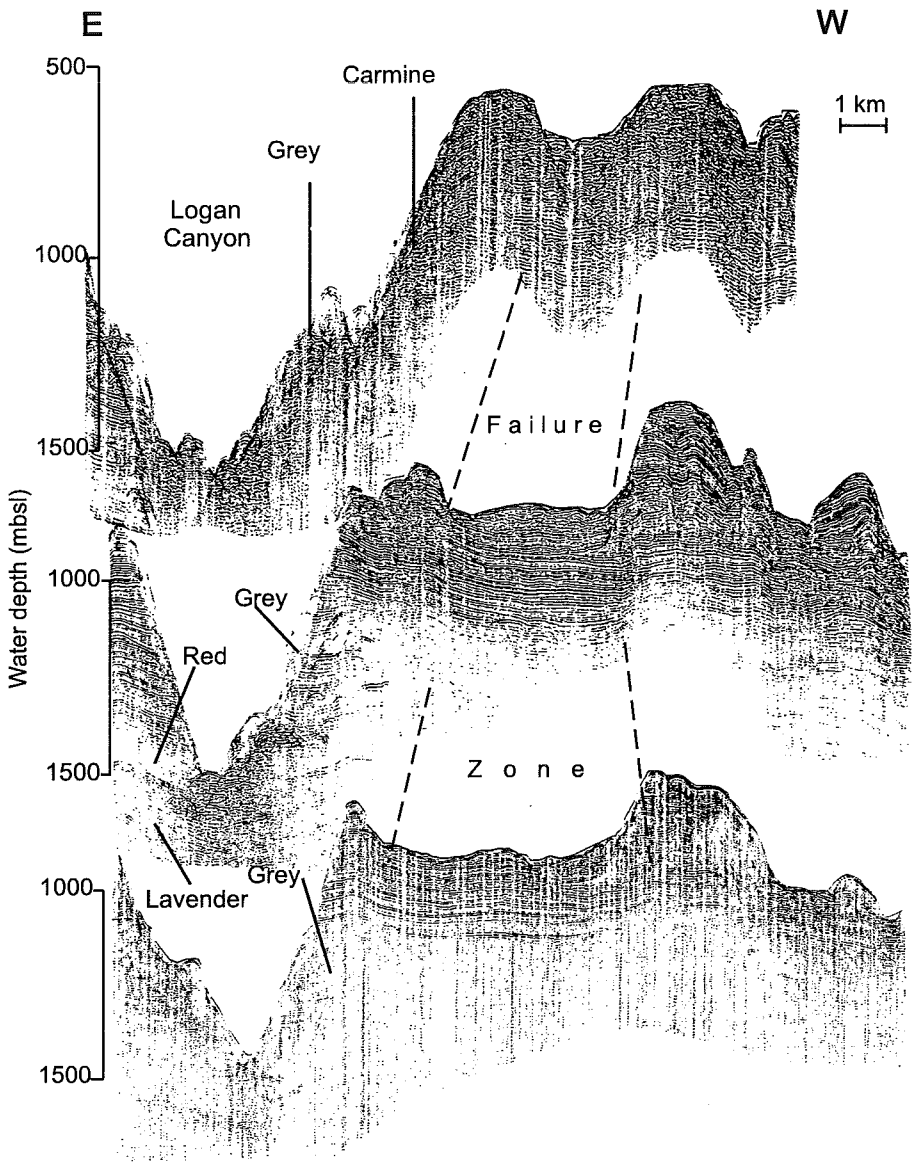

Fig. 7.12. Seismic reflection profiles showing large scar left by sediment failures on the Scotian Slope immediately west of Logan Canyon (cruise 92-052). (from Piper et al., 1999)

C:/IErnest/revised/fig7_12.cdr

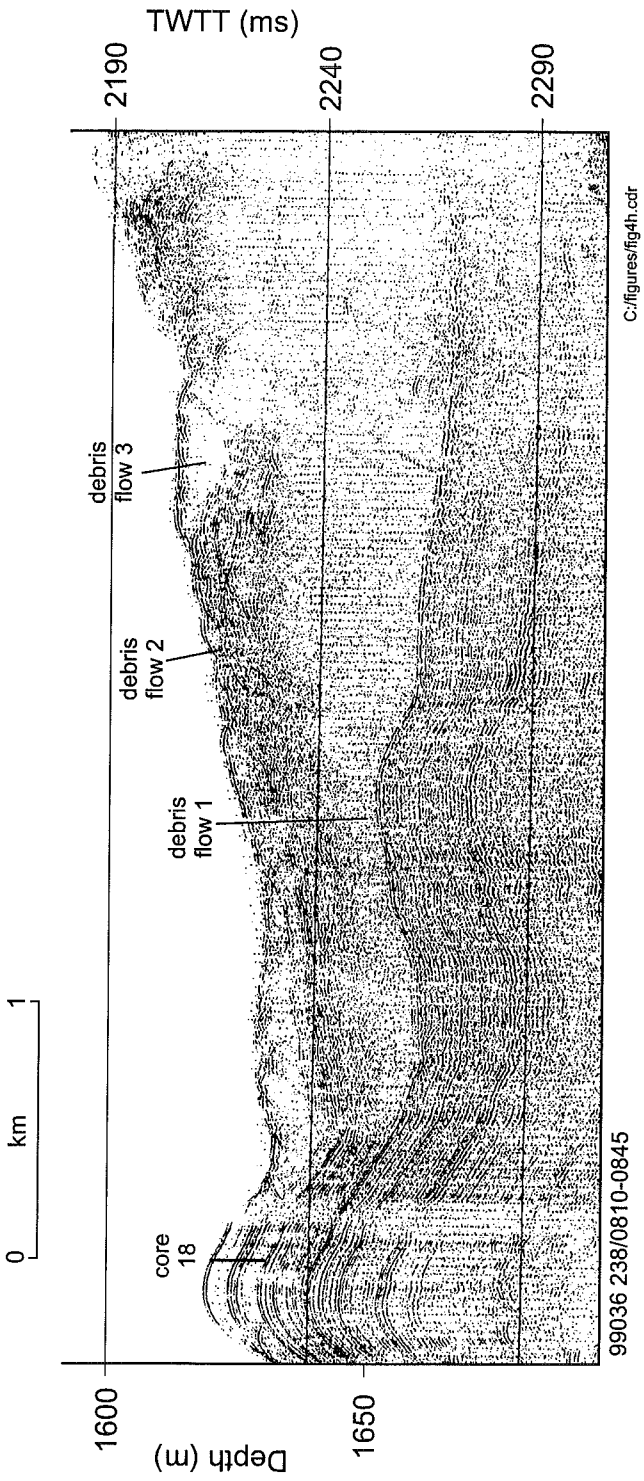

Fig. 7.13. Huntec high-resolution sparker profile across part of the Logan Canyon debris flow corridor, showing stacked debris flows passing laterally into stratified sediment, cored at 99036-018. 99036, 238/0810-0845.

C:/IEmest/revised/fig7_13.cdr

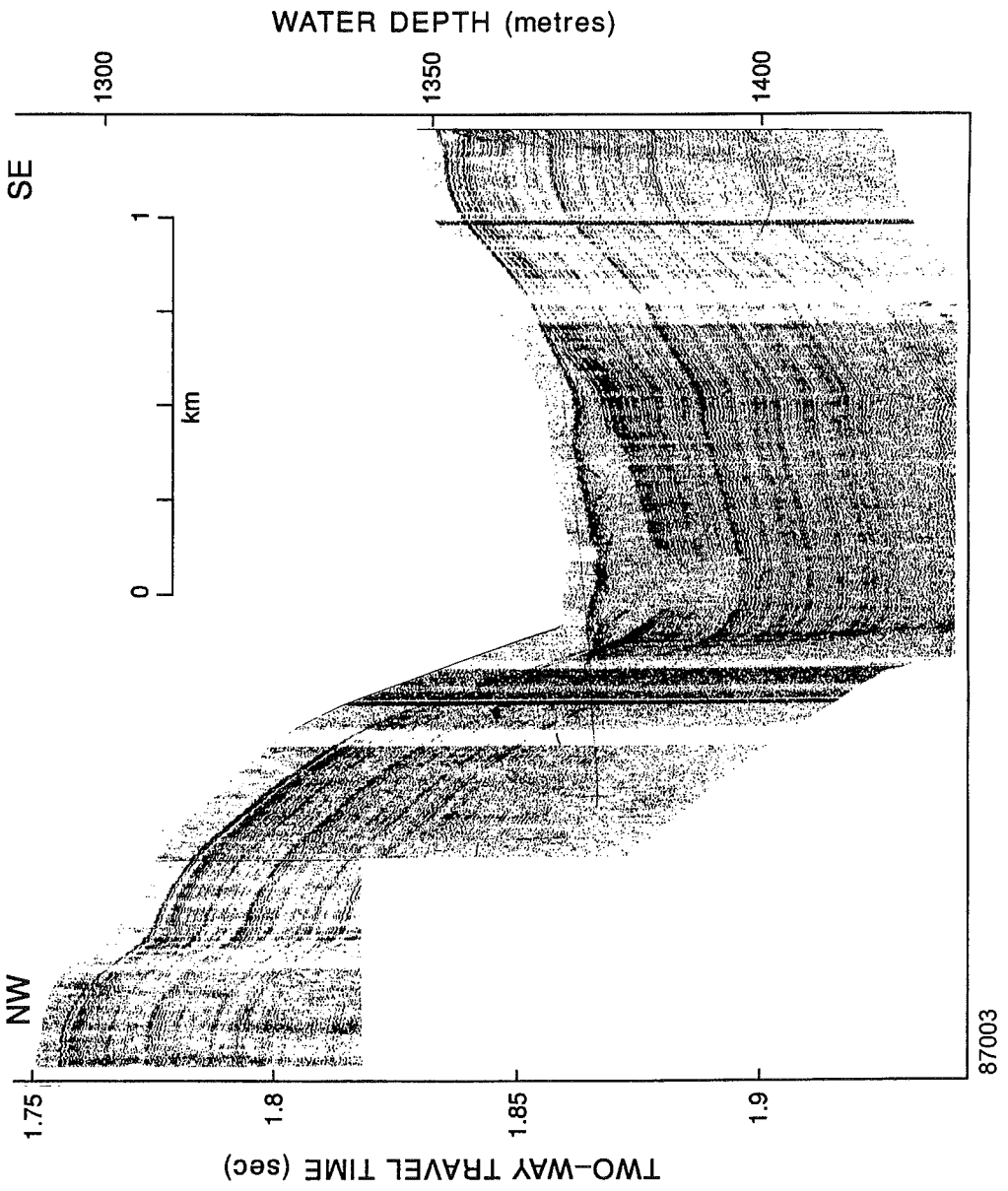

Fig.7.14. Huntec DTS profile showing debris flow in slope valley south of core site 87-07.

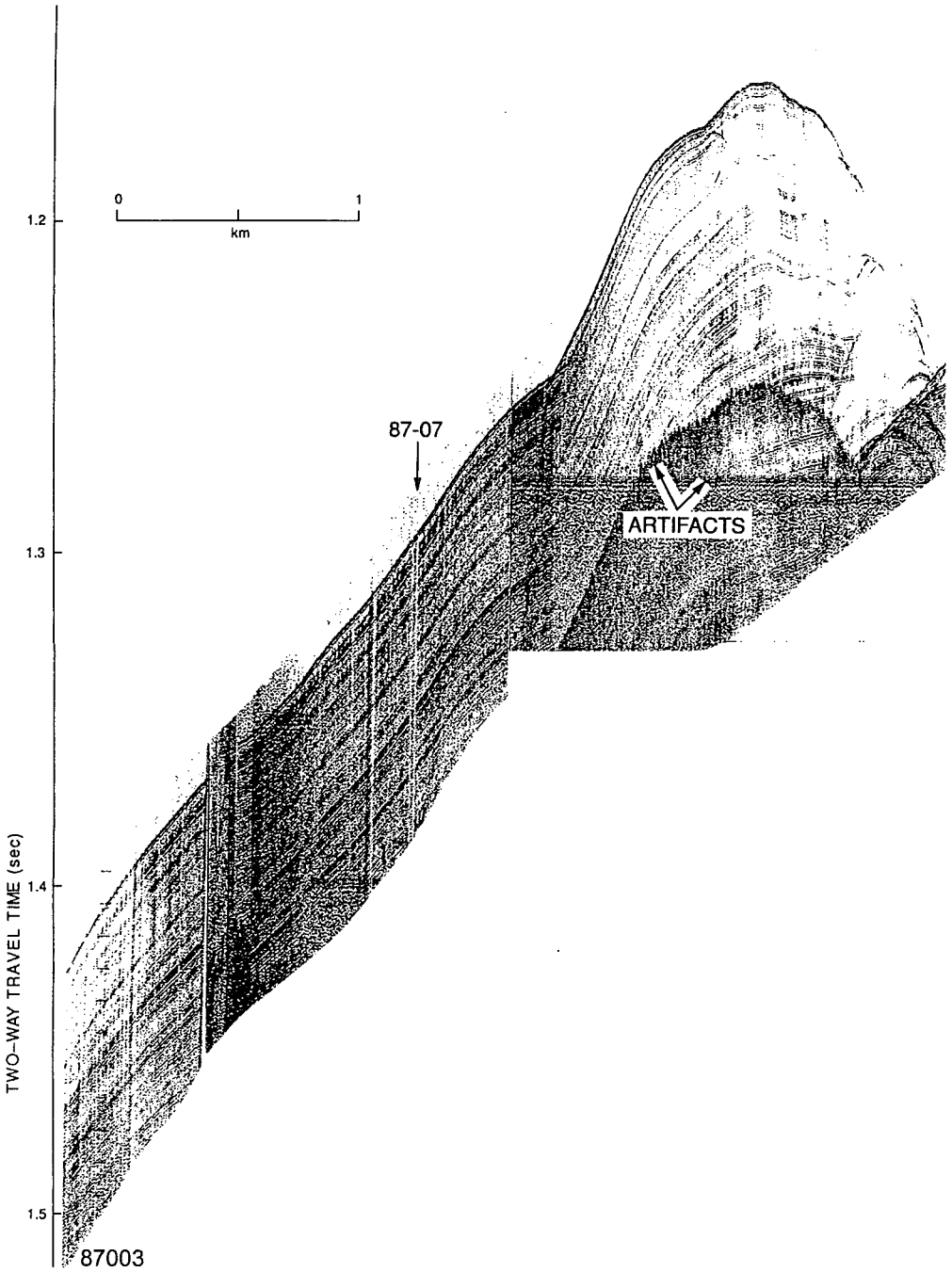

Fig. 7.15. Downslope Huntec DTS profile near core site 87-07.

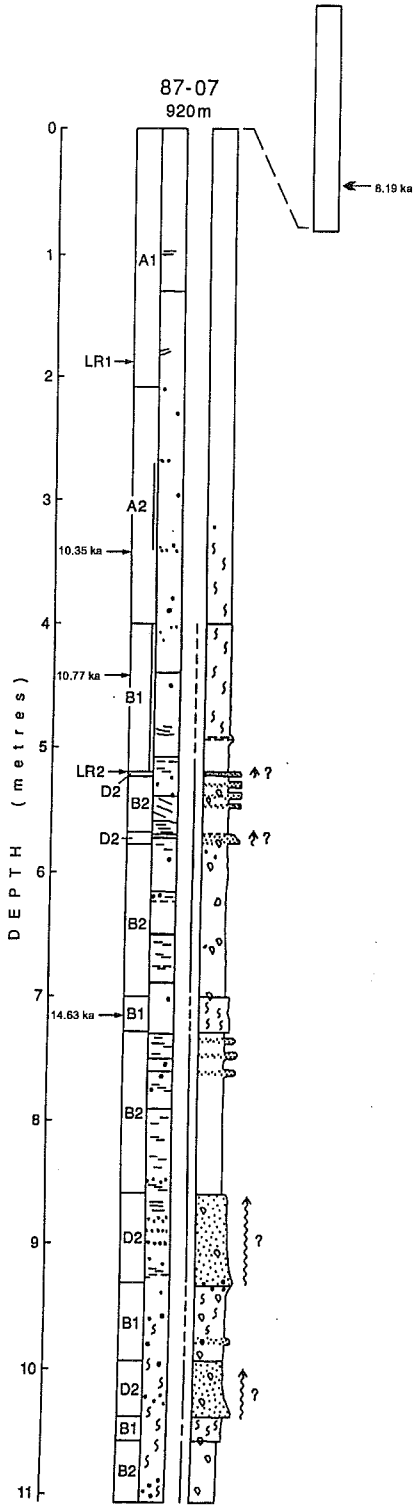

Fig.7.16. Summary of core stratigraphy in 87-003-007. Vertical bars within the facies column denote slightly browner intervals of olive grey mud. Legend in figure 1.5 .

C:/!Ernest/revised/fig7_16.cdr

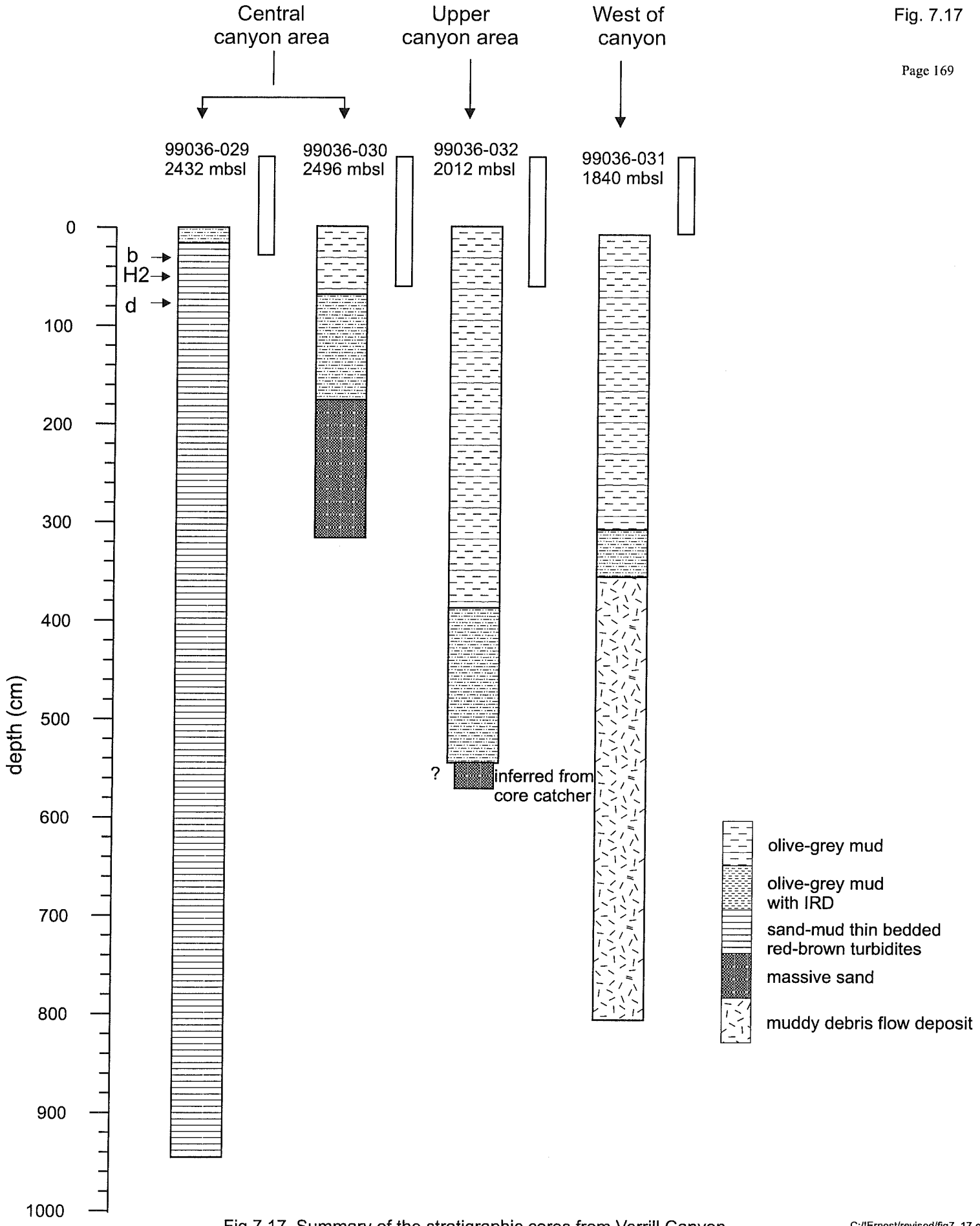

Fig.7.17. Summary of the stratigraphic cores from Verrill Canyon.

C:/!Ernest/revised/fig7_17.cdr

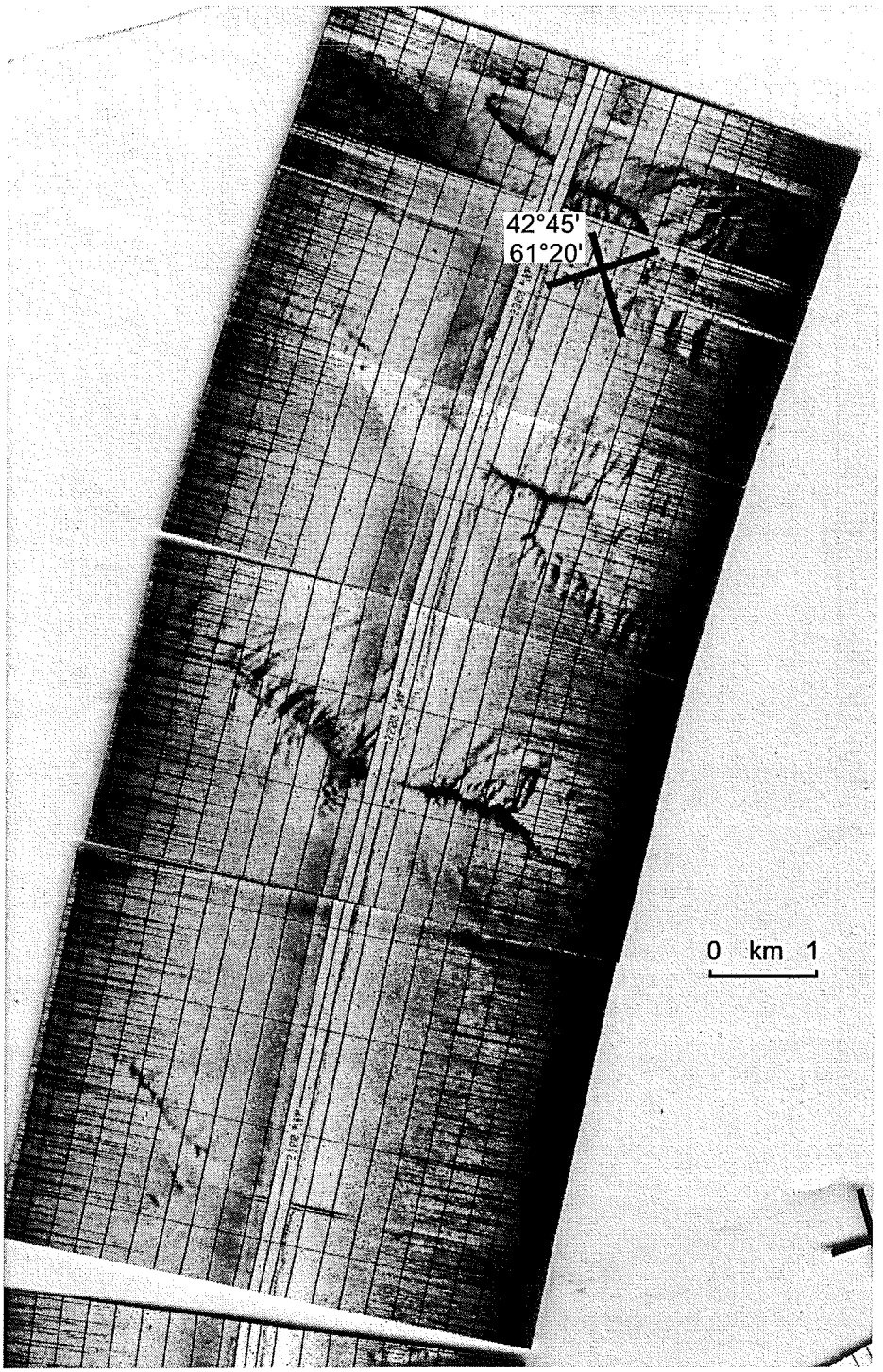

Fig. 7.18. Ridge and gully topography on the flanks of Verrill Canyon: 1983 SeaMARC imagery

8. Slope off Banquereau

8.1 Introduction and bathymetry

The continental slope of Banquereau is highly dissected by canyons (Fig. 8.1). Smaller canyons or gullies have an average 5 km spacing and head at about 300 mbsl, with typical depths of 200-500 m around the 600 m isobath. A few larger canyons head at about 100 mbsl and Shortland and Haldiman canyons substantially indent the shelf break.

The Geological Survey has carried out relatively little work on the continental slope in this area. A long high-resolution seismic strike line has been collected along the upper slope. In addition, more detailed surveys have been carried out near the Tantallon well, which is located on an inter-canyon ridge between Shortland Canyon and The Gully.

8.2 Late Cenozoic framework

Industry surveys at the Tantallon M-41 well site recognised four reflectors in the multichannel sparker profiles. These can be correlated with the well history report and logs, using the foraminiferal and palynology biostratigraphy in the well history report. The upper two reflectors (3 and 4) are also visible in GSC airgun seismic profiles and are identified in Fig. 8.2. Reflector 4 separates overlying acoustically stratified sediment from underlying more transparent sediment. It is within the well casing. Reflector 3 appears to be an unconformity and marks the base of the transparent unit. It corresponds approximately to the base of the casing in the well at 2260 m RT (720 mbsf), where the first samples are available. The topmost 20 m of sampling was identified as Late Pliocene on the basis of foraminifera, resting on Miocene. Thus reflector 3 is identified as a Pliocene-Miocene unconformity (regional reflector F of Piper and Normark, 1989). Reflector 2 is the base of a somewhat stratified unit overlying rather acoustically amorphous sediment. On the basis of sonic log response and velocities, this is identified at 2505 m RT and corresponds in the biostratigraphy to a Oligocene/Miocene unconformity. Reflector 1 is identified as the top Cretaceous.

The GSC has a single channel dip line run in 1986 (Fig. 8.2) and a strike line in about 300 m water depth on the upper slope (Skene, 1994). Neither shows interpretable instability features. The upper slope strike line (Fig. 8.3) shows a character similar to that off Logan Canyon, with a B reflector (base of glacially dominated section) marking the boundary between well stratified and relatively incoherent sediment. A few slope valleys are recognised below B, but the main development of gullies appears to be younger than B.

8.3 **Late Quaternary sedimentation**

High-resolution seismic data

Huntec deep-tow boomer lines across the Tantallon well site (Figs. 8.4, 8.5) show a well-stratified section that can be correlated to cores. The profile extends from failed strata on either flank to "Tantallon tongue". On the west side, the upper few metres of sediment appear to have failed on a slope of 14°.

Core stratigraphy

A series of cores were collected in undisturbed sediment and shallow slump scars resulting in a 16 m thick composite section (Fig. 8.6). The upper 2 m is a condensed latest Pleistocene - Holocene section, with a surface sand resulting from winnowing by Holocene storms (cf. Hill and Bowen, 1983). Underlying sediment comprises red clays with mudstone clasts and dropstones. They are interpreted as deposited from the proximal part of glacial meltwater plumes issuing from the Gulf of St Lawrence. Radiocarbon dates indicate extremely high sedimentation rates of 1 m per 200-300 years. These red clays are very cohesive, making piston cores difficult to split.

Geotechnical measurements

Geomechanical properties of the red muds at Tantallon can be compared with those near Verrill Canyon, where Mosher et al. (1994) performed an infinite slope analysis using average undrained shear strength and bulk density profiles. Average shear strengths of 8-11 kPa are found at 3-5 m subbottom at Verrill Canyon (Fig. 6.24); similar shear strengths occur in sediment inferred to have originally been buried about 16 m at Tantallon, implying a strength ratio of about 0.2. Likewise, bulk density at 8 m depth near Verrill Canyon is about 1.8 gm/cm^3 and is only 1.7 gm/cm^3 at Tantallon (Figs. 8.7, 8.8). We have not completed a new infinite slope stability analysis but these data show that sediment at Tantallon is substantially less stable than for Verrill Canyon (shown in Fig. 6.26).

8.4 **Geological history and hazard assessment**

Geological history

Based on limited data, the geological history of the slope of Banquereau appears similar to that off Sable Island Bank. Late Pliocene sedimentation shows only limited evidence of shallow slope valleys, although evidence has been removed by erosion beneath the major canyons. Some slope gullies formed in the early Quaternary, but much of the slope accumulated well stratified sediment. Widespread erosion appears to have

taken place only after the onset of shelf-crossing glaciation. Erosion of major canyons may be related to erosion of tunnel valleys on the shelf (Loncarevic et al. 1993), but the smaller gullies that head in 300 mbsl are probably similar to gullies elsewhere on the Scotian margin that head at the downslope limit of till deposition.

Slope stability

We have no data on the stability of canyon walls. This general issue has been discussed above for Verrill Canyon (see section 7.4). Some geotechnical data is available for late Quaternary sediment on the intervalley ridge at Tantallon. We have not completed a new infinite slope stability analysis but the geotechnical data discussed above show that sediment at Tantallon is substantially less stable than for Verrill Canyon (shown in Fig. 6.25).

Sticky clays

There are anecdotal reports of problems with "sticky clays" when drilling the Tantallon M-41 well, presumably caused by the same sort of clays as were sampled in the piston cores. Given that outwash plumes have issued from the Gulf of St Lawrence for at least the last 0.5 Ma (Piper et al. 1994), this facies may be several hundred metres thick, probably extending down to regional reflector (4).

Boulder bed problems

On the eastern Scotian Shelf, irregular tunnel valleys of subglacial origin are widespread north of Banquereau and on eastern Sable Island bank (Loncarevic et al. 1993), extending onto the northern part of Banquereau where they appear sediment-filled (Cruise report, PZ95-033B). These valleys are clearly visible on regional bathymetric maps. Similar valleys have been described beneath Sable Island (Boyd et al. 1988) and locally on the outer part of Banquereau (Amos and Knoll, 1987; Figure 10.20 of Piper et al. 1990). Some filled valleys are also visible on the prograded upper continental slope off Banquereau (Figure 4 of Skene 1994). Tunnel valleys are interpreted as subglacial water-cut valleys, perhaps resulting from catastrophic flood discharges (jokulhlaups). It is probable that tunnel valleys on the continental shelf lead to the deeply incised canyons on the continental slope, although this linkage has not been proved. Canyons on the eastern Banquereau and eastern Sable slopes are spaced at 4-5 km (Skene 1994), comparable with the spacing of tunnel valleys beneath Sable Island (Boyd et al. 1988) and less than the spacing of valleys along the northern edge of Banquereau (perhaps 10 km). Canyons are more widely spaced on the western Banquereau slope.

Large subglacial flows are likely to transport coarse-grained sediment including boulders. A section through the deposit of one jokulhlaup discharge has been observed from submersible on Eastern Valley of Laurentian Fan: it is a moderately sorted cobble conglomerate illustrated as Figure 5 of Hughes Clarke et al.

(1990) that has been moulded into prominent gravel waves (Piper et al., 1985a) with scattered boulders up to a metre in size. The canyons seaward of Banquereau and Sable Island Bank may well be floored by similar deposits. In addition, the eastern Scotian Slope was in the trajectory of icebergs from the Labrador Sea and Gulf of St Lawrence during the Pleistocene (Piper and Skene 1998) and scattered ice-rafted boulders are to be expected throughout the area.

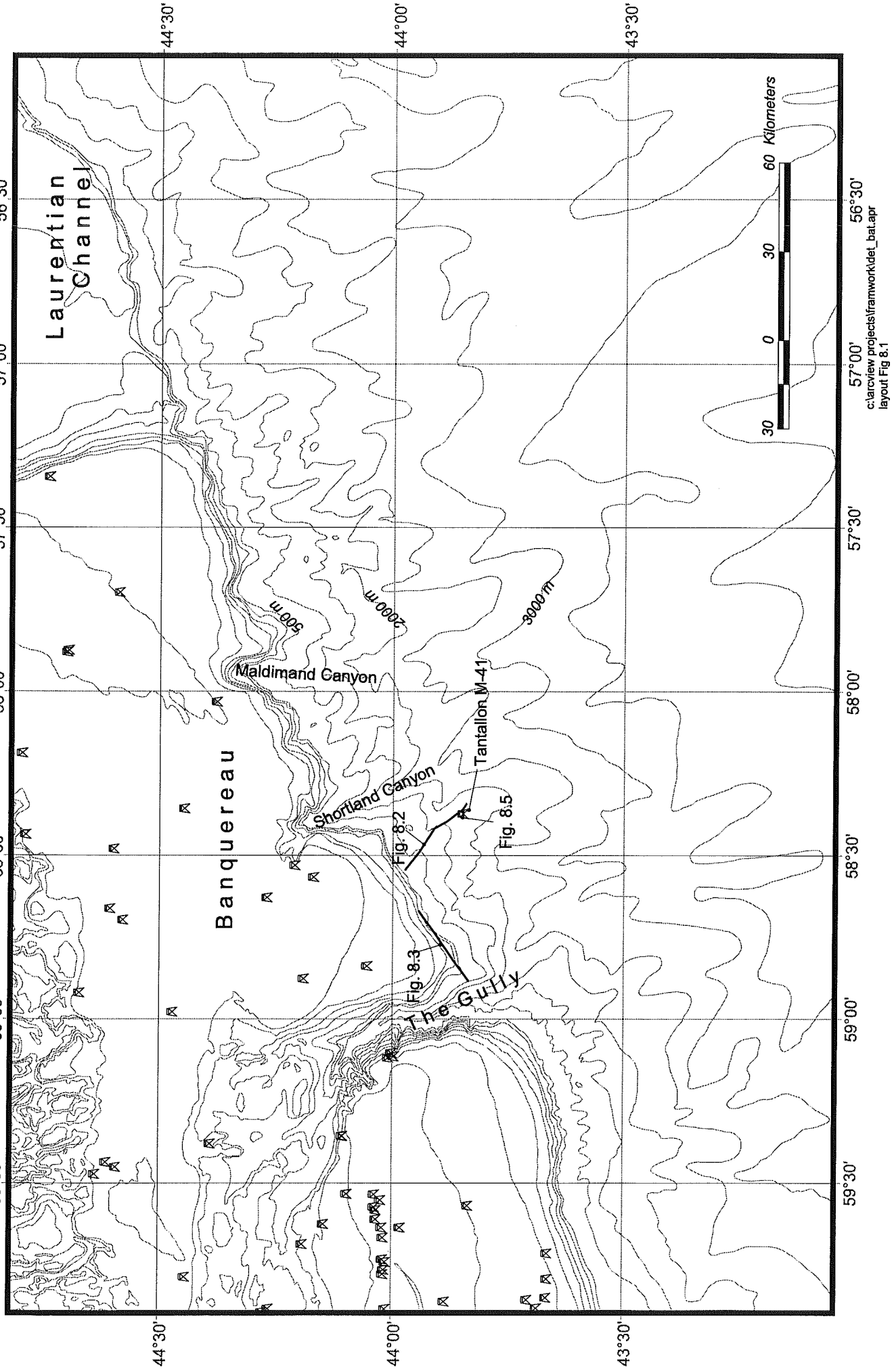

Figure 8.1: Regional map of the continental slope off Banquereau.

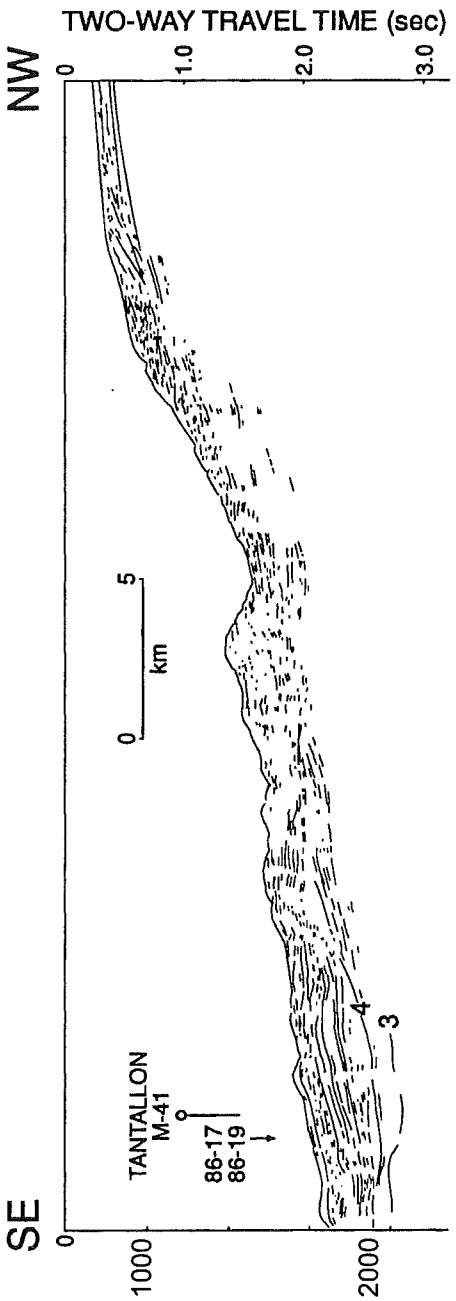

Fig. 8.2. Line drawing of seismic profile across the continental slope in the Tantallon area. Shows location of Tantallon M-41 well and piston cores 86-17 and 86-19. 3 and 4 are reflectors identified in well-site surveys: 4 corresponds to regional reflector F.

C:/fErnest/revised/fig8_2.cdr

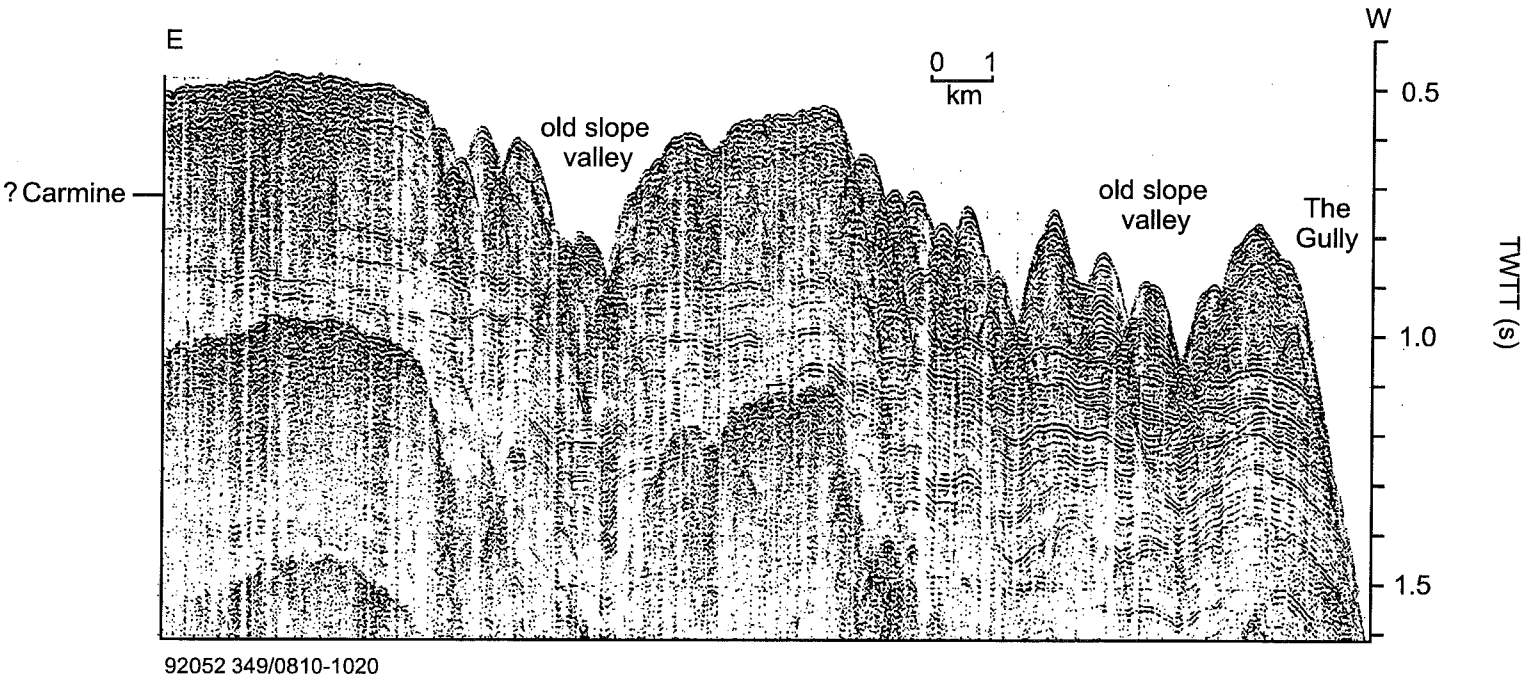

Fig.8.3. Strike airgun seismic profile on the upper slope in the Tantallon area.

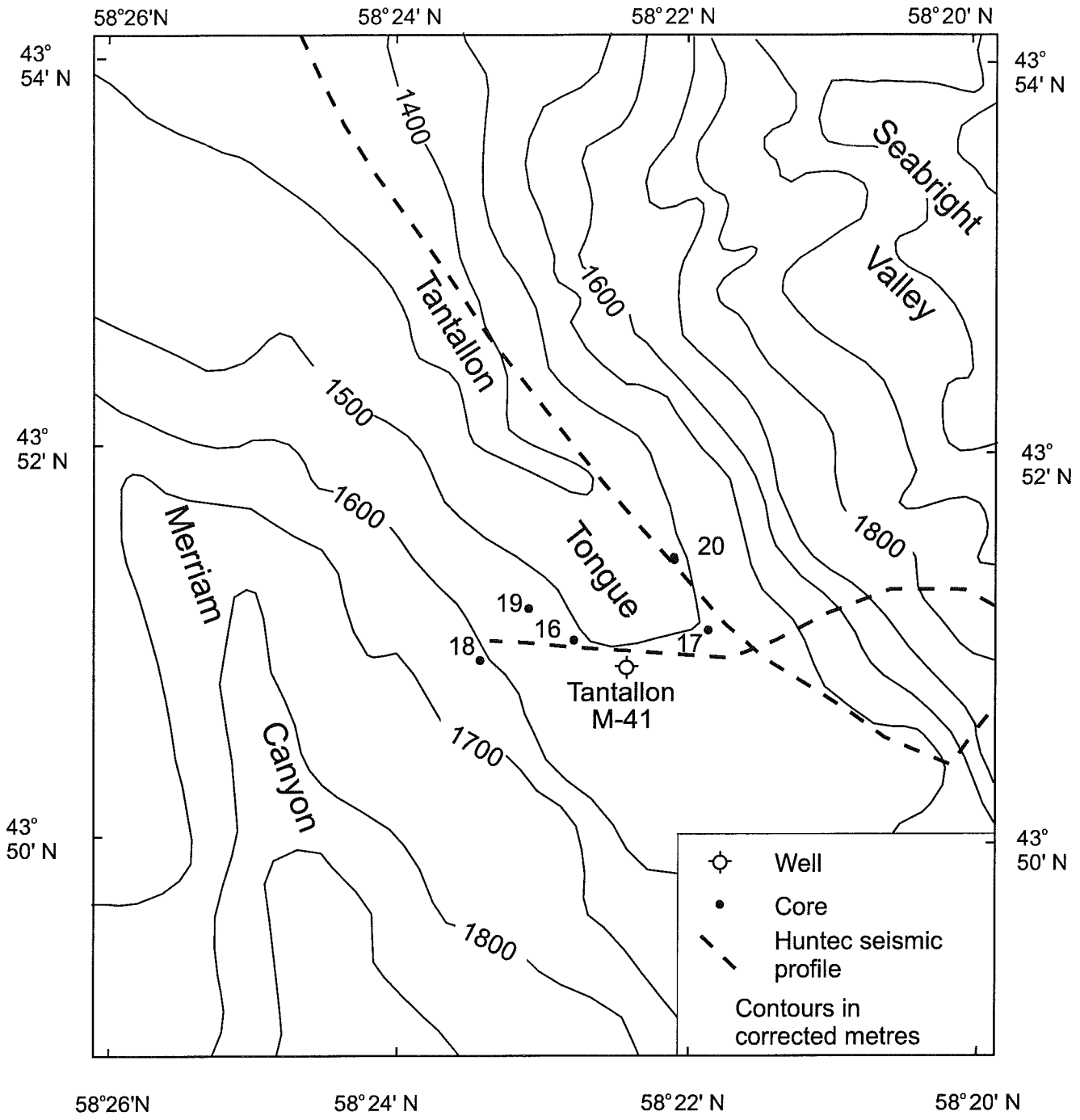

Fig. 8.4. Detailed bathymetry and data distribution near the Tantallon well site.

C:/!Ernest/revised/fig8_4.cdr

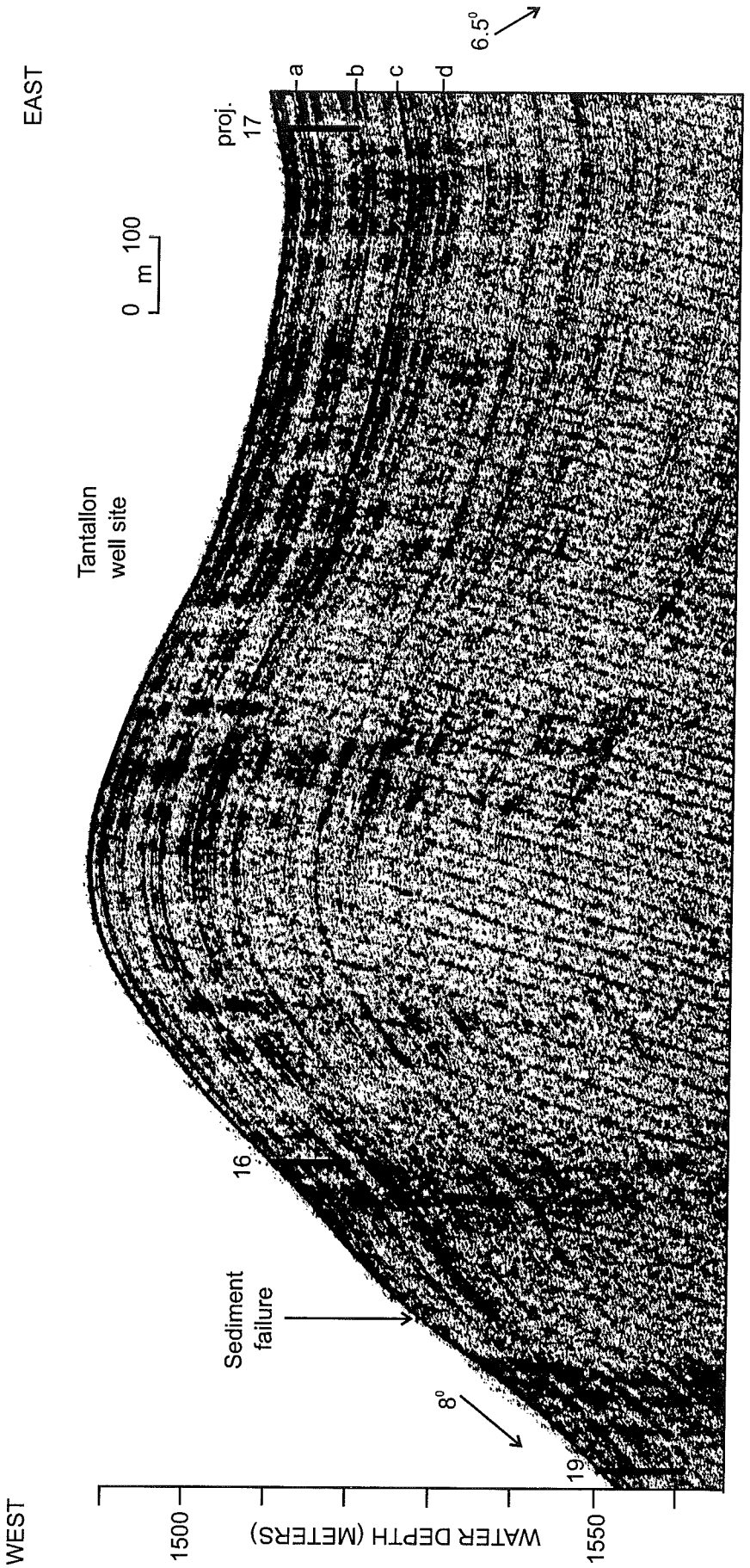

Fig. 8.5. Huntec DTS profile through the Tantallon well site, with the projected location of cores.

C:/IErnest/revised/fig8_5.cdr

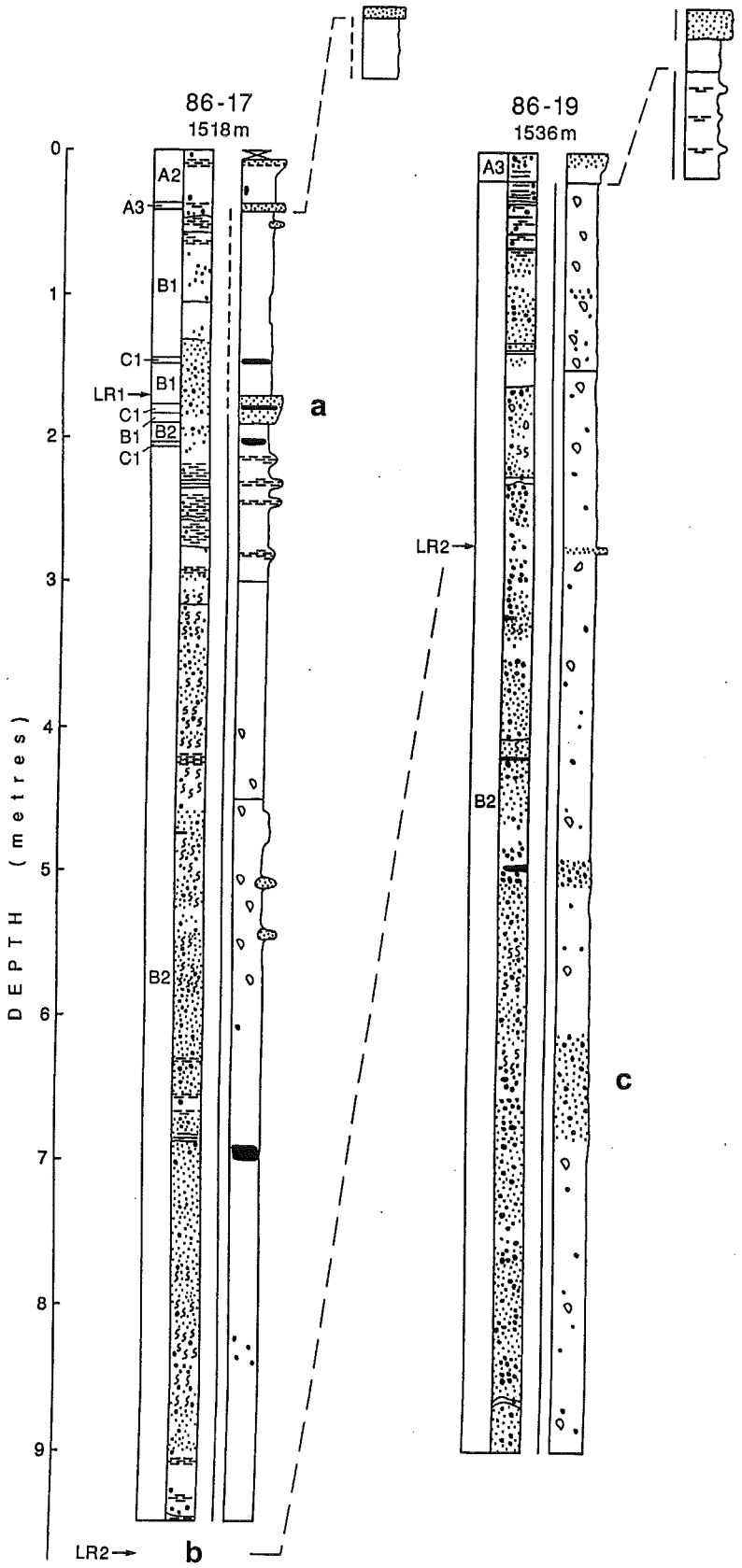

Fig. 8.6. Composite stratigraphic section based on piston cores. Legend in figure 1.5.

C:/IErnest/revised/fig8_6.cdr

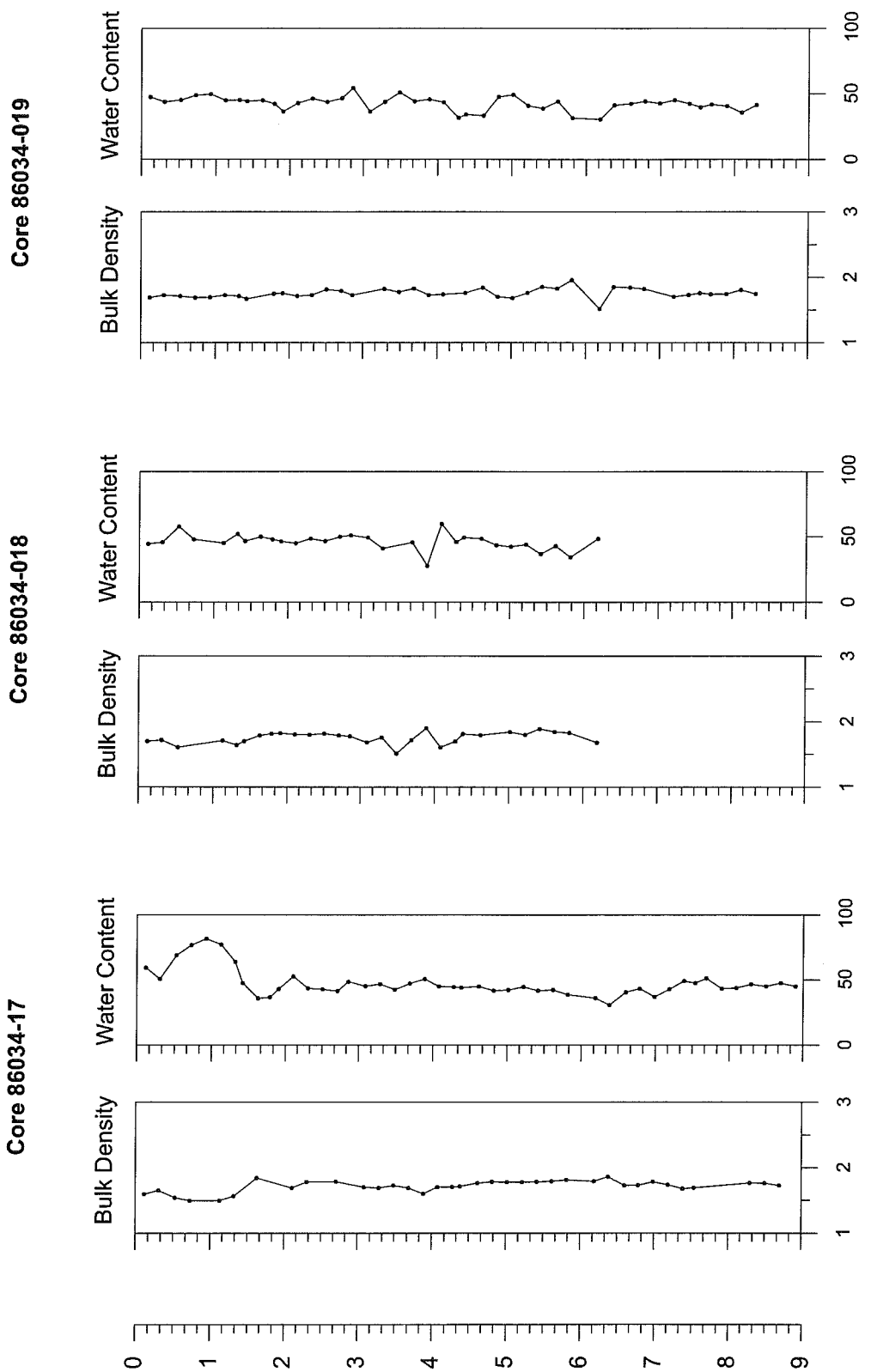

Fig. 8.7. Downcore geomechanical properties for cores around the Tantallon well site.

C:/IErnest/revised/fig8_7.cdr

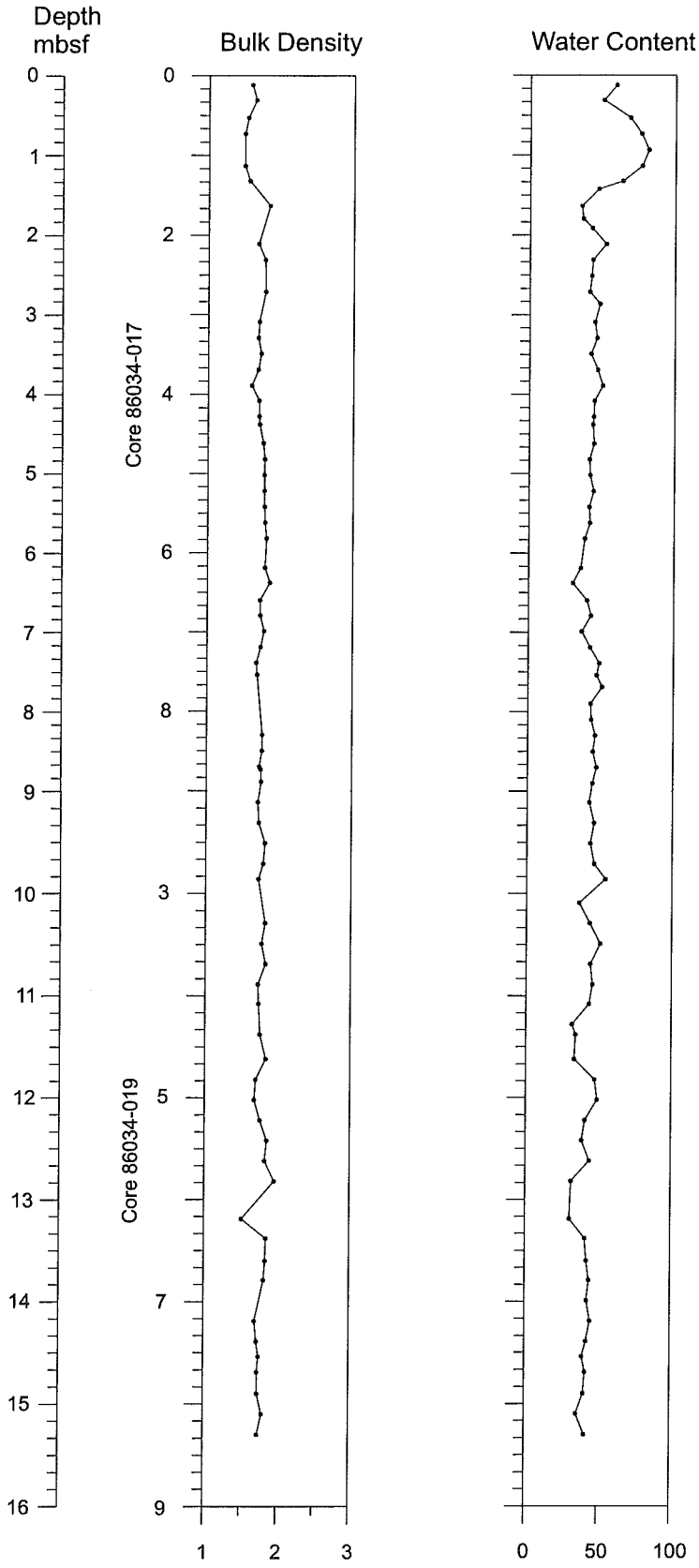

Fig. 8.8. Composite plot of downcore geomechanical properties near the Tantallon well site. Core 86034-019 is from a slump scar and measured properties may be quite different from in-situ properties at 10-16 mbsf.

C:/!Ernest/revised/fig8_8.cdr

9. Synthesis of stratigraphy and sedimentation

9.1 Late Cenozoic sedimentation as revealed by seismic reflection profiles

A cartoon synthesis of the late Cenozoic stratigraphy of the central part of the Scotian margin is shown in Figure 9.1. Data is currently insufficient to provide detail either off Browns Bank and westward or off Banquereau. The base of the glacial section (B) is well marked on the upper slope, where strata interfingering with tills from the shelf overlie more normal continental slope deposits. The basal Quaternary can be traced over much of the middle and lower slope as a prominently gullied horizon, locally with debris flows. Several horizons of valley cutting and gullying are visible in the Pliocene, the most widespread being at the Red and Lavender (D) reflectors. Possible correlations with the Scotian Rise are shown in Figure 2.8.

9.2 Late Quaternary sedimentation as revealed by cores

The distribution of sediment types in cores is summarized in Figure 9.2. Over much of the margin, there is a pronounced change from predominantly olive grey sediment of facies A to browner sediment of facies B. The age of this transition is constrained by several radiocarbon dates to between 12 and 14 ka. Although sediment colour may be partly diagenetic in origin, this colour change appears to correspond to a change in sediment petrography (Hill, 1981, Fig. 5-8). Distinctive thin beds of brick red sandy mud interbed with the extreme top of facies B and the base of facies A and are useful stratigraphic markers (Piper and Skene, 1998). Within the olive-grey facies A, there is a pronounced browner interval (termed unit 2c by Hill, 1981) at least in the area off Western Bank and Sable Island Bank. Basal ages are 8.9 ka off Western Bank and 10.3 ka off Sable Island Bank, suggesting an early Holocene or Younger Dryas age.

At the time of writing, there is no clear understanding of the regional variations in the proglacial facies that are older than 14 ka. This issue is currently being addressed, principally using cores collected in 1999. Principal upper slope lithologies are brownish muds with ice-rafted sand and gravel, sticky red muds in the east with ice-rafted detritus, and brownish mud turbidites with thin sand interbeds. These facies show a range of index properties (Fig. 9.3). Heinrich event 2, a mud rich in detrital carbonate dating from about 21 ka, is recognised in a few cores.

The available radiocarbon dates from debris flows and failures suggest that failures can be correlated between the Albatross and Shubenacadie areas (Piper and Skene, 1998). At least four discrete ages of failure are distinguised (Fig. 9.4). Further dating is currently underway to establish the ages of debris flows in other parts of the Scotian margin.

9.3 **Sedimentation rates**

Sedimentation rates can be estimated from dated piston cores and from dated seismic reflectors. Mean sedimentation rates in the Holocene (the last 10 000 years) are of the order of 10-20 cm/ky, with silts and muds largely swept off the outer banks. Where data exist, the early Holocene sedimentation rates appear much higher than those in the late Holocene.

Sedimentation rates during the last glacial maximum are probably regionally variable, depending on the proximity of the site to ice margins. In the Shubenacadie-Acadia area, principally muddy sediment accumulated in the 12-18 ka interval at about 60-100 cm/ky and in the 12-36 ka interval at 100 cm/ky. At the Tantallon well site, three radiocarbon dates of 15.1 ka to 16.5 ka imply a sedimentation rate of 450 cm/ky in the sticky red muds. In the area near the Shelburne well, a radiocarbon date of 28.1 ka implies a glacial sedimentation rate of only 15 cm/ky, again principally in muds, perhaps because of erosion.

Piper et al. (1994) present evidence that the age of the first major shelf-crossing glaciation in Laurentian Channel corresponds to isotopic stage 12, at about 0.5 Ma. If this is also the age of the first shelf-crossing glaciation on the Scotian Shelf, corresponding to regional reflector B, then this marker can be used to estimate mean sedimentation rates of the last half million years. Figure 2.4 shows that mean thickness on the central Scotian Slope is of the order of 200 metres, ranging from 50 m locally to over 300 m upslope. This corresponds to a mean sedimentation rate of 40 cm/ky.

Thicknesses of mid Quaternary to mid Pliocene sediment on the central Scotian Slope are in the range of 400-700 m (Fig. 2.5) and accumulated over perhaps two million years, corresponding to a sedimentation rate of 5-10 cm/ky. The base Quaternary marker (grey or C) is widely recognisable on the eastern Scotian Slope. South of Sable Island, intercanyon areas have up to 500 m of sediment above grey (Figs. 7.5, 7.6), corresponding to a mean Quaternary sedimentation rate of 30 cm/ky.

9.4 **The occurrence of large landslides**

There is sparse evidence of very large slides (involving > 50 m sediment thickness) on the Scotian margin. In contrast, farther southwest on the New England margin, very large slides are relatively common spatially and probably reflect the overall erosive character of that margin compared with the progradational Scotian margin (O'Leary, 1986a, b, 1992; O'Leary and Dobson, 1992). The largest slide complexes off southwest New England have headwall scarps 100 m high and the debris fields are commonly 50 km wide and 200 km long. Some were initiated in 700 m water depth, others as deep as 2000 mbsl. O'Leary and Dobson (1992) concluded that "the upper Pliocene to lower Pleistocene interval beneath the upper rise terrace is structurally weak; it began to flow in latest Pleistocene .... This deformation removed down-dip support for the Pleistocene section on the lower slope, leading to major mass movement.... Sliding and collapse was conditioned by

interstratal deformation and was probably triggered by epicentrally clustered earthquakes."

On the Scotian margin, Hughes Clarke et al. (1992) described a 100 km long slide, with a > 100 m headwall in 3500 m water depth, off northeast Georges Bank. What we have mapped as the Albatross debris flow on the Scotian margin resembles some of the smaller slides on the New England margin. On the other hand, the original interpretation of a giant slide in 1929 around the Grand Banks earthquake epicentre (Heezen and Drake, 1964) is now known to be incorrect (Moore, 1978; Piper et al. 1999) and only shallow surficial failure took place. The 75 m headwall in 2000 m water depth south of the Shubenacadie well (section 3.3) leads downslope to only a small channelled debris flow deposit.

Similar large slides are known in other parts of the world. One of the finest examples is the Storegga slide off Norway (Bugge et al., 1987, 1988). Gas hydrates are implicated in the origin of this slide (Paull et al., 1991) and it produced a 4 m high tsunami on the Scottish coast (Long et al. 1989). Similar slides off the Brazilian coast were cored by Ocean Drilling Program Leg 155 and geotechnical properties are reported by Piper et al. (1997). Again, gas hydrates are implicated in triggering these slides. Reviews of slides on the US Atlantic margin are provided by Embley (1980), Cashman and Popenoe (1985), and Schwab et al. (1992).

Some aspects of the O'Leary and Dobson (1992) interpretation of the New England margin might be questioned. Their chronology (that slides are essentially a latest Pleistocene to early Holocene phenomenon) seems improbable: on the Scotian margin, the record of debris flow deposits on the continental rise (discussed below: see also Piper et al. 1999) spans the Pleistocene and late Pliocene (Berry and Piper, 1993). Some of the seismic reflection features described by O'Leary (1986b) from seismic reflection profiles as deformational phenomena might equally well be accounted for by sediment deposition involving rapid changes in slope or facies. My experience is coloured by the 1929 event, where the evidence for deep failures was over-interpreted. This issue of whether seismic features are related to failure or deposition also arose in the relocation of the Albatross well-site in the 1980's. COGLA believed that the original site on Albatross Ridge (Fig. 5.13a) was on a slide: this interpretation was defensible, but I felt that the feature was purely depositional. The relocated well site in a channel resulted in boulder bed problems, I understand.

On the other hand, the pattern recognised by O'Leary and Dobson (1992) of interstratal deformation in the late Pliocene - early Pleistocene section off New England is also seen in areas that we have examined in detail off the Scotian margin. Such deformation is widespread in the Albatross - Shelburne area, leading in places to mud diapirism. Interstratal faulting is present in the Shubenacadie - Acadia area. If such weakness has led to major slides off southwestern New England with headwall scarps at 700 mbsl, it is possible that such slides could also occur on the Scotian margin.

9.5 **Correlation of failures with the continental rise record**

Correlation of slope failures with deposits on the continental rise is important because deposits on the rise provide information about the scale and timing of failures that leave little record on the slope. Such correlation is at present limited by available data and is summarized by Piper et al. (1999).

The correlations, if correct, are important because they show a history of debris flow deposition on the continental rise that goes back to the middle Pliocene (Fig. 2.8). This means that the triggering mechanism for debris flows does not directly involve the presence of icesheets on the outer shelf, since Atlantic Canada was likely not glaciated in the Pliocene and shelf-crossing glaciations probably first occurred around isotopic stage 16 or 12 (450-650 ka) (Piper et al. 1994). We have not determined why some areas of the rise have abundant debris flow deposits since the Pliocene, whereas others accumulated principally stratified sediment (Fig. 2.8). We speculate that it might be related to sedimentation rates or rates of leakage of petroliferous gas; it does not appear to correlate with regional gradient.

On the eastern Scotian Rise, the abundance and scale of debris flow deposits is greater in the late Pliocene and earlier Quaternary than it is in the later Quaternary. It is thought that the deep canyons on the eastern Scotian Slope were cut in the later Quaternary by ice-margin processes. If that is the case, it appears as though cutting of canyons has reduced the risk of very large sediment slides, perhaps by providing a pathway for draining excess pore pressures.

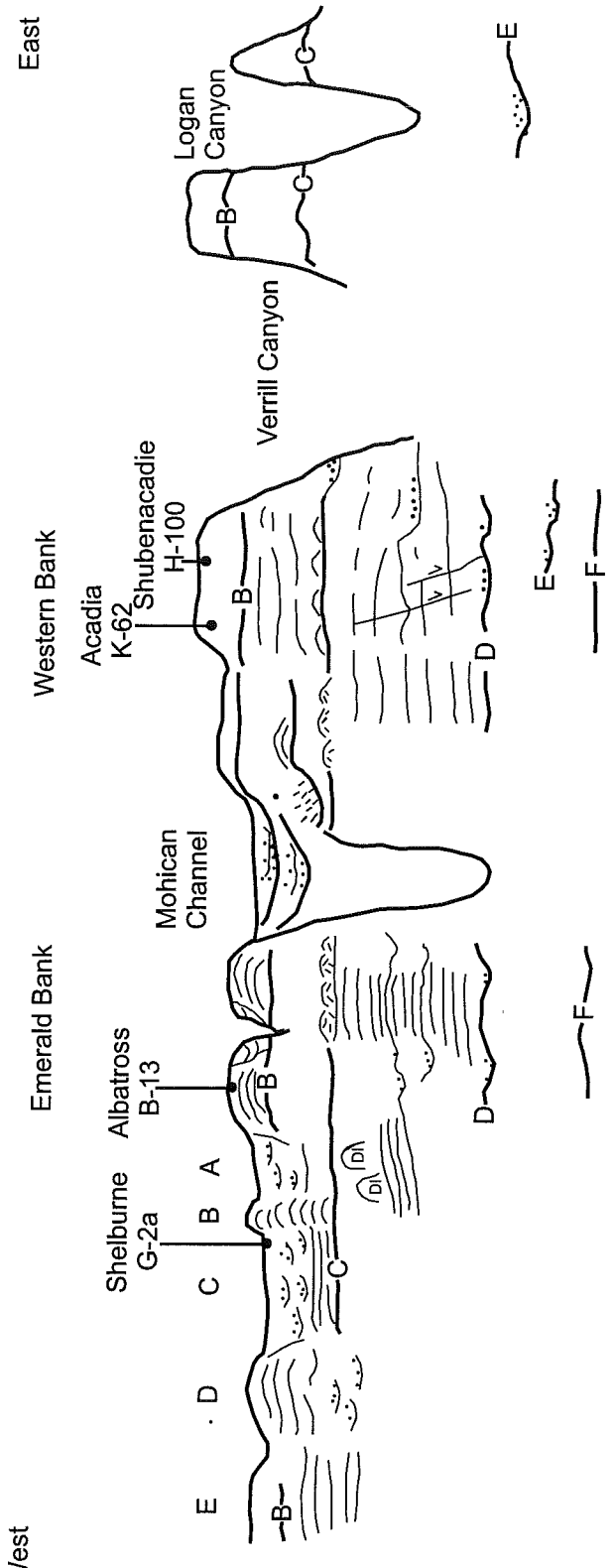

Fig. 9.1. Cartoon illustrating seismic architecture of the late Cenozoic on the Scotian margin.

C:/IErnest/revised/fig9_1.cdr

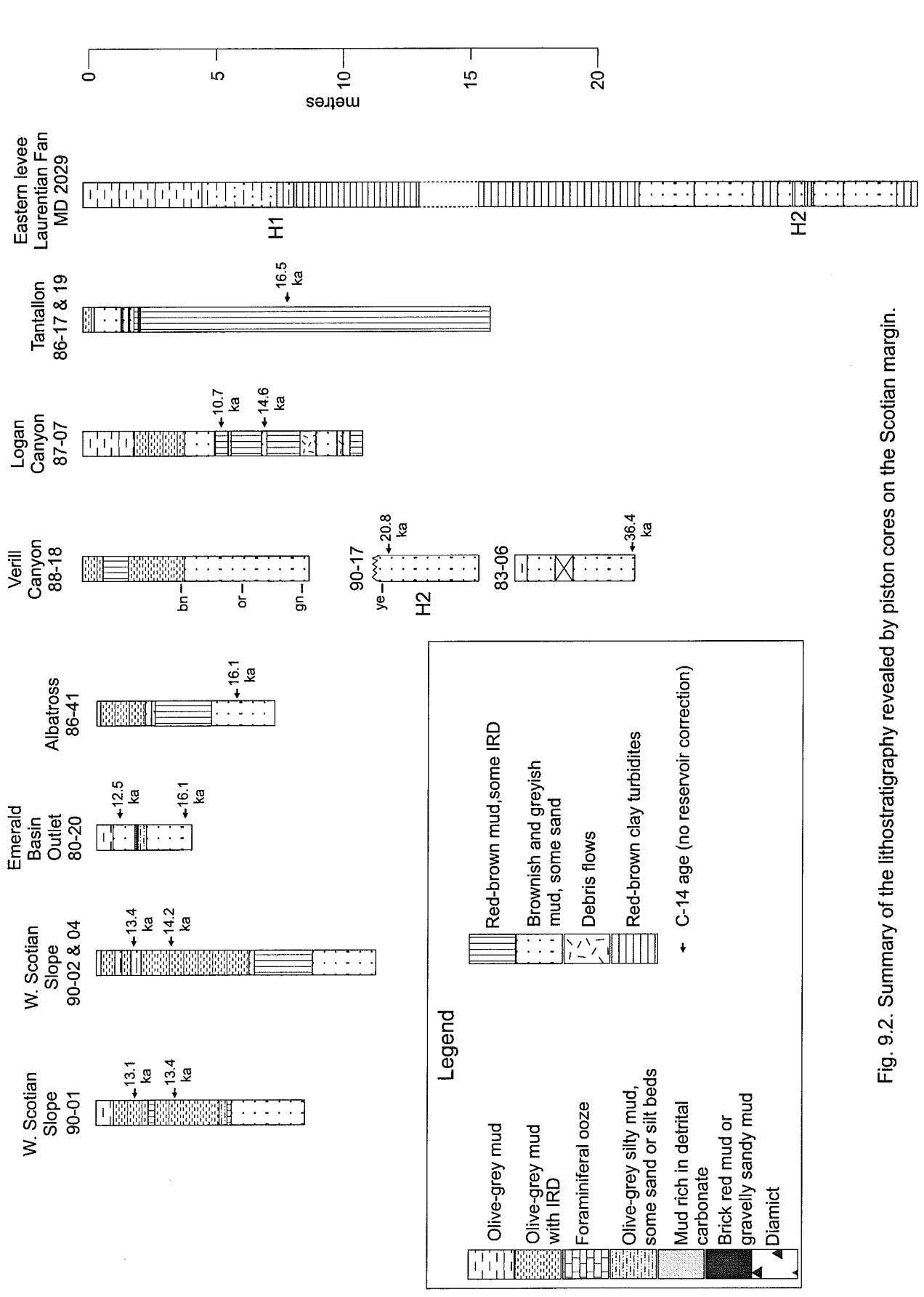

Fig. 9.2. Summary of the lithostratigraphy revealed by piston cores on the Scotian margin.

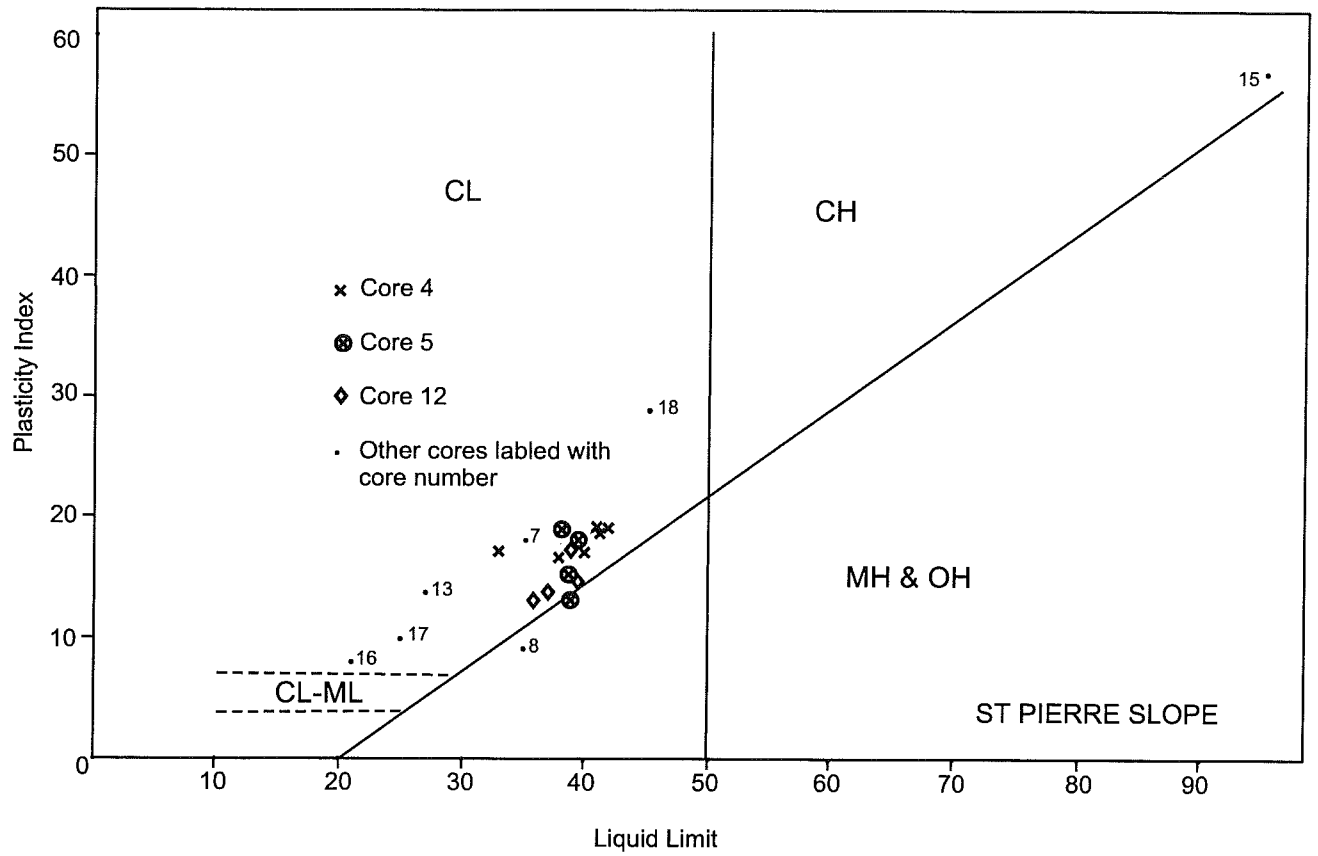

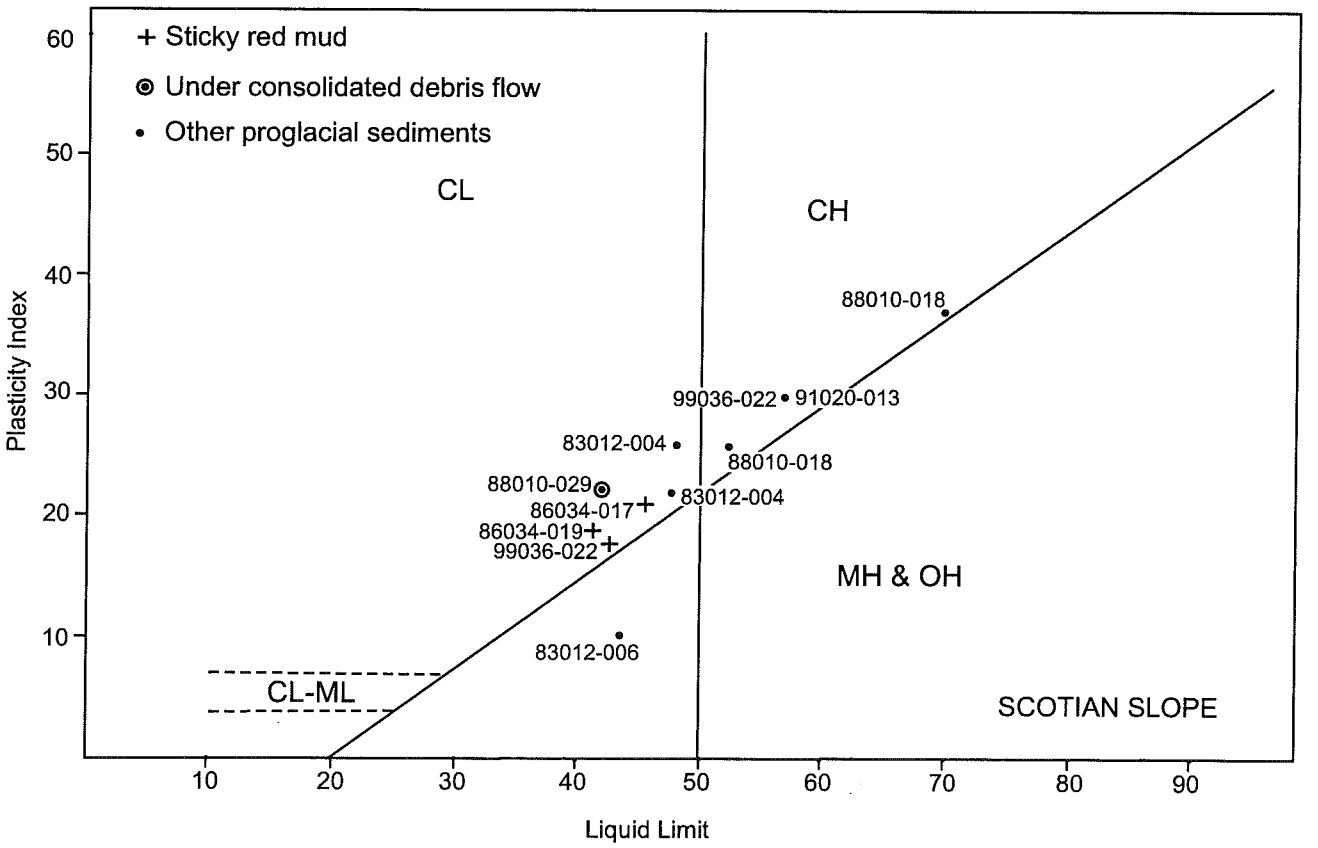

Fig. 9.3. Atterberg limits from piston cores. Above St Pierre Slope (from Masters 1986).

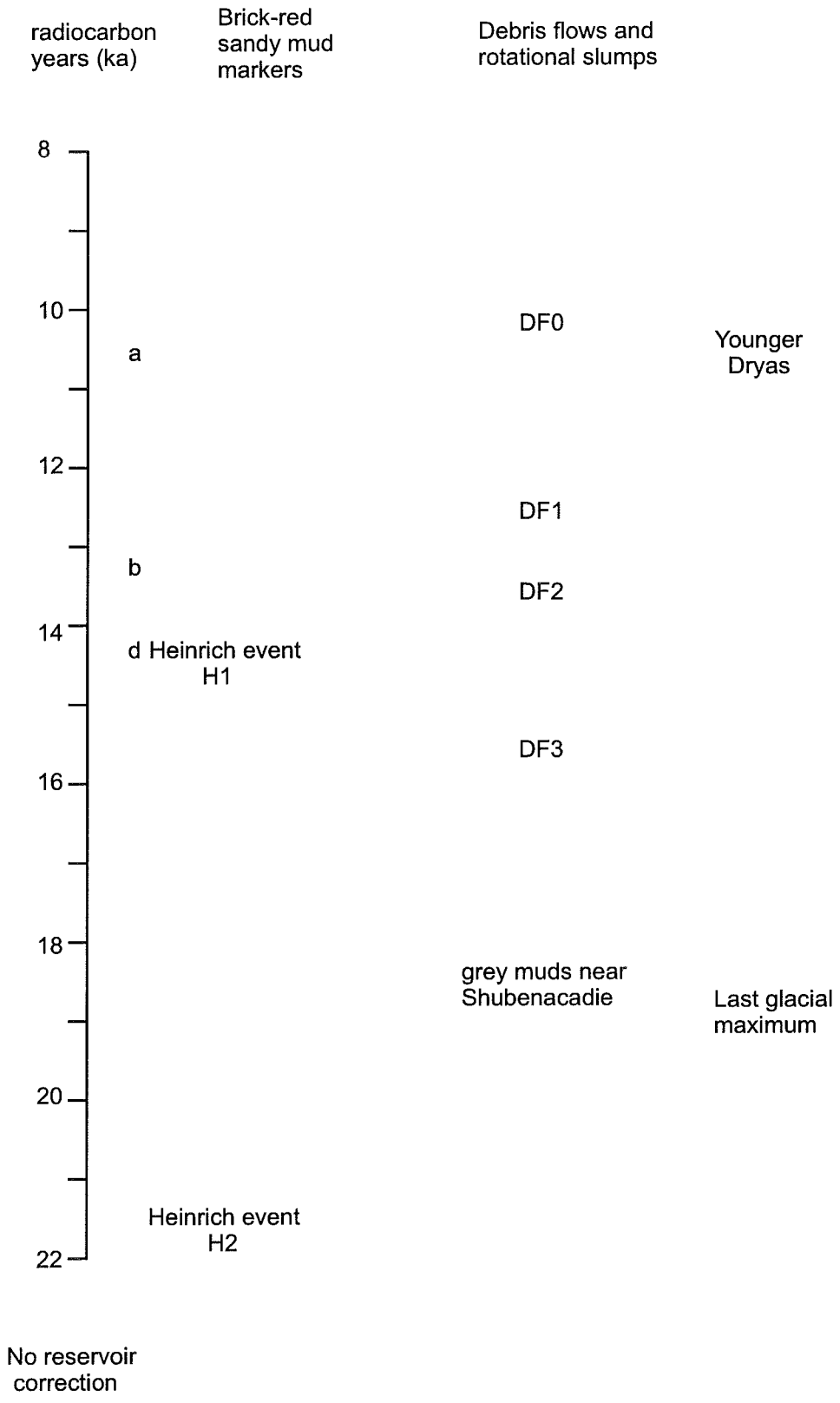

Fig.9.4. Summary of chronology of key late Pleistocene events on the Scotian Slope.

10. General assessment of hazards

10.1 Introduction

With the exception of the 1929 "Grand Banks" failure (Piper et al. 1999), evidence for large-scale sediment failure on the Scotian margin in the past 10 000 years is lacking. Nevertheless, failure has been widespread on the margin throughout the late Pliocene and Quaternary, suggesting that suitable conditions exist for large failures to take place. What is unclear is what triggers large failures. Failure is almost certainly triggered by rare earthquakes on the passive continental margin. The abundance of late glacial failures suggests that glaciation plays some sort of role, perhaps indirect, in triggering failure: whether this is through gas hydrates, ice loading, higher rates of sedimentation, or induced seismicity is discussed below. The role of these various processes must be understood if the thermal, micro-seismicity or loading impacts of eventual hydrocarbon production is to be assessed. The presence of widespread failure in the late Pliocene demonstrates that the direct results of shelf-crossing glaciation are not necessary for large failures to occur.

10.2 The role of shallow gas and gas hydrates

Evidence of shallow gas is sparse but widespread on the Scotian margin: it is recognised from pockmarks, from gassy cores, and from acoustic effects in high-resolution acoustic profiles. Gassy acoustically bright spots can also be mapped from confidential industry spec seismic surveys, which I understand confirm the patchy distribution of gas. Data available to the GSC is insufficient to define areas of more abundant gas but this could be done with recent industry seismic. High-resolution sidescan data (principally the IFREMER SAR system) shows that pockmarks are common on the continental slope. In areas where SAR 1-km swath sidescan imagery is available (Baltzer et al. 1994) between the Shubenacadie and Shelburne wells, pockmarks tend to be more abundant in water depths of 500-700 m than at 1000 - 2000 m (Figs. 5.24, 6.15). Pockmarks are generally interpreted as gas escape craters and this interpretation is supported by the presence of gas in piston cores in areas of pockmarks. Pockmarks are most readily formed and preserved in muddy substrates. They are most readily recognised in sidescan data in areas of smooth seabed.

Mapping of pockmarks in the Acadia-Shubenacadie area shows that they are most abundant in water depths of 500-900 m although they are present in all water depths to 2200 m. Lesser data near the Albatross well site shows a similar distribution. Several hypotheses can be suggested for this distribution.

1. That it is an artifact of bottom type. The paucity of pockmarks shallower than 500 m might be explained in this way, but the decrease in deeper water is more difficult to explain.
2. That it is a consequence of gas sources. It is not known whether the gas is biogenic or thermogenic, although

the latter seems more probable. Organic carbon content of later Quaternary muds is low (Pocklington et al., 1991). It is not obvious that there are systematic subsurface structures that would focus gas delivery into the 500-900 m window, although in confidential industry seismic, my impression is that shallow gas is commonly related to deeper structures.

3. That it is partly a consequence of a surficial cap of gas hydrates that reduces the vertical permeability of gas in deeper water. Estimates of the stability field of gas hydrate suggest that such a cap would thin out in water depths of 500-700 m (Martin Morrison, pers. comm., 1995). Gas migrating up-dip along the base of the hydrate layer would then preferentially escape to the surface where the hydrate cap thinned out or becomes discontinuous.

There is no direct evidence for the presence of gas hydrates on the Scotian margin. No bottom-simulating reflections or bottom-simulating wipeouts have been reported in publicly available data, although I understand that there is sparse evidence of BSRs in the new spec surveys. Hydrates have not been recovered in cores and no detailed geochemical measurements have been made on gas samples. Salinity has been routinely measured in many cores (to a precision of 1‰) as part of the laboratory procedure to determine bulk density and some cores have consistently low salinity that might indicate the melting of gas hydrates[1]. Measurement of core temperature[2] was made on two cruises (93026 and 99036) without any positive results. The abundance of gas in cores over a wide area and the presence of gas seeps on Laurentian fan (Mayer et al., 1987) suggests that sufficient gas is present to form hydrates. The physical conditions are suitable for hydrates. It therefore is probable that hydrates are present, but in sufficiently low concentrations that there is not a strong acoustic response.

If hydrates are present and influence the distribution of pockmarks then they probably also influence the occurrence of sediment failures. Excess pore pressures due to free gas beneath a thin hydrate cap may play an important role in producing the widespread sediment failures in 600 - 1000 m water depth.

The age of shallow sediment failures in the Shubenacadie to Albatross area is clustered around 15-12 ka (Piper and Skene, 1998), with one minor failure younger than 10.8 ka. There are two simple explanations for this pattern: (a) that they were triggered by ice-margin seismicity during ice retreat (cf. Stein et al. 1979) or (ii) that warming of slope waters as a result, principally of ice retreat in Laurentian Channel at about 14.5 ka ending underflows of cold water, allowed patchy gas hydrates to melt.

---

[1] since gas hydrates release fresh water when they sublime. The best example of lowered salinity is 3.6 - 6.2 mbsf in HU88010-18, where salinity is 32-33‰ compared with a "background" 34‰. Note, however, that in Emerald Basin Buckley (1991) has argued that low salinity is a direct consequence of low salinity glacial meltwater filling the basin. This mechanism is less probable on the continental slope.

[2] sublimation of gas hydrates is endothermic and may be detected by a fall in temperature when a core is first collected.

In summary, the evidence that hydrates may play a role in sediment instability on the Scotian Slope is:
(a) the chronology of large debris flows, extending back to the mid Pliocene, a time when slope waters would have been cool, but local glaciation absent, and the clustering of failures during times of warming of slope waters.
(b) the presence of shallow gas, suitable PT conditions, and anecdotal occurrence of rare BSRs.

10.3 **Earthquake risk**

Earthquake risk concepts on the east coast offshore of Canada are summarized by Keen et al. (1990) and updated numerical estimates are available from *http://www.seismo.nrcan.gc.ca*. A brief summary of issues is presented here. The eastern continental margin of Canada is relatively active compared with most passive continental margins, with two M>7 earthquakes this century (1929 off the Laurentian Channel and 1933 in Baffin Bay). The instrumental record of earthquakes is 30-70 years for this region; historical records suggest that off Nova Scotia there were no earthquakes comparable to the 1929 earthquake in the previous 150 years. The geological record on the continental margin suggests that there has been no such large earthquake in the previous 10 000 years, but that there were significant earthquakes in the late Pleistocene. The issues in assessing seismic risk are concerned with estimating both the recurrence interval and spatial distribution of past earthquakes: are the passive margin earthquakes concentrated in particular tectonic zones, such as the area of the 1929 earthquake, or are they evenly distributed along the continental margin. Keen et al. (1990) concluded that "the limited geological evidence, poor though it is, suggests that very large events are relatively widely spread, not concentrated in one area, and that the indicated return period in the range 10 000 to 100 000 years is longer than has been assumed in modelling seismicity from instrumental records ...". No new data since 1990 has changed this general assessment but the paucity of geological evidence must be emphasised.

10.4 **Is failure related to glacial processes?**

In a series of papers, Mulder has examined the relationships between glaciation and sediment failure. Mulder and Moran (1995) (modified in Mulder et al., 1999) examined the theoretical effects of a thick outer shelf ice sheet on stability on the upper slope. They show that bearing capacity failure under ice loading was a possible means of deep-seated failure at the shelf edge, although no geological evidence for failure of this style is known. They also analysed the effect of increased pore pressure in slope sediment as a result of ice loading on the outer shelf; they show that significant pore pressures might persist for 5 000 years after ice retreat to present water depths of 350 mbsl. Once again, there is no geological evidence that this process is important. Stein et al. (1979) discuss evidence that stresses arising from glacial unloading might be responsible for triggering earthquakes.

10.5 **The risk from storm-driven sediment transport**

Studies in the vicinity of the Albatross and Shelburne wells have shown the effect of large storms on transport of sand on the continental slope. Hill and Bowen (1983) showed that sorted sands and silts mantle the upper slope to water depths of 450-600 m. These are apparently derived from the outer continental shelf and remobilised by storm-driven, contour parallel currents.

North of the Albatross well, 1-km-swath SAR sidescan imagery showed a dendritic network of small middle-slope gullies (Baltzer et al., 1994, their Fig. 10). A push core on the floor of one such channel recovered 1.5 m of silty sand, with a 9.6 ka mollusc shell at 0.9 m. The sand occurred in beds 10-20 cm thick. These dendritic channels therefore appear to accumulate sand occasionally during the Holocene and may provide evidence of down-slope transport of sediment suspended on the outer shelf. On the Grand Banks margin, Savoye et al. (1990) found a 5 ka sand bed near the Titanic wreck that they interpreted as deposited from a storm-induced turbidity current from the shelf edge.

Storm-driven sediment transport is an issue to be considered in the development of any production facilities, but is not on a scale that would directly impact any exploration procedures.

10.6 **Boulder bed problems**

On the eastern Scotian Shelf, tunnel valleys are widespread (Loncarevic et al. 1993). Tunnel valleys are interpreted as subglacial water-cut valleys, perhaps resulting from catastrophic flood discharges (jokulhlaups). Tunnel valleys on the continental shelf probably lead to the deeply incised canyons on the continental slope, although this linkage has not been proved. Large subglacial flows are likely to transport coarse-grained sediment including boulders. Mohican Channel might also be a subglacial meltwater outlet.

In addition, the eastern Scotian Slope was in the trajectory of icebergs from the Labrador Sea and Gulf of St Lawrence during the Pleistocene (Piper and Skene 1998) and scattered ice-rafted boulders are to be expected throughout the area.

The geological framework studies in the Albatross - Shelburne area show common buried channels. Sediment supply to these channels, at least in the mid to late Quaternary (probably above the "rose" reflector) would have included glacial or fluvioglacial supply of gravel to boulders.

Bibliography

Amos, C.L. and Knoll, R., 1987. The Quaternary sediments of Banquereau, Scotian Shelf. Geological Society of America Bulletin, v. 99, p. 244-260.

Baltzer, A., 1994. Dynamique sedimentaire des marges de Nouvelle Ecosse et des entrées de la Manche au Quaternaire. Doctoral thesis, Université de Bretagne occidentale, 216 + 78 p.

Baltzer, A., Cochonat, P. and Piper, D.J.W., 1994. In situ geotechnical characterisation of sediments on the Scotian Slope, eastern Canadian continental margin. Marine Geology, v. 120, p. 291-308.

Berry, J.A., 1992. A detailed study of a debris flow system on the Scotian Rise. Unpublished M.Sc. thesis, Dalhousie University, 202 p.

Berry, J.A. and Piper, D.J.W., 1993. Seismic stratigraphy of the central Scotian Rise: a record of continental margin glaciation. Geo-Marine Letters, v. 13, p. 197-206.

Bonifay, D. and Piper, D.J.W., 1988. Probable Late Wisconsinan ice margin on the upper continental slope off St. Pierre Bank, eastern Canada. Canadian Journal of Earth Sciences, v. 25, p. 853-865.

Boyd, R., Scott, D.B. and Douma, M., 1988. Glacial tunnel valleys and the Quaternary history of the Scotian Shelf. Nature, v. 333, p. 61-64.

Buckley, D.E., 1991. Deposition and diagenetic alteration of sediment in Emerald Basin, the Scotian Shelf. Continental Shelf Research, v. 11, p. 1099-1122.

Bugge, T., Befrig, S., Belderson, R.H., Eidrin, T., Jansen, E., Kenyon, N.H., Holtedahl, H., and Sejrup, H.P., 1987. A giant three-stage submarine slide off Norway. Geo-Marine Letters, v. 7, p. 191-198.

Bugge, T., Belderson, R.H. and Kenyon, N.H., 1988. The Storegga Slide. Philosophical Transactions of the Royal Society A, v. 325, p. 357-388.

Campbell, D.C., 2000. Relationship of sediment properties to failure horizons for a small area of the Scotian Slope. Current Research, Geological Survey of Canada.

Carter, L., 1979. Significance of unstained and stained gravel on the Newfoundland continental slope and rise. Journal of Sedimentary Petrology, v. 49, p. 1147-1158.

Carter, L. and Schafer, C.T., 1983. Interaction of the Western Boundary Undercurrent with the continental margin off Newfoundland. Sedimentology, v. 30, p. 751-768.

Cartwright, J.A. and Dewhurst, D.N., 1998. Layer bound compaction faults in fine-grained sediments. Bulletin of the Geological Society of America, v. 110, p. 1242-1257.

Cashman, K.V. and Popenoe, P., 1985. Slumping and shallow faulting related to the presence of salt on the continental slope and rise off North Carolina. Marine and Petroleum Geology, v. 2, p. 260-271.

Christian, H.A. and Heffler, D.E., 1993. Lancelot - a seabed piezometric probe for geotechnical studies. Geo-Marine Letters, v. 13, p. 189-195.

Christian, H., Piper, D.J.W. and Armstrong, R., 1991. Geotechnical properties of seabed sediments from Flemish Pass. Deep Sea Research, v. 38, p. 663-676.

Clifford, V., 1986. The late Cenozoic seismo-stratigraphy of the East Scotian Slope. B.Sc. honours thesis, Saint Mary's University, 64 p.

Cochonat, P., Ollier, G. and Michel, J.-L., 1989. Evidence for slope instability and current-induced sediment transport; the R.M.S. Titanic wreck search area, Newfoundland Rise. Geomarine Letters, v. 9, p. 145-152.

Courtney, R.C. and Piper, D.J.W., 1992. The gravity signature of large Quaternary depocentres off southeastern Canada. Géographie Physique et Quaternaire, v. 46, p. 349-360.

DeClerk, H., 1990. Stratigraphie sismique haute resolution sur le talus continental au large de la Nouvelle-Ecosse. Institut Français du Petrole, Report IFP 38 503, 78 p.

Embley, R.W., 1980. The role of mass transport in the distribution and character of deep-ocean sediments with special reference to the North Atlantic. Marine Geology, v. 28, p. 23-50.

Gipp, M.R. and Piper, D.J.W., 1989. Chronology of Late Wisconsinan glaciation, Emerald Basin, Scotian Shelf. Canadian Journal of Earth Sciences, v. 26, p. 333-335.

Gipp, M.R. 1994. Late Wisconsinan deglacation of Emerald Basin, Scotian Shelf. Canadian Journal of Earth Sciences, v. 31, p. 554-566.

Gipp, M.R. 1996. Glacially-influenced marine sedimentation on continental margins: examples from areas of contrasting tectonic setting. Ph.D. thesis, University of Toronto, 139 p.

Gregory, D.N. and Bussard, C., 1996. Current statistics for the Scotian Shelf and Slope. Canadian Data Report of Hydrography and Ocean Sciences, 144, 167 p.

Heezen, B.C and Drake, C.L., 1964. Grand Banks slump. American Association of Petroleum Geologist Bulletin, v. 48, p. 221-225.

Hildebrand, L.P., 1984. Oceanographic setting. In. Wilson, R.C.H. and Addison, R.F., eds., Health of the Northwest Atlantic. Environment Canada and Department of Fisheries and Oceans, p. 8-30.

Hill, P.R., 1981. Detailed morphology and late Quaternary sedimentation of the Nova Scotian slope, south of Halifax. Unpublished Ph.D. thesis, Dalhousie University, Halifax, Nova Scotia, 331 p.

Hill, P.R., 1983. Detailed morphology of a small area on the Nova Scotian continental slope. Marine Geology, v. 53, p. 55-76.

Hill, P.R., 1984. Sedimentary facies of the Nova Scotian upper and middle continental slope, offshore Eastern Canada. Sedimentology, v. 31, p. 293-309.

Hill, P.R. and Bowen, A.J., 1983. Modern sediment dynamics at the shelf slope boundary off Nova Scotia; in

The Shelfbreak. Critical Interface on Continental Margins, eds. D.J. Stanley and G.T. Moore; Society of Economic Palaeontologists and Mineralogists Special Publication No. 33, p. 265-276.

Hill, P.R., Piper, D.J.W. and Normark, W.R., 1983. Pisces IV submersible dives on the Scotian Slope at 63°W. Geological Survey of Canada Paper 83-1A, p. 65-69.

Hughes Clarke, J.E., 1988. The geological record of the 1929 "Grand Banks" earthquake and its relevance to deep-sea clastic sedimentation. P.D. thesis, Dalhousie University, 171 p.

Hughes Clarke, J.E., Mayer, L.A., Piper, D.J.W. and Shor, A.N., 1989. Pisces IV submersible operations in the epicentral region of the 1929 Grand Banks earthquake. Geological Survey of Canada Paper 88-20, p. 57-69.

Hughes Clarke, J.E., Shor, A.N., Piper, D.J.W. and Mayer, L.A., 1990. Large scale current-induced erosion and deposition in the path of the 1929 Grand Banks turbidity current. Sedimentology, v. 37, p. 613-629.

Hughes Clarke, J.E., O'Leary, D. and Piper, D.J.W., 1992. The relative importance of mass wasting and deep boundary current activity on the continental rise off western Nova Scotia. Geologic evolution of Atlantic continental rises, ed. C.W. Poag and P.C. de Graciansky, van Nostrand Reinhold, New York, p. 266-281.

Hutchins, R.W., Dodds, J. and Fader, G.B., 1985. Seabed II. High resolution acoustic seabed surveys of the deep ocean. Proceedings of Society for Underwater Technology, London, England, 27 p.

Jansa, L.F. and Wade, J.A., 1975. Geology of the continental margin off Nova Scotia and Newfoundland. in Offshore Geology of Eastern Canada, ed. W.J.M. van der Linden and J.A. Wade, Geological Survey of Canada Paper 74-30, p. 51-105.

King, L.H. and Young, J.F., 1977. Paleocontinental slopes of East Coast geosyncline (Canadian Atlantic margin). Canadian Journal of Earth Sciences, v. 14, p. 2553-2564.

Keen, M.J., Adams, J., Moran, K., Piper, D.J.W. and Reid, I., 1990. Earthquakes and seismicity. in Geology of the continental margin off eastern Canada, ed. M.J.Keen and G.L.Williams. Geological Survey of Canada, Geology of Canada, no. 2, (also Geological Society of America, The Geology of North America, v. I-1), p. 793-798.

Klohn-Leonoff Ltd., 1993. Direct/triaxial shear testing. Report to the Geological Survey of Canada under contract 23420-2-M302/01-0SC, 7 pp. + appendix.

Long, D.E., Smith, D.E. and Dawson, A.G., 1989. A Holocene tsunami deposit in eastern Scotland. Journal of Quaternary Science, v. 4, p. 61-66.

McLaren, S.A., 1988. Quaternary seismic stratigraphy and sedimentation of the Sable Island sand body, Sable Island Bank, outer Scotian Shelf. M.Sc. thesis, Dalhousie University, 112p.

Mayer, L.A., Shor, A.N., Hughes Clarke, J.E. and Piper, D.J.W. 1987. Dense biological communities at 3850m on the Laurentian Fan. Deep Sea Research, 35, 1235-1246.

Marsters, J.C., 1986. Geotechnical analysis of sediments from the eastern Canadian continental slope, south of the St Pierre Bank. M.Eng. thesis, Technical University of Nova Scotia, 218 p.

Marsters, J.C., 1988. Geotechnical properties of sediments obtained during Hudson 86013 at Narwhal F-99 wellsite. Geological Survey of Canada Open File 1724, 63 p.

Moore, D.G., 1978. Submarine slides. In: Rockslides and avalanches, 1. Natural phenomena. Ed: B. Voight. Elsevier, Amsterdam, p. 564-604.

Moran, K. and Hurlbut, S.E., 1986. Analysis of potential slope instability due to wave loading on the Nova Scotian Shelf. Proceedings of the Third Canadian Conference on Marine Geotechnical Engineering, St Johns, Nfld.

Moran, K., Keen, M.J., Piper, D.J.W. and Adams, J., 1990. Slope stability. in Geology of the continental margin off eastern Canada, ed. M.J.Keen and G.L.Williams. Geological Survey of Canada, Geology of Canada, no. 2, (also Geological Society of America, The Geology of North America, v. I-1), p. 798-802.

Moran, K., Piper, D.J.W., Mayer, L.A., Courtney, R., Driscoll, A.H. and Hall, R., 1989. Scientific results of Long Coring on the eastern Canadian continental margin. Offshore Technology Conference,

Mosher, D.C., 1987. Late Quaternary sedimentology and sediment instability of a small area on the Scotian Slope. Unpublished M.Sc. thesis, Memorial University of Newfoundland, St. John's, Newfoundland, 249 p.

Mosher, D.C., Piper, D.J.W., Vilks, G., Aksu, A.E. and Fader, G.B., 1989. Evidence for Wisconsinan glaciations in the Verrill Canyon area, Scotian Slope. Quaternary Research, v. 31, p. 27-40.

Mosher, D.C., Moran, K. and Hiscott, R.N., 1994. Late Quaternary sediment, sediment mass-flow processes and slope stability on the Scotian Slope. Sedimentology, v. 41, p. 1039-1061.

Mountain, G.S. and Tucholke, B.E., 1985. Mesozoic and Cenozoic geology of the U.S. Atlantic continental slope and rise. In: Geologic evolution of the United States Atlantic margin, ed. C.W. Poag. Van Nostrand Reinhold, New York, pp. 293-342.

Mulder T., Cochonat P., Schieb T. and Tisot J.-P., 1992. Estimation de l'épaisseur de sédiment impliquée dans des glissements sous-marins à partir des données sur l'état de consolidation. Application à la Baie des Anges (S.E. de la France). C.R.Acad.Sci, Paris, t. 315, Série II: 1703-1709.

Mulder, T. and Moran, K., 1995. Relationship among submarine instabilities, sea-level variations and the presence of an ice sheet on the continental shelf: an example from the Verrill Canyon area, Scotian Shelf. Paleoceanography, v. 10, p. 137-154.

Mulder, T., Berry, J.A. and Piper, D.J.W., 1997. Links between geomorphology and geotechnical characteristics of large debris flow deposits in the Albatross area on the Scotian slope (E. Canada). Marine Georesources and Geotechnology, v. 15, p. 253-281.

Mulder, T., Moran, K. and Piper, D.J.W., 1999. Mechanisms for late Quaternary submarine landslides off Nova Scotia, Canada. Marine Geology (in press)

Myers, R.A. and Piper, D.J.W., 1988. Seismic stratigraphy of late Cenozoic sediments in the northern Labrador Sea: a history of bottom circulation and glaciation. Canadian Journal of Earth Sciences, v. 25, p. 2059-2074.

Neave, G. 1990. Shallow seismic velocities on the eastern Grand Banks and in Flemish Pass. Report to Geological Survey of Canada, 37 p.

O'Leary, D.W., 1986a. The Munson-Nygren slide, a major lower slope slide off Georges Bank. Marine Geology, v. 72, p. 101-114.

O'Leary, D.W., 1986. Seismic structure and stratigraphy of the New England continental slope and the evidence for slope instability. U.S. Geological Survey, Open-File Report 86-118, 182 p.

O'Leary, D.W., 1992. Submarine mass movements, a formative process of passive continental margins: the Munson-Nygren landslide complex and the southeast New England landslide complex. In: Submarine landslides: selected studies in the U.S. exclusive economic zone. Ed. Schwab, W.C., Lee, H.J., and Twichell, D.C., U.S. Geological Survey Bulletin 2002.

O'Leary, D.W. and Dobson, M.R., 1992. Southeastern New England continental rise: origin and history of slide complexes. Geologic evolution of Atlantic continental rises, ed. C.W. Poag and P.C. de Graciansky, van Nostrand Reinhold, New York, p. 214-265.

Paull, C.K., Ussler, W. III, and Dillon, W.P., 1991. Is the extent of glaciation limited by marine gas-hydrates. Geophysical Research Letters, v. 18, p. 432-434.

Piper, D.J.W., 1988. Glaciomarine sediments on the continental slope off eastern Canada. Geoscience Canada, v. 15, p. 23-28.

Piper, D.J.W., 1991. Surficial Geology and Physical Properties 6. Deep water surficial geology. in East Coast Basin Atlas Series: Scotian Shelf; Atlantic Geoscience Centre, Geological Survey of Canada, p. 121.

Piper, D.J.W., 1999. Cruise Report, Hudson 99-036. Unpublished report, Geological Survey of Canada (Atlantic), Bedford Institute of Oceanography, 49 pp. + appendices.

Piper, D.J.W., 2000. Pleistocene ice outlets on the central Scotian Slope. Current Research, Geological Survey of Canada, 2000-D, 8 p.

Piper, D.J.W. and Normark, W.R, 1989. Late Cenozoic sea-level changes and the onset of glaciation: impact on continental slope progradation off eastern Canada. Marine and Petroleum Geology, v. 6, p. 336-348.

Piper, D.J.W. and Sparkes, R., 1987. Proglacial sediment instability features on the Scotian Slope at 63°W. Marine Geology, v. 76, p. 1-11.

Piper, D.J.W. and Sparkes, R., 1990. Pliocene - Quaternary geology, central Scotian Slope. Geological Survey

of Canada Open File 2233.

Piper, D.J.W. and Skene, K.I., 1998. Latest Pleistocene ice-rafting events on the Scotian margin (eastern Canada) and their relationship to Heinrich events. Paleoceanography, v. 13, p. 205-214.

Piper, D.J.W. and Wilson, E. 1983. Surficial geology of the upper Scotian Slope west of Verrill Canyon. G.S.C. Open File 939.

Piper, D.J.W., Aksu, A.E., Mudie, P.J. and Skene, K.I., 1994. A 1 Ma record of sediment flux south of the Grand Banks. Quaternary Science Reviews, v. 13, p. 23-37.

Piper, D.J.W., Cochonat, P. and Morrison, M.L., 1999. Sidescan sonar evidence for progressive evolution of submarine failure into a turbidity current: the 1929 Grand Banks event. Sedimentology, v. 46, p. 79-97.

Piper, D.J.W., Farre, J.A. and Shor, A.N., 1985a. Late Quaternary slumps and debris flows on the Scotian Slope: Geological Society of America Bulletin, v. 96, p. 1508-1517.

Piper, D.J.W., Normark, W.R. and Sparkes, R., 1987. Late Cenozoic acoustic stratigraphy of the central Scotian Slope, eastern Canada: Canadian Bulletin of Petroleum Geology, v. 35, p. 1-11.

Piper, D.J.W., Pirmez, C., Manley, P.L., Long, D., Flood, R.D., Normark, W.R., and Showers, W., 1997. Mass transport deposits of Amazon Fan. Scientific Results, Ocean Drilling Program, v. 155, p. 109-146.

Piper, D.J.W., Shor, A.N., Farre, J.A., O'Connell, S. and Jacobi, R., 1985b. Sediment slides around the epicenter of the 1929 Grand Banks earthquake: Geology, v. 13, p. 538-541.

Piper, D.J.W., Skene, K.I. and Morash, N., 1999. History of major debris flows on the Scotian Rise, offshore Nova Scotia. Current Research 1999-E, p. 203-212.

Piper, D.J.W., Sparkes, R., Farre, J.A. and Shor, A. 1983. Mid-range sidescan and 4.5 kHz sub-bottom profiler survey of mass movement features, Scotian Slope at 61° 40'W. G.S.C. Open file 938.

Piper, D.J.W., Sparkes, R., Mosher, D.C., Shor, A.N and Farre, J.A. 1985c. Sediment instability near the epicentre of the 1929 Grand Banks earthquake. G.S.C. Open File 1311.

Piper, D.J.W., Mudie, P.J., Fader, G.B., Josenhans, H.W., MacLean, B. and Vilks, G., 1990. Quaternary Geology. Chapter 10 in Geology of the continental margin off eastern Canada, ed. M.J.Keen and G.L.Williams. Geological Survey of Canada, Geology of Canada, no. 2, (also Geological Society of America, The Geology of North America, v. I-1), p. 475-607.

Piper, D.J.W., Sparkes, R. and Berry, J., 1995. Bathymetry and echo-character maps of part of the Scotian Slope and Southwest Grand Banks Slope. Geological Survey of Canada Open File 3089.

Pocklington, R., Leonard, J.D. and Crewe, N.F. 1991. Sources of organic matter to surficial sediments from the Scotian Shelf and Slope, Canada. Continental Shelf Research, v. 11, p. 1069-1082.

Savoye, B., Cochonat, P. and Piper, D.J.W., 1990. Seismic evidence for a complex slide near the wreck of the Titanic: model of an instability corridor for non-channeled gravity events. Marine Geology, v. 91, p. 281-

298.

Schwab, W.C., Lee, H.J., and Twichell, D.C., 1992. Submarine landslides: selected studies in the U.S. exclusive economic zone. U.S. Geological Survey Bulletin 2002.

Schafer, C.T., Tan, F.C., Williams, D.F. and Smith, J.N., 1985. Late glacial to Recent stratigraphy, paleontology, and sedimentary processes: Newfoundland continental slope and rise: Canadian Journal of Earth Sciences, v. 22, p. 266-282.

Shor, A.N., 1984. Bathymetry. In: Ocean Margin Drilling Program Regional Data Synthesis Series, Atlas 2, Eastern North American Continental Margin and Adjacent Ocean Floor. 39° to 46° N and 54° to 64° W, A.N.Shor and E. Uchupi, editors, Woods Hole, Mass.: Marine Science International, Sheet 1.

Shor, A.N. and Piper, D.J.W., 1989. A large Pleistocene blocky debris flow on the central Scotian Slope. Geo-Marine Letters, v. 9, p. 153-160.

Shor, A.N., Piper, D.J.W., Hughes Clarke, J. and Mayer, L. A., 1990. Giant flute-like scour and other erosional features formed by the 1929 Grand Banks turbidity current. Sedimentology, v. 37, p. 631-645.

Skene, K.I., 1991. Quaternary geology of three selected transects of the continental slope off eastern Canada. Geological Survey of Canada Open File 2425, 71 p.

Skene, K.I., 1994. Stratigraphic interpretation and correlation of seismic reflection profiles from Parizeau cruise 92-052. Contract report to the Geological Survey of Canada.

Smith, J.N. and Schafer, C.T., 1984: Bioturbation processes in continental slope and rise sediments delineated by Pb-210, microfossil and textural indicators: Journal of Marine Research, v. 42, p. 1117-1145.

Stanley, D.J. and Silverberg, N. 1969. Recent slumping on the continental slope off Sable Island Bank, southeast Canada. Earth and Planetary Science Letters, v. 6, p. 123-133.

Stanley, D.J., Swift, D.J.P., Silverberg, N., James, N.P. and Sutton, R.G., 1972. Late Quaternary progradation and sand spillover on the outer continental margin off Nova Scotia, southeast Canada. Smithsonian Contributions to Earth Sciences, no. 8, 88 p.

Stea, R.R., Piper, D.J.W., Fader, G.B.J. and Boyd, R., 1998. Wisconsinan glacial and sea-level history of Maritime Canada and adjacent continental shelf: A correlation of land and sea events. Geological Society of America Bulletin, v. 110, p. 821-845.

Stein, S., Sleep, N.H., Geller, R.J., Wang, S., and Kroeger, G.C., 1979. Earthquakes along the passive margin of eastern Canada. Geophysical Research Letters, v. 6, p. 537-540.

Stow, D.A.V., 1977. Late Quaternary stratigraphy and sedimentation on the Nova Scotian outer continental margin: unpublished Ph.D. thesis, Dalhousie University, Halifax, Nova Scotia, 360 p.

Stow, D.A.V., 1978, Regional review of the Nova Scotian outer margin: Maritime Sediments, v. 14, p. 17-32.

Swift, S.A., 1985a: Late Quaternary sedimentation on the continental slope and rise off western Nova Scotia:

Geological Society of America Bulletin, v. 96, p. 832-841.

Swift, S.A., 1985b: Cenozoic geology of the continental slope and rise off western Nova Scotia: unpublished Ph.D. thesis, Woods Hole Oceanographic Institution.

Swift, S.A., 1987. Late Cretaceous - Cenozoic development of Outer Continental Margin, Southwest Nova Scotia. American Association of Petroleum Geologists Bulletin, v. 71, p. 678-701.

Syvitski, J.P.M., Fader, G.B., Josenhans, H.W., MacLean, B. and Piper, D.J.W. 1983. Seabed investigations of the Canadian East Coast and Arctic using PISCES IV. Geoscience Canada, 10, 59-68.

Thurber Consultants Ltd. 1985. Study of well logs from East Coast offshore wells to delineate gas hydrate occurrence. Report to Earth Physics Branch, EMR, 28 p.

Thurber Consultants Ltd. 1988. Update of well log studies Mackenzie Delta/ Beaufort Sea area, Arctic islands, and offshore East Coast. Volume 2, Hibernia and Terra Nova areas. Report to Earth Physics Branch, EMR, 24 p.

Uchupi, E. and Swift, S.A., 1992. Plio-Pleistocene slope construction off western Nova Scotia, Canada. In: The dynamics of coarse grained deltas. Ed. Dabris, C.J., Zazo, C. and Goy, J.L., Universidad Complutensa de Madrid, p. 15-36.

Wade, J.A. and MacLean, B.C., 1990. Aspects of the geology of the Scotian Basin from recent seismic and well data. Chapter 5, in Geology of the continental margin off eastern Canada, ed. M.J.Keen and G.L.Williams. Geological Survey of Canada, Geology of Canada, no. 2, (also Geological Society of America, The Geology of North America, v. I-1), p. 190-238.